Series II, Volume 6 April 24, 1961 Number 3

BULLETIN

OF THE

AMERICAN PHYSICAL SOCIETY

INCLUDING THE

PROGRAMME OF THE

1961 SPRING MEETING

WASHINGTON, D. C.

April 24–27, 1961

PUBLISHED BY THE AMERICAN PHYSICAL SOCIETY, COLUMBIA UNIVERSITY, NEW YORK 27, NEW YORK
SIX ISSUES EACH YEAR

BULLETIN

of the

AMERICAN PHYSICAL SOCIETY

Published six times per year

Subscription price: $5.00 per year

Back number prices: $4.00 for the triennial Membership List; $1.00 for other issues.

The Bulletin of the American Physical Society is published six times a year, once in February, once in March, once in April, once in June, once in November, and once in December, at Prince and Lemon Streets, Lancaster, Pennsylvania. Correspondence should be addressed to American Physical Society, Columbia University, New York 27, New York.

Second class postage paid at Lancaster, Pa.

Table of Contents

Page

Programme of the 1961 Spring Meeting at Washington:

Preamble 220

Epitome 222

Main Text 224

Index 316

Pertaining to the Oliver E. Buckley Solid-State Physics Prize 315

Reservation form for Sheraton-Park Hotel 321

Announcement of 1961 June Meeting at Mexico City 323

Announcement of 1961 Thanksgiving Meeting at Chicago 323

Announcements of topical conferences 323–324

Important Announcement Concerning the Membership List 324

Calendar of Meetings and Deadlines 325

Instructions for the Preparation of Abstracts 326

List of Officers of the Society 327

April 24, 1961 Series II, Vol. 6, No. 3

BULLETIN

OF THE

AMERICAN PHYSICAL SOCIETY

1961 Spring Meeting at Washington, D. C., April 24–27, 1961

OUR change from a three-day to a four-day Spring meeting, made last year, has come, if not just in the nick of time, at any rate at the last opportunity before the nick. The Washington meeting has reached its turn for one of the population-explosions which unpredictably affect one after another of our annual cycle of conventions, and, since its previous record was our all-time all-place record, we now have another of these last. Another piece of luck, for which we can claim no credit, is the coming-into-being of two new large auditoria—the Cotillion Rooms North and South—in the Sheraton-Park Hotel. But for these we could not have found adequate space conveniently located for the seven simultaneous sessions which occupy every one of the eight half-days of the congress. We continue to enjoy the East Building Lecture Room of the National Bureau of Standards. Our valiant and industrious Local Committee, headed as usual by R. D. Huntoon and W. R. Tilley, and comprising D. F. Bleil, R. T. Cook, W. C. Hall, A. I. Mahan, J. H. McMillen, R. B. Roberts, S. F. Singer, and L. Slack, will have more work than ever.

The **official hotel is the Sheraton-Park,** already well known to us for many years. It will find rooms in other hotels when its own provision is fully booked: but this is on the assumption that our members will be prompt in booking, and their applications for space should be received not later than April eighteenth. A transcript of the standard reservation card of the Sheraton-Park Hotel appears on page 321: those who have disregarded the admonition (to reserve early) that has been put into previous issues of this Bulletin should tear it out and mail it as soon as they read these words.

The **registration desk** will be located in the Esplanade of the Sheraton-Park (the large room between lobby and Sheraton Hall). It will be open from 6:00 to 9:00 on Sunday evening, a great courtesy of which all should avail themselves who come soon enough to Washington: these will thus benefit themselves and the staff. The message center and information desk will be found in the northeast corner of the lobby, as it was last year. Here will be found blackboards for notices of post-deadline papers, changes in halls or in the womens' programme, and anything else to be brought to the attention of our members. We do not accept messages from anyone who has not yet registered and paid the fee.

The **registration fee** has ascended to $2.50, but the marvel is that the Local Committee expects to come out even without making it still bigger. Those who deem it high should observe the practices of other societies!

Invited speakers are named on the Epitome and the titles of their papers are given in the Main Text. Among them we mention M. L. Goldberger, the winner of the 1961 Dannie Heineman Prize in mathematical physics, and W. F. Libby, the 1960 Nobel Laureate in Chemistry (his fellow laureate in physics appeared last year before the Spring meeting as recipient of the American Physical Society Prize sponsored by Hughes Aircraft Company). Our Divisions of Solid-State Physics and of Plasma Physics have each arranged a half-day session of invited papers.

Five hundred and thirty-seven, the number of contributed papers, exceeds by eighty-four the maximum heretofore attained. The upsweep is concentrated in no single field of physics: it is more nearly a uniform expansion: plasma physics went from two sessions (in 1960) to three, neutron physics from two to three, semiconductors from one to two, theoretical physics from six to eight (but did not quite reach the figure attained at New York) and nuclear reactions stretch clear from beginning to end of the meeting. One of our expectations was happily not realized. We expected a mighty inrush of papers from solid-state physicists who would have found themselves unable or unwilling to make the long journey to the March meeting this year translated

to Monterey: there are no symptoms of such a phenomenon. For the arrangement of papers in theoretical physics the Society owes a great debt to N. M. Kroll; and also to the Deputy Secretary who took over the distribution of the abstracts pertaining to nuclear reactions, radioactive nuclei, and neutrons.

It is devoutly hoped that we shall now have several years of near-constancy in which to adapt ourselves to meetings of this magnitude before the next population-explosion comes along. Else, where do we go from here?

Our banquet will be held on Wednesday evening in the Sheraton Hall. G. T. Seaborg, newly chosen head of the Atomic Energy Commission, will be the after-dinner speaker, and the 1961 Dannie Heineman Prize will be awarded to M. L. Goldberger. The banquet (scheduled for 7:30 p.m.) will be preceded by a cocktail party in the balcony of Sheraton Hall from 6:30 onward. Your dinner ticket, priced at five dollars, will admit you to the cocktail party, but you cannot go to the party without paying for the dinner. There are only two places where a member of the Society present at the meeting may spend Wednesday evening with propriety: one is Sheraton Hall, the other is his bedroom if but only if he has a contagious cold or some ailment so severe that his doctor forbids him to go out.

The **National Bureau of Standards** will be host at a tea on Tuesday from 4:30 to 6:30 p.m. in the Manse on the Bureau grounds.

The **Register for Women's Activities** will be open from 8:30 a.m. to noon, Monday and Tuesday, April 24 and 25. A **Get-Acquainted Coffee Social** has been arranged for Monday morning, 9:30 to 11:00 in a place later to be determined. Special tours have been planned for Wednesday with advance registration necessary since the number will be limited. Included will be a special visit to the White House at 9:15 a.m., luncheon at the Continental Hotel at 1 p.m. ($2.50), followed by a meeting with ladies of the Congress and a tour of the Capitol. Those wishing to attend limited functions should make reservations in advance with Mrs. A. G. McNish at National Bureau of Standards, Washington 25, D. C., and include their check for the luncheon if desired.

The American Institute of Physics will conduct a **Placement Service Register** in the Exhibit Hall of the Sheraton-Park Hotel, April 24–27. The Register will be open from 9:00 to 6:00 p.m.

There will be a **book exhibit** in the Florentine Foyer at which twelve of the leading book publishers will display the latest scientific and technical books and publications. It will be open from 9:00 a.m. to 5:30 p.m. on all days excepting Thursday, when it will close at 2:00 p.m. All are cordially invited to browse.

The **Council of The American Physical Society** will meet at 9:30 a.m. on Monday, April 24, in the Woodley Room in Section F of the Sheraton-Park Hotel.

The **Nominating Committee of the American Physical Society** will meet at 4:00 p.m. on Tuesday, April 25, in the Conference Room in the South Building of the National Bureau of Standards.

Post-deadline ten-minute papers, pertaining to very recent achievements of very special significance, will be considered for admission to the programme if abstracts are received not later than Tuesday, April 18, at the office of Dr. R. D. Huntoon, National Bureau of Standards, Washington 25, D. C. The titles of such as are accepted will appear on a blackboard near the registration desk. Session Y has been set aside for them, but it is not impossible that some may be placed at the ends of sessions relevant in topic and not already too long for elongation.

The **1961 June meeting in Mexico City** is announced on page 323, and attention is very specially called to two features: the deadline for hotel reservations, and the request for *three* (not just two) copies of each abstract, the third being meant for translation into Spanish and publication in the bulletin which our sister society the Sociedad Mexicana de Fisica will bring out. There will be no Summer Meeting other than this in 1961. A preliminary announcement of the **Thanksgiving meeting at Chicago** will be found on page 323.

Announcements of topical conferences will be found on pages 323 and 324.

Instructions for the preparation of abstracts are printed on page 326 of this Bulletin. Read and heed them! An extra instruction is given: use a typewriter ribbon that is decently fresh! Some of the abstracts that come to us are so faint that it is a wonder that the printers can read them.

Errata pertaining to abstracts in this issue will be published in a later issue of this Bulletin if received not later than Monday, May first, by Miss Ruth F. Bryans, American Institute of Physics, 335 East 45 Street, New York 17, New York. Do not send in the abstract defaced with erasures and corrections. Write out your corrections in the form "Instead of . . . read. . . ." Add nothing.

KARL K. DARROW, *Secretary*
American Physical Society
New York 27, New York

EPITOME OF THE 1961 SPRING MEETING

(Personal names are those of invited speakers. NBS stands for National Bureau of Standards; all sessions not so marked are at Sheraton-Park Hotel.)

Monday Morning

10:15	A.	Spins, I. Burgundy Room.
10:00	AA.	Nuclear Reactions, I. Continental.
10:00	B.	Radioactive Nuclei, I. Cotillion Room South.
10:00	BA.	Magnetism. Franklin Room.
10:30	C.	Segall, Kip. Sheraton Hall.
10:30	CA.	Weinberg, Nilsson. Cotillion Room North.
10:00	CB.	Theory I.: Nuclear Structure, I. Adams-Hamilton Room.

Monday Afternoon

2:00	D.	Spins, II; Stroke. Burgundy Room.
2:00	DA.	Nuclear Reactions, II. Continental Room.
2:00	E.	Radioactive Nuclei, II. Cotillion Room South.
2:15	EA.	Division of Plasma Physics: Lenard, Coensgen, Post, Drummond. NBS East.
2:00	F.	General nuclear physics, mostly apparatus. Sheraton Hall.
2:00	FA.	Metals. Adams-Hamilton Room.
2:00	FB.	Theory, II: many-body problems, statistical mechanics. Cotillion Room North.

Tuesday Morning

10:15	G.	Spins, III. Adams-Hamilton Room.
9:30	GA.	Nuclear Reactions, III. Continental Room.
9:30	H.	Fast neutrons. Cotillion Room South.
9:45	HA.	Hayward, Kessler, De Benedetti, Walker. Sheraton Hall.
9:45	J.	Accelerators; K. Green. Cotillion Room North.
9:30	JA.	Division of Solid-State Physics: Rubin, Maradudin, Wallis, Kahn. NBS, East.
9:45	JB.	Theory, III: dispersion-relations and quantum electrodynamics. Burgundy Room.

Tuesday Afternoon

2:00	K.	Spins, IV. Adams-Hamilton Room.
2:00	KA.	Nuclear Reactions, IV. Continental Room.
2:00	L.	Cold-neutron scattering and solid-state physics. Cotillion Room South.
2:00	LA.	Cosmic rays and space. Sheraton Hall.
2:00	M.	Electron physics. NBS, East.
2:00	MA.	Cryogenics. Cotillion Room North.
2:00	MB.	Theory, IV: properties and interactions of elementary particles. Burgundy Room.

Wednesday Morning

10:30	N.	Molecules. Adams-Hamilton Room.
9:30	NA.	Nuclear Reactions, V. Continental Room.
10:30	P.	Neutron spectroscopy. Cotillion Room South.
9:45	PA.	Yagoda; cosmic-ray studies with satellites. Sheraton Hall.
10:00	Q.	Fluid dynamics. NBS, East.
10:15	QA.	Mitchell; general solid-state physics, I. Cotillion Room North.
9:30	QB.	Theory V: atomic and general theory. Burgundy Room.

Wednesday Afternoon

2:00	R.	Optical and X-ray physics; astrophysics; M. S. Green. Adams-Hamilton Room.
2:00	RA.	Nuclear Reactions VI: heavy ion-reactions. Continental Room.
2:00	S.	Hofstadter; nucleonic structure and scattering. Sheraton Hall.
2:00	SA.	Plasma, I. NBS, East.
2:00	T.	Strange Particles. Cotillion Room South.
2:00	TA.	General Solid-State Physics II. Cotillion Room North.
2:00	TB.	Theory V: Nuclear Reactions. Burgundy.

Wednesday Evening at 7:00

Sheraton Park Hotel

Banquet of The American Physical Society; Seaborg.

Thursday Morning

9:30 U. General; physics; masers; Ramsey. Cotillion Room South.
9:30 UA. Barschall, Wildermuth, Satchler, Johnson. Cotillion Room North.
9:30 V. Goldberger, Libby, Kunzler, Matthias. Sheraton Hall.
9:30 VA. Plasma II. NBS, East.
9:30 W. Muons and pions. Continental.
9:30 WA. Semiconductors I. Burgundy Room.
9:30 WB. Theory VII: general theory, mostly relativity. Adams-Hamilton.

Thursday Afternoon

1:30 X. Shapiro, Friedman, Naugle. Sheraton Hall.
1:30 XA. Nuclear Reactions VII (including fission). Continental Room.
1:30 Y. Post-deadline papers, if any. Franklin Room.
1:30 YA. Plasma III. NBS, East.
1:30 Z. Pions. Cotillion Room South.
1:30 ZA. Semiconductors II. Cotillion Room North.
1:30 ZB. Theory VIII: Nuclear Structure II. Adams-Hamilton Room.

PROGRAMME

MONDAY MORNING AT 10:15

Burgundy Room

(N. F. RAMSEY presiding)

Spins, I

A1. Nuclear Spins of N^{13} and C^{11}.* J. L. SNIDER, M. POSNER, A. M. BERNSTEIN, AND D. R. HAMILTON, *Princeton University.*—The nuclear spins of 10-min N^{13} and 20-min C^{11} have been measured by the atomic beam magnetic resonance method to be $\frac{1}{2}$ and $\frac{3}{2}$, respectively. Powdered melamine was bombarded with 18 Mev protons giving N^{13} in the reaction $N^{14}(p,pn)N^{13}$, while C^{11} was made by $B^{11}(p,n)C^{11}$. The radioactivity, in the form of gaseous molecules, was continually flushed with neon through a 375-ft pipe into the apparatus. After dissociation in a microwave discharge, atoms traveled through a modified focusing atomic beam apparatus to the detector. N^{13} atoms were collected on iron foils heated to 1050°C. Resonances in the $^4S_{\frac{3}{2}}$ atomic ground state were observed at frequencies up to 1.7 Mc/sec. C^{11} was collected on silver-plated copper collectors held at ≈ -100°C. Resonances in the $^2P_2$ and $^2P_1$ metastable atomic states were observed up to 1.3 Mc/sec. Both activities were detected by counting the decay positrons. The spins of N^{13} and C^{11} are the same as those of their charge conjugate nuclei C^{13} and B^{11} as expected on the basis of charge symmetry of nuclear forces. Measurements of the hyperfine structure splittings in both isotopes are in progress.

* This work was supported by the U. S. Atomic Energy Commission and the Higgins Scientific Trust Fund.

A2. Spins of Sc^{44} and Sc^{44m}.* D. L. HARRIS AND J. D. MCCULLEN, *Princeton University.*—The nuclear spins of Sc^{44} and Sc^{44m} have been measured with the six-pole focusing-magnet atomic beams machine. The radioactive isotope was made in the Princeton cyclotron by a (p,pn) reaction on pure Scandium metal. The beam was produced at a color temperature of ~1600°C using a tantalum double oven, and was collected on copper disks. Resonances were observed at several fields in both the $^2D_{\frac{3}{2}}$ and $^2D_{\frac{1}{2}}$ electronic states, yielding the following results: $I=2$ for the ground state (3.96*h*), $I=6$ for the metastable level (2.44*d*). Work is in progress to measure the hyperfine structure for these levels, as well as to determine the spin of Ti^{45}, which is also present in the beam.

* This work was supported by the U. S. Atomic Energy Commission and the Higgins Scientific Trust Fund.

A3. Nuclear Magnetic Resonance of Lanthanum Metal.* D. S. SCHREIBER AND R. M. COTTS, *Cornell University.*—Two resonances have been found in La metal particles; one Knight shifted by $k_1=+0.64\%$ as previously reported,[1] and a second line shifted by $k_2=+0.21\%$. The metal is known to exist in two phases predominately hcp below 280°C and fcc above 280°C. However, both phases can exist together depending upon thermal history and cold working. The shifts remain constant in the temperature range 25° to 380°C. The second line (k_2) has a thermal relaxation time T_1 approximately 20 times that of the first line (k_1). The linewidths are about 11 g each. The first line is slightly asymmetric, but becomes symmetric and narrows about 25% above 280°C. Upon heating, the intensity of the first line increases rapidly near 280°C, which indicates that a relaxation of random quadrupole interactions accompanies the phase transition. Upon cooling, the increased intensity persists down to 230°C, and further cooling returns the intensity to its room temperature value. X-ray powder diffraction shows that the first line appears only when some fcc is present and that both lines are seen when both the hcp and fcc phases are present.

* Supported in part by the National Science Foundation.
[1] W. E. Blumberg, J. Eisinger, V. Jaccarino, and B. T. Matthias, Phys. Rev. Letters 5, 52 (1960).

A4. *g*-Value of the 0.123 Mev State of Sm^{152}.* R. W. BAUER AND M. DEUTSCH, *MIT.*—Recently published measurements of this *g* value have given contradictory results, largely because of the difficulty of evaluating the paramagnetic correction to the magnetic field. We have measured the rotation, in a magnetic field of 26 kgauss, of the gamma ray angular correlation from *liquid* sources of Eu^{152} at four temperatures: 300°K (aqueous solution of Eu Cl_3), 1100°K, 1300°K, and 1500°K (melt of Eu Cl_3). The rotation appeared to be independent of temperature within an experimental uncertainty of about 15%. This suggests that the paramagnetic correction is quite small, as suggested by the calculations of Kanamori and Sugimoto.[1] Without correction, the weighted mean of our measurements is $g=0.375\pm0.03$. With the corrections cited in footnote 1, this is reduced to 0.351 ± 0.03.

* This work is supported in part by funds provided by the U. S. Atomic Energy Commission, the Office of Naval Research, and the Air Force Office of Scientific Research.
[1] J. Kanamori and K. Sugimoto, J. Phys. Soc. Japan 13, 754 (1958).

A5. Hyperfine Structure and Nuclear Moments of Lutetium-177.* F. R. PETERSEN AND H. A. SHUGART, *University of California, Berkeley.*—The hyperfine structure separations for radioactive lutetium-177 ($I=7/2$) have been measured in both the $^2D_{\frac{3}{2}}$ and $^2D_{\frac{5}{2}}$ electronic states by the atomic beam magnetic resonance method. Seven "flop-in" transitions in the $^2D_{\frac{3}{2}}$ state and ten in the $^2D_{\frac{5}{2}}$ state corresponding to the high field transition $M_J=\pm\frac{1}{2}\leftrightarrow\mp\frac{1}{2}$ have been observed. The interaction constants a and b fitted to these observations are $a(^2D_{\frac{3}{2}})=194.84(2)$ Mc/sec, $b(^2D_{\frac{3}{2}})=1466.71(12)$ Mc/sec, $a(^2D_{\frac{5}{2}})=147.17(1)$ Mc/sec, $b(^2D_{\frac{5}{2}})=1805.93(14)$ Mc/sec. The uncorrected nuclear magnetic moment calculated from the interaction constant a is $\mu_I=+2.0(2)$ nm. The sign of the moment was determined from the g_I-dependent $\Delta F=\pm1$ transitions for which the magnetic field dependence of the frequency was zero at high fields. The uncorrected nuclear electric quadrupole moment calculated from the interaction constant b is $Q=+5.0(6)$ barns. Uncertainties in both moments will be considerably reduced when more precise measurements of the hyperfine structure and moments of stable Lu^{175}, currently in progress by George J. Ritter and Hin Lew, are published.[1]

* Supported in part by the U. S. Air Force Office of Scientific Research and the U. S. Atomic Energy Commission.
[1] George J. Ritter, National Research Council, Ottawa, Canada, private communication (1960).

A6. Effects on Proton Magnetic Resonance in Hydrated Crystals Induced by Quadrupolar Nuclei.* A. A. SILVIDI AND J. W. MCGRATH, *Kent State University.*—Long proton relaxation times sometimes are reduced by spin-exchange of energy between the protons and nearby quadrupolar nuclei via magnetic dipole-dipole interaction.[1] This can occur[2] for orientations of a hydrated crystal and magnitudes of an extenral magnetic field, such that, a Zeeman-split quadrupolar frequency matches the NMR frequency of the proton. If T_1 for the quadrupolar nucleus is short, T_1 for the proton is reduced and

proton resonance absorption is enhanced. This effect has appeared in single crystals of $BaBr_2 \cdot H_2O$.[3] We are using proton resonance enhancement as a detector of quadrupolar resonances of Ba^{137}. Data fit orientation-frequency values computed[2] for an asymmetry parameter of 0.66 and principal axes of the electric field gradient tensor; x antiparallel to a, y and z parallel to c and b, respectively. a, b, and c are crystallographic axes. ν_Q is 24.3 Mc/sec.

* Supported by the National Science Foundation.
[1] D. E. Woessner and H. S. Gutowsky, J. Chem. Phys. 29, 804 (1958).
[2] J. W. McGrath and A. A. Silvidi, J. Chem. Phys. 33, 644 (1960).
[3] C. Dean, Phys. Rev. 96, 1053 (1954).

A7. Dynamic Proton Polarization in Crystals at Low Temperatures.* O. S. LEIFSON† AND C. D. JEFFRIES, *University of California, Berkeley.*—Dynamic polarization of protons in $La_2Mg_3(NO_3)_{12} \cdot 24H_2O$, with a small fraction of the La^{3+} replaced by paramagnetic Ce^{3+}, has been produced by strongly inducing the (relatively) forbidden electron transition[1] of the Ce^{3+}. An apparatus for simultaneously observing the cerium electron resonance at 9400 Mc/sec and the proton nuclear resonance at 16 Mc/sec at liquid helium temperatures is described. For fixed electron resonance frequency, the dependence of the dynamic proton polarization on magnetic field and microwave power agrees with theory.[2] In the liquid helium temperature range and for fixed Ce^{3+} concentrations ranging from 0.05% to 5%, the electron relaxation time $T_{1e} \propto (\text{temperature})^{-16}$ and the nuclear spin-lattice relaxation time $T_{1n} \propto (\text{temperature})^{-7}$. The maximum polarization of protons produced at x-band and 1.5°K was 3.1%, which represents a maximum proton polarization enhancement of 140 times thermal equilibrium as compared to the theoretically maximum value of 605.

* Supported in part by the Office of Naval Research and the U. S. Atomic Energy Commission.
† Now at the U. S. Army Signal Research and Development Laboratories, Fort Monmouth, New Jersey.
[1] C. D. Jeffries, Phys. Rev. 117, 1056 (1960).
[2] O. S. Leifson and C. D. Jeffries, Phys. Rev. (to be published).

A8. Nuclear Magnetic Resonance of B^{11} in the Alkali-Borate Glass Systems.* J. G. O'KEEFE AND P. J. BRAY, *Brown University.*—Previous investigation[1] of the alkali-borate glass systems has shown that the amount of 4-coordinated boron (N_4) is a function of the alkali modifier concentration. It was noted in this work that the experimental procedure used led to an overestimation of N_4 at high alkali modifier concentrations. The four alkali-borate glass systems, $K_2O-B_2O_3$, $Na_2-B_2O_3$, $Li_2O-B_2O_3$, and $BaO-B_2O_3$ were re-investigated using a different technique. In this investigation, the intensity of the resonance due to 4-coordinated boron in the glass sample was compared with the intensity of the boron resonance in a crystalline compound containing only 4-coordinated boron. The results show that the maximum number of 4-coordinated boron atoms is of the order of 25% rather than 50% as stated in the earlier work. The data for all four systems may be fitted by a single curve on a graph of N_4 versus alkali modifier concentration.

* Research supported by Office of Naval Research.
[1] A. H. Silver and P. J. Bray, J. Chem. Phys. 29, 984 (1958).

A9. Nuclear Magnetic Resonance in Gallium Phosphide. M. J. WEBER, L. RIMAI, AND L. NEURINGER, *Raytheon Company.*—Pulsed and c.w. measurements have been made of the nuclear magnetic resonance of Ga^{69}, Ga^{71}, and P^{31} in polycrystalline GaP. The resonance line shapes are approximately Gaussian with linewidths ~10% greater than the calculated dipolar widths. The additional width may be attributed to indirect nuclear exchange broadening as observed in other III–V compounds. The spin-lattice relaxation time T_1 was measured in the temperature range 77–700°K using pulsed NMR techniques. At room temperature, $T_1(Ga^{69}) = 0.45 \pm 0.03$ sec, $T_1(Ga^{71}) = 1.15 \pm 0.08$ sec, $T_1(P^{31}) = 100 \pm 30$ sec. The ratio $[T_1(Ga^{69})/T(Ga^{71})] \approx [Q(Ga^{71})/Q(Ga^{69})]^3$, where Q is the quadrupole moment, is observed at all temperatures and indicates that the gallium relaxation is caused by time-dependent quadrupole interactions. The gallium T_1's can be fitted to Van Kranendonk's temperature dependence for a two-phonon relaxation process using a Debye temperature $\theta_D \sim 400$°K. The phosphorus relaxation is approximately temperature independent between 77–460°K. Possible relaxation mechanisms will be discussed.

MONDAY MORNING AT 10:00

Continental Room

(T. KRUSE presiding)

Nuclear Reactions, I

AA1. Angular Distribution of the Reaction $Be^9(Li^7,\alpha)B^{12}$.* J. M. BLAIR AND R. K. HOBBIE, *University of Minnesota.*—The techniques used[1] to study the reaction $Be^9(Li^6,\alpha)B^{11}$ have been extended to the reaction $Be^9(Li^7,\alpha)B^{12}$. At energies near 3.3 Mev $Q = 10.46$ Mev. Alpha particles are separated from other reaction products by measuring both dE/dx and E. A solid state detector provides sufficient resolution to separate levels through the second excited state; the 2.62 and 2.72 Mev levels appear as one peak.

* Supported in part by the joint program of the U. S. Atomic Energy Commission and the Office of Naval Research.
[1] J. J. Leigh and J. M. Blair, Phys. Rev. 121, 246 (1961).

AA2. Nucleon Reduced Widths and Charge Independence. ALBERT ALTMAN AND JERRY B. MARION, *Convair, San Diego,* AND WILLIAM M. MACDONALD, *University of Maryland.*—The mirror levels at 8.89 Mev in B^{10} and 7.37 Mev in Be^{10} have been re-analysed under the assumption of d-wave formation of these levels and hence a $J^\pi = 3^-$ assignment. The previously assumed 3^+ assignment (formed by p waves) gave poor agreement with the isotopic spin addition and ratio rules.[1] With this new assignment, which agrees well with recent high energy stripping data[2] and is not excluded by the elastic scattering experiment,[3] agreement with the isotopic spin rules is achieved without the necessity of invoking different neutron and proton interaction radii. The resulting isotopic-spin impurity of the B^{10} level (8.89 Mev) is $\alpha^2 < 2.5 \times 10^{-3}$ in *intensity*, the upper limit holding only if the reduced width of the impurity state is as large as that of the normal state.

[1] W. M. MacDonald and J. B. Marion, Bull. Am. Phys. Soc. 5, 34 (1960).
[2] M. H. Macfarlane and J. B. French, Revs. Modern Phys. 32, 567 (1960).
[3] H. B. Willard, J. K. Bair, and J. D. Kington, Phys. Rev. 98, 669 (1955).

AA3. Energy Dependence of the $B^{10}(d,p)B^{11}$ Reaction.* B. ZEIDMAN AND J. L. YNTEMA, *Argonne National Laboratory.*—The $B^{10}(d,p)B^{11}$ ground state reaction has been investigated at deuteron energies of 12.5, 15.5, 18.5, and 21.5 Mev. The energies below 21.5 Mev were obtained by degrading and re-

focusing the beam from the Argonne 60-in. cyclotron. The angular distributions cover a range of angles between 7° and 165° except for the 12.5-Mev data which extends only to 90°. At forward angles, a peak is observed at all energies. At the lowest energies, the first peak in the angular distribution is well fitted by Butler theory with the customary radius of 5 f, but there are significant deviations from the Butler theory at higher energies which cannot be compensated for by adjustment of the interaction radius. The peak cross section increases with increasing energy, contrary to the trend expected from the energy dependence of the Butler theory.

* Work performed under the auspices of the U. S. Atomic Energy Commission.

AA4. Gamma Rays from the Bombardment of Light Nuclei with Lithium Ions.* S. BASHKIN, E. BERKOWITZ, J. DAVIES, AND E. NORBECK, *State University of Iowa.*—Thick targets of Li^6F, Li^7F, Be^9, B^{10}, B^{11}, carbon, titanium nitride, and CaF_2 have been bombarded with Li^6 ions having an energy of 2.8 Mev. A sodium iodide crystal, 3-in. diam×3 in. long, viewed the gamma radiation through a conical collimating aperture in a 4-in. thick lead shield, A 256-channel analyzer sorted the detector pulses. The gain of the detecting system was calibrated with a variety of gamma rays of known energy. In each case, a number of relatively low energy gamma rays appear. They give evidence that a neutron, proton, or small cluster of neutrons and protons is transferred between the incident and target nuclei, leaving a residual nucleus in a low-lying excited state. Reactions which might lead to the observed gamma rays will be discussed.

* Supported in part by the U. S. Atomic Energy Commission.

AA5. Excitation Functions of the $Li^7(\alpha,n)B^{10}$ and $Li^6(\alpha,n)B^9$ Reactions.* M. K. MEHTA, W. E. HUNT, H. S. PLENDL, AND R. H. DAVIS, *Florida State University.*—The neutron yield from the $Li^7(\alpha,n)B^{10}$ reaction has been measured as a function of bombarding energy from threshold at 4.37 to 14.5 Mev α-particle energy (lab). Neutrons were detected by three paraffin embedded BF_3 counters subtending an angle of about $-15°$ to $+15°$ with respect to the beam direction. Prominent peaks in neutron yield were observed at 5.23, 5.6, 7.05, 8.46, 9.22, 10.09, 12.66, and 13.95 Mev (lab) alpha-particle energy. These correspond to levels in the compound nucleus B^{11} at 12.00, 12.24, 13.16, 14.05, 14.53, 15.09, 16.73, and 17.55 Mev, respectively, which compare well with those reported in previous work.[1] The measured ground state and first excited state thresholds of this reaction are 4.37 and 5.50 Mev (lab). A general rise in the neutron yield with indications of many contributing resonances has been observed between 14.5 and 18.0 Mev bombarding energy. The observed threshold for the reaction $Li^6(\alpha,n)B^9$ is 6.63 Mev (lab) which corresponds to a Q value of -3.98 Mev in good agreement with earlier work.[1] Energy calibrations are based on an $Al(p,n)$ threshold at 5.800 Mev and the estimated error in the present determination is ±0.02 Mev. Neutron yield from the reaction $Li^6(\alpha,n)B^9$ increases by a factor of ten between 7 and 16 Mev bombarding energy of the α particles.

* Supported in part by the U. S. Air Force Office of Scientific Research.
[1] F. Ajzenberg-Selove and T. Lauritsen, Nuclear Phys. 11, 1 (1959); R. Day and M. Walt, Phys. Rev. 117, 1330 (1960).

AA6. Be^9+p and Be^9+d Reactions at Low Energies.* J. A. BIGGERSTAFF, R. F. HOOD, AND M. T. MCELLISTREM, *University of Kentucky.*—Differential cross sections for proton and deuteron induced reactions in beryllium have been measured in a solid-target reaction chamber from 20° to 167° in the incident energy range from 0.75 to 2.0 Mev. Protons, deuterons, tritons, and alpha-particles produced in the bombardment of self-supporting Be foils were detected with a thin CsI(Tl) scintillator. Particle groups were identified on the basis of reaction kinematics and CsI(Tl) fluorescent decay times.[1] Characteristics usually attributed to direct reaction amplitudes were apparent in all reactions studied. The low Q-value $Be^9(p,d)Be^9$ and high Q-value $Be^9(d,t)Be^9$ reactions were compared, and yield very similar angular distributions over the energy range studied. The $Be^9(d,\alpha)Li^7$ reactions to the ground and first excited states of Li^7 show similar angular distributions near 2 Mev, but dissimilar distributions at lower energies. Data for the $Be^9(d,p)Be^{10}$ and $Be^9(p,\alpha)Li^6$ reactions have also been obtained.

* This work partially supported by the U. S. Atomic Energy Commission.
[1] J. A. Biggerstaff, R. F. Hood, and M. T. McEllistrem, Bull. Am. Phys. Soc. Ser. II 5, 441 (1960).

AA7. Positions, Widths, and Cross Sections. of C^{12} Levels from the $B^{10}(He^3,p)C^{12}$ Reaction.* C. P. BROWNE, W. E. DORENBUSCH, AND J. R. ERSKINE,† *University of Notre Dame.*—Proton groups from the $B^{10}(He^3,p)C^{12}$ reaction leading to levels up to 16.2-Mev excitation were analyzed with a broad-range spectrograph. The bombarding energy was 3.74 Mev and spectra were taken at 11 angles from 5° to 139°. Preliminary values for excitation energies are 4.441, 7.651, 9.644, 10.856, 11.863, 12.712, 14.088, 15.107, and 16.107 Mev. Widths of the 9.6-, 10.8-, 11.9-, and 14.1-Mev levels are 36±6, 340±30, 247±30, and 248±15 kev, respectively. Widths of the other levels are less than 15 kev. No levels were found at 9.0, 11.1, 13.3, or 15.6 Mev. A level 2 Mev wide at 10.1 Mev would not have been seen above the high background from three-particle breakup. Yields at each angle were measured relative to the yield of the $B^{10}(He^3,d)C^{11}$ reaction. An angular distribution of this reaction was obtained. Absolute differential cross sections were found by comparing the yields with the known yield from the $B^{10}(d,p)B^{11}$ reaction. Cross sections are of the order of 0.15 mb/sr.

* Supported by the joint program of the Office of Naval Research and the U. S. Atomic Energy Commission.
† Now at Massachusetts Institute of Technology.

AA8. Gamma-Ray Decay of the 7.66-Mev Level of C^{12}.* DAVID E. ALBURGER, *Brookhaven National Laboratory.*—Proton-gamma-gamma triple coincidence measurements are being carried out on the $B^{10}(He^3,p)C^{12}$ reaction at $E_{He^3}=2.2$ Mev using a geometry described previously.[1] Protons are detected in a ¾-in. diam. by ½-in. thick CsI scintillator, the gamma-ray detectors are 5-in.×5-in. NaI crystals, and the coincidence resolving time is ~8 mμsec. The pulse-height spectrum of protons in triple coincidence with the two gamma-ray counters, both channeled from 2.4–5.0 Mev, contains a line (~3 counts/hr) corresponding to the 7.66-Mev level of C^{12}. This line is interpreted as resulting from the 3.23–4.43-Mev cascade gamma-ray decay of the 7.66-Mev level, although the possibility of an inelastic scattering effect is not excluded. When the ratio of the triples to singles counting rates of the 7.66-Mev proton line is corrected by the appropriate gamma ray efficiency factors, the 3.23-Mev gamma-ray branch is found to be 3×10^{-4} per decay of the 7.66-Mev level. This preliminary result, which at present is accurate to about 50%, is in agreement with the theoretical single-particle estimated branch of 2×10^{-4}.

* Work performed under the auspices of the U. S. Atomic Energy Commission.
[1] D. E. Alburger and R. E. Pixley, Phys. Rev. 119, 1970 (1960).

AA9. Proton Polarization in $C^{12}(\vec{p},p)C^{12}$. S. J. MOSS, R. I. BROWN, D. G. MCDONALD, AND W. HAEBERLI, *University of Wisconsin.**—The polarization of protons elastically scattered from C^{12} has been measured in 10° intervals for laboratory scattering angles from 20° to 140° at eight energies between 4.7 and 8.7 Mev. Protons scattered by self-supporting carbon targets (150–200 kev) entered a helium cell. The left-right asymmetry of the doubly scattered protons was measured with junction detectors at a mean scattering angle of 125°. The analyzing power of helium was taken from Brockman.[1]

The angular distribution of polarization at 6.2 Mev is characterized by a maximum at 70° ($P=+0.92\pm0.08$) and a minima at 40° ($P=-0.83\pm0.01$) and 100° ($P=-0.70\pm0.05$), where P is positive in the direction $\mathbf{k}_{in}\times\mathbf{k}_{out}$. As the energy is increased, the forward angle minimum decreases in absolute value, while the back angle minimum increases. The maximum remains above $P=+0.70$ at all energies measured. Agreement with other measurements at 7 Mev (see Evans)[2] and 8 Mev (see Rosen)[3] is good.

* Work supported by the U. S. Atomic Energy Commission and the Wisconsin Alumni Research Foundation.
[1] K. Brockman, Phys. Rev. 110, 163 (1958).
[2] J. E. Evans, *Proceedings of the Symposium on Polarization Phenomena, Basel, Switzerland, 1960* (to be published).
[3] L. Rosen, *Proceedings of the International Conference on Nuclear Structure* (University of Toronto Press, Toronto, Canada, 1960).

AA10. Elastic Scattering of Alpha Particles from C^{13}.* C. M. Jones, G. C. Phillips, R. W. Harris, and E. H. Beckner, *Rice University.*—The elastic scattering of alpha particles from C^{13} has been measured in the energy range 2.5 to 4.8 Mev using a recently constructed precision small volume gas scattering chamber. Excitation curves have been taken at the center of mass angles 66°7′, 70°7′, 90°0′, 99°15′, 109°24′, 125°16′, 140°16′, 149°27′, and 166°35′, and angular distributions have been measured at laboratory energies of 2.820, 3.377, 3.989, and 4.640 Mev. The data will be presented and a preliminary phase shift analysis of the data will be discussed.

* Supported in part by the U. S. Atomic Energy Commission.

AA11. α Particles from the 16.11 Mev State in C^{12}. Melvin J. Bina and Ralph E. Segel, *Aeronautical Research Laboratory.*—The 16.11-Mev state in C^{12} is formed by the well-known 163-kev $B^{11}+p$ resonance.[1] Thick boron targets were bombarded with protons just above the resonance energy and the resulting alpha-particle spectra were measured with silicon detectors. Two alpha-particle groups were seen: a sharp group due to breakup through the ground state of $Be^8(\alpha_0)$ and a continuum due to breakup through the broad 2.9-Mev Be^8 first excited state (α_1). Spectra were taken at every 15° from 45° to 165°. An over-all ratio $\alpha_1:\alpha_0=20:1$ was found which implies $\Gamma\alpha_0=325\pm50$ ev if the width of the 16.11-Mev state is taken to be mainly due to the alpha width. This value of $\Gamma\alpha_0$ is some factor of three larger than is listed in the literature.[1]

[1] F. Ajzenberg-Selove and T. Lauritsen, Nuclear Phys. 11, 1 (1959).

AA12. Elastic Scattering of He^3 by C^{12}.* P. D. Forsyth and G. S. Mani, *Rice University.*—The elastic scattering of He^3 from carbon has been studied in the energy range 1.5 to 5.5 Mev. The target was a thin, self-supporting foil of natural carbon. The scattered particles were detected by solid state counters. Preliminary results will be presented and compared with the He^3 reactions on the same nucleus.

* Supported in part by the U. S. Atomic Energy Commission.

AA13. Study of the Gamma Ray Yield from the $C^{12}(\alpha,\alpha'\gamma_{4.43})C^{12}$ Reaction.* G. E. Mitchell, E. B. Carter, and R. H. Davis, *Florida State University.*—The excitation function for $C^{13}(\alpha,\alpha'\gamma_{4.43})C^{12}$ has been measured from 7.3 to 17.0 Mev. Gamma rays produced in thin (<0.1 mg/cm², 99% C^{12}) targets were detected with a 3-in. by 3-in. NaI (Tl) crystal. Resonances were observed at bombarding energies of 7.94 ($\Gamma=120$ kev), 8.14 ($\Gamma=50$ kev), 8.95 ($\Gamma=90$ kev), 10.08 ($\Gamma\sim400$ kev), and 10.19 ($\Gamma=40$ kev) Mev, where the widths quoted are observed widths. The corresponding excitation energies in O^{16} are 13.10, 13.25, 13.86, 14.71, and 14.79 Mev. The first three levels have been previously studied via $N^{15}+p$ reactions.[1,2] Above 11 Mev bombarding energy, there appear to be many unresolved levels. Most of the angular distributions throughout the region of well resolved resonances show a maximum in the vicinity of 30° and a minimum at 90°.

* Supported in part by U. S. Air Force Office of Scientific Research.
[1] F. Ajzenberg-Selove and T. Lauritsen, Nuclear Phys. 11, 1 (1959).
[2] Bashkin, Carlson, and Douglas, Phys. Rev. 114, 1543 (1959).

Monday Morning at 10:00

Cotillion Room South

(A. Schwarzschild presiding)

Radioactive Nuclei, I

B1. Recoil Energy Spectrum for the β Decay of He^6. C. H. Johnson, Frances Pleasonton, and T. A. Carlson, *Oak Ridge National Laboratory.*—The energy spectrum of the Li^6 recoils following the β decay of He^6 was observed with the spectrometer which was used for an earlier investigation[1] of A^{37}. The spectrometer uses both magnetic and electrostatic deflectors in series so that the separate spectra of singly and doubly charged Li^6 ions can be observed and then combined into the total spectrum. Three states of differential pumping reduce the background so that better than 1% counting statistics are readily obtained over most of the spectrum. Preliminary results[2] presented at the 1958 Gatlinburg Conference showed the Gamow-Teller interaction to be predominantly axial-vector. After that conference the spectrometer was modified and work was continued with an aim to improve and to establish the accuracy of the experiments. The major modification was the installation of a new electron multiplier whose efficiency is nearly independent of electrostatic focusing of the incident Li^6 ions. Measurements are now completed and at the present stage of analysis we find the correlation coefficient to be -0.33 ± 0.01 in agreement with $-\frac{1}{3}$ for the axial-vector interaction.

[1] A. H. Snell and F. Pleasonton, Phys. Rev. 100, 1396 (1955).
[2] F. Pleasonton, C. H. Johnson, and A. H. Snell, Bull. Am. Phys. Soc. 4, 78 (1959).

B2. Electron Shake-off Following $He^6 \xrightarrow{\beta^-} Li^6$. T. A. Carlson, Frances Pleasonton and C. H. Johnson, *Oak Ridge National Laboratory.*—The extent of electron shake-off following the β decay of He^6 has been experimentally determined with a specially designed mass spectrometer. By use of both a magnetic and an electrostatic analyzer in tandem, measurements were made on the charge distribution and recoil energy spectra of the resulting lithium ions. The percentages of the total number of decays for the different charged ions are as follows: Li^+, 89.4 ± 0.3; Li^{++}, 10.6 ± 0.3; Li^{+++}, 0.052 ± 0.005. From the comparison of the recoil spectra for variously charged ions, an estimate was obtained of the role that kinetic energy plays in electron shake-off. This mode of excitation seems to account for about 4% of the total Li^{++} found and about $\frac{1}{3}$ of

the Li^{+++}. The results of the experiment are compared with theoretical calculations and are found to be in good agreement.

B3. Lifetime and *g* Factor of the First Excited State in Fe^{56}. F. R. METZGER,* *Bartol Research Foundation.*—With the gamma rays from a gaseous source of Co^{56} as the exciting radiation, resonance fluorescence from the first excited state of Fe^{56} has been observed. From a study of the self-absorption of the resonance radiation, a width $\Gamma=(6.4\pm1)\times10^{-5}$ ev was obtained. Making use of the large magnetic field at the position of the iron nuclei,[1] an attempt has been made to observe the rotation of the radiation pattern when the iron scatterer is placed in an external field which is perpendicular to the plane of the incident and the resonantly scattered gamma rays. The spin sequence 0–2–0 which characterizes the resonance scattering from the 2+ level in Fe^{56} gives rise to a very anisotropic radiation pattern and thus provides a high sensitivity of the counting rate to rotation. Together with the large magnetic field this makes it feasible to observe the minute Larmor precession of the excited Fe^{56} nuclei during the lifetime of 10^{-11} sec. Preliminary experiments indicate a positive magnetic moment for the first excited state of Fe^{56}, the *g* factor being $g\approx+0.5$.

* Assisted by the Office of Naval Research.
[1] S. S. Hanna, J. Heberle, G. J. Perlow, R. S. Preston, and D. H. Vincent, Phys. Rev. Letters 4, 513 (1960).

B4. Superallowed β^+ Decay of K^{38m}, Sc^{42}, Ti^{43}, and the Lowest $T=0$ Level in Sc^{42}. HORST JUNG AND JOACHIM JÄNECKE,* *Max-Planck-Institut fur Kernphysik, Heidelberg* (introduced by W. C. Parkinson).—The shortlived β^+ activities have been produced by α,n reactions with the Heidelberg cyclotron and measured with a scintillation detector. The maximum β^+ energies of 5.00±0.10 Mev (K^{38m}), 5.32±0.15 Mev (Sc^{42}), and 5.81±0.20 Mev (Ti^{43}) are in agreement with the predictions of a semiempirical formula[1] and with the known K^{38m} values. The measured half-lives agree with the known half-lives and the ft values of K^{38m} and Sc^{42} agree with the ft value of O^{14}. From the existence of the superallowed decay of Sc^{42}, it follows that there is isomerism and/or inversion of the lowest $T=0$ and $T=1$ states. In a search for a long-lived Sc^{42} activity, natural and enriched K compounds were bombarded with α particles up to 43 Mev. A weak activity of about 14 d half-life was found,[2] but this could be interpreted as P^{32}, produced from Cl^{35} only with high energy α particles.[3] Since no isomerism in Sc^{42} could be found, it is probable that the lowest $T=0$ and $T=1$ levels are inverted as in Cl^{34}.

* Present address: The University of Michigan.
[1] J. Jänecke, Zt. Physik 160, 171 (1960).
[2] H. Walke, Phys. Rev. 57, 163 (1940).
[3] *cf.* N. T. Porile, Bull. Am. Phys. Soc. Ser. II, 5, 405 (1960).

B5. Decay of As^{74}. E. EICHLER, R. L. ROBINSON, G. D. O'KELLEY, AND NOAH R. JOHNSON, *Oak Ridge National Laboratory.**—New light has been shed on the level structure of Ge^{74} by studying the radiations from As^{74}. After subtraction of the positron annihilation-in-flight continuum from the singles spectrum, the following γ ray peaks (and relative intensities) were resolved: 0.60 (100), 0.635 (30), 1.20 (0.4), 1.6 (0.02), 2.18 (0.04), and 2.53 (0.01) Mev.[1] By gating on the 0.60-Mev γ ray, coincidence peaks were extracted from the continuum at 0.60, 0.70, 0.88, 0.99, 1.11, and 1.59 Mev. A measurement of the directional correlation of the 0.60–0.60 Mev cascade yielded coefficients $A_2=-0.248\pm0.044$ and $A_4=0.251\pm0.070$, which are consistent with a 2–2–0 spin sequence and a value of approximately 3 for δ, the mixing coefficient, which agrees with the Davidov-Filippov[2] prediction of 2.7. These data and those obtained from a study of the decay of Ga^{74} lead to energy levels in Ge^{74} at 0.598 (2^+), 1.20 (2^+), 1.47 (4^+), 1.71, 2.18, 2.53, 2.95, 3.05, 3.17, 3.33, 3.41, 3.57, and 3.83 Mev. A new value, 18.0±0.2 days, was obtained for the As^{74} half-life.

* Operated by Union Carbide Corporation for the U. S. Atomic Energy Commission.
[1] *cf.* Nuclear Data Sheets for results of other workers.
[2] A. S. Davidov and G. F. Filippov, Nuclear Phys. 8, 237 (1959).

B6. Positron Decay of Y^{88}.† J. I. RHODE,* O. E. JOHNSON, AND W. G. SMITH, *Purdue University.*—The weak (≈0.2%) positron mode of decay of Y^{88} was studied using a 4π β ray scintillation spectrometer which recorded only those positrons in coincidence with the simultaneous detection of two annihilation quanta and a 1.84-Mev γ ray. The Fermi-Kurie plot constructed from the experimental positron distribution is linear above 280 kev, and the linear extrapolation of a straight line least-squares fitted to the data above 280 kev yields an end-point energy of (766±10)kev. This positron transition is to the 2^+, first excited state of Sr^{88} at 1.84 Mev. The positron spectrum does not show the once forbidden unique shape that would be expected if the previous asignment of 4^- for the Y^{88} ground state was correct. Below 280 kev the Fermi-Kurie plot deviates from the extrapolated striaght line in a manner which could indicate the presence of other weak positron transitions. The results of various coincidence studies using the β and γ radiations associated with the decay of Y^{88} will be presented. The bearing of these measurements on the interpretation of the low energy portion of the positron distribution and the Y^{88} decay scheme will be discussed.

† Supported in part by U. S. Atomic Energy Commission.
* National Science Foundation Predoctoral Fellow.

B7. Y^{88}-Sr^{88} Mass Difference.* S. M. SHAFROTH, *Bartol Research Foundation.*—In order to investigate a reported[1] 200-kev discrepancy in the Y^{88}-Sr^{88} mass difference, depending on whether it is obtained from Y^{88} positron decay[2] or from the $Sr^{88}(p,n)Y^{88}$ threshold, we have remeasured the latter quantity (4454±8 kev) as well as the $Sr^{88}(p,n)Y^{88*}$ (394 kev γ) threshold (4848±6 kev). The 394-kev γ threshold could in principle be located to better than 1 kev since the γ yield $\sim(E_p-E_{Th})^{\frac{1}{2}}$ over an extended range of E_p. The (p,n) threshold gives Y^{88}-$Sr^{88}=3621\pm8$ kev and the (p,n,γ) threshold combined with the measured γ energy (394±2 kev) gives 3617±6 kev. These results are in essential agreement with Nelson *et al.*[1] and in disagreement with Ramaswamy and Jastram,[2] whose positron end point energy leads to Y^{88}-$Sr^{88}=3422\pm31$ kev. A preliminary search using a natural strontium target reveals no evidence for a 200-kev γ at $E_p<4848$ kev or for an additional neutron group at $E_p<4454$ kev such as might be expected from positron decay experiments.[2] Thus this experiment gives no evidence for new levels in Y^{88} or Sr^{88}. Therefore we feel that the positron decay should be studied further.

* Assisted by the U. S. Atomic Energy Commission.
[1] J. W. Nelson, H. S. Adams, R. H. Davis, J. D. Fox, N. P. Heydenburg, H. S. Plendl, R. K. Sheline, and G. M. Temmer, Bull. Am. Phys. Soc. 5, 424 (1960).
[2] M. K. Ramaswamy and P. S. Jastram, Nuclear Phys. 19, 243.

B8. 3.14 Hr Isomeric Level in Y^{90}.† J. E. CLINE, R. L. HEATH, C. W. REICH, AND E. H. TURK, *Phillips Petroleum Company.*—A previously unreported 3.14 hr isomeric activity has been produced in Y^{90} by thermal neutron irradiation of Y^{89}. The decay of the isomeric level is characterized by the emission of two cascade γ rays of 0.482 and 0.203 Mev. Conversion coefficient measurements indicated that the isomeric level at 0.685 Mev decays by *M*4 or *E*5 radiation to an intermediate level at 0.203 Mev followed by a predominantly *M*1 transition to the ground state of Y^{90}. Gamma-gamma directional correlation measurements and internal conversion measurements indicate that the level at 0.203 Mev has spin and parity of 3^- and that the level at 0.685 Mev has spin 7 or 8 and has even parity. Shell model configurations have been tentatively assigned to these levels. These assignments will be

compared to those proposed by Bartholomew[1] from neutron capture γ-ray studies.

† Work performed under the auspices of the U. S. Atomic Energy Commission.
[1] G. A. Bartholomew, P. J. Campion, J. W. Knowles, and G. Manning, Nuclear Phys. 10, 590 (1959).

B9. Decay of Y^{92}.* M. E. BUNKER, J. D. KNIGHT, J. W. STARNER, AND B. J. DROPESKY, *Los Alamos Scientific Laboratory.*—The decay of the fission product Y^{92} (3.53 hr) has been studied with scintillation spectrometers and a solenoidal β spectrometer (0.8% momentum resolution). The observed γ rays have the following energies (Mev) and relative intensities: 0.448 (17), 0.49 (3.7), 0.56 (23), 0.84 (5.2), 0.90 (6.2), 0.932 (100), 1.12 (1.8), 1.39 (34), 1.83 (2.9), and 2.06 (0.4). These data, along with results of our γ-γ coincidence and angular correlation measurements, indicate the existence of the following levels in Zr^{92} (energies in Mev): 0.932 (2^+), 1.380 (0^+), 1.49 (4^+), 1.83 (2^+), 2.05 (2^+), and 2.32 (3^-). The spins of the 1.380-, 1.49-, and 2.32-Mev levels were determined through study of the angular correlations of the (0.448–0.932)-, (0.56–0.932)-, and (1.39–0.932)-Mev γ-γ cascades, respectively. The other spins were assigned primarily through selection-rule arguments. The 3.64-Mev ground-state β transition has an intensity of 86% (log ft=7.8) and a first-forbidden unique shape, establishing the spin and parity of Y^{92} as 2^-. There are direct β transitions to each of the Zr^{92} excited states given above. Except for the transition to the 3^- state (log ft=7.1), the corresponding log ft values are all ~8.5.

* Work performed under the auspices of the U. S. Atomic Energy Commission.

B10. A Long-Lived Isomer of Rh^{103}.* M. I. KALKSTEIN, *Air Force Cambridge Research Laboratories.*—A long-lived tail to the decay curve of 210-day Rh^{103} K x rays has been observed in rhodium samples obtained from high altitude collections of nuclear weapons debris. Decay of a standard, prepared prior to the 1958 weapons production, has been followed for over 2 yr and indicates a half-life of roughly 2.5 yr. There is little or no evidence for a long-lived component in the decay curve of the β radiation of Rh^{103}. This is taken as evidence that the decay of the long-lived isomer is predominantly by electron capture with very little branching by β, positron, or low energy isomeric transitions. Gamma-ray spectra measurements exhibit a longer-lived component as has also been observed by McGowan and Stelson.[1] In addition, a comparison of the γ-ray spectrum of rhodium activity produced by the reaction of a low flux of 14 Mev neutrons on rhodium with that produced by a large nuclear weapon reaction on rhodium, gives convincing evidence for the mass assignment of the 5-yr Rh^{101m} isomer.[2]

† Supported in part by the U. S. Atomic Energy Commission.
[1] F. K. McGowan and P. H. Stelson, Bull. Am. Phys. Soc. 5, 448 (1960).
[2] D. J. Farmer, Phys. Rev. 99, 659A (1955); and Kazuo Hisatake, James T. Jones, and J. D. Kurbatov, Bull. Am. Phys. Soc. 1, 217 (1956).

B11. M3 Isomeric Transition in Sn^{113}.* MARCEL SCHMORAK, GUY T. EMERY, AND GERTRUDE SCHARFF-GOLDHABER, *Brookhaven National Laboratory.*—Selinov and Chikladze[1] discovered Sn^{113m}(27±3 min) and concluded that the 79.3 kev isomeric transition is $M4$ from the K/L ratio. We have observed a 20±1 min activity in tin enriched in Sn^{112} irradiated with slow neutrons. The scintillation spectrum showed K x rays and a single γ ray of 79±3 kev. The K conversion coefficient (ϵ_K=95) and the half-life show that the isomeric transition is $M3$. A (12±3)% K electron capture branch from the isomeric level was found, and an upper limit of 10^{-4} was placed on the ratio of positron emission to electron capture. The latter value limits the decay energy to <1.15 Mev and since it is known from previous work to be >0.76 Mev, a log ft value of 4.3±0.2 for the decay from the isomeric state to the $(9/2)^+$ ground state of In^{113} results. The proposed spins and parities are thus $\frac{7}{2}^+$ for Sn^{113m} and $\frac{1}{2}^+$ for Sn^{113}. These results will be compared with the theoretical predictions of Kisslinger and Sörensen.

† Work performed under the auspices of the U. S. Atomic Energy Commission.
[1] I. P. Selinov and V. L. Chikladze, Zhur. Eksp. i Teoret. Fiz. 38, 1012 (1960) [English translation: Soviet Phys.—JETP 11, 728 (1960)].

B12. Lifetime of the First Excited State in Sn^{117}.* ANGELA C. LI,† MARCEL SCHMORAK, AND A. SCHWARZSCHILD, *Brookhaven National Laboratory.*—The half-life of the 161-kev transition in Sn^{117} was measured by the delayed coincidence method. The 14-day Sn^{117m} was produced by neutron bombardment of enriched Sn^{116}. Conversion-electron—conversion electron coincidences were observed using diphenyl-acetylene scintillators. A 6BN6 time to pulse height converter was used to determine the lifetime. The "prompt" time distribution exhibits exponential slopes which decrease a factor of 2 in 1.5×10^{-10} sec. The slopes observed with the Sn source yield $\tau_{\frac{1}{2}}=(3.1\pm0.3)\times10^{-10}$ sec for the first excited state. Since the energies of the conversion electrons from both members of the cascade are almost identical, the coincidences exhibit the lifetime on both sides of the time spectrum. Time spectra observed in electron-γ ray coincidences resulted in the same lifetime. It is known that the transition is essentially pure $M1$ and is l forbidden, occurring between the $d\frac{3}{2}$ and $s\frac{1}{2}$ states. The measured lifetime is 60 times slower than single particle speed. It is interesting to compare this with the similar 24-kev transition in Sn^{119} which is retarded by a factor of 80±20.

* Work performed under the auspices of the U. S. Atomic Energy Commission.
† Graduate student—New York University.

MONDAY MORNING AT 10:00

Franklin Room

(R. M. BOZORTH presiding)

BA1. On the Indirect Exchange Model for Ferromagnetic Metals. S. H. LIU, *IBM Research Laboratory.*—The ferromagnetic properties of rare earth metals and their alloys are discussed in terms of the indirect exchange model. It is shown that in calculating the Curie temperatures of these metals the simple theory of Fröhlich and Nabarro and Zener is applicable. The second-order energy terms calculated by Ruderman and Kittel, Kasuya, and Yosida are important in discussing the low temperature properties. Some numerical results are obtained which are in good agreement with the experiments.

BA2. Fe^{57} Mossbauer Effect in Cu-Ni Alloys. G. K. WERTHEIM AND J. H. WERNICK, *Bell Telephone Laboratories.*—The Mossbauer effect of Fe^{57} produced by the decay of Co^{57} diffused into Cu-Ni alloys covering the range of composition from pure Ni to pure Cu has been observed with an absorber of $K_4Fe^{57}(CN)_6\cdot3H_2O$. Measurements were made at 4°K to determine the isomer shift, the magnetic field at the Fe^{57} nucleus, and the linewidth. The isomer shift increases slowly in the ferromagnetic range (0 to 60% Cu) and considerably faster in the paramagnetic range (60 to 100% Cu). This is

consistent with an interpretation relating the isomer shift to the location of the Fermi level through its effect on the filling of the 3*d* shell of the iron. The magnitude of the shift between Cu and Ni is small, however, leading to the conclusion that the iron *d* shell, unlike the *d* band in the alloy, is filled only to a very small extent by the Cu *s* electrons. The field at the iron nucleus decreases from 2.82×10^5 oe in pure nickel to 2.46×10^5 oe in a 45% Cu alloy. In the same range of composition the magnetization in the alloy decreases by 75%. No hfs was observed in a 55% alloy. The origin of the probably negative hyperfine field at the Fe nucleus is the exchange polarization of inner *s* electrons by the ferromagnetically coupled *d* spins. An additional contribution to the field results from the exchange interaction between conduction *s* electrons and *d* electrons.

BA3. A Study by the Mössbauer Method of the hfs Splitting of Au^{197} Alloyed in Cobalt and Nickel. L. D. ROBERTS, *Oak Ridge National Laboratory*, AND J. O. THOMSON, *University of Tennessee*.—Au^{197} has a $\frac{3}{2}^+$ ground state and a $\frac{1}{2}^+$ first excited state at 77 kev. Although gold is normally nonmagnetic, when it is alloyed in iron it partakes of the ferromagnetism of the latter through a magnetic polarization process.[1] This polarization produces a hfs splitting of the above ground and excited states of gold. The previous work[1] on iron alloys has been extended to one at.% gold in cobalt and to one at.% Au in nickel. The measurements were made at helium temperatures by the Mössbauer method using a Pt^{197} metal source and either of the above Au-Co or the Au-Ni alloys as absorber. In the case of Co, two lines are observed, each being an unresolved triplet. The separation of these lines is approximately 0.80 cm/sec with a line width of about 0.6 cm/sec and a chemical shift of about 0.4 cm/sec. For the excited nuclear state, these measurements give $|\mu_n H_0| = 3.3\times10^8$. For the Ni alloy, only one line is observed. Its width is about 0.6 cm/sec, the chemical shift is about 0.4 cm/sec and $\mu_n H_0 \sim 0$.

[1] L. D. Roberts and J. O. Thomson, Bull. Am. Phys. Soc. 6, 75 (1961).

BA4. Magnetic and Crystallographic Study of Neodymium-Substituted Yttrium and Gadolinium Iron Garnets. S. GELLER, H. J. WILLIAMS, AND R. C. SHERWOOD, *Bell Telephone Laboratories*.—A study of the garnet systems $\{R_{3-x}Nd_x\}Fe_2Fe_3O_{12}$, R=Y or Gd, indicates, as expected, that the moment contributed by the Nd^{3+} ion adds to that of the resultant contributed by the iron, sublattices similar to results of earlier work by others on intermetallic systems involving rare earths and also on Nd- and Pr-substituted yttrium iron garnets. This has been explained on the basis that in *L-S* ions Nd and Pr, **J** is generally directed oppositely to **S**. If the 0°K moments of the Gd^{3+} and Fe^{3+} ions are taken as 7.0 and 5.0 μ_B when R=Gd and 1.0 μ_B when R=Y. Also a null method involving the garnet system $\{Gd_{3-x}Y_xNd\}Fe_2Fe_3O_{12}$ gives a 0°K moment of 1.2 μ_B for the Nd^{3+} ion. The possible causes of the differences will be discussed. Maxima have been found for amounts of Nd substitution in Y, Gd, and Sm iron garnets. These data, in turn, lead to prediction regarding maximum substitution of Nd in most other rare earth iron garnets and also predict a maximum lattice constant close to 12.538 A for any iron garnet.

BA5. Magnetism of Dilute Solutions of Iron-Group Elements in Platinum Metals. R. M. BOZORTH, D. D. DAVIS, AND J. H. WERNICK, *Bell Telephone Laboratories*.—Ferromagnetic Curie points θ and ferromagnetic moments per iron-group atom n_A have been derived from measurements at low temperatures and high fields (to 1.3°K, 12 koe). The lowest concentration of Ni in Pd to support ferromagnetism is about 2 at.%; the limiting concentration of Co in Pd is below 0.1 at.%, when the average distance distance between Co atoms is about 10 at. diam.[1] Values of θ, n_A, and the limiting concentration for ferromagnetism are sensitive to both solute and solvent atoms, for they depend on the atomic moments of each kind of atom and on the exchange interaction between atoms of one kind in a medium of another. The values of θ and n_A in dilute Co-Pd alloys[1] are quickly reduced by substitution of Rh or Ag for some of the Pd. When Cu replaces Pd in alloys containing 1 at.% Co the ferromagnetic moment of the Co-Pd complex is quickly reduced from its maximum of about 9 Bohr magnetons per cobalt atom and goes to zero at about 40 at.% Cu. Dilute Co-Rh, Ni-Rh, and Ni-Pt alloys are not ferromagnetic; even $Ni_{0.4}Pt_{0.6}$ is paramagnetic at 1.3°K.

[1] R. M. Bozorth, Wolff, D. D. Davis, Compton, and J. H. Wernick, Phys. Rev. (to be published).

BA6. Magnetization of Nickel Single Crystals. ALVIN W. JENKINS, JR., AND LAMBROS TTERLIKKIS, *University of Denver*.—A calculation of the magnetization curves of nickel single crystals is made by the method of Lawton and Steward[1] for arbitrary orientation of the crystal in the field. The anisotropy coefficients are calculated from experimental curves with the applied field in symmetry directions, and it is found that only K_1 can be determined reliably with the data used. The calculated off-axis curves agree well with experimental results. A correcting field determined from the easy-axis magnetization curve is utilized to compensate for internal strain effects. The relation between the calculated field minus the observed field, and the easy-axis field suggests a possible method for measuring internal strain energy in ferromagnetic crystals.

[1] H. Lawton and K. H. Steward, Proc. Roy. Soc. (London) A193, 72 (1948).

BA7. Antiferromagnetic Resonance in FeF_2 at Far-Infrared Frequencies.* R. C. OHLMANN,† *University of California, Berkeley*.—Antiferromagnetic resonance in single crystals of FeF_2 was observed between 1.5° and 66°K (T_N=78.4°K), in the frequency region from 25 cm^{-1} to 100 cm^{-1}. The resonance frequency at $T\approx0$ was found to be $\bar{\nu}(0)=52.7\pm0.2$ cm^{-1}. From this frequency the uniaxial anisotropy constant at absolute zero, $K(0)$, was inferred to be 1.1×10^8 ergs/cm^3 (40 cm^{-1}/atom). Measurements of the splitting of the line caused by an external magnetic field gave $g_{||}=2.25\pm0.05$. The anisotropy energy in FeF_2, being primarily due to the crystalline field-spin-orbit interaction, may be described by a term $\Sigma_i DS_{iz}^2$ in the Hamiltonian. By including this interaction in the molecular-field treatment, we have determined $D=-9\pm2$ cm^{-1} and have calculated the temperature dependences of the sublattice magnetization, the anisotropy constant, the resonance frequency, and the line width, the last two being compared with the experimental results and found to be in reasonable agreement. The line widths were found to follow a T^4 law above 15°K.

* Supported in part by the National Science Foundation, the Alfred P. Sloan Foundation, and the Office of Naval Research.

† Present address: Westinghouse Research Laboratories, Pittsburgh, Pennsylvania.

BA8. Several Soluble One-Dimensional Antiferromagnets. E. LIEB, T. SCHULTZ, AND D. MATTIS, *IBM Research Center*.—The ground state properties and thermodynamics of several one-dimensional quantum mechanical antiferromagnetic chains with nearest neighbor interactions have been found exactly. Two of the models have the Hamiltonians

$$H_1 = S_1\cdot S_2 + S_2^z S_3^z + S_3\cdot S_4 + S_4^z S_5^z + \cdots;$$

and

$$H_2 = \sum_{j=1}^{N} (S_j\cdot S_{j+1} - S_j^z S_{j+1}^z).$$

H_1 and H_2 have no long-range order in the ground state, but some anisotropic modifications of them do have order. Aside from the inherent mathematical interest of such soluble models, the physical properties are also interesting; and we find that the thermodynamics and order can depend sensitively on the

model chosen and that one cannot guess these properties *a priori*.

BA9. Ferromagnetic Nucleation Sources on Iron Whiskers. R. W. DE BLOIS, *General Electric Research Laboratory.*—Previous experimental work has established that the near perfection of some selected iron whiskers brings the axial magnetic field required to nucleate the reversal of magnetization close to the theoretical coercive force limit of $2K/M_s$ (560 oe at 20°C).[1] Further experiments now show an approximately constant shift of the nucleation-field contour along an iron whisker with change in temperature, increases in nucleation field of several hundred oersteds along the lengths and at the tips of several iron whiskers following electropolishing, and a correlation between observed microscopic surface imperfections and regions of nucleation-field minima. These results support current ideas that abrupt surface contour variations are primarily responsible for reducing the observed nucleation fields for iron whiskers to below the ideal value.

[1] R. W. De Blois and C. P. Bean, J. Appl. Phys. **30**, 225S (1959).

BA10. Polarization of γ Rays from Co^{56} Nuclei Oriented in Cerium Zinc Nitrate.* R. C. SAPP, D. K. BRICE, AND W. W. STROHM, JR., *University of Kansas.*—A model for the influence of magnetic interaction on nuclear orientation of cobalt isotopes in cerium double nitrate has recently been proposed[1]; it involves multiaxial spin alignments of the cobalt nuclei as a result of interaction with the cerium ions through a dipolar "internal field." Quantitative determination of the degree of γ ray polarization affords an independent check on this model below 7×10^{-2}°K. Such measurements have been undertaken by utilizing the polarization dependence of the Compton scattering cross section. Measurement of the degree of polarization is strongly dependent on correctly assessing the effects of prompt background and finite geometry of the polarimeter, and the building of adequate statistics. If these factors are properly evaluated, it appears that the degree of linear polarization p_1 is consistent with the internal field model.

* Assisted by the National Science Foundation and the Office of Naval Research.

[1] M. W. Levi, R. C. Sapp, and J. W. Culvahouse, Phys. Rev. **121**, 538 (1961).

MONDAY MORNING AT 10:30

Sheraton Hall

(CONYERS HERRING presiding)

Invited Papers

C1. Theoretical Energy Band Structures for the Noble Metals. BENJAMIN SEGALL, *General Electric Research Laboratory.* (30 min.)

C2. Cyclotron Resonance in Metals. A. F. KIP, *University of California, Berkeley.* (40 min.)

MONDAY MORNING AT 10:30

Cotillion Room, North

(D. R. INGLIS presiding)

Invited Papers

CA1. Some Effects of Pair Correlation for Deformed Nuclei. STEVEN WEINBERG, *University of California, Berkeley.* (30 min.)

CA2. Muons and Electrons. S. G. NILSSON, *University of California, Berkeley.* (30 min.)

MONDAY MORNING AT 10:00

Adams-Hamilton Room

(R. F. CHRISTY presiding)

Theoretical Physics, I: Nuclear Structure, I

CB1. Approximate Total Nuclear Binding Energy.* KIUCK LEE, *Marquette University.*—The usual method of evaluating the approximate total nuclear binding energy from the single particle energies is modified to account for the empirical total binding energy. Namely, $\frac{1}{2}\sum_i[\langle V_i\rangle - e_i]$ is subtracted, instead of $\frac{1}{2}\sum_i\langle V_i\rangle$, from the sum of the single particle energy e_i to avoid counting the two body interactions twice, which is equivalent to the introduction of the velocity-dependent potential. The total energies of typical nuclei estimated from this equation, using a realistic potential and the resulting eigenfunctions and eigenvalues determined by Green[1] without considering the Coulomb effect, is in good agreement with those values obtained from the Weiszaecker's empirical formula. Details of the calculation will be discussed.

* Supported by the National Science Foundation.

[1] A. E. S. Green, Phys. Rev. **102**, 1325 (1956).

CB2. Pear-Shape Nuclear Deformation.* RICHARD A. HAERTLE AND KIUCK LEE, *Marquette University.*—Nilsson's calculation[1] is extended to evaluate exact single-particle levels

for a pear-shaped nuclear deformation. The transform of the potential used by Lee and Inglis[2] is considered for simplicity. The exact eigenvalues are obtained with the help of IBM 7070, using the harmonic oscillator representation after Nilsson. Preliminary results show considerable depression in some single-particle levels for large deformation, indicating the possible stability of such deformation in heavy nuclei. Details of the calculation will be presented.

* Supported by the National Science Foundation.
[1] S. A. Nilsson, Kgl. Danske Videnskabe Selskab, Mat. Fys. Medd. **29**, No. 16 (1955).
[2] Kiuck Lee and D. R. Inglis, Phys. Rev. **108**, 774 (1957).

CB3. S-State Interaction and Nuclear Properties.* S. A. MOSZKOWSKI, *University of California, Los Angeles.*—The properties of nuclear matter are being studied assuming a nonlocal S state two-body interaction of the form (in momentum space) $V(k,k') = -U_1 g_1(k) g_1(k') + U_2 g_2(k) g_2(k')$, where $g_1(k) = \exp(-\lambda k^2)$, $g_2(k) = k^2 g_1(k)$. The second term simulates a short-range repulsion. However, the interaction is nonsingular, so that a perturbation expansion converges rapidly. By suitable choice of parameters, it is possible to approximately fit low-energy two-body scattering data and also the binding energy and equilibrium density of nuclear matter. It would seem that any satisfactory representation of the nucleon-nucleon interaction should fit at least *these* quantities. In this sense, the above interaction may be more realistic than conventional local interactions used in many shell model calculations to date, which fit low-energy two-body data, but not the properties of nuclear matter. Of course, the S state interaction cannot fit high-energy data or polarizations, but perhaps this might not be too important for low-energy nuclear properties. We have used this interaction for a calculation of other nuclear properties, e.g., symmetry energy, surface energy, and surface thickness and obtain reasonable agreement with empirical values.

* This work was supported in part by the Office of Ordnance Research.

CB4. Lowest State of a Nucleus with a Specified Angular Momentum According to the Fermi Gas Model. DANIEL SPERBER, *Armour Research Foundation.*—The energy of the lowest state of a nucleus with a specified angular momentum is calculated on the basis of the Fermi gas model. It is assumed that all observable quantities are sums of contributions from single particles. The total energy is minimized, keeping in mind the subsidiary conditions: (a) specified number of nucleons and (b) specified angular momentum. As a result of the variational calculation, the following information about the lowest state with a specified angular momentum was obtained: (i) the shape of the occupied region in momentum space for each point in coordinate space, (ii) the shape of the deformed nucleus, and (iii) an effective moment of inertia for the rotational motion. Two potentials were used: a square well potential with a supplementary surface-tension energy proportional to the surface area of this potential well, and the individual nucleon moving in a harmonic oscillator well.

CB5. Nuclear Many-Body Problem.* FRANZ MOHLING, *Cornell University.*—The methods of quantum statistics previously developed by the author have been applied to the determination of properties of the ground state of nuclear matter. An expansion in powers of the pair function of quantum statistics is made and expressions are derived for the momentum distribution, pair correlation function, ground-state energy, and effective single-particle energies. The leading terms of these expressions can be interpreted in terms of an effective two-body potential for nuclear matter. A model of nuclear matter which consists of weakly interacting quasi-particles, whose energies are the effective single-particle energies, is therefore suggested. The proposed expansion is likely to converge rapidly, since by explicit computation for an S wave (square-well+hard-core) nuclear interaction, the two-pair term for the ground-state energy is shown to be $\lesssim 10\%$ of the one-pair term. The analysis is limited to the region of nuclear densities for which the thermodynamic potential is negative.

* Supported in part by joint contract of Office of Naval Research and U. S. Atomic Energy Commission.

CB6. Refinement of α-Decay Branching Relations for Odd-Mass Spheroidal Nuclei.* JOHN O. RASMUSSEN, *University of California, Berkeley.*—The branching ratio relationships proposed by Bohr, Fröman, and Mottelson[1] have been applied with considerable success to the $L=2$ groups of favored α decay of odd-A nuclei. They would be exact in the limit either of infinite nuclear moment of inertia or zero electric quadrupole moment. Two kinds of corrections are made to the BFM predictions in this work. First, there is a small correction arising from Coriolis mixing. Second, there are quadrupole coupling effects. We treat the quadrupole effects approximately by calculating the quadrupole coupling energy at the classical turning point of each partial wave and assume this energy to have an exponential effect on the intensity. For U^{233} the BFM theory predicts alpha intensities of 83.7, 14.6, 2.29, 0.094, and 0.0081%, respectively, to the first five states of the ground rotational band. After our corrections the predictions become, for $l=2$ and 4 in phase, 83.5, 14.6, 1.88, 0.092, 0.0043% and, for $l=2$ and 4 out of phase, 84.4, 14.1, 1.55, 0.051, and 0.0058%.

* Work under auspices of the U. S. Atomic Energy Commission.
[1] Bohr, Fröman, and Mottelson, Kgl. Danske Videnskab. Selskab, Mat. Fys. Medd. **29**, No. 10 (1955).

CB7. Magnetic Octupole Moments of Deformed Nuclei.* S. A. WILLIAMS AND J. P. DAVIDSON, *Rensselaer Polytechnic Institute.*—The magnetic octupole moment of an odd-A nucleus described by the axially symmetric collective model has been calculated. The results of this calculation have been applied to those nuclei whose energy spacings are reasonably well described by this model as well as to the seven nuclei whose octupole moments have been measured, although the latter lie well outside of what is normally considered to be the region of applicability of the model. The parameters involved have been determined by fitting the measured values of the lower moments, transition probabilities and energy spacings. The assumption has been made that the orbital gyromagnetic ratio g_l for the odd particle is that of a free particle. Then, from the total gyromagnetic ratio of the particle, which is determined from the magnetic dipole moment and $M1$ transition probabilities, the spin gyromagnetic ratio g_s was determined. A table comparing the theoretical results with the seven experimental results will be shown, as well as a predictive table of magnetic octupole moments for other nuclei.

* Supported by the National Science Foundation.

CB8. Octupole Vibrations of Spheroidal Even-Even Nuclei.* P. O. LIPAS† AND J. P. DAVIDSON, *Rensselaer Polytechnic Institute.*—The systematically occurring $K=0-$ and $K=2-$ bands observed in deformed even-even nuclei are explained by allowing the nuclear surface to have two octupole degrees of freedom, corresponding to the spherical harmonics Y_{30} and $Y_{3\pm3}$, in addition to the usual β and γ quadrupole degrees of freedom. The appropriate hydrodynamic moments of inertia are used, and the Schrödinger equation is solved approximately for small oscillations about a spherioidal equilibrium shape. In addition to the usual β and γ vibrations one thus finds a "b vibrational band" ($K=0-$, $I=1, 2, 5, \cdots$) and a "g vibrational band" ($K=2-$, $I=2, 3, 4, \cdots$), in qualitative agreement with experiment. Not knowing the mass and elastic parameters associated with the various degrees of freedom, one cannot make quantitative predictions of vibrational band heads. When β and b bands are observed in the same nucleus, in

most cases they are found to lie within 300 kev of each other. Likewise γ and g bands are separated by no more than 300 kev in the strongly deformed regions ($94 \lesssim N \lesssim 110$ and $N \gtrsim 138$).

* Supported in part by the National Science Foundation.
† An International Atomic Energy Agency Fellow, 1959–1960.

CB9. Rotor-Particle Model for Odd-A Nuclei.* B. E. CHI AND J. P. DAVIDSON, *Rensselaer Polytechnic Institute.*—Energy levels of a single nucleon coupled to an even-even core are obtained by diagonalizing the collective Hamiltonain given by $H=\hbar\omega_0(h_r+h_p)$, where

$$h_r=P\kappa\Sigma(I_\nu-j_\nu)^2/\sin^2(\gamma-2\pi\nu/3),$$

$$h_p=N+\tfrac{3}{2}-\beta\cos\gamma r^2Y_2^0(\vartheta,\varphi)-2^{-\frac{1}{2}}\beta\sin\gamma[Y_2^{-2}(\vartheta,\varphi)+Y_2^{-2}(\vartheta,\varphi)]-2\kappa\mathbf{l}\cdot\mathbf{s}.$$

The symmetrized spherical top-spherical oscillator states $|NIMKj\Omega\rangle$ are used as a basis, N being the principal quantum number of the oscillator. Elements connecting different values of N are ignored. The parameter κ is that of Nilsson's,[1] β and γ are the usual deformation parameters, and P is a mass parameter for the rotor. The energy level structure, static moments, and reduced matrix elements have been calculated as a function of P, β, and γ. Results for odd-A nuclei in the region $A \approx 25$ will be discussed.

* Supported in part by the National Science Foundation.
[1] S. G. Nilsson, Dan. Mat. Fys. Medd. 29, 16 (1955).

CB10. Rotational Motion in a Many-Particle System. T. SASAKWA, *M.I.T.*—Based on quite orthodox quantum mechanics, it is shown that in an N-particle system we can always divide the whole motion into three parts: the center of mass motion, the rigid rotation as a whole, and the intrinsic translational motion. The resulting formulas have nice similarity with the corresponding formulas in classical mechanics. The story is quite general and may find its application to molecular physics as well as nuclear physics.

CB11. On Nuclear Forces in the Radional Field. ANATOL J. SHNEIDEROV, *Polycultural Institution of America.*—*Radion* is a subparticle 10^{-26} cm in diameter. Parallel streams of these subparticles intersect space in all directions. Such streams penetrate *macro*cosmic bodies, exerting a differential pressure J_{sf} on their structures. Gravitation force resulting from the pressure J_{sf} on such bodies is $f_g=(J_{sf}\beta^2)(q_1s_1\cdot q_2s_2)/R^2 = J_{sf}(\pi r_1^2\varphi_1\cdot\pi r_2^2\varphi_2)/R^2$ dynes. This is identical with Newton's formula, but expresses mass M as a product of its *mola* q (the sum of masses of all elementary particles in M) and *mass defect* s. Here $s=1-(\frac{3}{4})r\delta\beta+(\frac{3}{5})(r\delta\beta)^2-(\frac{1}{8})(r\delta\beta)^3+\cdots$, where r is radius δ is *molal density* $=q/(\frac{4}{3})\pi r^3$, $\beta\approx 5.31\cdot 10^{-12}$ cm²/g is radional absorption coefficient, and $J_{sf}\beta^2$ is gravitation constant. An analogous formula is derived for *micro*cosmic bodies (protons, neutrons, electrons, etc.), impervious to radions. Here $f_e=2J_s(\pm\pi r_1^2)\cdot(\pm\pi r_2^2)/R^2$ dynes, R being a distance between the bodies, and J_s the pressure of the radional field. This formula is experimentally accurate when $R\gg(r_1+r_2)$, but diverges from the inverse square law when R grows smaller. The f_e reverses its sign when R becomes commensurable with (r_1+r_2), and changes its sign again when the pair is forced still closer to each other. These two changes in sign explain the potential barrier and the Majorana-Heisenberg forces. Saturation and the Levy's force are explained.

MONDAY AFTERNOON AT 2:00

Burgundy Room

(H. A. SHUGART presiding)

Spins, II

D1. Pulse Relaxation Experiments on the Fe^{3+} Ion in $K_3[Co,Fe](CN)_6$.* T. M. BRAY, G. C. BROWN, AND A. KIEL, *The Johns Hopkins University.*—The pulse saturation decay technique was used to investigate the relaxation processes in diluted potassium ferricyanide at 8.7 kMc and at liquid helium temperatures. In general, two distinct relaxation times were observed below 3°K. The more rapid of the two relaxations we believe is due to cross-relaxation, the slower is the usual spin-lattice relaxation time. In most samples, the spin lattice relaxation time was strongly temperature dependent above 2.6°K, that is, the Raman processes dominate the direct spin-lattice relaxation and at 4.2°K, T_1 was comparable with the cross-relaxation time T_{12} ($\sim$50–200 μsec). The concentration dependence of the relaxation times was also studied in these experiments. The concentration dependence appears to be related to the presence of exchange coupling which will be briefly discussed.

* Supported by the Air Research and Development Command of the U. S. Air Force.

D2. Nuclear Resonances in TaC and NbC. LAWRENCE H. BENNETT, *National Bureau of Standards.*—The nuclear magnetic resonances of Ta^{181} in TaC powder and Nb^{93} in NbC powder have been measured at room temperature and each shows a small (about 0.1%) diamagnetic shift. Since both TaC and NbC are metallic conductors at room temperature, and NbC is considered a superconductor at helium temperatures, these negative "Knight" shifts are unusual. Diamagnetic shifts previously observed[1,2] in alloys (or intermetallic compounds) containing transition metals were of the non-transition element only. The transition element, vanadium, displayed paramagnetic shifts of the same order of magnitude as the Knight shift in metallic vanadium. The resonance results on the carbides will be discussed with relation to other physical properties of these materials and the problem of sample characterization will be considered.

[1] R. G. Shulman, B. J. Wyluda, and B. T. Matthias, Phys. Rev. Letters 1, 278 (1958).
[2] W. E. Blumberg, J. Eisinger, V. Jaccarino, and B. T. Matthias, Phys. Rev. Letters 5, 149 (1960).

D3. Linewidth Broadening of the F^{19} Nuclear Resonance in MnF_2 near the Néel Temperature. P. HELLER AND G. B. BENEDEK, *Harvard University.*—Using a system capable of temperature stabilization to within one millidegree for long periods of time, we have studied the line width of the F^{19} resonance in MnF_2 as a function of temperature near the Néel temperature T_N ($\sim$68°K). In the paramagnetic state the line broadens markedly as T_N is approached. At a given temperature, this broadening depends strongly on the direction of the applied field H_0 with respect to the crystal axes, being more marked with H_0 along the c axis than with H_0 along the a axis. We take as T_N the temperature at which the line broadens to the point of disappearance with H_0 along the

a axis. This point can be determined to within about 1 millidegree. In the temperature range $0.090°K \leq T - T_N \leq 4°K$, the line widths vs temperature can be represented by the empirical formula

$$\delta H(T) = (\delta H)_0 + k/(T - T_N),$$

where $k = 2.2$ gauss °K, $(\delta H)_0 = 24.5$ gauss for H_0 along the a axis and $k = 6.5$ gauss°K, $(\delta H)_0 = 24$ gauss for H_0 along the c axis. With H_0 along a, we have also made observations at temperatures as close as 18 millidegrees above T_N. Preliminary results indicate that the line shape changes in this region.

D4. Spin Relaxation of Optically Aligned Rubidium Vapor in Helium.* R. A. BERNHEIM, *Columbia University.*—The spin relaxation time of rubidium vapor has been measured at 50°C as a function of helium buffer gas pressure. The measurement was performed by interrupting the optical pumping radiation after the method of Franzen.[1] The vapor was contained in an uncoated 300 cc spherical bulb. The analysis of the data yields a value of 0.54 ± 0.02 cm²/sec for the diffusion coefficient of rubidium in helium gas, and $6.2 \pm 0.2 \times 10^{-24}$ cm² for the disorientation cross section for a collision between an aligned ground state rubidium atom and a helium atom.

* Supported by the U. S. Air Force Office of Scientific Research.
[1] W. Franzen, Phys. Rev. **115**, 850 (1959).

D5. Ultrasonic Excitation in Nuclear Magnetic Resonance in KI. A. H. SILVER, *Ford Motor Company.*—Changes which occur in the NMR absorption spectrum of I^{127} in KI as a function of acoustic excitation have been studied. The NMR line, observed at $\nu_0 = 5$ Mc/sec with a Pound-Watkins type detector, is inhomogeneously broadened by strain. Longitudinal acoustic waves with $\nu_A = 10$ Mc/sec are generated by an X-cut quartz transducer and propagated along a [100] direction perpendicular to H_0. This distortion of the lattice induces $\Delta m = \pm 2$ quadrupolar transitions resulting in saturation of some of the five $\Delta m = \pm 1$ magnetic dipole transitions and in enhancement of others. Because the six levels are not all equally spaced, some of the spin-spin relaxation processes are attenuated. The nuclei do not assume a Boltzmann distribution in the presence of the acoustic excitation. The change in absorption at the center of the line is a function of the satellite distribution and is observed by varying $(\nu_A - 2\nu_0)$. For $\nu_A = 2\nu_0$, the absorption is reduced to 45% of its equilibrium value in the sample studied. The effects of shear waves and of mechanical resonance will also be discussed.

D6. Nuclear Quadrupole Resonance Isotope Effect in Solid Nitrogen. T. A. SCOTT AND P. J. HAIGH, *University of Florida.*—Solid nitrogen, which at natural abundance consists of 99.6% N^{14} ($I = 1$), has been observed to exhibit a single pure quadrupole resonance due to this nucleus in the α phase below 35.5°K. The resonance frequency shows a strong temperature dependence. When the sample is enriched in N^{15} ($I = \frac{1}{2}$), the resonance of the N^{14} is split into two distinct lines. For an approximately equal isotopic mixture, the splitting is 8.2 kc at 4.2°K and decreases with increasing temperature. The observations have been interpreted in terms of a difference between the torsional oscillations of $N^{14}-N^{14}$ and $N^{14}-N^{15}$ molecules. The $N^{14}-N^{14}$ molecules should have a larger amplitude of oscillation, which according to Bayer theory would result in a smaller electric field gradient at the nuclear site and a lower quadrupole frequency.

D7. NMR Study of Dislocation Effects and Elastic Axial Compression Effects in NaI Single Crystals.* H. O. HOOPER AND P. J. BRAY, *Brown University.*—The anomalous angular distribution[1] in the intensity of the I^{127} NMR spectra of single crystals of NaI rotated about [110] and [100] type directions perpendicular to the magnetic field has been studied. This intensity anomaly due to the changing amount of first-order quadrupolar broadening of the line is attributed to oriented dislocations in these previously unstrained crystals. The full intensity of the NMR line (i.e., quadrupolar broadening approaches zero) is observed when H_0 is along a [100] type direction. Calculations have been carried out to determine the orientation of screw and edge dislocations that would give rise to such an anomaly. When H_0 is along a [100] type direction, the NaI crystals have been axially compressed in an elastic manner. As the stress was increased, the peak-to-peak height of the derivative curve of the I^{127} line was diminished by as much as 15%, while the integrated intensity is unchanged. Using this compression data, the value of the Sternheimer antishielding parameter for I^{127} in NaI has been estimated.

* Research supported by a Frederick Gardner Cottrell grant from the Research Corporation.
[1] J. F. Hon and P. J. Bray, J. Appl. Phys. **30**, 1425 (1959).

D8. The Pressure and Temperature Dependence of the Co^{59} NMR Chemical Shifts in Cobaltic Complexes. J. A. ARMSTRONG AND G. B. BENEDEK, *Harvard University.*—Accurate measurements have been made of the pressure and temperature dependences of the Co^{59} NMR chemical shifts in aqueous solutions of $K_3Co(CN)_6$, $Na_3Co(NO_2)_6$, and $Co(NH_3)_6Cl_3$, and in solutions of $Co(C_5H_7O_2)_3$ in three solvents. The pressure range was from 1–10 000 kg/cm² and the temperature range was 0–100°C. Griffith and Orgel[1] and Freeman *et al.*[2] have shown that in these complexes the chemical shift σ is determined primarily by the energy splitting (Δ) between the ground state and the first excited state of the same multiplicity. The pressure dependence of σ is interpreted in terms of the pressure dependence of Δ. Using theoretically estimated values for the compressibilities of the complex ions, the dependence of Δ on the cobalt ligand distance (R) has been obtained. If one wirites $\Delta = KR^{-n}$, it is found that $n = 4.8 \pm 1$, 12 ± 2.4, and 6.5 ± 1.3 for the first three complexes, respectively. The temperature dependence of σ can be expected to arise out of the thermal expansion of the complex and the mean squared modulation of Δ produced by the normal vibrations of the ligands. A semiquantitative calculation of both these effects has been made, giving results in satisfactory agreement with the experiments.

[1] J. S. Griffith and L. E. Orgel, Trans. Faraday Soc. **53**, 601 (1957).
[2] R. Freeman, G. R. Murray, and R. E. Richards, Proc. Roy. Soc. (London) **A242**, 455 (1957).

D9. Hyperfine Fields in $KMnF_3$ via Exchange Polarization. A. J. FREEMAN, *Ordnance Materials Research Office* AND R. E. WATSON,* *AVCO RAD.*—NMR studies in iron series fluorides have revealed large hyperfine interactions between the fluorine nuclei and the $3d$ magnetic electrons of the transition metal ions. These have been interpreted as arising from unpaired spins in the F^- orbitals. This unpairing has been thought to arise (1) because of an admixture of covalent bonding into the purely ionic configuration or (2) by the unpairing action of the Pauli principle (Pauli "distortion") which affects those fluorine orbitals which have the same spin as the cation $3d$ orbitals differently from those orbitals which have opposite spin. In either method, the unpaired s electrons produce an isotropic hyperfine interaction whereas the $2p$ electrons produce an anisotropic interaction, the degree of unpairing being determined by the squares of the overlap integrals (S^2) between the free F^- orbitals and the $3d$ electrons on the cation. We have done an exchange (or spin) polarized Hartree-Fock calculation for the F^- ion in the exchange field arising from its paramagnetic Mn^{+2} nearest neighbors (as in $KMnF_3$). Since exchange acts differently on the F^- electrons of differing spin, different radial functions are obtained for electrons of opposite spin. The isotropic hyperfine field arises from the "paired" $2s$ *and* $1s$ shells, whereas, the anisotropic field comes from the "paired" $2p$ electrons. Large deviations from the previous types of analyses have been found.

* The work of this author was supported in part by the Ordnance Materials Research Office.

D10. Paramagnetic Resonance of Ag^{2+} in Solution.* JUAN A. MCMILLAN AND BERNARD SMALLER, *Argonne National Laboratory.*—Solutions of Ag^{2+} produced by oxidation in nitric and sulphuric solutions in H_2O and D_2O were observed for paramagnetic resonance at 9 kMc/sec. At room temperature, a broad line at $g=2.133\pm0.005$ was observed. Fozen solutions, at 77°K, showed a strong symmetric g-anisotropy that permitted the resolution of the hyperfine splitting due to interaction with silver nuclei. Measurements made with natural silver gave the following results: $g_{\parallel}=2.274\pm0.001$; $g_{\perp}=2.074\pm0.001$; contact term $a=37$ gauss; dipole-dipole interaction splitting $B_{\parallel}=11$ gauss; and $B_{\perp}=-5.5$ gauss. From Polder's relations, the ^2D transitions would occur at $\Delta_{\parallel}=-53500\ c^{-1}$ and $\Delta_{\perp}=48750\ c^{-1}$. The solutions are brown, which suggests an uv absorption tail that could be compatible with these results although it seems likely that the electron hole is not localized in the paramagnetic ion. Experiments made with pure ^{107}Ag and ^{109}Ag samples exhibited a hyperfine splitting ratio of 1.11 ± 0.07, in agreement with the accepted value 1.150.

* Based on work performed under the auspices of the U. S. Atomic Energy Commission.

D11. Effect of Illumination on the Paramagnetic Resonance of Ni^{3+} in Rutile. H. J. GERRITSEN AND E. SABISKY, *RCA Laboratories.*—Electron spin resonance was observed in nickel doped rutile and ascribed to the lowest doublet of Ni^{3+}, although Ni^{+} cannot be completely ruled out. There are four ions in the unit cell, in contrast to many other ions studied in rutile. These ions are magnetically identical along the c axis with g value of 2.085. In the plane perpendicular to the c axis, the axes of the four g tensors make angles of $\pm35°$ with the crystal a axes, having values of 2.084 and 2.254. This center is observed at room temperature and below, and ascribed to Ni^{3+} at a Ti^{4+} site with one of the neighboring oxygen ions as O^{-}. If one illuminates the sample, a broad additional spectrum appears at room temperature. It narrows below 200°K, and its intensity can be made comparable to the above mentioned spectrum. The symmetry is, however, that of a Ti^{4+} site with the customary two nonequivalent ions in the unit cell. It is ascribed to the recapturing of an electron by the O^{-}. Illumination at helium temperature shows two more rather intense nickel spectra which can be ascribed speculatively to other neighboring oxygens losing electrons.

D12. A New Method of Measurement of Dielectric Constant and Loss Tangent at Microwave Range.* AKIRA OKAYA AND LEE F. BARASH, *Columbia University.*—A piece of dielectric material acts as a microwave resonator due to large reflection at the surface, if ϵ is 10 or more and the loss tangent is 0.01 or less. TiO_2 (Rutile) and some other crystals have shown good resonance characteristics in centimeter- and millimeter-wave-range. The detailed interpretation of dielectric resonator characteristics will be discussed. The temperature, frequency dependence of ϵ and $\tan\delta$, and the accurate measurement of an anisotropic ϵ will be presented.

* Work supported jointly by the U. S. Army Signal Corps, the Office of Naval Research, and the U. S. Air Force Office of Scientific Research.

Invited Paper

D13. Distribution of Charge and Magnetization in Nuclei As Seen by Extra-Nuclear Electrons. HENRY H. STROKE, *M.I.T.*

MONDAY AFTERNOON AT 2:00

Continental Room

(H. E. GOVE presiding)

Nuclear Reactions, II

DA1. Scattering of Alpha Particles by Carbon. A. J. FERGUSON AND G. J. MCCALLUM, *Chalk River Laboratories.*—Elastic and inelastic scattering of alpha particles by carbon in the energy range 6.5 Mev to 11.0 Mev has been studied using the Chalk River tandem accelerator. Both solid and gaseous targets have been used. The detectors were silicon p-n junctions having an energy resolution less than 1%. Resonances are observed at 7.05 Mev, 7.92 Mev, 8.15 Mev, 8.98 Mev, 10.22 Mev, and 11.0 Mev, the probable error of all energies being 30 kev. Below 7.5 Mev, the results are consistent with those of Bittner and Moffat.[1] Inelastic alpha particles feeding the 4.43 Mev state of C^{13} are observed and show all the above resonances excepting the 7.05 Mev one. The 7.92 Mev and 8.15 Mev resonances have the tentative assignments 0+ and 3−, respectively.

[1] J. W. Bittner and R. D. Moffat, Phys. Rev. **96**, 374 (1954).

DA2. (α,n) Thresholds on C^{12}, Si^{28}, S^{32}, and S^{34}.* J. W. NELSON, E. B. CARTER, G. E. MITCHELL, R. H. DAVIS, *Florida State University.*—Using alpha particle beams of one to six millimicroamperes from the Florida State University Tandem Van de Graaff accelerator, the following ground state neutron thresholds have been observed: C^{12} 11.484 ± 0.045, Si^{28} 10.00 ± 0.12, S^{32} 9.98 ± 0.07, S^{34} 5.37 ± 0.15 Mev. Energies of alpha particles were determined by magnetic analysis assuming the $Al(p,n)$ threshold to be 5.800 Mev. Thick targets were used for all determinations. Annihilation gamma rays from positron decay of the product nuclei were measured in the C^{13}, Si^{28}, and S^{32} experiments while a BF_3 proportional counter was used to detect neutrons from S^{34} targets. Indications for excited state thresholds have been observed in Si^{28}, S^{32}, and S^{34}. Analysis of these data in terms of known residual nucleus states will be presented.

* Supported in part by the U. S. Air Force Office of Scientific Research.

DA3. $C^{12}(p,p'\gamma_{12.8,15.1})C^{12}$ Excitation Functions between 15 and 20 Mev.* E. K. WARBURTON AND H. L. BERK, *Princeton University.*—The 90° excitation functions for the $C^{12}(p,p'\gamma)C^{12}$ reaction proceeding through the 12.8- and 15.1-Mev levels were measured for incident proton energies between about 15 and 20 Mev. The ground state gamma rays from these states were produced in a 3.4 mg/cm² polystyrene target and detected at 90° by a 5-in.×4-in. NaI(Tl) crystal. The excitation curve for the 12.8-Mev gamma ray increases rather smoothly with energy in this range, while that for the 15.1-Mev gamma ray has an apparent threshold at 16.9 Mev and resonances at 17.5, 18.1, and 19.3 Mev. The absolute energy scale is uncertain to 100–200 kev. The center-of-mass widths of these resonances are about 270, $\lesssim$200, and 250 kev, respectively. These resonances correspond to N^{13} states at 18.1, 18.7, and

19.8 Mev excitation. It is suggested that the 17.5-Mev resonance is responsible for the anomalous behavior[1] of the $C^{12}(p,p)C^{12}$ reaction in this energy region. The $C^{13}(p,\gamma)N^{13}$ 90° cross section was measured at a few proton energies.

* This work was supported by the U. S. Atomic Energy Commission and The Higgins Scientific Trust Fund.
[1] W. Daehnick, M. Garrell, R. Wood, and R. Sherr, Bull. Am. Phys. Soc. 6, 25 (1961).

DA4. (d,p) Polarization Measurements of Excited-State Reactions in C^{13}, Mg^{24}, and Ca^{40}.* W. P. JOHNSON† AND D. W. MILLER, *Indiana University.*— A proton polarimeter has been built for use in conjunction with a heavy-particle magnetic spectrometer which allows measurements to be made of the polarizations of proton groups corresponding to nearby nuclear states. The following (d,p) polarizations were measured at a deuteron energy of 10.8 Mev and a laboratory scattering angle of 12.5°, listed according to the residual nuclear state and using the Basel convention for the quantization axis $(n=k_d\times k_p)$. C^{13} ground state: -0.32 ± 0.5; C^{13} 3.09-Mev state: $+0.03\pm0.04$; Mg^{25} 3.40-Mev state: -0.05 ± 0.05; Ca^{41} 1.95-Mev state: $+0.014\pm0.043$; Ca^{41} 3.95-Mev state: -0.21 ± 0.05. The Mg result agrees within experimental errors with the polarization magnitude predicted by Martin *et al.*[1] from $(d,p\gamma)$ angular correlation measurements. If the two Ca states investigated are single-particle p-neutron states with $j=\frac{3}{2}$ and $\frac{1}{2}$, respectively, the ratio of the corresponding proton polarizations should be -0.5.[2] The experimental ratio, which is subject to large error because of the near zero result for the 1.95-Mev state, is -0.07 ± 0.20.

* Supported by the joint program of the Office of Naval Research and the U. S. Atomic Energy Commission.
† Now at the University of Colorado.
[1] J. P. Martin, K. S. Quisenberry, and C. A. Low, Phys. Rev. 120, 492 (1960).
[2] R. Huby, M. Y. Rafai, and G. R. Satchler, Nuclear Phys. 9, 94 (1958).

DA5. Excitation Curves and Angular Distributions for the Reaction $C^{12}(He^3,n)O^{14}$.* GHIAS UD DIN, HSIN-MIN KUAN, AND T. W. BONNER, *Rice University.*—Excitation curves at 0° and 90° and the total yield from the reaction $C^{12}(He^3,n)O^{14}$ have been measured for He^3 bombarding energies of from 1.8 to 5.1 Mev. The excitation curve at 0° shows three separate peaks at 2.33, 2.87, and 4.70 Mev. At 90° there is a broad peak centered at 2.5 Mev as well as a less pronounced peak at 4.7 Mev. The total yield of O^{14}, obtained by measuring the beta particles from O^{14} and the 2.31 Mev γ rays, is similar to the neutron yield at 90°. The neutrons have an angular distribution which is spherically symmetric at 1.87 Mev. At energies of 2.33 and 2.87 Mev the distribution peaks in the backward direction; at energies of 4.02 to 5.08 Mev there is a forward peaking which becomes more pronounced at the higher energies. Angular distributions at 4.63, 4.80, and 5.08 Mev are similar to those obtained by others at higher energies, except for the fact that the ratio of forward to backward intensities is smaller. The angular distributions can be explained in terms of double stripping at the higher energies, but it is not certain whether the pronounced resonance structure at 2.5 Mev is due to a wide state of the compound nucleus or to a resonance in the stripping process.

* Supported by the U. S. Atomic Energy Commission.

DA6. A Calculation of the $C^{12}(He^3,n)O^{14}$ Cross Section at Low Energies.* W. R. GIBBS, *Rice University,* AND W. TOBOCMAN,† *Case Institute of Technology.*—Calculations have been carried out using the distorted wave Born approximation to compute the differential and total cross sections for the $C^{12}(He^3,n)O^{14}$ reaction. The assumption that the di-proton is captured as a single particle is made. The results show a qualitative similarity to the experimental results.[1] The most striking feature of the total cross section calculation is that anomalies resembling broad resonances as a function of energy are found.

* Supported in part by the National Science Foundation.
† Now on leave of absence from Rice University.
[1] G. U. Din, H. Kuan, and T. W. Bonner (preceding abstract).

DA7. The (γ,n) Cross Section of C^{13}.* S. KOWALSKI, W. BERTOZZI, P. T. DEMOS, C. P. SARGENT, AND W. TURCHINETZ, *M.I.T.*—The time of flight technique has been used to measure the (γ,n) cross section of C^{13} at photon energies from 6–18 Mev. This technique has been previously employed in the determination of the $Be^9(\gamma,n)$ cross section.[1–3] The cross section of γ absorption exhibits resonances at about 7.7, 8.9 Mev and higher energies. Data will be presented for the (γ,n) cross section including angular distributions of the emitted photoneutrons.

* This work is supported in part by the U. S. Atomic Energy Commission, the Office of Naval Research, and the U. S. Air Force Office of Scientific Research.
[1] F. R. Paolini, Ph.D. Thesis, M.I.T., 1960 (unpublished).
[2] Karlsruhe Photonuclear Conference, 1960.
[3] *Proceedings of the International Conference on Nuclear Structure, Kingston, Canada* (University of Toronto Press, 1960), pp. 710, 928.

DA8. The $C^{13}(He^3,n)O^{15}$ Reaction.* R. G. JOHNSON, L. F. CHASE, JR., AND F. J. VAUGHN, *Lockheed Missiles and Space Division Research Laboratory.*—The $C^{13}(He^3,n)O^{15}$ reaction has been investigated by observing the neutrons with time-of-flight techniques. Carbon targets enriched to 58 percent C^{13} were used and were prepared by cracking methyl iodide onto hot tantalum backings. Neutron groups were observed corresponding to O^{15} being left in the ground state, the 5.20 and 5.25-Mev states which were unresolved, the 6.15-Mev state, and the 6.79- and 6.86-Mev states which were unresolved. The excitation function for the ground-state group was measured at 10° relative to the incident beam direction for He^3 energies from 2.3 to 3.2 Mev. The yield increases monotonically in this region. Angular distributions for the ground-state group were measured from 0° to 155° at 2.60, 2.85, and 3.10 Mev. The distributions, which were peaked near 0° and exhibited a secondary maximum near 100°, suggest that the reaction proceeds by a direct-reaction mechanism. A comparison of the data with the double stripping theory of Newns[1] will be presented.

* Supported jointly by the Lockheed General Research Program and the U. S. Atomic Energy Commission.
[1] H. C. Newns, to be published.

DA9. Elastic Scattering and Capture of Protons by C^{14}.* JERRY D. HENDERSON, *The University of Texas.*—The elastic scattering of protons by C^{14} has been studied at four angles in the proton bombarding energy region of 0.6 to 2.7 Mev. The targets used were thin, self-supporting carbon foils enriched in C^{14}, and a solid state junction detector allowed separation of the C^{12} and C^{14} scattering groups through a large part of the energy range. Scattering anomalies corresponding to known levels in N^{15} were observed at 1.16, 1.31, 1.50, and 2.08 Mev. In addition, a large anomaly was present at 2.5 Mev. This level was observed in the $C^{14}(p,\gamma)N^{15}$ reaction, but has not been reported in studies of other competing reactions, indicating that it decays only by proton and γ-ray emission. Preliminary analysis of the data indicates a D-state assignment. It appears that this state may be the isobaric analog of the first excited state of C^{15}, i.e., $T=\frac{3}{2}$. A phase-shift analysis of the data is being undertaken. The yield of ground state γ-rays from proton capture by C^{14} has been studied from 1.1 to 3.2 Mev, and will be discussed in relation to the scattering data.

* Assisted by the U. S. Atomic Energy Commission.

DA10. The $C^{14}(d,n)N^{15}$ Reaction.* W. L. IMHOF, H. A. GRENCH, AND R. G. JOHNSON, *Lockheed Missiles and Space Division.*—The $C^{14}(d,n)N^{15}$ reaction has been studied by observing the neutrons with time-of-flight techniques. Peaks are observed in the time-of-flight spectra corresponding to neutron

groups which leave N^{15} in the ground state, the 5.28- and 5.31-Mev states which are unresolved, the 6.33-Mev state, and partially resolved higher states. Using a 0.27 mg/cm² target enriched in C^{14} to 28%, the excitation function for the ground state group has been measured at 30° for deuteron energies from 0.93 to 3.20 Mev. Broad peaks are observed in the yield curve at 1.3, 2.1, and 2.75 Mev. Angular distributions for the ground state group have been obtained from 0° to 150° at 1.31, 1.62, 2.10, 2.33, 2.75, and 3.08 Mev. The distributions are distinctly different at each energy, although at the four lowest energies pronounced peaking in the backward direction is observed. With better energy resolution, angular distributions were also measured for the other neutron groups at bombarding energies of 2.10 and 2.33 Mev.

* Supported jointly by the Lockheed General Research Program and the U. S. Atomic Energy Commission.

DA11. Angular Distributions of (n,d) Pickup Reactions in N^{14}, P^{31}, and S^{32} at 14 Mev.* M. R. ZATZICK AND D. R. MAXSON, *Brown University.*—Absolute differential cross sections for the $N^{14}(n,d)$ reactions leading to the ground state and the 3.68 Mev level in C^{13} were measured at ten forward angles and three backward angles. $P^{31}(n,d)Si^{30}$ and $S^{32}(n,d)P^{31}$ reaction leading to the ground states of the final nuclei were observed in 5 degree steps of laboratory angle. Deuteron energy spectra were recorded on a 20-channel analyzer, and discrimination against particles of different Z/M was accomplished by gating the analyzer with averaged dE/dx pulses from the two proportional counters. Natural elements were used for all of the targets. The experimental angular distrbutions will be compared with Butler pickup curves, and reduced widths will be extracted from the data.

* Supported in part by U. S. Atomic Energy Commission.

DA12. $N^{14}(tn)O^{16*}(p)N^{15}$, a Two-Stage Nuclear Reaction.† NELSON JARMIE, M. G. SILBERT, AND DARRYL B. SMITH, *Los Alamos Scientific Laboratory.*—A remarkably clear example of a two-state nuclear reaction has been observed. During an investigation of the proton energy spectra (at a lab angle of 30° and with 2.6-Mev tritons)[1] from the $N^{14}(t,p)N^{16}$ reaction, several anomalous, broad, steep-sided "lumps" were observed. These lumps have been identified as protons from the two-stage process: $N^{14}(t,n)O^{16*}$, $O^{16*}(p)N^{15}$. The identification was aided by noting that the energy width and position was predicted exactly by the two-stage assumption if the reaction went by way of the excited O^{16} in its sharp states at 16.22 and 14.94 Mev. In addition, the lumps moved in energy as expected when the triton energy was changed, and did not move like the proton peaks in the reaction producing N^{16}. The width of the lump arises primarily from the fact that the O^{16*} nucleus comes from the first reaction with a distribution of recoil energies and directions. A comparison of the two-stage process with other possible channels will be made. It is interesting to consider the possibility that these two-stage groups have been mistaken for broad peaks in the spectra of a one-stage reaction in an experiment with relatively poor resolution.

† Work performed under the auspices of the U. S. Atomic Energy Commission.

[1] For experimental details, see N. Jarmie and M. G. Silbert, Phys. Rev. 120, 914 (1960).

DA13. Neutron Capture γ-Ray Angular Correlation Measurements. G. A. BARTHOLOMEW AND J. F. VERVIER, *Chalk River Laboratories.*—Angular correlation apparatus described previously[1] has been used to determine level spin information. In N^{15}, the 4.50–6.33 Mev correlation shows that $J>\frac{1}{2}$ for the 6.33 Mev level. In Fe^{57}, the 7.28–0.350 and 7.29–0.228 Mev correlations show $J=\frac{1}{2}$ for the 0.364 Mev level. In Cu^{61}, the 7.63–0.277 and 7.29–0.607 Mev corerelations show $J=1$ or 2 for both the 0.277 and 0.607 Mev levels. In Zr^{92}, the 6.30–1.42, 6.30–0.929, and 1.42–0.929 Mev correlations, with the assumption that the 6.30 Mev γ-ray is $E1$, show the capturing level has $J=2$ and the 2.34 Mev level, $J=3$. In Hg^{200}, the 6.44–1.59 Mev correlation shows the capturing state and 1.59 Mev level have $J=0$ and 1, respectively.

[1] G. Manning and G. A. Bartholomew, Phys. Rev. 115, 401 (1959).

DA14. Elastic Scattering of Neutrons by Oxygen.* A. SAYRES, *Columbia University.*—Differential cross sections for the elastic scattering of neutrons by oxygen will be presented for neutrons between 3 and 4 Mev. A proportional counter filled alternately with CO_2 and hydrocarbons was bombarded by neutrons produced by the $T(p,n)He^3$ reaction. Recoil spectra were recorded on a 256-channel analyzer. Differences of the observed recoil spectra yielded the oxygen recoil spectra whose shapes are proportional to the differential cross section versus $\cos\theta_{CM}$. The absolute cross sections were obtained by normalizing to know total cross sections. By using the scatterer as the detector, multiple scattering corrections are negligible. The spectra were corrected for analyzer dead time and the finite resolution of the detector. Some implications of these measurements will be discussed.

* This work partially supported by the U. S. Atomic Energy Commission.

DA15. $O^{16}(n,p)N^{16}$ Reaction Cross Section. K. W. SEEMANN AND W. E. MOORE, *Knolls Atomic Power Laboratory.**—The cross section for the reaction $O^{16}(n,p)N^{16}$ has been measured in the neutron energy range $12.5<E_n<16.5$ Mev. Neutrons were produced by the $T(d,n)He^4$ reaction, using 1 Mev deuterons from a Cockcroft-Walton accelerator.[1] A triple coincidence proton recoil neutron spectrometer was used to measure the absolute neutron yield from the tritium as a function of angle. An oxygen-bearing liquid scintillator was bombarded in an annular ring concentric with the accelerator tube. After bombardment, the scintillant was transferred remotely and automatically to a shielded photomultiplier assembly where the beta decay of the 7.35 sec N^{16} was observed. The relative intensity profile of the d-t neutrons as seen by a separate monitor, and the N^{16} activity, were displayed in sequence on a 256 channel analyzer operating as a multichannel time analyzer. Thus fluctuations in neutron intensity during a single run can be included in the data analysis. Preliminary analysis yields a cross section of 34 ± 6 mb at 14.4 Mev. Data at other energies will be presented.

* Operated by the General Electric Company for the U. S. Atomic Energy Commission.

[1] Built and operated by the General Engineering Laboratory, General Electric Company, Schenectady, New York.

MONDAY AFTERNOON AT 2:00

Cotillion Room, South

(D. E. ALBURGER presiding)

Radioactive Nuclei, II

E1. Decay of $Te^{121,*}$ B. A. BISHARA, M. K. RAMASWAMY, W. L. SKEEL, AND P. S. JASTRAM, *The Ohio State University.*—Natural antimony was bombarded with 6-Mev protons from the Ohio State University Cyclotron. In addition the Sb K x ray, gamma rays of 70, 164, 215, 506, 576, and 1120 kev were observed in a NaI scintillation spectrometer. The 70-,

506-, and 576-kev gamma rays are attributed to the Te^{121} ground-state decay; the 215- and 1120-kev gamma rays to the decay of the metastable state of Te^{121}; and the 164-kev gamma ray to Te^{123m}. Gamma-gamma coincidences have been observed in the decay of Te^{121}. A decay scheme for Sb^{121} will be presented including a measurement of the lifetimes of the accessible excited states.

* Supported by the U. S. Atomic Energy Commission.

E2. Beta-Gamma Angular Correlation in the Decay of Sb^{124}.* R. G. Wilkinson, K. S. R. Sastry, and R. F. Petry, *Indiana University.*—The directional correlation between the first forbidden nonunique outer beta-ray group of Sb^{124} and the 603-kev cascade gamma ray in Te^{124} has been measured at eleven beta-ray energies with an accuracy of about 2%. Measurements were made with a small shaped magnetic field beta-gamma coincidence spectrometer having 5% transmission, 5% energy resolution, and a coincidence resolving time of 40 mμsec. The correlation coefficient is negative and ranges from -0.21 to -0.38 in the energy interval 3.2 to 5.1 (mc^2 units). It will be shown that the results can be analyzed quite satisfactorily with the "modified B_{ij} approximation" of the theory of Kotani and Ross,[1] as it applies to a $3(\beta)2(\gamma)0$ first forbidden transition.

* Supported by the joint program of the Office of Naval Research and the U. S. Atomic Energy Commission.
[1] T. Kotani and M. Ross, Progr. Theoret. Phys. (Kyoto) **20**, 643 (1958).

E3. Beta-Gamma Angular Correlation in the Decay of Sb^{124}.* Helmut J. Fischbeck and Marcellus L. Wiedenbeck, *University of Michigan.*—The directional correlation between the first forbidden nonunique 2.31-Mev β transition and the successive 0.603-Mev γ ray in Sb^{124} has been measured at eight β-ray energies. A thin lens spectrometer with a momentum resolution of 7% was used for the analysis of the β-ray energy. The measured angular correlation coefficient, ϵ, ranges from $-(0.28\pm0.03)$ to $-(0.404\pm0.008)$ in the energy interval 1.24 to 2.09 Mev, and is in agreement with an earlier measurement by Steffen.[1] It will be shown that an analysis of the data in the "modified B_{ij} approximation" ($Y\neq0$, $x=u=0$) using Kotani's[2] notation for a $3(\beta)2(\gamma)0$ transition is consistent with the experiment and yields two possible values for the matrix element ratio Y($Y=0.40\pm0.05$ and $Y=1.04\pm0.09$). This result may be compared with a slope factor measurement by Langer and Smith[3] which gives $Y=1.1\pm0.2$ if the modified B_{ij} approximation is assumed to hold.

* Work supported by the U. S. Atomic Energy Commission.
[1] R. M. Steffen, Phys. Rev. Letters **4**, 290 (1960).
[2] T. Kotani, Phys. Rev. **114**, 795 (1959).
[3] L. M. Langer and D. R. Smith, Bull. Am. Phys. Soc. **5**, 245 (1960).

E4. Levels in Pm^{147}. G. T. Ewan, R. L. Graham, and J. S. Geiger, *Chalk River Laboratories.*—The conversion electron spectrum of Nd^{147} is being studied at momentum resolutions of 0.03–0.1% using the Chalk River iron-free $\pi\sqrt{2}$ β-ray spectrometer. Conversion lines have been observed corresponding to transitions in Pm^{147} with energies (kev): 91.06 ± 0.04 (99.2% $M1$+0.8% $E2$), 120.47 ± 0.05 (98% $M1$+~2% $E2$), 196.64 ± 0.07 ($M1$, <10% $E2$; or $E1$), 275.36 ± 0.08 ($M1$, <30% $E2$), 319.39 ± 0.08 (~80% $M1$+~20% $E2$), 439.82 ± 0.1 and 530.95 ± 0.1 ($M1$, <50% $E2$). The multipolarity assignments are derived by comparing the experimental L_I:L_{II}:L_{III} conversion line intensity ratios with the theoretical values of Sliv. Additional weak γ rays of energies 400 ± 15 kev, 600 ± 15 kev, and 690 ± 15 kev are observed in the NaI scintillation spectrum. Gamma-gamma coincidence measurements and energy sums establish levels in Pm^{147} at 0, 7/2+; 91.06 (5/2+); 410.45 (3/2+); 489.17, 530.93, (5/2+) and 685.81, (5/2 or 3/2+) kev. No evidence is observed for the existence of a level at 182 kev recently proposed by Wendt and Kleinheinz.[1] The spin assignments are partly based on a combination of the above multipolarity assignments and the gamma-gamma angular correlation results of Bodenstedt *et al.*[2] However, their measurements are not fully consistent with the present spin choices and multipolarity assignments.

[1] H. Wendt and P. Kleinheinz, Nuclear Phys. **20**, 169 (1960).
[2] E. Bodenstedt *et al.*, Z. Physik **160**, 33 (1960).

E5. Electron Capture Decay of Tb^{158}.* H. R. Lewis, Jr., R. A. Naumann, and J. L. Power, *Princeton University.*—A terbium sample has been prepared with initial isotopic composition: 157=41%, 158=18% 159=41%, 160=0.05%. The gamma radiations accompanying the decay of this sample have been studied by scintillation spectrometry and the conversion electrons have been examined using a permanent magnet electron spectrograph. In addition to the well-known radiations accompanying the decay of terbium 160, conversion electrons, attributed to a 182.7-kev transition and a 79.7-kev transition, have been observed and assigned to the gamma cascade de-excitation of the lowest 4+ excited state in gadolinium 158 following electron capture decay of terbium 158. The scintillation spectra revealed 970-kev radiation to be also associated with the decay of terbium 158. The strong population of a 4+ state in gadolinium 158 is consistent with the assignment 3− for the nuclear spin and parity of long-lived terbium 158, analogous to the measured[1] spin and inferred parity found for terbium 160. On the assumption that the 2+→0+ transitions following the decay of terbium 158 and terbium 160 are equally probable, a half-life of 1200 ± 400 yr is deduced for terbium 158. No evidence has been obtained as yet for radiations accompanying the decay of terbium 157.

* Supported in part by the U. S. Atomic Energy Commission.
[1] A. Cabezas, I. Lindgren, R. Narrus, and M. Rubinstein, Bull. Am. Phys. Soc. **5**, 504 (1960).

E6. Radioactive Decay of Yb^{165}, Tm^{165}, and Er^{165}.* G. G. Staehle, R. G. Wilson, and M. L. Pool, *The Ohio State University.*—The radioactive chain initiated by the decay of Yb^{165} has been studied by the method of gamma-ray spectrometry. Enriched Er^{162} was irradiated with helium nuclei to produce Yb^{165}. The half-life of this previously unreported activity is 9 min. The observed radiations were the thulium K x ray; annihilation radiation, gamma rays of 80.2, 945, 1090, 1275, and 1440 kev; and composite gamma radiation from 635 to 755 kev and 780 to 845 kev. Gamma rays of 210 and possibly 95 kev are in coincidence with the 1090-kev gamma ray. The daughter activity, Tm^{165}, was studied by means of gamma-gamma coincidence measurements. From the coincidence data, relative gamma-ray intensities, and from previously reported conversion electron data, a level scheme for Er^{165} has been constructed. The level scheme shows 63 transitions and 20 levels. Transition probabilities and electron branching ratios are calculated. Er^{165} was produced by neutron irradiation of enriched Er^{164}. The only radiation observed was a 10-hr K x ray which is in agreement with previously reported information.

* Supported in part by the Office of Naval Research.

E7. Levels of Os^{188}.* L. B. Warner and R. K. Sheline, *Florida State University.*—Forty-one hour Ir^{188} has been produced by $Re^{187}(\alpha,3n)Ir^{188}$ and studied in the Gerholm electron-electron coincidence spectrometer and a conventional gamma-gamma spectrometer, both with fast-slow electronics. Seventeen hour Re^{188} and 21 min Re^{188m} were produced by $Re^{187}(n,\gamma)Re^{188}$ and examined with fast-slow gamma-gamma coincidence equipment.[1] The weak positron spectrum of Ir^{188} has been analyzed and found to consist of branches with end points at (1656 ± 10) kev and (1211 ± 45) kev, yielding $Q_{\beta^+}=(1811\pm10)$ kev. Coincidence relations and conversion electron energies,[2] while confirming the main features of previously proposed decay schemes, suggest additional or adjusted states at 2225, 2106, 1846, 1732, and 1461 kev, which

are all populated in the decay of Ir^{188}. A discussion of the level scheme of Os^{188} and the decays feeding it will be given in terms of the Collective Model.

* Work supported in part by the U. S. Atomic Energy Commission and the U. S. Army Office of Ordnance Research.
[1] Work performed at, and with the cooperation of, the Chemistry Division of the Oak Ridge National Laboratory.
[2] Based in part on unpublished high-resolution conversion electron spectra kindly supplied by R. A. Naumann and similar spectra obtained in cooperation with O. B. Nielsen.

E8. Excited States in Xe^{126}.* R. E. SUND, R. G. ARNS, L. I. YIN, AND MARCELLUS L. WIEDENBECK, *The University of Michigan.*—Gamma transitions in Xe^{126} following the decay of the 25-min I^{126} have been studied using coincidence techniques. Directional correlation measurements for the 567-kev —439-kev cascade were taken at six angles in each quadrant (every 15° from 90° to 165°), and the corrected expansion coefficients were found to be $A_2 = -0.180 \pm 0.028$ and $A_4 = +0.269 \pm 0.047$. Conversion electrons corresponding to these gamma transitions have been observed in a magnetic spectrometer. These measurements confirmed the existence of excited states at 439 kev (2+) and 1006 kev (2+). The spectrograph measurements show tentative evidence for a 0+ excited state at 1016 kev which is de-excited by weak transitions to the first excited state and to the ground state.

* Supported in part by the U. S. Atomic Energy Commission and the Michigan Memorial-Phoenix Project.

E9. Rotational and Vibrational Levels in U^{233}. S. BJØRNHOLM,* A. B. KNUTSEN, AND O. B. NIELSEN, *Institute of Theoretical Physics, Copenhagen* (introduced by J. O. Rasmussen).—The β decay of 1.3 *d* Pa^{233} has been investigated with a six-gap β spectrometer, scintillation spectrometers, and coincidence techniques. Energies, intensities, and multipole orders of 21 transitions have been established. Three are electric monopole transitions. The decay scheme comprises 12 levels. Multipole assignments and branching ratios allow accurate determinations of spins, parities, and, in most cases, K-quantum numbers. The levels group into rotational bands built on intrinsic excitations of vibrational character. Excited states with $(K, I, \pi) = (0.1-)$ at 564 kev, (0.0+) at, 693 kev, and (2.2+) at 868 kev are interpreted as the $(K=0)$ octupole, the β, and the γ vibrations, respectively. In addition, there are two negative parity states at 1018 and 1052 kev. It has been found that the β-vibrational levels are populated by ($E2$) γ transitions from the γ-vibrational band.

* Presently on leave at Lawrence Radiation Laboratory, Berkeley, California.

E10. Gamma Rays From the Decay of Pu^{239} and Pu^{240}.* E. L. MURRI† AND J. E. CLINE, *Phillips Petroleum Company.*—Studies have been made of the gamma radiation emitted following the alpha decay of the nuclides Pu^{239} and Pu^{240}. Samples of 99.83% and 95.70% Pu^{239} and Pu^{240}, respectively, were obtained from ORNL. Prior to the experiments, a chemical repurification of the samples was performed to remove contaminant activities from the Pu decay products (in particular Am^{241}). Considerable care was taken in the isotopic identification of the gamma rays. Gamma rays from the decay of Pu^{239} and their absolute intensities (in terms of %/alpha decay) are given as: 0.057 (1.6×10^{-2}%), 0.105 (1.4×10^{-2}%), 0.130 (5.4×10^{-3}%), 0.150 (7.7×10^{-4}%), 0.170 (2.4×10^{-4}%), 0.207 (6.8×10^{-4}%), 0.235 (1.4×10^{-4}%), 0.263 (1.5×10^{-4}%), 0.316 (1.9×10^{-4}%), 0.340 (1.1×10^{-3}%), 0.380 (2.5×10^{-3}%), 0.418 (1.6×10^{-3}%), and 0.450 Mev (3.2×10^{-4}%). Gamma rays from Pu^{240} and their absolute intensities are given as 0.0448 (3.6×10^{-2}%), 0.060 (2×10^{-3}%), 0.1025 (9.1×10^{-3}%), 0.155 (5.1×10^{-4}%), 0.203 (4.8×10^{-4}%), 0.263 (2.5×10^{-5}%), and 0.317 Mev (3.6×10^{-5}%). Tentative level schemes for the nuclei U^{235} and U^{236}, based on coincidence studies, will be discussed.

* This work performed under the auspices of the U. S. Atomic Energy Commission.
† U. S. Atomic Energy Commission Radiological Physics Fellow at Vanderbilt University; presently at Consumers' Power Company, Jackson, Michigan (introduced by J. E. Cline).

E11. Identification of an Isomeric Pair in Am^{244}.* SUSANNE E. VANDENBOSCH, PAUL DAY, AND DALE J. HENDERSON, *Argonne National Laboratory.*—A new 11-hr beta emitter produced in neutron irradiations of enriched (99.9%) Am^{243} was chemically identified as an isotope of americium and is assigned to an isomer of Am^{244}. The decay scheme was studied using a beta spectrometer in addition to gamma-gamma and gamma-beta coincidence scintillation counting techniques. These measurements establish levels in Cm^{244} at 0(0,0+), 43 (0,2+), 142 (0,4+), 296 (0,6+), 503 (0,8+), and 1042 (6+) kev. All levels except the 1042-kev level are rotational levels commonly found in even-even actinide isotopes. The 1042-kev level decays by highly retarded $E2$ transitions which suggests that it is a (6,6+) intrinsic level. The only beta group observed has an end point energy of 383 kev and populates the 1042-kev level. The 26-min isomer of Am^{244} decays by beta emission principally to the ground state of Cm^{244}. Theory predicts two spin states for Am^{244}, 6− and 1−, obtained by couplings of a 7/2+ [624]↓ neutron and a 5/2− [523]↓ proton. Spin assignments of 6− to the 11-hr ground state Am^{244} isomer and 1− to the 26-min isomer are consistent with the data, although other assignments are possible.

* Based on work performed under the auspices of the U. S. Atomic Energy Commission.

MONDAY AFTERNOON AT 2:15

National Bureau of Standards, East Building

(M. N. ROSENBLUTH presiding)

Symposium of the Division of Plasma Physics

EA1. Exact Statistical Mechanics of a One-Dimensional Plasma Model. A. LENARD, *Princeton University.* (30 min.)

EA2. Production and Confinement of Hot Plasma in a Multistage Mirror Machine. F. COENSGEN, *Lawrence Radiation Laboratory, Livermore.* (30 min.)

EA3. Present Understanding of Plasma Confinement in Mirror Machines. R. F. POST, *Lawrence Radiation Laboratory, Livermore.* (30 min.)

EA4. Transconductance Properties of Plasma. J. A. DRUMMOND, *Boeing Scientific Laboratories.* (30 min.)

MONDAY AFTERNOON AT 2:00

Sheraton Hall

(W. C. PARKINSON presiding)

General Nuclear Physics, Mostly Apparatus

F1. Influence of Pressure on the Mean Lifetime of Positrons in Liquids.* ROBERT STUMP, *University of Kansas.*—The mean life of positrons forming positronium has been measured in a number of liquids as a function of pressure and temperature. Liquids used include water, isopropyl alcohol, benzene, and glycerine. Pressures ranged from 1–6000 atm, temperatures from 0° to 300°C. The results may be summarized as follows: the number of positrons in the long lived-component (o-positronium) is essentially independent of pressure, whereas the lifetime decreases linearly with the volume of the liquid.

* Supported by the U. S. Air Force Office of Scientific Research.

F2. Stopping Power of Gases for Charge-Invariant Atomic Projectiles. S. K. ALLISON, J. CUEVAS, AND M. GARCIA-MUNOZ, *University of Chicago.*—In 1949, Warshaw,[1] following a conversation with Fermi, pointed out that the observed stopping power, ϵ, for protons of velocities $\sim(c/137)$, should be considered a mixture of ϵ for protons (ϵ_1) and for hydrogen atoms (ϵ_0) because of the charge exchange phenomena. By following Fermi's suggestions, Warshaw estimated $\epsilon_0=0.46\ \epsilon_1$ for H^0 and He^0 atoms of these velocities in H_2. In our work, a beam of singly charged ions is brought to charge equilibrium in converter cell No. 1. The ionic and atomic beam then enters a 54-cm absorption tube with apertures of 0.1 cm, placed in a transverse magnetic field of ~3000 gauss. Only those entering neutral particles *which remain neutral through it,* can emerge. Some of these become ions again in converter cell No. 2 and their energy is accurately measured by electrostatic deflection. With enough gas in the absorption tube for a dE of $\sim-0.8\%$ the emergent flux falls by a factor 10^{-6}—10^{-7} due mainly to charge exchange, but individual particle counting is still possible. This beam gives a greatly reduced stopping power; for instance at 75 kev ($1.7c/137$) where the normal or weighted mean of ϵ_0 and ϵ_1 is 7.4×10^{-15} ev/(atom/cm^2) for a hydrogen beam in H_2, we find $\epsilon_0=2.6$ such units.

[1] S. D. Warshaw, Phys. Rev. **76**, 1759 (1949).

F3. High Intensity Nanosecond Ion Buncher.* L. D. CHISHOLM, W. E. DANCE, D. C. RALPH, AND R. C. MOBLEY, *Louisiana State University.*—Following a previously proposed method for producing short intense monoenergetic ion buncher,[1] a complete variable path magnetic ion buncher was constructed. Tests over the past two years have indicated good bunching, but available ion beam intensity and instrumental resolution were too low for detailed measurements. Recently a high-current (100 μa), high-resolution ion beam and corresponding high-resolution pulse measuring equipment have shown performance in accordance with design predictions. Measurements with ½-Mev protons indicate pulse lengths $\leq$1 nsec peak currents $\geq$4 ma and a bunching ratio of $\geq$40. Average bunched current is ~30 μa. Bunching is accomplished by deflecting successive portions of a continuous monoenergetic ion beam from an electrostatic accelerator over progressively shorter paths between focii of a multifocusing 103° deflection magnet in a manner such that all ions coalesce essentially simultaneously at one focal point in high intensity short duration ion pulses. Sinusoidal electrostatic deflection at 8.8 Mc/sec, linearized by cylindrical electrostatic lenses[2] provides the required sweep.

* Supported in part by the U. S. Atomic Energy Commission.
[1] R. C. Mobley, Phys. Rev. **88**, 360 (1952).
[2] R. C. Mobley, Bull. Am. Phys. Soc. 1, 179 (1956).

F4. Response of Silicon Surface Barrier Detectors to Fission Fragments. H. W. SCHMITT, J. H. NEILER, F. J. WALTER, AND R. J. SILVA, *Oak Ridge National Laboratory.*—The pulse-height response of silicon surface barrier detectors to fission fragments has been found not to be strictly proportional to fragment energy. A linear relationship in the range of fission fragment energies is exhibited, but extrapolation to zero pulse height yields a finite energy (analogous to the ionization defect for fission fragments stopped in gases[1]). Thus $E=a\times PH+\delta$, where E=fragment energy, PH=pulse height, and δ for these detectors has been termed[2] "pulse height defect." Values of δ from 6 to 26 Mev have been found, depending on silicon resistivity and applied bias voltage. The systematics of this behavior will be discussed.

[1] H. W. Schmitt and R. B. Leachman, Phys. Rev. 102, 183 (1956).
[2] Proceedings of Solid State Nuclear Particle Detectors Conference, Asheville, North Carolina (1960).

F5. Performance of a Large Luminosity Beta-Ray Spectrometer.* A. A. BARTLETT AND ROBERT A. RISTINEN, *University of Colorado.*—An inside-out $\sqrt{2}\pi$ double-focusing spectrometer of the Siegbahn type has been constructed. The magnet is made of low-carbon iron with the flux return on the outside. The design radius is $r_0=30$ cm and the maximum transmission is 5% of 4π. Several coils in series provide the magnet excitation and the use of shunts in parallel with individual coils provides flexibility in adjusting the field shape. The design of the entrance slits allows the study of small groups of rays anywhere in the maximum transmitted solid angle. By means of these coil and slit adjustments one can achieve a focusing that is independent of the angle ϕ_z in the range $-0.6\leq\phi_z\leq+0.6$ radians. Under these conditions the dependence of the focusing on ϕ_r is symmetric about a negative value of ϕ_r and it is approximately quadratic. A representative performance is: a resolution of 0.4% at a transmission of 2% of 4π with a source 1.5 by 40 mm. Because of the radial defocusing, larger sources must be used in order to achieve reasonable line shapes at full transmission.

* Work supported by the National Science Foundation.

F6. Charged Particle Optics of Magnetic Sector Spectrometers with $H=H_\phi\propto r^{-1}$ [z,r,Φ Cylindrical Coordinates with z-axis=Object-Image Line].* A. H. JAFFEY, C. A. MALLMANN, J. SUAREZ-ETCHEPARE, AND T. SUTER, *Argonne National Laboratory and Argentine Atomic Energy Commission.*—The charged particle optics of symmetric and asymmetric spectrometers of this kind[1] is developed,[2] taking into account the effects of fringing fields. Formulas are given for: the images of point and extended sources, the resolution, and transmission. The suppression of ghost peaks arising from multiloop trajectories is studied. Methods and tables for the calculation of instruments are given, and some general considerations concerning the choice of design parameters are presented. The correction (for fringing field effects) of sector profiles of instruments already constructed is analyzed; formulas are given which permit calculation of the modifications to the profiles required to insure good focusing with high transmission. Tables include: general trajectory functions; profile curves, dispersion and transmission functions for symmetrical

instruments. A tabulated comparison is made between instruments constructed in various laboratories.

* Based on work performed under the auspices of the U. S. Atomic Energy Commission and the Argentine Atomic Energy Commission.
[1] In its multiple-gap form, this design has been used in "sliced-orange" spectrometers as, for example, in O. Kofoed-Hansen, J. Lindhard, and O. B. Nielsen, Mat. Fys. Medd. Dan. Vid. Selsk. 25, No. 16 (1950).
[2] To be published as ANL-6222.

F7. A Two-Crystal Gamma-Ray Spectrometer of Relatively High Efficiency. L. C. NORTHCLIFFE, *Yale University*.—Two NaI(Tl) crystals, separately packaged and viewed by separate photomultiplier tubes, are placed with the plane faces of the crystal containers in contact. Incident gamma rays are collimated parallel to the contact plane. Coincident output pulses are separately amplified, stretched, and fed to the horizontal and vertical plates of an oscilloscope. The event is recorded as a spot by intensifying the scope trace. A time exposure photograph of the spots displays the gamma-ray spectrum. Since the crystal containers inhibit the passage of electrons, coincident output pulses are associated with pair production or Compton scattering in one of the crystals (barring coincident incidence of two gammas). For a monoenergetic gamma ray the spots resulting from Compton interactions accumulate along a diagonal, while those resulting from pair production show up in in unique locations. Relatively complex spectra are quickly displayed and easily interpreted. For more quantitative measurements the coincident pulses are summed and gated into a multichannel analyzer. The pulse height spectra are considerably improved over those from a single crystal, with only a modest sacrifice in efficiency.

F8. An Exact Analytic Treatment for Scintillation Counter Time Resolution Functions.* J. V. KANE AND M. A. EL-WAHAB,† *Brookhaven National Laboratory*.—Expressions will be given for time response functions of scintillation counters employing a mathematical model to introduce various time spreads. It is shown that for exponential time spreads these functions are obtained in closed analytic form. The statistics are treated exactly and numerical values are given for several cases of interest.

* Work performed under the auspices of the U. S. Atomic Energy Commission.
† On leave from the University of Alexandria, U. A. R.

F9. On the Optimum Design Parameters of a Hydrogen Bubble Chamber.* R. W. THOMPSON, *University of Chicago and Argonne National Laboratory*, AND T. H. FIELDS, *Carnegie Institute of Technology and Argonne National Laboratory*.—The methods of operations research are being applied to the problem of determining the length L and strength of magnetic field H for the ANL hydrogen bubble chamber. We define a figure of merit as the ratio of "physics" to the cost of the program. "Physics" is defined as the relative statistical weight of experimental results, and depends not only upon L and H but upon n, the number of interactions needed in an event, and m, a variable related to the sources of momentum error. The cost of the program is represented by an algebraic function of L and H, an important uncertainty being the cost of future data reduction systems. The chamber length which maximizes the figure of merit for most classes of experimentation is much larger than existing chambers and implies a cost exceeding that of a large accelerator. If we apply an economic constraint, and arbitrarily fix the cost of the program to be the same as that of other large hydrogen chambers, an optimum is found for $L=1.5$ m, $H=40$ kgauss. This optimum is rather independent of the type of experiment. These optimum parameters might be appreciably changed if a cryogenic magnet were used.

* Work performed under the auspices of the U. S. Atomic Energy Commission.

F10. Solid Bubble Chamber. JOHN H. ATKINSON, JR., *Aeronutronic Division of Ford Motor Company*.—A solid plastic material has been discovered which shows the tracks of ionizing particles. The base material is a thermoplastic in which a metastable ionization sensitive material is dispersed. Exposure to a 12-Mev proton beam released nitrogen gas along the ionized paths of the incident protons. This gas was trapped by the base plastic matrix as small bubbles. The bubbles expand to approximately 3 μ in diameter upon heating the material to 125°C. Heating also sets the plastic and preserves the image. The developed image bubbles act as scattering centers for light since the ratio of index of refraction for the bubbles to the plastic medium is approximately 1/1.5. Space flight applications of the detection process are attractive since the material is relatively light weight with specific gravities around 1.5 and can be easily developed in flight. The gas image can be allowed to diffuse out if the plastic is not heated. Thus exposures can be made at a particular time during a flight without background interference from earlier exposures. Telemetry of the undeveloped image is also possible, allowing inflight observation of the changing particle flux. No sensitivity to minimum ionizing particles has been observed.

F11. A Three-Parameter Multichannel Recorder Analyzer System.* MICHAEL G. STRAUSS AND CURTIS C. ROCKWOOD, *Argonne National Laboratory* (introduced by L. M. Bollinger).—The system described consists of one record station and one search station now in operation, and an additional record station under construction. Nuclear events described by three parameters are recorded on magnetic tape by the record stations. The completed tapes are then analyzed off line by the search station. Each parameter is encoded by eight binary characters or 256 channels; thus the available number of channels is $(256)^3$ or approximately 16 700 000. The maximum recording rate is 150 events per second with a pulse pair resolution of 300 μsec. During search of the recorded tape, restrictions are imposed on two parameters. If both are satisfied, the third variable of the corresponding event is stored in one quadrant of a 1024-word core memory. Thus in a neutron experiment, for example, a single tape pass containing 3×10^6 events and lasting 3 min will produce four time-of-flight spectra, each as function of two coincident gamma rays of preselected energies. The four spectra may be viewed on a cathode-ray tube or read out simultaneously by a typewriter, punch paper tape, and X-Y recorder. The entire system is made of solid-state devices.

* Work performed under the auspices of the U. S. Atomic Energy Commission.

F12. Properties of Spherical NaI(*Tl*) Crystals and Their Use in the Measurement of Continuous Gamma-Ray Energy Spectra. J. I. TROMBKA AND MARCELLUS L. WIEDENBECK,* *University of Michigan*.—Both the shape of the gamma-ray pulse height spectra and the intrinsic efficiency measured using cylindrical NaI(*Tl*) crystals are dependent upon source-detector geometry. Experimental and theoretical[1] results show that this geometrical dependence is greatly reduced if spherical crystals are used. Thus in cases where the source detector geometry cannot be specified, it is still feasible to deduce the true gamma-ray energy spectra from the measurement of pulse height spectra. The aforementioned properties are of particular interest in gamma-ray shielding studies. Using a spherical NaI(*Tl*) crystal and using a method developed by this group for obtaining the true gamma ray energy spectrum from the measured pulse height spectrum,[2] it has been possible to determine degraded energy spectra produced by the scattering of gamma rays when passing through various materials. Experimental results will be presented.

* Supported in part by U. S. Atomic Energy Commission and the Michigan Memorial Phoenix Project.
[1] Private Communication from W. F. Miller and W. J. Snow, Applied Mathematics Division, Argonne National Laboratory.
[2] J. I. Trombka and M. L. Wiedenbeck, Bull. Am. Phys. Soc. 5, 417 (1960).

F13. Fast Transient High-Intensity Gamma-Ray Solid-State Detectors.* WILLIAM F. LINDSAY, *Lawrence Radiation Laboratory, Livermore.*—Feasibility studies have been conducted to provide design criteria for using reverse-biased *p-n* junction diodes of select design as current detectors of high-intensity fast transient gamma radiation. The sensitivity of a silicon *p-n* junction is calculated to be $S \simeq 10^{-18}$ amp/cm² of junction area per gamma Mev/cm² sec of incident gamma flux per μ of depletion layer width for 1- to 2-Mev gamma rays. Select commercially available diodes and transistors operated as reverse-biased *p-n* junction diodes were irradiated in a Godiva-type[1] pulsed reactor and in a linear accelerator bremsstrahlung beam. The observed signals gave device sensitivities in agreement with that calculated. For radiation pulse widths of from 0.10 to 250 μsec, frequency response characteristics were as expected from device alpha cutoff and recovery time ratings. Conclusions concerning design criteria for further development of this type of detector to provide increased sensitivity and higher-frequency response will be discussed.

* Work done under the auspices of the U. S. Atomic Energy Commission.
[1] T. F. Wimett *et al.*, "Time behavior of Godiva through prompt critical," Los Alamos Rept. LA-2029, April 1956.

F14. Computer Scanning of Hodoscope Pictures.* L. Q. NIEMELA AND A. BOYARSKI, *M.I.T.*—Machine scanning of hodoscope pictures is in progress, using the M.I.T. TX-0 computer. Events are recorded by photographing 360 gated lights, connected to scintillation counters arranged in a suitable geometry to follow particle paths in K meson decays. This binary information is read into the computer by focusing an oscilloscope spot, whose position is under computer control, onto the film, with a photomultiplier collecting the transmitted light and giving a yes-no signal back to the computer. A small search raster hunts for events; upon finding one, appropriate measurements are made to locate the position of the event on the film. A programmed spot scan then interrogates each possible light position. The lights appear as 0.1×0.3 mm dots on the film, and are covered by a 3×6 pattern of TX-0 spot positions. An event is read in $\frac{1}{3}$ sec, and the film is advanced under computer control. The machine is programmed to recognize and analyze only interesting events, to make cross checks, and to print out range curves, angular correlations, and complete data on rare events.

* This work is supported in part by the U. S. Atomic Energy Commission, the Office of Naval Research, and the U. S. Air Force Office of Scientific Research.

MONDAY AFTERNOON AT 2:00

Adams-Hamilton Room

(R. SMOLUCHOWSKI presiding)

Metals

FA1. Specific Heat of an Electron Gas in the Region of Metallic Densities.* SETH D. SILVERSTEIN, *University of Illinois.*—The influence of electron interaction on the electronic specific heat has been calculated utilizing an interpolation procedure similar to that employed by Nozieres and Pines[1] for the correlation energy. The contributions to the electron self-energy, and its derivative at the Fermi surface has been calculated in the region of low momentum transfer q, by the use of the random phase approximation, and in the region of large q, using second-order perturbation theory[2] with the neglect of the interaction between particles of parallel spin. The contributions from intermediate valves of q are obtained by making a smooth interpolation between the low and high q regions. The results for the alkali metals (including an effective mass contribution for the kinetic energy) are for the ratio of the interacting to the electron specific heat C/C_0: Li, 1.12; Na, 1.12; K, 1.19; Rb, 1.19; Cs, 1.20.

* This research supported by the Office of Ordnance Research, U. S. Army.
[1] P. Nozieres and D. Pines, Phys. Rev. 111, 442 (1958).
[2] J. G. Fletcher and D. C. Larson, Phys. Rev. 111, 455 (1958).

FA2. Electron-Phonon Interaction in Metals. JOHN J. QUINN, *RCA Laboratories.*—An effective interaction between conduction electrons in a metal is derived by summing to infinite order all diagrams which contribute to the scattering of two electrons in the "pair approximation."[1] This effective interaction can logically be separated into two parts, one involving no phonon processes, and the remainder. The former gives the usual screened Coulomb interaction for the degenerate electron gas. The latter represents the "effective" electron-phonon interaction. This effective interaction gives rise to a renormalized phonon frequency which contains both a real and imaginary part. In the limit of low frequency and long wavelength, the real part reduced to the Bardeen-Pines result.[2] The imaginary part gives rise to attenuation of sound waves in the crystal; the attenuation coefficient shall be calculated explicitly.

[1] K. Sawada, Phys. Rev. 106, 372 (1957).
[2] J. Bardeen and D. Pines, Phys. Rev. 99, 1140 (1955).

FA3. Effective Mass of Electrons in Sodium.* EDWARD A. STERN, *University of Maryland,* AND WILLIAM E. HARTE, *Department of Defense.*—By measuring the angle of rotation of the plane of polarization of light after normal reflection from a flat metal surface in a normal magnetic field, an average effective mass of the conduction electrons can be calculated.[1] The room-temperature results of this measurement (the so-called Faraday effect on reflection) on sodium metal is presented. Because the Fermi surface in bcc sodium, the room-temperature phase, is essentially a sphere, an average electron effective mass is the actual effective mass. This value is compared with theoretical values and with the value obtained from specific-heat measurements. Because the specific-heat mass is more affected by electron-electron interactions than the Faraday mass, a comparison between the two masses shows very graphically the importance of many body effects in sodium.

* Research supported by U. S. Signal Corps.
[1] E. A. Stern, Bull. Am. Phys. Soc. 5, 150 (1960).

FA4. Effective Charge of Quasi-Particles in a Metal.* E. R. BURKE AND RICHARD A. FERRELL, *University of Maryland.*—According to Stern[1] the charge of a quasi-particle in a metal e^* is related to the effective mass m^* by the equation $e^*/m^* = e/m$, when only electron-electron interactions play a role and lattice effects can be ignored. The unstarred quantities are the free charge and mass of an electron. Stern has further pointed out that this simple relationship no longer holds when electron-phonon interactions are taking place. We have performed an explicit calculation in lowest order perturbation

theory of the deviation from Stern's formula and will present numerical results in which the percentage deviation is expressed in terms of the percentage contribution to the effective mass due to electron-phonon emission and absorption. Since the e/m ratio is modified by the electron-phonon interactions, it is clear that the latter can significantly influence the cyclotron resonance frequency in a metal.

* Research supported by the U. S. Air Force Office of Scientific Research.
[1] E. A. Stern (submitted for publication to Phys. Rev.).

FA5. Gold Crystals One Atom Thick.* R. L. HINES, *Northwestern University*.—When gold is evaporated in a vacuum onto an appropriate single-crystal substrate, the gold forms a single crystal with definite orientation with respect to the substrate. If the flux of gold atoms is large compared to the flux of residual gas molecules and if a clean substrate surface is exposed at the start of evaporation by cleaving a mica crystal in the vacuum system, then very thin gold crystals can be made. A gold film 300 A tihck deposited in a vacuum of 10^{-6} mm Hg on a mica surface cleaved outside of the vacuum system shows a fracture pattern characteristic of an amorphous film. However, a gold film 300 A thick grown at a rate of 30 A/sec in a vacuum of 4×10^{-7} mm Hg on a mica surface freshly cleaved in the vacuum (mica temperature of ~100°C) shows a fracture pattern consisting of straight edges intersecting at angles of 60° and 120°. The thickness of the film is determined from its reflection coefficient using published data of reflection coefficient versus gold film thickness. The thinnest film obtained to date has a reflection coefficient due to the gold of 0.010 which gives a thickness of 7 A or only 3 atom layers. The film still shows fracture along lines with hexagonal symmetry.

* This research is supported by the Advanced Research Projects Agency of the U. S. Department of Defense.

FA6. Temperature Dependence of Electrical Resistance of Thin Metal Films in Different Environments. HELMUT SCHWARZ,* *R.C.A.*—The resistance of vacuum-deposited thin-metal films as a function of temperature was measured in vacuum, air, argon, and silicone oil. The films were formed by the deposition of a nickel-chromium alloy on ceramic substrates. Measurements were made of uncoated films and of films which were coated with a protective layer of silicone monoxide in thickness from 5 000 to 10 000 angstrom units. When measured under vacuum, resistors displayed a temperature coefficient of resistance lower than that obtained in air, argon, or silicone oil. In an argon environment, the films had lower coefficients of resistance than in air or silicone oil. Even when the metal films were protected by a 10 000 A thick layer of silicone monoxide, their temperature-coefficient behavior differed in different gas environments. Most of the temperature coefficients measured in the temperature range from −55° to +150°C were between 5 and 50 parts per million per degree centigrade.

* Now with Hamilton Standard Division, United Aircraft Corporation, Windsor Locks, Connecticut.

FA7. Radiation Effects on the Mechanical Properties of Tungsten.* D. R. MUSS AND J. R. TOWNSEND, *University of Pittsburgh*.—Young's modulus (Y) and internal friction (δ) were measured in polycrystalline tungsten between 78°K and room temperature at audio frequencies. This measurement was made in place, in the University of Pittsburgh cyclotron, where the samples were bombarded by 14 Mev deuterons. Pre-irradiation observations of δ as a function of temperature show what seems to be a Bordoni peak at about 140°K with a width of about 60°K. The estimated activation energy for this relaxation process is 0.24 ev. This estimate was made from observation of the shift in peak temperature for two different frequencies. Room-temperature results for Y and δ as a function of incident flux are similar to those published by Thompson and Holmes[1] for copper, i.e., Y increases and δ decreases with incident flux. Both of these effects saturate at about 10^{16} deuterons/cm². With still higher incident flux Y then decreases linearly with incident flux, a result attributable to the bulk effect of immobile vacancies. The slope of this bulk effect is $0.011\%/10^{16}$ deuterons/cm².

* This work was supported by the U. S. Air Force Cambridge Research Center.
[1] D. O. Thompson and D. K. Holmes, J. Appl. Phys. **27**, 713 (1956).

FA8. Annealing of Radiation Induced Defects in Tungsten.* J. R. TOWNSEND AND D. R. MUSS, *University of Pittsburgh*.—The Bordoni peak in tungsten reported in the preceding abstract was removed by a room-temperature irradiation of 10^{16} deuterons/cm². The main peak was replaced by a number of narrow peaks (widths from 2–5°K), the largest of which were strain amplitude and frequency dependent. After light irradiation (~10^{15} deuterons/cm²) at 78°K the internal friction (δ) was measured as a function of temperature between 78°K and room temperature. About 10 very large, narrow peaks were found superimposed on the original Bordoni peak. These internal friction peaks are an order of magnitude higher than the background, and are of the order of 2°K wide. Measurement of δ vs T subsequent to this anneal gives the same Bordoni peak as before irradiation with the peak height reduced by about 10%. Two possible explanations for the large annealing fine structure in the internal friction are suggested: (1) The stress-induced motion of mobile interstitials, and (2) The relaxation of dislocations interacting with an atmosphere of defects.

* This work was supported by the U. S. Air Force Cambridge Research Center.

FA9. Chemical Etch Pits and Dislocations in Copper. A. W. RUFF, JR., *National Bureau of Standards*.—The relation between chemical etch pits and dislocations has been studied in thin single-crystal foils of copper. Both deformed and as-grown sheet crystals in {111} orientations have been employed. Surface studies were conducted at low magnifications by optical microscopy and at high magnifications by electron microscopy using replica techniques. In addition, a procedure was developed for etching thin foils so that both the etch pits and dislocations were simultaneously revealed by transmission electron-microscopy methods. There is considerable evidence that there is not a one-to-one correspondence between the seetch pits and the emergence points of glide or notwork dislocations. Electron micrographs will be presented which indicate that etch pits are also nucleated by small dislocation loops near the surface. These loops are produced throughout the sample during deformation. Some elements of diffraction contrast theory concerning dislocation visibility will be reviewed.

FA10. Pressure and Temperature Dependence of High-Temperature Creep in Lead.* B. M. BUTCHER AND A. L. RUOFF, *Cornell University*.—The activation energy E_c for steady-state creep of 99.9999% lead was calculated from relative strain rates obtained by the method of rapidly changing temperature over the range 60 to 200°C. The activation volume V_c was obtained in a similar manner over the range 1–10 kbars. Here E_c which was independent of the deviatoric stress, was slightly larger (about 0.1 ev) for lead (as it appears to be in other metals) than the self-diffusion activation energy E_d. For certain[1] diffusion-controlled (I) mechanisms these values should be identical. When vacancy creation in a supersaturated atmosphere (II) is rate controlling,[2] E_c should be twice the energy of vacancy formation $2E_f$. Since $2E_f$ in several fcc metals[3] is about 1.10 E_d, excellent agreement is found with (II); V_c should be 0.84 Ω_0 for (I)[4] and we estimate from

other data[5] 1.40 Ω_0 for (II). Experimentally, we find $V_c = 0.85 \pm 0.02\ \Omega_0$.

* Supported by the U. S. Atomic Energy Commission and the Advanced Research Projects Agency.

[1] J. Lothe, J. Appl. Phys. 31, 1077 (1960).
[2] A. Seeger, Phil. Mag. 46, 1194 (1955).
[3] R. O. Simmons and R. W. Balluffi, Phys. Rev. 119, 600 (1960).
[4] N. H. Nachtrieb, H. A. Resing, and S. A. Rice, J. Chem. Phys. 31, 135 (1959).
[5] D. Lazarus, Conference on Very High Pressures, Bolton Landing, New York (1960).

FA11. Effect of Additional Elements on the Period of the CuAu II Superlattice. ROBERT S. TOTH AND HIROSHI SATO, *Ford Motor Company.*—The superlattice CuAu II is characterized by a long period, or regular antiphase domain. This type of antiphase domain is not peculiar to CuAu only, but frequently occurs in other alloys. The effect of additional elements on the long period superlattice of CuAu II was determined in order to supplement the existing data[1] systematically and also in the hope that it would lead to some explanation as to why such a long period structure is stable. Single crystal CuAu II films were made by employing the thin-film technique. The films were made by successive evaporations of Au and Cu, respectively, onto a heated NaCl substrate. Additional elements of various concentrations were then evaporated onto, and diffused into, the films. Elements from each group in the periodic table which could be readily evaporated from *W* boats were selected. The effects noted included an increase or decrease of the period, or a complete destruction of the long period superlattice, depending upon the type and concentration of the additional element. For example, the addition of Group III *B* elements Al, Ga, or In resulted in a decrease of the domain size *M* from 5.0 to 1.5 for concentrations of 2 to 23 atom %, respectively, while the addition of 4 atom % Ge or Pd into CuAu completely destroyed the CuAu II superlattice.

[1] S. Ogawa, D. Watanabe, H. Watanabe, and T. Komoda, J. Phys. Soc. Japan 14, 936 (1959).

FA12. Low-Temperature Specific Heats of Dilute Cu-Co Alloys. L. T. CRANE AND J. E. ZIMMERMAN, *Ford Motor Company.*—The specific heats of dilute alloys of cobalt in copper have been investigated in the temperature range from 1.5° to 4.5°K. Both cobalt and copper samples were of spectroscopic purity and specimens were prepared by chill casting from the melt and fast quenching after annealing. Measurements were made on eight specimens having cobalt concentrations in the range from ¼ to 2½ weight percent. Results show a complex specific heat anomaly which is divisible into two parts: the specific heat in excess of that of pure copper (1) is linear in temperature and a quadratic function of concentration at the higher temperatures in this range and (2) exhibits at the lower temperatures a strong additional increase which appears to have a characteristic temperature proportional to cobalt concentration. Comparison with the measurements on dilute Cu-Mn alloys shows that the magnetic interaction in Cu-Co and Cu-Mn must be quite different. Calculation of the entropy accounted for between 1.5 and 4.5°K shows that the available atomic cobalt spins are not being aligned at these temperatures.

FA13. Ultrasonic Attenuation Measurements in Copper.* EUGENIE V. MIELCZAREK, D. SHELLEY, AND PAUL H. E. MEIJER, *The Catholic University of America.*—Measurements of the magneto-acoustic effect have been made in copper at orientations every few degrees around the 001 axis. Longitudinal waves were propagated along the 001 axis and the magnetic field was kept perpendicular to this axis. Measurements in the 110±1° direction as a function of magnetic field show seven minima. These minima give a momentum of $1.29 \pm 0.03 \times 10^{-19}$ g cm sec^{-1} in this direction. This is the momentum of an outside orbit in particular a dogbone orbit. This value is in fair agreement with that measured by Morse (1.22×10^{-19} g/cm/sec^{-1}). The measurements around the 001 axis show a definite shift in the minima positions toward lower values of $(\lambda H)^{-1}$ at about 110+25°. In the 100 direction seven minima are observed. Two of these minima are displaced to such an extent, in both attenuation and field, with respect to the other minima that they obviously belong to another orbit. The two orbits contributing to the resonance are a belly orbit and probably an orbit which occurs for an electron having $k_z \neq 0$. Measurements have also been made at several frequencies with the wave vector q along the 110 axis and with H in the 111 direction. Here the last minimum appears split (similar to our observations in Silver).

* This research is sponsored by the Office of Naval Research.

FA14. Relation Between Stored Energy and Dilatation of Irradiated Graphite. ROBERT W. KEYES, *IBM Research Laboratory.**—This work uses Zener's theory of stored energy to calculate the stored energy of irradiated graphite from the *c*-axis expansion. According to Zener's theory the stored energy per unit volume is

$$E_S = [(\partial \log C/\partial P)_T - \beta]^{-1}\delta,$$

where $(\partial \log C/\partial P)_T$ is the isothermal pressure derivative of an elastic modulus and β is the isothermal compressibility. The dilatation δ is essentially equal to $(\Delta c/c)$ in graphite. From Gruneisen theory $(\partial \log C/\partial P)_T = (2\gamma + \frac{1}{3})\beta$, and the Gruneisen constant γ can be obtained from measured values of the thermal expansion coefficient, the specific heat, and β. We find that $\gamma = 1.3$. Use of $\beta = 2.9 \times 10^{-6}$ bar^{-1} gives $E_S = 4000(\Delta c/c)$ in cal/cm^3. This value is $(\frac{1}{3})$ to $(\frac{1}{4})$ of those observed.

* This paper placed on Monday at the speaker's request.
[1] C. Zener, Trans. Am. Inst. Mining Met. Eng. 147, 61 (1942).

MONDAY AFTERNOON AT 2:00

Cotillion Room North

(G. E. UHLENBECK presiding)

Theory, II: Many-Body Problems, Statistical Mechanics

FB1. Explicit Collective Coordinate Transformation of a Many-Boson System. JEROME K. PERCUS, *New York University,* AND GEORGE J. YEVICK, *Stevens Institute of Technology.*—The Fourier components of matter density for a condensed boson system behave to a considerable extent as independent oscillating variables. This suggests rewriting the Hamiltonian in terms of an appropriate finite number of such components and their conjugate momenta. Numerous approximate procedures for doing so have been investigated in the past. In the case of a periodically bounded *N*-body system in one space dimension, an explicit transformation results from the observation that the *N* lowest components vanish at regular lattice

spacing, so that a MacLaurin series may be developed about this N-dimensional point. The required momentum and Jacobian transformations easily follow as well. For three space dimensions, the analogous process is available if we consider only the longitudinal part of the Hamiltonian. In either event, a diagrammatic technique has been obtained for facilitating the transformation. The resulting Hamiltonian is nearly diagonal, and both variation and perturbation methods are readily set up for its solution. Transverse variables in the three-dimensional case may also be inserted perturbationwise, and their effect in coupling longitudinal modes determined, but there is a good deal of latitude in the definition of the transverse variables, and correspondingly in their treatment.

FB2. Quasi Particle-Quasi Particle Interaction in a Many Fermion System.* D. KOBE AND W. CHESTON, *University of Minnesota.*—The states of a many Fermion system possessing an energy gap can be explored using the formal techniques of Bogoliubov and Belyaev. To a good approximation, these states correspond to those of a system of independent quasi particles the major effect of the Fermion pairing forces being included in the introduction of the quasi particles. The Green's function for an interacting two quasi particle system has been constructed and examined in the limits of large and small energy gap. Under certain conditions, the modification of the states of the system caused by the quasi particle interaction is large and it is not possible to calculate the modification treating the quasi particle interaction as a perturbation. These effects are also present when one attempts to formally sum the equivalent stationary state perturbation series.

* Supported by the U. S. Atomic Energy Commission.

FB3. Time-Dependent Pair Correlation Function for a Degenerate Fermion Gas.* J. R. CULLEN AND RICHARD A. FERRELL, *University of Maryland.*—Let P^1 be a single-particle projection operator in a small region of configuration space centered about point 1 and $P_2(t)$ be a corresponding operator at point 2 and at the later time t in the Heisenberg picture. Then van Hove's time-dependent pair correlation function, defined in connection with the scattering properties of the fermion gas, is given essentially by the vacuum expectation value $\langle P_2(t)P_1\rangle$. On the other hand, the true joint probability of finding a particle at point 1 and, in addition, another particle at point 2 time t later is given by $\langle P_1P_2(t)P_1\rangle$. These two functions can be expected to be identical only for the case $t=0$, for which the projection operators commute (and $P_1^2=P_1$). Explicit expressions can be exhibited for the one-dimensional free-fermion gas.

* Research supported in part by the U. S. Air Force Office of Scientific Research.

FB4. Linear System Which Approaches a Second-Order, Order-Disorder Phase Transition.* GEORGE A. BAKER, JR., *Los Alamos Scientific Laboratory.*—The calculation of the partition function for a simple, one-dimensional, order-disorder model is reduced to the solution of a certain functional equation. This equation is solved exactly and it is shown that in the limit of indefinitely long range interactions the model exhibits a finite discontinuity in the specific heat.

* Work performed under the auspices of the U. S. Atomic Energy Commission.

FB5. Three-Dimensional Lattice Gas in Random Phase Approximation.* M. COOPERSMITH AND R. BROUT, *Cornell University.*—The three-dimensional lattice gas is examined in the light of Brout's recent work[1] on high density ferromagnetism. It is observed that the spherical model approximation to the Ising model partition function with magnetic field is a function of $1-R^2$, where R is the magnetization or long range order. By identifying the pressure of the lattice gas with the free energy of the Ising model, we note that the pressure of the lattice gas is a function of $\rho(1-\rho)$ in the same approximation, where ρ equals density equals $(1-R)/2$. The relationship between the vapor and liquid phases is therefore made manifestly evident, the expansion parameter for the vapor phase being the density of particles, ρ and for the liquid phase being the density of holes, $1-\rho$. Machine calculations of Ising model and lattice gas isotherms are made and will be presented. Considerations on the extension of lattice gas condensation to the condensation of real gases will also be given.

* Supported in part by the Office of Naval Research.
[1] R. Brout, Phys. Rev. **118**, 1009 (1960).

FB6. Some Partition Problems with Analogies in Quantum Statistics. R. L. INGRAHAM, *New Mexico State University* (introduced by Otto Theimer).—The problem of counting spin configurations in Ising lattices which satisfy various algebraic conditions is formally similar to computing the entropy of certain many-particle systems obeying Fermi Dirac statistics. Steepest descent methods have been used to solve several of these problems, and the analogies with quantum statistical formulas have been brought out.

FB7. Radial Distribution Functions for the Lennard-Jones Potential. A. A. BROYLES, *University of Florida.*—A comparison will be made between radial distribution functions computed various ways for a system of particles interacting with the Lennard-Jones 6-12 potential where kT/ϵ is 2.74. The Monte Carlo calculations of Wood and Parker[1] will be compared with the solutions to various integral equations such as the Born-Green and Percus-Yevick equations.

[1] W. W. Wood and F. R. Parker, J. Chem. Phys. **27**, 720 (1957).

FB8. Complex Cluster Integrals for an Augmented Gaussian Gas.* TOMOYASU TANAKA, PAUL H. E. MEIJER, AND JOHN N. FOX, *Catholic University of America.*—It has been shown[1] that complex cluster integrals can be evaluated very easily if the actual f-function $f=\exp-\phi(r)/kT-1$ is replaced by $f_0=-\exp-\lambda r^2$. A possibility of using a more realistic f-function is suggested also by the same authors.[1] We have carried out the actual calculation of the cluster integrals of of four and five particles with the augmented Gaussian function in the form $f=(-1+Br^2)\exp-\lambda r^2$, where B and λ are determined as functions of temperature by comparing with the Lennard-Jones potential. It is shown that the integration problem is reduced to the evaluation of higher derivatives of the so called tree determinant. The method is also applicable to the evaluation of more complicated clusters.

* Supported by U. S. Air Force contract.
[1] E. W. Montroll, T. H. Berlin, and T. W. Hart, *Changements de Phases* (Paris, 1952), p. 211.

FB9. Quantum Mechanical Irreversible Ensembles.* CHARLES R. WILLIS, *Boston University.*—In a previous report[1] we developed models for the description of the interaction of an arbitrary quantum system coupled with reservoirs of free bosons or free fermions. The equation satisfied by the system density matrix was derived using a perturbation expansion in powers of λc, where λ is a coupling constant and c is the density of the resevoir. If a further assumption is applied to our equation we obtain the Bloch equation.[2] We now have extended the "H theorem" proved in reference 1 for a simple class of interactions to all interactions for the Bloch equation and a much wider class of interactions for our equation. The lack of dependence of the "H theorem" on the interaction of the system with the reservoir for the Bloch equation is shown to be due to the property that the Bloch condition divides the elements of the density matrix into noninteracting sets relaxing independent of each other.

* Supported by the U. S. Air Force Cambridge Research Center.
[1] C. R. Willis and P. G. Bergmann, P11, AFOSR-TN-57-623.
[2] R. K. Wangness and F. Bloch, Phys. Rev. **89**, 728 (1953).

FB10. Statistical Theory of the Dielectric Constant of an Imperfect Gas.* A. N. KAUFMAN, *Lawrence Radiation Laboratory, Livermore,* AND K. M. WATSON, *Lawrence Radiation Laboratory, Berkeley.*—A description is given of the state and dielectric properties of a gas of interacting molecules in a weak, nonuniform electrostatic field $\mathbf{E}_0(\mathbf{r})$. The molecules may be polar or nonpolar, and interact by Coulomb forces, which have a long-range (dipole-dipole) component, and by the Pauli principle, which gives rise to short-range repulsion. When the applied field varies slowly over molecular dimensions, a relation is obtained between the polarization $\mathbf{P}(\mathbf{r})$ and the macroscopic field $\mathbf{E}(\mathbf{r})$ (suitably defined): $\mathbf{P}(\mathbf{r})=(4\pi)^{-1}(K-1)\mathbf{E}(\mathbf{r})$. The Clausius-Mossotti function $(K-1)/(K+2)$ is expressed as a power series in density, the coefficients of which are the traces of molecular cluster operators. Approximate evaluation of these coefficients leads to the Kirkwood and Jansen-Mazur dielectric theories.

* This work was done under the auspices of the U. S. Atomic Energy Commission.

FB11. Equilibrium Statistical Mechanics of the One-Dimensional Plasma.* STEPHEN PRAGER, *University of Minnesota.*—The interaction of two charges in one dimension corresponds to the three dimensional interaction of two uniformly charged parallel plates, that is the potential is ∧- or ∨-shaped depending on whether the charges are of like or unlike sign. The partition function for an electrically neutral system of such charges can be obtained rigorously, without recorse to any approximations. The resulting thermodynamic functions agree with those predicted by the one-dimensional Debye-Hückel theory in the limit of high pressures, but considerable deviations appear as the pressure is reduced. At very low pressures the system behaves as though made up of neutral molecules.

* Work supported by the U. S. Air Force Office of Scientific Research.

FB12. Transport Properties of Polar Gases. L. MONCHICK, *Applied Physics Laboratory,* AND E. A. MASON, *University of Maryland.*—A model for the kinetic theory of polar gases is proposed in which it is assumed that the transfer of rotational energy may be safely ignored and that the relative configuration of two colliding molecules remains fixed throughout the most significant part of the trajectory; e.g., the turning point. The Chapman-Enskog theory retains its usual form except that the collision integrals must be averaged over all configurations. The calculations have been carried out for the Stockmayer potential, (12-6-3),

$$\phi=4\epsilon_0[(\sigma/r)^{12}-(\sigma/r)^6+\delta(\sigma/r)^3]$$

for values of kT/ϵ_0 ranging from 0 to 100 and of δ from -2.5 to 2.5. The transport properties that may be calculated from these integrals are the viscosity, diffusivity, and thermal diffusivity. The over-all agreement between experiment and this model for polar gases is comparable to that of the Lennard-Jones (12-6) model for nonpolar gases.

FB13. Theory of Drag in a Rarefied Atmosphere.* M. H. ROSE, *Institute of Mathematical Sciences, New York University.*—The problem considered is that of the drag on a body in steady motion through a rarefied, neutral gas when collisions are no longer negligible. By using a Boltzmann equation with a modified collision term suggested by Krook,[1] it is possible to obtain the space dependence of moments of the distribution function for distances within a mean free path from the body (it is assumed that the mean free path is much larger than some characteristic dimension of the body). Values of the drag are calculated for both low and high Mach numbers. The method used is similar to Grad's in deriving the asymptotic solution far from the body.[2]

* The work presented here is supported by the Institute of Mathematical Sciences, New York University, under contract with the U. S. Atomic Energy Commission.

[1] P. L. Bhatnager, E. P. Gross, and M. Krook, Phys. Rev. **94**, 511 (1954).

[2] H. Grad, "Equations of flow in a rarefied atmosphere," NYO-2543, New York University (1959).

FB14. Statistics of Random Events Scaled by an Arbitrary Factor. WESLEY O. DOGGETT, *North Carolina State College.*—The statistical nature of a random sequence of pulses scaled by an arbitrary factor is investigated. Expressions relating the average input rate of pulses to the observed average rate of the scaled-down pulses are given and verified experimentally. The fractional standard deviation of the scaled-down pulses is theoretically evaluated. Several generalized hyperbolic functions required in this analysis were numerically evaluated by the University's Univac 1105 digital computer and are presented graphically.

TUESDAY MORNING AT 10:15

Adams-Hamilton Room

(S. GESCHWIND presiding)

Spins, III

G1. Electron Paramagnetic Resonance of Irradiated Borosilicate Glasses.* SOOK LEE AND P. J. BRAY, *Brown University.*—ESPR spectra have been obtained from gamma-, proton, and x-ray irradiated borosilicate glasses. All spectra consist of asymmetric broad lines of width 51 gauss, which are well resolved into 5 equidistant lines of separation 14 gauss. Neutron irradiation produces the same spectra except for the addition of a single sharp, intense line with $g=2.0012$ superimposed on one of the 5 lines. Measurements of g-value and response to microwave saturation and annealing indicate that this sharp line is due to trapped electrons in the silica network in the glasses, as described by Weeks[1] in neutron-irradiated pure silica. Spectra consisting of the broad resonance with 5 lines have also been obtained from irradiated sodium, potassium, and lithium borate glasses, but not in the case of irradiated boron-free alkali silicate glasses.[2] It would appear, therefore, that this resonance is due to paramagnetic centers produced in the B_2O_3-Na_2O, $-Li_2O$ or $-K_2O$ networks in the glasses. Centers produced in the silica network in the glasses seem to give no contribution to the resolved 5-line spectra.

* Research supported by the U. S. Atomic Energy Commission.

[1] R. A. Weeks, J. Appl. Phys. **27**, 1376 (1956).

[2] J. S. van Wieringen and A. Kats, Philips Research Repts. **12**, 432 (1957).

G2. Effects of Heat Treatment Prior to Irradiation on Paramagnetic Resonance of Fused Silica.* A. J. SHUSKUS AND O. R. GILLIAM, *University of Connecticut,* AND P. W. LEVY, *Brookhaven National Laboratory.*—Paramagnetic resonance has been observed in room temperature uv irradiated Corning 7943 fused silica. The line shape and g value are the same as

those observed by Weeks[1] in gamma and neutron irradiated fused silica, and optical absorption is developed at 212 mμ. When samples are flame-heated to softening and quenched in water, the resonance is weakly observable before irradiation. Also, quenching causes optical absorption at 247 mμ, which does not appear to correlate with the ESR absorption. Significant enhancement in the spin resonance of uv irradiated samples results from quenching prior to irradiation. Other fused silicas behave similarly except Corning 7940, which gives no paramagnetic absorption. For a 10^6-r Co^{60} gamma irradiation of 7943 at 300°K, two ESR lines of equal intensity, each 5 gauss wide and separated about 75 gauss, are detected. Quenching before irradiation enhances them. Prior to our interpretation of these lines, Weeks and Nelson[1] reported evidence that their intensity is proportional to the OH concentration in the lattice, measured by infrared, and they postulated proton hyperfine structure. By deuterium substitution we have confirmed that the splitting arises from proton hyperfine interaction.

* Supported by the U. S. Atomic Energy Commission.
[1] R. A. Weeks, J. Appl. Phys. **27**, 1376 (1956); R. A. Weeks and C. M. Nelson, Oak Ridge National Laboratory Rept. (3017), August 31, 1960.

G3. Electron Spin Resonance of X-Irradiated Single Crystals of Normal and Deuterated *dl*-Aspartic Acid.* THADHO S. JASEJA AND ROY S. ANDERSON, *University of Maryland and Clark University.*—A single crystal of normal *dl*-aspartic acid and one in which the NH_2 and OH protons were replaced by deuterium, were x-irradiated and examined by electron spin resonance at room temperature. No marked difference in the resonance patterns of both kinds of crystals were observed at any orientation in the magnetic field. Analysis of the spectrum suggested that the radicals formed were $(CO_2H)CH_2\dot{C}H(CO_2H)$. One of the hyperfine interactions was found to be anisotropic and the other interactions were quite isotropic. This is similar to the results obtained with succinic acid.[1] The two methylene protons in the aspartic acid radical were found to be total nonequivalent and cause isotropic splittings of 116 and 20 mc. This may indicate that there is a larger twist of the methylene group in this radical than in succinic acid.[1] This larger twist may result from the presence of NH_2 or ND_2 in the parent molecule. Thus it must be assumed that the orientation of the radical formed in the crystal lattice remain the same as that of the parent molecule in the undamaged lattice, as done in the case of succinic acid.[1]

* Supported by the National Security Agency.
[1] C. Heller and H. M. McConnell, J. Chem. Phys. **32**, 1535 (1960).

G4. Overhauser Effects and Other Relaxation Processes for Cobalt Ions in Cerium Zinc Double Nitrate.* J. W. CULVAHOUSE AND W. P. UNRUH,† *University of Kansas.*—A microwave cavity with two modes of oscillation, has been used to investigate the relaxation process for the hyperfine levels of the cobalt X ions in cerium zinc double nitrate.[1] One of the transitions of the hyperfine structure is saturated with high power while the signal due to another transition is observed with low power. At cobalt concentrations greater than 0.05%, cross relaxation processes of the type described by Bloembergen[2] are dominant. For dilute samples, saturation of the forbidden transitions produces changes in the intensity of the allowed transitions which are rather close to those calculated for a simple model. A small Overhauser effect can be produced, the size of which implies that the direct nuclear relaxation is somewhat faster than the relaxation for the forbidden transition. The nuclear relaxation is of the order of 1 sec and the relaxation time for the allowed transitions is about 5×10^{-2} sec.

* Supported in part by the National Science Foundation and the Office of Naval Research.
† National Science Foundation Predoctoral Fellow.
[1] R. S. Trenam, Proc. Phys. Soc. (London) **A66**, 118 (1953).
[2] N. Bloembergen, S. Shapiro, P. S. Pershan, and J. O. Artman, Phys. Rev. **114**, 445 (1959).

G5. Paramagnetic Spectrum of Interstitial Hydrogen Atoms in CaF_2. J. L. HALL* AND R. T. SCHUMACHER,† *Carnegie Institute of Technology.*—We have observed a paramagnetic resonance spectrum in suitably prepared CaF_2 which we ascribe to interstitial atomic hydrogen. The crystal structure of CaF_2 is for this purpose appropriately described as a simple arrangement of F^- ions with every other body center occupied by a Ca^{++} ion. The hydrogen atom is in a body center position. The observed spectrum can be described by the following spin Hamiltonian:

$$\mathcal{H}_s=g_e\beta_0\mathbf{S}\cdot\mathbf{H}_0+\sum_{i=0}^{8}\boldsymbol{\mu}_i\cdot\mathfrak{T}^{(i)}\cdot\mathbf{S}-\sum_{i=0}^{8}\boldsymbol{\mu}_i\cdot\mathbf{H}_0.$$

S is the electron spin, $\boldsymbol{\mu}_i$, $1\leq i\leq 8$, is the fluorine nuclear magnetic moment, $\boldsymbol{\mu}_0$ is the proton magnetic moment, and $\mathfrak{T}^{(i)},0\leq i\leq 8$. is the electron-nuclear hyperfine tensor. We obtain $|\mathfrak{T}_{zz}^{(0)}|=|\mathfrak{T}_{yy}^{(0)}|=|\mathfrak{T}_{zz}^{(0)}|=521$ gauss, $\mathfrak{T}_{zz}^{(i)}=\mathfrak{T}_{yy}^{(i)}=24$ gauss, $\mathfrak{T}_{zz}^{(i)}=63.2$ gauss, $1\leq i\leq 8$. The z directions are along body diagonals of the simple cube. g_e is very close to the free electron g value. Lines arising from $\Delta m_s=\pm1$, $\Delta m_z=0$, ±1 are predicted by $\mathcal{H}_s$, and are observed with the expected intensity. Sample preparation will be discussed.

* National Carbon Predoctoral Fellow.
† Alfred P. Sloan Fellow.

G6. Electron Spin Resonance of Irradiated Chloroacetamide and Chloroacetic Acid. ROGER P. KOHIN, *University of Maryland,* AND ROY S. ANDERSON, *Clark University.*—Single crystals of chloroacetamide and chloracetic acid were x-irradiated at room temperature. Both samples yielded similar electron spin resonance signals having complex anisotropic hyperfine structure due to the chlorine and hydrogen nuclei. The Cl^{35} nucleus contributed a maximum anisotropic hyperfine coupling of 55 Mc, which is comparable to the 35 Mc quadrupole splitting observed in the undamaged molecule.[1] The minimum contribution of the chlorine nucleus was much smaller and unresolvable. In this intermediate field region, if $\mathbf{B}$ is not parallel to the symmetry axis of the electric field gradient, $\Delta m_{Cl}=\pm1$, ±2 transitions may be more intense than $\Delta m_{Cl}=0$ transitions. m_{Cl} represents the component of $\mathbf{I}_{Cl}$ along $\mathbf{B}$ in the high field approximation. Deuteration of the chloracetamide amino group showed that the amino protons contributed a small hyperfine coupling of 13 Mc or less. One proton showed a large hyperfine coupling of 85 Mc maximum. The other protons having small hyperfine interactions could not be identified but may be from adjacent molecules hydrogen bonded to the chlorine atom. Hyperfine structure from the nitrogen nucleus could not be resolved but contributed to the line width. The radical was tentatively identified as $\cdot CHClCOOH$ or $\cdot CHClCONH_2$.

[1] H. C. Allen, Jr., J. Am. Chem. Soc. **74**, 6074 (1952).

G7. Electro Spin Resonance Studies of Radicals Formed by X-Irradiation of Amino Isobutyric Acid: Motional Effect in Free Radical Spectra. MINORU FUJIMOTO AND ROGER P. KOHIN, *University of Maryland,* AND ROY S. ANDERSON, *Clark University.*—Electron spin resonance studies were made between 10° and 300°K on the single crystal of amino isobutyric acid irradiated by x rays at room temperature. The spectrum showed a reversible change with temperature. At room temperature the spectrum consisted of seven sharp isotropic hyperfine components having a nearly binomial intensity distribution, from which the radical was identified as $(CH_3)_2\dot{C}$-COOH. As the temperature was lowered, this pattern gradually broadened and then changed to a strongly anisotropic spectrum below 50°K. This change can be interpreted as an effect of restricted motion of the two methyl groups in the radical. A determination of the possible structure of the radical in the low temperature phase was attempted from the analysis of hyperfine structure.

G8. Electron Spin Resonance of Irradiated Rutile.* C. G. YOUNG, A. J. SHUSKUS, AND O. R. GILLIAM, *University of Connecticut*, AND P. W. LEVY, *Brookhaven National Laboratory*.—At least ten radiation-induced electron spin resonances have been observed in clear Linde rutile which has been gamma irradiated at 77°K. The observations were made at 77°K using the sample as a dielectric X band cavity resonator. Four lines are of comparable intensity and much more intense than the others. Bleaching and annealing behavior of these indicate two different paramagnetic centers, each in two nonequivalent sites. For this high field pair, $g_x[110]=1.92\pm0.01$, $g_y[1\bar{1}0]=1.89\pm0.01$, $g_z[001]=1.80\pm0.01$; for the low field pair, $g_x=2.00\pm0.01$, $g_y=4.50\pm0.01$, $g_z=3.43+0.01$. These lines have anisotropic linewidths varying from 15 to 50 gauss. Brief exposure to room light causes bleaching, at different rates, of each of these pairs. The irradiation also causes the Fe^{3+}, Cr^{3+}, plus about forty other impurity lines to decrease in size, while bleaching or annealing reverses the process. Another pair of radiation-induced lines, each about one gauss wide, showing a weak multiline hyperfine structure, has $g_x=1.964\pm0.001$, $g_y=1.914\pm0.001$, $g_z=1.935\pm0.001$. This center also anneals away readily. All of the radiation-induced effects could also be observed by irradiation for a few hours at 77°K by an unfiltered uv low-pressure mercury lamp. These results and their interpretations will be discussed.

* Supported by the U. S. Atomic Energy Commision.

G9. Effect of Buffer Gases on Atomic Hyperfine Frequencies.* GEORGE A. CLARKE, *Columbia University*.—Recent experiments on the effect of buffer gases (B) on the atomic hyperfine frequencies of the hydrogen isotopes show a dependence of the fractional frequency shift $\Delta\nu/\nu_0$ on the buffer gas and the hydrogen isotope. In principle, the fractional frequency shift, as a function of the internuclear coordinates $\mathbf{R}$, is obtained from the expectation value of the hyperfine Hamiltonian using, in the two body collision approximation, an appropriately antisymmetrized system wave function $\Psi_{H-B}(\mathbf{r}_e;\mathbf{R})$. The quantity of physical interest, the statistically averaged frequency shift, can be computed classically using the intermolecular energies associated with the system wave function. This procedure has been carried out for the H-He system using as an approximation to the system wave function the antisymmetrized product of $1s$ state orbitals. The calculation results in a fractional frequency shift which is in good agreement with experiment. Corrections to the classical distribution function for this near-classical system have been made in order to ascertain the nature of the mass dependence. For this most favorable system calculation shows that the quantum statistical correction is small ($\sim2\%$).

* Supported by the U. S. Air Force Office of Scientific Research.

G10. Radio-Frequency Zeeman Transitions in the $2^3P_{2,1}$ States of He^4.* B. B. AUBREY, L. Y. CHOW, VERNON W. HUGHES, AND R. SWIFT, *Yale University*.—The optical-rf atomic beam magnetic resonance method has been used to observe rf transitions between the Zeeman sublevels of the $2^3P_{2,1}$ states of helium in weak magnetic fields. A beam of helium atoms in the metastable 2^3S_1 state is formed. The C-field region is illuminated with resonance radiation for the $2^3S\rightarrow2^3P$ transition so that atoms are excited to the 2^3P states in which thay have a lifetime of about 10^{-7} sec. The excitation of the atoms to the ^3P states and their subsequent decay back to the $^3S_1$ state produces a "light flop." While the atoms are in the 2^3P states they are subjected to a radio-frequency magnetic field so that transitions are induced between the Zeeman sublevels of the 2^3P states and can be observed as changes in the light flop. At the weak magnetic fields of 10 to 30 gauss employed, the transitions between the ^3P Zeeman sublevels and those between the $^3S_1$ Zeeman sublevels are not completely resolved, and the observed line shape is not a simple superposition of independent Zeeman transitions in the ^3P and $^3S_1$ levels, but indicates interference effects which must arise from the strong coupling by optical and radio-frequency fields between all the states.

* This research has been supported in part by the U. S. Air Force Office of Scientific Research.

TUESDAY MORNING AT 9:30

Continental Room

(D. A. BROMLEY presiding)

Nuclear Reactions, III

GA1. Excitation Function of the $O^{16}(\alpha,\alpha'\gamma)O^{16}$ Reaction.* W. E. HUNT, M. K. MEHTA, R. H. DAVIS, AND J. W. NELSON, *Florida State University*.—Excitation function for the reaction $O^{16}(\alpha,\alpha'\gamma)O^{16}$ has been measured for α-particle bombarding energies (lab) from 10.0 Mev to 16.5 Mev by observing the yield of the 6.14-Mev γ ray and the unresolved 6.92-Mev and 7.12-Mev γ rays from the second, third, and fourth excited states in O^{16}, respectively, using a 3-in.×3-in. NaI crystal at 0° with respect to the α beam. Prominent peaks in the yields of 6.14-Mev γ ray occur at 11.97, 12.76, 13.27, 14.42, 14.85, 15.73, and 16.07 Mev α-particle energy (lab) which correspond to the energy levels in Ne^{20} at 14.33, 14.96, 15.37, 16.29, 16.63, 17.33, and 17.61 Mev, respectively. Peaks in the combined yield of 6.92 and 7.14 γ rays occur at 12.02, 12.51, 12.76, 13.69, 14.53, 14.85, 15.51, and 16.07-Mev α-particle energy (lab). These correspond to levels in Ne^{20} at 14.37, 14.76, 14.96, 15.70, 16.37, 17.16, and 17.61 Mev. Peaks in the two yields do not always occur at the same energy, indicating that the α particles from the same level in compound nucleus Ne^{20} do not always populate all the three levels in O^{16}. The levels seen in this work are in good agreement with those seen in yields of α_0, α_γ, α_1, α_2, α_3, in the reaction $F^{19}(p,\alpha)O^{16}$ reported earlier.[1]

* Supported in part by the U. S. Air Force Office of Scientific Research.
[1] F. Ajzenberg-Selove and T. Lauritsen, Nuclear Phys. 11, 1 (1959).

GA2. Lifetimes of the Low-Lying Levels of O^{18} and F^{18}. A. E. LITHERLAND, *Clarendon Laboratory, Oxford*,* AND B. ADAMS, D. ECCLESHALL, AND M. YATES, *Atomic Weapons Research Establishment, Aldermaston*.—Excited O^{18} and F^{18} nuclei traveling at about 10^9 cm/sec have been produced by bombarding tritium with 11- to 16-Mev oxygen ions from the Aldermaston Tandem Accelerator. The attenuation of the doppler shifts, of the gamma rays from the decay of these excited nuclei, have been observed when the nuclei were slowed down in magnesium and copper.[1] By using recent data[2,3] on the specific loss of heavy ions in solids it was possible to interpret the observed doppler shifts in terms of the mean lives of the nuclear levels involved.[4] The mean lives of the

1.98, 3.63, and 3.93 levels in O^{18} were found to be 3 ± 1, 2.2 ± 0.6, and ≤0.3 picoseconds, respectively. In F^{18} the mean lives of the 0.94, 1.04, 1.70, 2.10, and 2.53 Mev levels were ≥4, ≤0.4, 2.0 ± 1.0, 0.8 ± 0.3, and 1.2 ± 0.4 psec, respectively.

* Seconded from the Chalk River Laboratories, Atomic Energy of Canada, Ltd.
[1] The thin tritium in titanium (100 $\mu g/cm^2$) targets deposited on magnesium and copper were supplied by Dr. E. J. Wilson, Radiochemical Laboratory, Amersham, England.
[2] D. I. Porat and K. Ramavataran, Proc. Roy. Soc. (London) A252, 394 (1959).
[3] P. G. Roll and F. E. Steigert, Nuclear Phys. 17, 54 (1960).
[4] S. Devons, G. Manning, and D. St. P. Bunbury, Proc. Phys. Soc. (London) A68, 18 (1955).

GA3. Lifetime of the 4.25-Mev Level in Ne^{20}. M. A. CLARK, H. E. GOVE, AND A. E. LITHERLAND, *Chalk River Laboratories.*—The reaction $C^{12}(C^{12}\alpha\gamma)Ne^{20}$ using carbon ions up to 21 Mev from the Chalk River tandem accelerator is being employed to study properties of levels in Ne^{20} and, in particular, thier lifetimes by the Doppler shift method.[1] Alpha particles were measured at 0° to the beam in a *p-n* junction counter and the spectra of gamma rays in coincidence with particular alpha groups were measured in a large NaI(Tl) crystal at angles from 0° to 135° to the beam. In the cascade de-excitation of the 4.25-Mev level in Ne^{20} it was found that the ratio of the energy of the 2.62-Mev gamma ray to that of the 1.63 Mev varied with angle as $1+(0.007\pm0.002)\cos\theta$ when 18-Mev incident carbon ions were used and the recoiling Ne^{20} ions were stopped in aluminum. From this result and the measured mean life of the 1.63-Mev level of $7.6\pm3.3\times10^{-13}$ sec[2] an upper limit of 5×10^{-13} sec is obtained for the mean life of the 4.25-Mev level. Other properties of the levels in Ne^{20} at 4.25, 4.97, and 5.63 Mev obtained from these measurements will be discussed.

[1] Litherland, Adams, Eccleshall and Yates (preceding abstract).
[2] Devons, Manning, and Towle, Proc. Phys. Soc. (London) A69, 173 (1956).

GA4. $O^{18}(p,d)O^{17}$ Reaction.* J. C. LEGG, *Princeton University.*—Enriched Al_2O_3 targets, containing 90.2%, were bombarded by 17.6-Mev protons from the Princeton University cyclotron. Protons, deuterons, and tritons were separated from each other by means of a pulse multiplier used with a dE/dx, E counter telescope. A proportional counter was used as the dE/dx counter, and both NaI and diffused junction silicon detectors were used as the E counter. Deuterons were observed going to the ground state and the first two excited states of O^{17} with $l=2$, 0, 1 angular distributions, respectively. Absolute cross sections for the ground state and first excited state deuterons were in reasonable agreement with the results of the $O^{18}(d,t)O^{17}$ experiment of Armstrong and Quisenberry.[1] Tritons leading to the ground state of O^{16} were observed with an angular distribution consistent with an $l=0$ assignment.

* This work was supported by the U. S. Atomic Energy Commission and the Higgins Scientific Trust Fund.
[1] J. C. Armstrong and K. S. Quisenberry, Phys. Rev. (to be published).

GA5. (Abstract withdrawn.)

GA6. Gamma Radiation from Ne^{20}.* W. W. EIDSON,† R. D. BENT, AND R. A. LA SALLE *Indiana University.*—A search has been made for states of Ne^{20} with excitation energies between 5 and 10 Mev which decay predominately by gamma emission. Excited states in this energy range are unbound to alpha emission and will decay predominately by gamma emission only if they have "unnatural" (0^-, 1^+, 2^-, 3^+, 4^-, 5^+, $\cdots$) spin and parity. The $Ne^{20}(\alpha,\alpha'\gamma)$ reaction was studied using particle-gamma coincidence techniques and the 22-Mev alpha particle beam from the Indiana University cyclotron. Several gamma-emitting states have been discovered in the 5–19-Mev energy range which appear to decay predominately to the 4.2- or 4.9-Mev states.

* Supported by the joint program of the Office of Naval Research and the U. S. Atomic Energy Commission.
† National Science Foundation predoctoral Fellow.

GA7. Elastic Scattering of 15-Mev Deuterons by Light and Medium Weight Nuclei,* C. A. LOW, JR., AND K. S. QUISENBERRY, *University of Pittsburgh.*—A program has been started to investigate elastic scattering of 15-Mev deuterons using the magnetic spectrograph of the University of Pittsburgh cyclotron. The energy resolution of this detection system is such that the deuterons scattered from different elements in a mixed target can usually be separated at all but the lowest scattering angles. Deuterons scattered through laboratory angles from about 10° to 90° have been observed from carbon, oxygen, magnesium, aluminum, and potassium. A comparison has been made between natural Mg and Mg^{25}. Results from other individual isotopes will also be discussed. Aluminum was studied with an incident energy spread which was varied from about 40 kev to 450 kev, and no differences were observed. Plots of the ratio of the scattering cross section to the calculated Rutherford cross section show a marked diffraction-like pattern in most cases. Some, such as potassium, differ greatly from the more usual pattern. The aluminum results agree substantially with those of Cindro and Wall.[1]

* Work done in the Sarah Mellon Scaife Radiation Laboratory and assisted by the program of the Office of Naval Research.
[1] Nikola Cindro and N. S. Wall, Phys. Rev. 119, 1340 (1960).

GA8. Collective Enhancement in $Mg^{24}(p,p')$.* E. ROST† AND N. AUSTERN, *University of Pittsburgh,* AND G. R. SATCHLER, *Oak Ridge National Laboratory.*—The differential cross section for the excitation of the first excited state of Mg^{24} by the inelastic scattering of 18-Mev protons has been calculated on a direct interaction model using the distorted wave Born approximation. It was found that the magnitude of the cross section could not be explained by any reasonable single-particle or surface-interaction model. However, a more complete interpretation using rotational-model wave functions and a sum of two-body interactions[1] proved to be successful in fitting the magnitude, as well as the general features of the angular distribution, without any unknown parameters. The two-body interaction used was a simple central potential which fits low-energy $^1S_0$ nucleon-nucleon scattering. The optical potentials used were those which fit the elastic scattering data. All the nucleons in Mg^{24} were found to contribute to the inelastic scattering.

* Work done in the Radiation Laboratory and assisted by the joint program of the Office of Naval Research and the U. S. Atomic Energy Commission.
† National Science Foundation Cooperative Graduate Fellow.
[1] W. T. Pinkston and G. R. Satchler, *Proceedings of the International Conference on Nuclear Structure,* edited by Bromley and Vogt (University of Toronto Press, Toronto).

GA9. Experimental Nuclear Energy Levels of Mg^{25} and Their Interpretation,* R. K. SHELINE AND R. A. HARLAN, *Florida State University.*—Using the reaction $Al^{27}(d,\alpha)Mg^{25}$ and a magnetic spectrograph 66 levels in Mg^{25} have been determined below 8.7-Mev excitation. An interpretation of the levels utilizing the Bohr-Mottelson collective model will be presented. Results indicate that below 4.8 Mev, agreement

with the model is good, while above this energy, deviations from experimental level density and energies can be qualitatively explained by additional intrinsic and vibrational states, Coriolis coupling, and the uncoupling of paired nucleons in higher-spin rotational states. A statistical treatment,[1] used in determining the nuclear temperature of Mg^{25} as ≈ 2.45 Mev, indicates that the average level spacing begins to become smaller than experimental energy resolution above 7.7 Mev.

* Supported in part by the U. S. Office of Ordnance Research and the U. S. Atomic Energy Commission.
[1] T. Ericson, Nuclear Phys. 11, 481 (1959).

GA10. Mean Life of the 1.61-Mev Level of Mg^{25}.* V. K. RASMUSSEN, F. R. METZGER, AND C. P. SWANN, *Bartol Research Foundation.*—Reasons for regarding the 1.61-Mev level of Mg^{25} and the 2.21-Mev level of Al^{27} as the second, $\frac{3}{2}^+$, members of the $K=\frac{5}{2}^+$ rotational band based on the ground state have recently been reviewed by Gove.[1] We have measured the mean life of the 1.61-Mev level using nuclear resonance fluorescence techniques. The $Mg^{25}(p,p')$ reaction, with 4-Mev protons from the Bartol-ONR generator on Mg^{25} targets, was found to be a suitable source of the exciting γ radiation. Form the self-absorption of the resonance radiation, and assuming spin $\frac{3}{2}$, $\tau=(2.5_{-0.4}{}^{+0.6})\times 10^{-14}$ sec. The angular distribution of the resonance scattering was found to be $1+(0.42\pm 0.03)P_2 +(0.03\pm 0.01)P_4$. Neglecting possible polarization of the incident radiation, this corresponds to an $E2/M1$ amplitude ratio of $\delta=-0.19\pm 0.015$ and a value of $B(E2)/B(E2)_{SP}$ of 6.5. According to Gove, Lemberg's revised value[1] for this ratio, as measured by Coulomb excitation, is 5. Collective effects are thus implied. If the spin of the 2.21-Mev level of Al^{27} is taken as $\frac{7}{2}^+$, then the work of Metzger *et al.*[2] gives $B(E2)/B(E2)_{SP}=4.9$ for $\delta=+0.5$, but only 0.16 for $\delta=-0.08$. More direct evidence as to the spin of these levels is desirable.

† Assisted by the Office of Naval Research.
[1] H. E. Gove, International Conference on Nuclear Structure, Kingston, 1960.
[2] Metzger, Swann, and Rasmussen, Nuclear Phys. 16, 568 (1960).

GA11. Excitation Curves for the Reactions $Mg^{24}(n,p)Na^{24}$ and $Cu^{65}(n,p)Ni^{65}$. J. P. BUTLER AND D. C. SANTRY, *Chalk River Laboratories* (introduced by L. G. Elliott).—Fast neutron cross sections for the reactions, $Mg^{24}(n,p)Na^{24}$ and $Cu^{65}(n,p)Ni^{65}$ have been measured by the activation method for neutron energies from 5.7 to 20.4 Mev relative to the known cross section of the $S^{32}(n,p)P^{32}$ reaction.[1] Monoenergetic neutrons were obtained from the $D(d,n)He^3$ and $T(d,n)He^4$ reactions, using a Tandem Van de Graaff accelerator. By irradiating samples at definite angles to the deuteron beam relative cross sections in the energy range 12.5 to 20.4 Mev were obtained by employing the known neutron angular distribution of the $T(d,n)He^4$ reaction.[2] These data were normalized at 14.5 Mev to the $S(n,p)$ cross section. The $Mg(n,p)$ cross section rises rapidly from 5.7 to 8.0 Mev and then it increases slowly reaching its maximum value of 190 ± 10 mb in the region of 14 Mev. The $Cu(n,p)$ cross section increases slowly from 5.7 Mev and reaches its maximum value of 11 ± 1 mb at 10 Mev.

[1] L. Allen, Jr., W. A. Biggers, R. J. Prestwood and R. K. Smith, Phys. Rev. 107, 1363 (1957).
[2] S. J. Bame, Jr., and J. E. Perry, Jr., Phys. Rev. 107, 1616 (1957).

GA12. Radiative Capture of Protons by Mg^{25}.* F. W. PROSSER, JR., D. H. NEHER, AND R. W. KRONE, *University of Kansas.*—The γ-ray spectra resulting from proton capture by Mg^{25} have been measured for 20 resonances in the range of proton bombarding energies from 0.956 Mev to 1.717 Mev. Of these, the complete spectrum of only the resonance at 0.956 Mev has been investigated previously.[1] The spectra are in general complex and involve several of the lower-lying states in Al^{26}. The branching ratios for these states as determined by Green, *et al.*,[1] were used in the preliminary analysis of the pulse height distributions. The stronger cascades observed and the proton energies, in Mev, of the resonances at which they were predominant are as follows: compound state → 2.07-Mev state → 0.42-Mev state → ground state (0.956, 1.197, 1.634, and 1.701); c.s. → 4.19 → 0.42 → g.s. (1.207, 1.240, and 1.377); c.s. → 0.42 → g.s. and c.s. → g.s. (1.028, 1.046, 1.086, 1.150, 1.166, 1.589, 1.652, and 1.717); c.s. → 1.76 → 0.42 → g.s. (0.987); c.s. → 3.16 → several states (1.527); unassigned (1.105, 1.138, and 1.285). At all of the resonances weaker transitions were observed which leave the Al^{26} in its 0^+ isomeric state. Coincidence spectra are being obtained to complete the identification of the weaker transitions and to confirm the branching ratios of the lower-lying states. Angular distributions will be obtained to allow spin and parity assignments to be made for the several compound states and previously unassigned lower states in Al^{26}.

† Supported in part by the U. S. Atomic Energy Commission.
[1] L. L. Green, J. J. Singh, and J. C. Willmott, Proc. Roy. Soc. (London) A69, 335 (1956).

GA13. Gamma-Ray Resonance Yields from Aluminum Bombarded by Hydrogen Molecular Ions.* D. G. COSTELLO, W. L. WALTERS, AND R. G. HERB, *University of Wisconsin.*—In previous work on the $Al^{27}(p,\gamma)Si^{28}$ reaction by Dahl, Costello, and Walters[1] the curious asymmetry and resonance energy shift in yield curves taken with diatomic hydrogen ions was investigated. To fit the curves the electron accompanying the ion is assumed to be torn away instantaneously upon impact with the target and the mutual Coulomb repulsion of the protons alters their laboratory energies enough to appreciably distort the yield curves. New experimental data at higher energy resolution have revealed more structure in the yield curves. The earlier analysis has been extended to take into account higher vibrational states of the ion and the different internuclear separations of the constituent protons prior to break-up. Results of the analysis are compared with the data.

* Work supported by the U. S. Atomic Energy Commission and the Wisconsin Alumni Research Foundation.
[1] P. F. Dahl, D. G. Costello, and W. L. Walters, Nuclear Phys. 21, 106 (1960).

GA14. Studies of (p,α) Reactions up to 12 Mev.* H. S. ADAMS, J. D. FOX, N. P. HEYDENBURG,† AND G. M. TEMMER,† *Florida State University.*—We have studied the excitation curves and some angular distributions of alpha particles from $Al^{27}(p,\alpha)Mg^{24}$ (at least 7 states in Mg^{24}) and $Na^{23}(p,\alpha)Ne^{20}$ (at least four groups). A small Si junction counter was used as a detector. Strong resonances are still observed in the region of 20-Mev excitation energy in Si^{28}. We are extending this survey to heavier nuclei.

* Supported in part by the U. S. Air Force Office of Scientific Research.
† Also DTM, Carnegie Institution of Washington.

GA15. Gamma Radiations from Low Levels of Al^{27}.† R. D. BENT AND W. W. EIDSON, *Indiana University.*—The $Al^{27}(\alpha,\alpha',\gamma)$ reaction was investigated using particle-gamma coincidence techniques and the 2.2-Mev alpha particle beam from the Indiana University cyclotron. A strong 0.79 ± 0.03-Mev gamma ray transition between the 3.0- and 2.21-Mev states of Al^{27} was observed. This result, together with other data,[1] suggests that the 3.0- and 2.2-Mev states are the $9/2^+$ and $\frac{7}{2}^+$ members of a rotational band based on the $\frac{5}{2}^+$ ground state.

† Supported by the joint program of the Office of Naval Research and the U. S. Atomic Energy Commission.
[1] E. Almqvist, D. A. Bromley, H. E. Gove, and A. E. Litherland, Nuclear Phys., 19, 1 (1960).

TUESDAY MORNING AT 9:30

Cotillion Room, South

(J. B. MARION presiding)

Fast Neutrons

H1. Angular Distribution of Fast Photoneutrons.* G. C. REINHARDT AND W. D. WHITEHEAD, *University of Virginia.*—The angular distribution of photoneutrons with energies above the ($Si^{28}n,pAl^{28}$) threshold has been measured for several elements between yttrium and bismuth, using 55-Mev bremsstrahlung from the University of Virginia 70-Mev synchrotron. Neutrons were detected at nine angles from 30° to 150° by cylindrical containers holding 50 g of pure silicon, and the 2.54-min Al^{28} activity was measured with geiger counters. Angular distributions were anisotropic and showed marked forward asymmetry. A least squares fit of the data to curves of the type $A+B\sin^2\theta+C\cos\theta$ showed B somewhat smaller and C larger than values determined at lower bremsstrahlung energies. There is evidence in support of previously reported peaking of the ratio B/A at $N=82$ and 126.

* Supported by the U. S. Air Force Office of Scientific Research.

H2. Time-of-Flight Measurements of Photoneutron Energy Spectra in the Kilovolt Region. I. Technique and the (n,γ) Cross Section of Ag.* D. B. MCCONNELL, W. BERTOZZI, P. T. DEMOS, C. P. SARGENT, AND W. TURCHINETZ, *M.I.T.*—A modification of the time-of-flight technique developed at the M. I. T. Linear Accelerator[1,2] has allowed measurements to be undertaken in the kilovolt region of neutron energy spectra produced by nuclear photodisintegration. Neutron flight times over a 1.6-m flight path are measured with a timing resolution of about 10^{-8} sec. Neutrons are detected with the aid of large liquid scintillators, by the (n,γ) reaction in silver. The technique will be described. Using the known $Be^9(\gamma,n)$ cross section results will be presented for the energy dependence of the (n,γ) cross section of silver in the energy range 10–500 kev.

* This work is supported in part by the U. S. Atomic Energy Commission, the Office of Naval Research, and the Air Force Office of Scientific Research.
[1] W. Bertozzi, Ph.D. Thesis M.I.T., 1958 (unpublished).
[2] F. R. Paolini, Ph.D. Thesis, M.I.T., 1960 (unpublished).

H3. Time-Of-Flight Measurement of Photoneutron Energy Spectra. II. Spectra from Pb and Bi in the Kilovolt Region.* W. TURCHINETZ, W. BERTOZZI, P. T. DEMOS, D. B. MCCONNELL, AND C. P. SARGENT, *M.I.T.*—The technique described in the preceeding abstract has been used to extend to the kilovolt region the earlier measurements of photoneutron energy spectra from Pb and Bi.[1] The neutron spectra produced by the absorption of 10-Mev bremsstrahlung have been measured from 10–500 kev. Several lines appear in the Pb spectrum at about (20), (30), 40, 95, (120), 180, and 250 kev. The Bi spectrum is almost smooth. Data will be related to the results of other experiments.[2,3] The implications of such measurements in the determination of $\Gamma_{\gamma 0}$ and D will be discussed.

* This work is supported in part by the U. S. Atomic Energy Commission, the Office of Naval Research, and the Air Force Office of Scientific Research.
[1] W. Bertozzi, F. R. Paolini, and C. P. Sargent, Phys. rev. 110, 790 (1958).
[2] K. Reibel and A. K. Mann, Phys. Rev. 118, 701 (1960).
[3] Karlsruhe Photonuclear Conference, 1960, I5.

H4. Differential Elastic Scattering of 15.2-Mev Neutrons by Ta, Th, and U.* C. I. HUDSON, JR., AND W. SCOTT WALKER, *University of Virginia.*—A need for additional data from (d,t) neutrons elastically scattered by deformed heavy nuclei has prompted a measurement of the elastic angular distributions of 15.2 Mev neutrons on Ta, Th, and U. The associated particle technique was used with a time-to-pulse-height converter to measure the time of flight of neutrons over a distance of 179 cm. The percent energy resolution at 15.2 Mev was 16%. The neutron detector was a 13-cm diam by 15-cm long plastic scintillator. Cylindrical scatterers were used and angular distributions were taken from 10° to 162° in 2° to 10° intervals. For comparison with a spherical nucleus, the angular distribution for Bi was also measured. The data were corrected for finite geometry and multiple scattering. Several thicknesses of Ta and Bi were used to check the multiple scattering corrections. Estimates were made of the contributions due to inelastic scattering from low-lying levels. The data will be compared with optical model computations.

* Supported jointly by the U. S. Army Office of Ordinance Research and the U. S. Atomic Energy Commission.

H5. Total Neutron Cross Section of the Isotopes of Selenium. H. MUENZER,* K. NISHIMURA,† AND W. M. GOOD, *Oak Ridge National Laboratory.*—The total cross section of Se^{76}, Se^{77}, Se^{78}, Se^{80}, and Se^{82} for neutrons has recently been measured in the energy range 4 kev to about 50 kev. The average resolution was 12 nsec/min. The resonances in Se^{77} were small and the sample thin, so that no structure was observed, only an average cross section in the neighborhood of 6 b. Resonances were observed in the other isotopes as follows:

Se^{76}: 4.95, 5.95, 6.60, 7.80, 9.25, 12.9, 24.5, 34.8
Se^{78}: 5.70, 8.50, 10.0, 17.0, 26.8, 29.2, 31.0, 32.5, 40.0, 45.0
Se^{80}: 3.96, 4.84, 11.7, 18.3, 20.9, 24.0, 30.0, 40.4, 48.0
Se^{82}: 6.60, 13.8, 23.0, 26.5

Results of analysis of these resonances cannot be given in this abstract. It is perhaps worth observing, however, that the trend of level spacing in these isotopes with number of neutrons is parallel to that in the case of the germanium isotopes. This and other comparisons between germanium and selenium will be given.

* H. Muenzer, Visiting Investigator from the Institut fuer Radiumforschung und Kernphysik, der Oesterreichischen Akademie der Wissenschaften, Vienna, Austria.
† K. Nishimura, Visiting Investigator from Japan Atomic Energy Research Institute, Tokoyo, Japan.

H6. Neutron Total Cross Section of Pb^{208} with 3-kv Resolution. J. L. FOWLER AND E. C. CAMPBELL, *Oak Ridge National Laboratory.*—Since the total cross section of Pb^{208} measured with 10-kv resolution shows considerable unresolved structure in the 1–2 Mev range,[1] it is necessary to examine this region with better energy resolution. Therefore, the total cross section has been determined by the standard transmission technique with the $Li(p,n)$ neutron source about 3 kv thick over this neutron energy range. The samples (~120 g) were in the form of 1⅛-in.-diam cylinders of 99.75% Pb^{208}.[2] Neutrons were detected with approximately 10% efficiency by use of a stilbene crystal from which pulses due to gamma rays were depressed by means of the Brooks-Owen technique. Inscattering corrections to the data were calculated by use of published differential cross sections of normal lead, and corrections were made for the second group of $Li(p,n)$ neutrons. In the energy interval 1.0 to 1.9 Mev, at least 46 resonances were observed. These had peak cross sections corresponding to J values in the range ½ to ⅞. Widths of the resonances varied from less than 3 kev to ~100 kev.

[1] J. L. Fowler, E. G. Corman, and E. C. Campbell, *Proceedings of the International Conference on Nuclear Structure*, edited by D. A. Bromley and E. W. Vogt (The University of Toronto Press, Toronto, Canada, 1960), p. 474.
[2] The enriched Pb^{208} isotope was obtained from the Isotopes Division of the Oak Ridge National Laboratory.

H7. Spectra of γ Rays from Capture of (30±10) kev Neutrons. F. W. K. FIRK AND J. H. GIBBONS, *Oak Ridge National Laboratory.*—Current interest in the "direct capture" theory of Lane and Lynn[1] has prompted the measurement of γ-ray spectra from capture of (30±10) kev neutrons by Ag, Au, Cu, Fe, Lu, and Ni using a 9 in.×6 in. NaI(Tl) spectrometer. The ORNL 3-Mev pulsed Van de Graaff (10^{-8} sec proton burst, 700 μa peak current) has been used to produce (30±10) kev neutrons from the reaction $Li^7(p,n)Be^7$. Nanosecond time-of-flight techniques have enabled capture γ-rays from the sample to be distinguished from those produced by the Li target and those from capture by iodine in the crystal. By using flight paths of 50 cm from the Li target to the sample and from the sample to the NaI(Tl) crystal, it has been possible to measure γ-ray spectra of samples having capture cross sections ~20 mb. Transitions to the ground and low-lying states were observed in several cases and these preliminary results will be discussed.

* Now visiting Oak Ridge National Laboratory from Atomic Energy Research Establishment, Harwell, England.
[1] A. M. Lane and J. E. Lynn, Nuclear Phys. **17**, 563 (1960).

H8. Average Neutron Cross Sections in the kev Region.* K. K. SETH, R. H. TABONY, L. W. WESTON, AND H. W. NEWSON, *Duke University.*—Average neutron total cross sections for Cu, Zn, Zr, Na, Mo, Sn, Rh, Pd, Ag, Cd, Gd, Nd, Pt, Au, and Tl as determined in the energy region 1 to 650 kev[1] have been analyzed for the statistical parameters $\langle \Gamma_n^{(1)}/D \rangle$ and R'. A discussion is presented of the various methods which have been proposed[2-4] for analysis of average cross sections and the results for $\langle \Gamma_n^{0}/D \rangle$, $\langle \Gamma_n^{(1)}/D \rangle$ and R' are discussed in terms of the optical model.

* Work supported by the U. S. Atomic Energy Commission.
[1] K. K. Seth, E. G. Bilpuch, and H. W. Newson, Bull. Am. Phys. Soc. **5**, 18 (1960).
[2] D. J. Hughes, R. L. Zimmerman, and R. E. Chrien, Phys. Rev. Letters **1**, 461 (1958).
[3] R. G. Thomas, Phys. Rev. **97**, 224 (1955).
[4] K. K. Seth, Revs. Modern Phys. **30**, 442 (1960).

H9. Elastic and Inelastic Scattering of 6-Mev Neutrons.* R. M. WILENZICK, K. K. SETH, P. R. BEVINGTON, AND H. W. LEWIS,† *Duke University.*—The angular distributions of neutrons scattered from C, Fe, Y, Mo, Sn, Cd, and Bi have been measured using a pulsed beam time-of-flight system for an incident neutron energy of 6 Mev. A gamma ray discriminator utilizing pulse shape discrimination in a liquid scintillator was successfully used to eliminate tube noise and gamma ray background. Energy distributions of the emitted neutrons were taken in 10° intervals for angles between 20° and 140°. Absolute differential elastic and inelastic cross sections were determined by comparison with the differential n-p scattering cross section and by using Fe as a secondary standard. Results of the analysis of the experiment will be compared with predictions of the statistical theory.

* Work supported by the U. S. Atomic Energy Commission.
† Now on leave at the American University of Beirut, Beirut, Lebanon.

H10. Neutron Time-of-Flight Spectrometer.* R. R. BORCHERS, H. W. LEFEVRE, AND C. H. POPPE, *University of Wisconsin.*—A fast neutron time-of-flight spectrometer has been constructed for use with the tandem electrostatic accelerator. The beam pulses obtained by chopping the negative ion beam prior to entry into the accelerating tube had a minimum duration of 4 nsec measured both before and after acceleration. The length of the pulse is determined by the energy spread in the negative ion beam. Shorter bursts are obtained by chopping the accelerated beam, although the deflected beam increases background. Chopping both before and after acceleration reduces background substantially. A dc bias applied to the negative ion deflection plates allows suppression of either of the two beam bursts associated with each rf cycle by a factor of 1000. This improves the accuracy of charge integration and reduces the problem of spectral overlap. Beam bursts with a peak current of 2 μa and a duration of less than 2 nsec are obtained. Time intervals are measured with a vernier chronotron.[1] A commercial 256-channel memory is used for storage. Over-all time resolution is 2.5 nsec.

* Work supported by the U. S. Atomic Energy Commission and the Wisconsin Alumni Research Foundation.
[1] H. W. Lefevre and J. T. Russel, Rev. Sci. Instr. **30**, 159 (1958).

H11. Deuteron Breakup.* H. W. LEFEVRE, R. R. BORCHERS, T. H. MAY, AND W. BENENSON, *University of Wisconsin.*—Spectra of neutrons produced by breakup of deuterons on the hydrogen and helium isotopes have been obtained by time-of-flight spectrometry. The hydrogen, deuterium, and helium spectra were obtained at deuteron energies of 8, 9, and 10 Mev at laboratory angles up to 70°. The tritium and helium-3 spectra were observed at 0° for a deuteron energy of 6.7 Mev. Gas target thickness for most of the measurements was two atmosphere centimeters and the energy resolution used was 1.7 nsec/m. Neutrons were detected in a Pilot B plastic scintillator 7.6 cm in diameter by 2.5 cm thick mounted on a RCA 7046 photomultiplier tube. The detector bias level was maintained at about 1 Mev. All of the angular distributions showed strong forward peaking of the breakup neutrons. The continuous neutron spectrum from deuterons on tritium was observed to have two maxima.

* Work supported by the U. S. Atomic Energy Commission and the Wisconsin Alumni Research Foundation.

H12. Activation Cross Sections for 14.5-Mev Neutrons for B^{11}, O^{16}, Al^{27}, and F^{19}. JUHANI KANTELE, *University of Arkansas* (introduced by R. W. Fink).—In the present work a few activation cross sections for 14.5±0.8 Mev have been measured. By using a pneumatic transport equipment, end-window beta proportional counter, and thin powder samples, the following cross-section values were obtained, the value 556 mb[1] for $Cu^{63}(n,2n)$-reaction having been used as a standard: $B^{11}(n,p)$, 3.2±0.4 mb; $O^{16}(n,p)$, 39±4 mb. The former value is in excellent agreement with a recent work.[2] The important cross section for $Al^{27}(n,p)$ was studied by three different methods, namely, by comparing activities induced in Al and Cu foils, and in Al_2O_3 powder, using beta proportional counter, and with the aid of gamma decay of activities produced in Al_2O_3. Weighted mean result from these was 87±8 mb which agrees with the 4π-counter work of YASUMI.[1] From irradiations of AlF_3 powder and Teflon, the cross-section values 16.5±2 mb and 57±7 mb were obtained for $F^{19}(n,p)$ and $F^{19}(n,\alpha)$, respectively, using the above aluminum cross section as a standard. In all foregoing cases conventional corrections have been made before obtaining the cross-section values given.

[1] S. Yasumi, J. Phys. Soc. (Japan) **12**, 443 (1957).
[2] J. A. DeJuren and R. W. Stooksberry, Phys. Rev. **120**, 901 (1960).

H13. A Reproducible Precision Long Counter for Measuring Fast-Neutron Flux.* J. DE PANGHER, *General Electric Company, Hanford.*—A design[1] based on the Hanson-McKibben counter[2] was evolved and three precision long counters were constructed out of polyethylene and retaining structures. These counters designated as PLC-H-1, PLC-NBS-1 and PLC-H-2 were built at Hanford, at the National Bureau of Standards and at a commercial machine works. The use of a good quality BF_3 tube and a small retractable internal PuBe neutron source readily permits accurate standardization in different laboratories. Comparison tests with accelerator neutrons and with neutrons from radioactive sources showed that the responses of the counters agreed to within 1.2% before any alterations were made and to within 0.4% after the central

polyethylene core of PLC-H-2 was exchanged for another one. Performance characteristics will be discussed.

* This work was done under the auspices of the U. S. Atomic Energy Commission.
[1] Machine drawings are available from the Cooper-Trent Blueprint and Microfilm Corporation, 2701 Wilson Boulevard, Arlington 1, Virginia.
[2] A. O. Hanson and J. L. McKibben, Phys. Rev. 72, 763 (1947).

H14. $(n,2n)$ Reactions in Cu^{63}, Ag^{107}, and Sb^{121}.* L. A. RAYBURN, *Argonne National Laboratory and University of Georgia.*—Cross sections for the $(n,2n)$ reaction in Cu^{63}, Ag^{107}, and Sb^{121} have been measured for incident neutron energies from 12 to 19.5 Mev. The two 511-kev gamma rays from the annihilation of positrons in the irradiated samples were counted in coincidence by using two NaI scintillation spectrometers. For Cu^{63}, the value of this cross section varied from 65 to 675 mb; for Ag^{107}, from 600 mb to a maximum of approximately 925 mb at an incident neutron energy of 15 Mev and then decreased to about 700 mb; for Sb^{121}, from 700 mb to a maximum of approximately 1050 mb at an incident neutron energy of 15 Mev and then decreased to about 800 mb. Where these measurements overlap those of other investigators, the values are in general agreement.

* Work performed under the auspices of the U. S. Atomic Energy Commission.

TUESDAY MORNING AT 9:45

Sheraton Hall

(V. JACCARINO presiding)

Invited Papers

HA1. Nuclear Matrix Elements from Beta-Gamma Nuclear-Spin Correlations. R. W. HAYWARD, *National Bureau of Standards.* (30 min.)

HA2. Atomic Beams and the Standard of Length. K. G. KESSLER, *National Bureau of Standards.* (30 min.)

HA3. Nuclear Size and Quadrupole Effects in Mossbauer Absorption. S. DE BENEDETTI, *Carnegie Institute of Technology.* (30 min.)

HA4. Interpretation of the Isomer Shift of Iron 57. L. R. WALKER, *Bell Telephone Laboratories.* (30 min.)

TUESDAY MORNING AT 9:45

Cotillion Room, North

(G. N. GLASOE presiding)

Accelerators

J1. Properties of Shapiro-Type Accelerator Pulsing System.* J. LOWE, J. V. KANE, AND M. A. EL-WAHAB,† *Brookhaven National Laboratory.*—A radio-frequency deflection system has been installed on the BNL 3-Mev Positive Ion Van de Graaff machine. Short bursts of radiation are produced by allowing the continuous beam to pass through an electrostatic focusing lens, then the RF deflection plates, and finally to impinge upon a slanted target. This is a special case of the method proposed by F. L. Shapiro.[1] The period between beam bursts is 130 nsec and the beam time on target is $\sim 10^{-10}$ sec for 2-Mev deuterons with an average current reduction to about 2% of the unswept value. Thus an effective beam compression of approximately 20 times is obtained by this method. Details of the construction and operating parameters of the system will be presented.

* Work performed under the auspices of the U. S. Atomic Energy Commission.
† On leave from the University of Alexandria, United Arab Republic.
[1] F. L. Shapiro, Instrumental and Exptl. Tech. U.S.S.R. 1, 33 (1957).

J2. Production of an 18-Mev Alpha Particle Beam in a Tandem Van de Graaff Accelerator.* E. B. CARTER AND R. H. DAVIS, *Florida State University.*—An analyzed beam of 8 mμa of He^{++} has been identified by gamma-rays the $Be^9(\alpha,n\gamma_{4.43})C^{12}$ reaction, by tracks in Ilford K2 plates of particles scattered from Au foils, and by the $C(\alpha,n)O^{16}$ reaction threshold. A mixture of helium and hydrogen is normally used in the duoplasmatron ion source, but the importance of hydrogen is not clear since significant traces have been found after four hours of operation of the unmodified ion source with the hydrogen inlet valve turned off. The beam from the negative ion source has a momentum consistant a He^+ assignment for beam from the duoplasmatron ion source and He^- from the charge exchange canal. The terminal voltage is consistant with a He^- beam in the first half of the tandem accelerator. Hydrogen as a charge exchange gas yields a beam 25% larger than air and five times larger than helium. Modifications of the ion source to study mixtures of gases will be discussed.

* Supported in part by the U. S. Air Force Office of Scientific Research.

J3. Multiple-Gap Spectrograph for Charged-Particle Reaction Studies.* H. A. ENGE AND W. W. BUECHNER, *M.I.T.*—An 11-ton magnetic iron ring with magnetizing coils and 25 gaps provide magnetic fields for 25 broad-range magnetic spectrographs simultaneously facing a target in the center of the ring. Gaps are 7.5° apart, accepting reaction products at from zero to 172.5° in 7.5° steps. Geometry of each gap and associated nuclear-track plateholder is similar to the MIT-broad-range, single-gap spectrograph.[1] An electrostatic quadrupole lens focuses a reduced image of the energy-defining slit for the electrostatic generator onto a rotating gas or solid target. The whole spectrograph is enclosed in a vacuum tank.

* This work has been supported in part with funds provided by the U. S. Atomic Energy Commission, by the Office of Naval Research, and by the U. S. Air Force Office of Scientific Research.
[1] C. P. Browne and W. W. Buechner, Rev. Sci. Instr. 27, 899 (1956).

J4. Analysis of the Loading the Beam of a Synchrotron on the Radio-Frequency Power Amplifier and Accelerating Cavity.* C. H. M. TURNER, J. H. MARTIN, T. DEPARRY, AND D. SHIRER, *Argonne National Laboratory.*—The relationship between the dynamics of a beam in a synchrotron, its bunching and phasing with respect to the rf voltage across the accelerating gap of a cavity is well known. The loading of the cavity by a bunched beam has received little attention, and is no longer negligible when the first harmonic component of the beam current through the accelerating gap is $\gtrsim$current flowing through the resistive component of the self-impedance of the cavity. An equivalent circuit is derived containing two independent current "sources" due to the power amplifier and beam current. The greater the beam intensity the further the inductance of the cavity should be tuned from resonance to maintain the same program of the rf voltage and beam phasing during an acceleration cycle. The currents delivered by, and the power dissipated at the anodes of the power amplifier can then be minimized. A simple measure of the distortion of the sinusoidal accelerating voltage waveform is obtained by assuming that the bunches are infinitely short.

* Research performed under the auspices of the U. S. Atomic Energy Commission.

J5. Broad-Range Spectrograph for Cyclotron. R. N. MATHUR AND E. BLEULER, *Purdue University.*—As part of the program of nuclear reaction studies, a broad-range magnetic spectrograph has been designed and built. The spectrograph has a uniform-field, sector type magnet (up to 17 000 gauss) with a gap width of 1 in. and is mounted to rotate about a horizontal axis passing through the target position at an angle of 77.5° to the beam direction. This provides a useful angular range 0° to 155°. Particles with radii of curvature between 35 and 53 cm in the magnetic field are detected in nuclear emulsion plates. With partial entrance-edge focussing the z-acceptance angle varies with increasing R from about 1° to 0.6° for a detector width of 0.5 in. The exit edge is designed to yield second-order focussing for three values of R. Preliminary measurements of the properties of the spectrograph have been made with thin Po^{210} α-particle sources. With maximum acceptance angles, peaks of half-widths less than 2 mm are obtained over the entire length of the photographic plates. The dispersion varies along the length of the plates, but is of the order of 0.1% in energy per mm.

J6. Shaped Drift Tubes for Proton Linear Accelerators.* R. L. GLUCKSTERN, *Yale University.*—Solutions of Maxwell's equations for an unloaded cylindrical cavity driven by isolated currents and charges are obtained. With judicious choice of cavity parameters one can enclose the region of charges and currents within a surface everywhere normal to the electric field. In this way one can obtain the resonant frequency of cylindrical cavities loaded with rounded drift tubes. The method is similar to that of Christofilos.[1] Several possible drift tube shapes have been calculated in connection with the design of a linear proton accelerator. Power loss calculations and resonant parameters will be compared with those of Walkinshaw[2] for both the 2π-mode and π-mode drift tube loaded cavities. The method has also been extended to wave guide structures with shaped irises.

* Supported in part by U. S. Atomic Energy Commission contract.
[1] N. C. Christofilos, CERN Symposium 1956, p. 176.
[2] Walkinshaw, Sabel, and Outram, Atomic Energy Research Establishment, Harwell, TM 104, 105 (1954).

J7. Pole Shape Design in FFAG Magnets.* S. C. SNOWDON AND R. S. CHRISTIAN, *Midwestern Universities Research Association.*—In the design of spiral sector FFAG magnets the desired magnetic field increases along the spiral as r^k where r is the radius from the center of the machine and k is the mean field index. Since k usually is a large number between 10 and 100, it is necessary to obtain the increase in magnetic field by shaping the spiral pole rather than by continually increasing the current density. A computer program UNICYL has been developed to obtain the magnetostatic potential and fields from an integral scaling FFAG magnet structure employing distributed windings. In particular the program searches for a surface of constant potential which, apart from saturation effects, may be used to shape the pole faces. In connection with the fabrication of a 14-ton spiral sector model magnet, a decomposition of the surface into a sequence of contours has been arranged so that numerically controlled milling operations can be used to produce the desired pole. The basis of the magnetostatic calculation program and the resulting potential surface will be discussed.

* Supported by the U. S. Atomic Energy Commission.

J8. Axial Motion Behavior in the Resonant Extraction of Cyclotron Beams.* H. G. BLOSSER AND M. M. GORDON, *Michigan State University.*—The nonlinear 3/3 resonance driven by a suitable field bump is indicated by computational studies to be a precise and economical mechanism for accomplishing extraction of the beam from a three sector medium energy cyclotron.[1] In such a system the resonance is utilized to excite large coherent radial oscillations of the cyclotron beam. An often encountered source of difficulty arises from the marked tendency of the axial focusing frequency to shift to the $2\nu_r=\nu_z$ resonance as the radial amplitude builds up. As an aid to understanding and control of this axial frequency shift, a study has been made of the field features determining the axial focusing of the extraction orbits. Since these orbits move for a substantial fraction of their circumference in regions of the field not crossed by normal orbits, field changes necessary to bring the axial frequency into the desired range can be accomplished without appreciably affecting the properties of orbits in the normal acceleration region. Results for several types of such field modifications will be presented.

* Supported in part by U. S. Atomic Energy Commission.
[1] H. G. Blosser and M. M. Gordon, Midwestern Universities Research Association, Rept. 593 (unpublished); Bull. Am. Phys. Soc. 6, 9 (1961).

J9. FFAG Accelerator with Cryogenic Air-Core Magnet.* CYRIL D. CURTIS, *Midwestern Universities Research Association.*—The air-core magnet of a radial sector FFAG accelerator has field-producing coils whose current density contours for minimizing cost of power plus construction form in cross section, a family of nesting circles. A comparison between 15-Bev accelerators with cryogenic coils of copper, aluminum, and sodium and with iron magnets shows the possibility of savings in total power consumption and in over-all accelerator construction cost for air-core magnets. A formula for a two-way accelerator which includes cost of construction and cost of power for a specified lifetime of accelerator operation is given as a function of accelerator radius and other parameters. Coupled to this is a restrictive equation imposed by the maximum field gradient permissible. From this formula the optimum radius giving minimum cost appropriate for a particular magnet material can be determined. Curves of accelerator cost vs radius are presented. Retention of radiation damage to the coils at very low temperatures raises doubt about the usefulness of such an accelerator for high-average current beams ($\sim$30 μa). Examination of this problem suggests, however, that the time interval permitted before necessary coil annealing need not be prohibitively short.

* Supported by the U. S. Atomic Energy Commission.

Invited Paper

J10. The Brookhaven Alternate-Gradient Synchrotron. K. GREEN, *Brookhaven National Laboratory.* (30 min.)

TUESDAY MORNING AT 9:30

National Bureau of Standards, East Building

(P. EWALD presiding)

Programme of the Division of Solid-State Physics

JA1. Statistical Dynamics of Cubic Lattices and Kramer's Equation. R. J. RUBIN, *National Bureau of Standards.* (30 min.)

JA2. Dynamical Theory of Disordered Lattices. A. A. MARADUDIN, *Westinghouse Research Laboratory.* (30 min.)

JA3. Lattice Anharmonicity and Optical Absorption in Polar Crystals. R. F. WALLIS, *U. S. Naval Research Laboratory.* (30 min.)

JA4. Electron Scattering in Strong Magnetic Fields. A. KAHN, *National Bureau of Standards.* (30 min.)

TUESDAY MORNING AT 9:45

Burgundy Room

(J. S. TOLL presiding)

Theory III: Dispersion Relations and Quantum Electrodynamics

JB1. Subtractions in Dispersion Relations.* MASAO SUGAWARA AND AKIRA KANAZAWA,† *Purdue University.*—In order to further clarify the subject of subtractions in dispersion relations, the following theorem has been proved: Let $f(z)$ be analytic except for some poles and cuts (extending to $\pm\infty$) on the real axis and diverging not worse than z^N, where N is a finite positive integer, as $|z|\to\infty$. Suppose $f(x)/x^n$, where x is real and n is zero or a positive integer, has a finite limit as x goes to infinity along one of the cuts. We can then show that $f(z)/z^n$ has also a finite limit as $|z|\to\infty$ which is the same as or the complex conjugate of the limit of $f(x)/x^n$, depending upon how we approach the limit. This theorem allows us to write down dispersion relations with the minimum number of subtractions when the behavior of the amplitude is known at infinity along one of the cuts. We apply this theorem to forward and double dispersion relations for pion-nucleon scattering, assuming that the total cross section approaches a finite limit as the energy goes to infinity. The double dispersion relations are simpler than those conjectured by Mandelstam[1] on the basis of perturbation theory.

* Supported by the National Science Foundation.
† On leave from Hokkaido University, Sapporo, Japan.
[1] S. Mandelstam, Phys. Rev. 115, 1741 (1959).

JB2. Impulse Approximation and the Construction of Wave Functions. R. E. CUTKOSKY, *Carnegie Institute of Technology.*—There are many different formal ways of constructing a Schrödinger-like equation from dispersion relations, which lead to essentially the same result in the nonrelativistic limit. The most satisfactory method will be the way which leads to a wave function which is particularly useful for correlating different kinds of experimental results. Now, it is well known that the impulse approximation is a good first approximation in many problems. The important feature of the impulse approximation is that the properties of the probe and of the system being studied can be separated, with the latter being represented by its wave function. This suggests that we should define "wave functions" by means of idealized experiments for which the impulse approximation is exact. This leads to a definition based on a systematic elimination of explicit reference to anomalous thresholds in the dispersion theory analysis of the impulse approximation.

JB3. Pion-Hyperon Resonances and the Relative Σ-Λ Parity. RICHARD H. CAPPS, *Northwestern University.*—The various scattering and reaction amplitudes among the particle pairs $\Lambda\pi$, $\Sigma\pi$, and $\bar{K}N$ in states of total angular momentum $\frac{1}{2}$ are considered, under the assumption that the intrinsic parity of the Λ is opposite to that of the Σ and of the $\bar{K}N$ pair. The effects of the poles associated with real (positive energy) baryons are investigated, using the matrix N/D method of Bjorken.[1] Several possible pion-hyperon resonances are discussed. Consideration is also given to the $j=\frac{3}{2}$ states; it is shown that measurements of the angular distribution of the up-down asymmetry in the decay of Σ^+ particles produced in the reaction $K^-+p\to\pi^-+\Sigma^+$ by K^- mesons of momentum in the range 200–400 Mev/c would provide a clue to the relative parity of the Σ and Λ.

[1] J. D. Bjorken, Phys. Rev. Letters 4, 473 (1960).

JB4. Theory of πN Scattering in the Strip Approximation to the Mandelstam Representation.* VIRENDRA SINGH† AND B. M. UDGONKAR,‡ *Lawrence Radiation Laboratory, Berkeley.*—The strip approximation to the Mandelstam representation is applied to the πN problem, and the basic equations given. The asymptotic behavior of the invariant amplitudes in the physical regions is discussed in terms of the unitarity condition on partial-wave amplitudes, the constancy of high-energy scattering cross sections, and the Pomeranchuk theorem. It is shown that this behavior implies that no subtractions should be necessary except in the $J=\frac{1}{2}$ wave of the πN channel and the $J=0$ wave of the $\pi\pi\to N\bar{N}$ channel. This obviates the difficulties encountered by earlier workers when they subtracted higher waves.

* Work done under the auspices of the U. S. Atomic Energy Commission.
† On deputation from Tata Institute of Fundamental Research, Bombay, India.
‡ On deputation from Atomic Energy Establishment, Trombay, India.

JB5. Theory of the High Energy p-$\bar{p}$ Total Cross Section. CHARLES J. GOEBEL, *Institute for Advanced Study.*—The Mandelstam dispersion representation, if only the two-meson-exchange "box" diagrams of the spectral function are kept, provides an "on-the-mass-shell Williams-Weizsacker approximation" for the calculation of absorptive amplitudes. It has the

usual advantages of an on-the-mass-shell formalism; it also allows a simple decomposition into partial waves, so that unitarity limits (important for strongly interacting particles) can be explicitly satisfied. As an example, the high energy p-p total cross section ($\approx$40 mb) has been calculated, using the π-p cross section ($\approx$30 mb). By making an additional approximation which amounts to the (absurd) assumption that the π-p interaction is zero ranged, the result is only 17 mb. But in the "Mandelstam-W-W" formula it is explicit that the longer the range of the π-p interaction, the larger will be the cross section for the peripheral p-p interactions, which agrees with the intuition. It then follows that a significant proportion of high energy p-p interactions take place through the exchange of a "chain-of-pions"; further implications of this will be described.

JB6. On the Spectral Functions of Some Feyman Diagrams in $K \to 3\pi$ Decay. C. KACSER,* *Princeton University*, AND G. BARTON,† *Institute for Advanced Study.*—We examine in perturbation theory the discontinuities across the branch cuts arising from the first few diagrams in an attempt to disentangle effects depending on the K mass from those of the $\pi\pi$ interaction. For instance, in the vertex-type diagrams, when the mass parameter λ of the internal double pion line lies in the range $M^2-\mu^2<2\lambda^2<2(M-\mu)^2$, an additional, anomalous, branch point appears above the normal threshold. This happens only when the K is unstable. On integrating over λ this anomalous branch point moves down to the normal threshold at $s=4\mu^2$, but may nevertheless affect the discontinuity across the cut.

* Supported in part by the U. S. Air Force Office of Scientific Research, Air Research and Development Command.
† Supported by a grant to the Institute from the National Science Foundation.

JB7. Proton Compton Scattering at High Energy. A. P. CONTOGOURIS, *Cornell University.*—The cross section and the angular distribution for Compton scattering on protons is calculated at various energies in the region of and above the peak corresponding to the 3-3 pion-nucleon resonance. For this, the use of a set of approximate dispersion relations for the scattering amplitudes is discussed and justified. It is shown that the recent experimental data[1] up to 420-Mev photon laboratory energy can be well accounted by the Low diagram[2] and the contributions to single pion photoproduction in the s- and the first two resonant states. The effect of small admixtures of electric quadrupole in the radiation producing the first photopion resonance is also examined; it is shown to improve the angular distributions significantly.

[1] J. De-Wire, M. Feldman, and R. Littauer, Bull. Am. Phys. Soc. 4, 253 (1959), and private communication.
[2] G. F. Chew, 1958 Annual International Conference on High-Energy Physics at CERN, p. 98.

JB8. Small-Angle Coulomb Scattering. R. H. PRATT AND S. D. DRELL, *Stanford University.*—The low momentum transfer region of strong interaction processes may be discussed in terms of one-pion-exchange graphs. This success of "extrapolation to poles" suggests, as an extension, "extrapolation to cuts" corresponding to low-mass intermediate states containing two or more particles. We find that this extrapolation may be performed in the case of electromagnetic interactions, owing to the vanishing photon mass, which also causes the one-photon pole and the threshold of the many-photon cuts to coincide. For small-angle scattering of relativistic electrons in a pure Coulomb field $(\sin^4\phi/2)(d\sigma/d\Omega)=a_0+a_1\sin\phi/2+\cdots$, where a_0 is given precisely by the one-photon pole and a_1 (obtained exactly to all orders in $Z\alpha$) comes from the many-photon terms. For scattering by finite nuclei, we further find that, for fixed momentum transfer, the ratio of second to first Born approximation decreases as (energy)$^{-1}$ at high energies. Simple approximations are given for determining charge form factors of intermediate Z nuclei by electron and positron scattering.

JB9. Pion Production in Electron-Positron Collisions.* FRANK CHILTON, *University of Washington.*—Electron-positron colliding beams offer the possibility of studying certain strongly interacting particles without the presence of other strongly interacting particles. Pion production is particularly interesting because of the presumably fundamental role of the pion in strong interactions. Charge conjugation invariance, in addition to the usual symmetries of rotational invariance, etc., permits the complete classification of the initial electron-positron states, just as for positronium. However, in these high energy processes the states are more conveniently determined as states of definite helicity and total angular momentum. Various selection rules governing pion production in electron-positron collisions are obtained. The cross sections for the reactions $e^++e^-\to\pi^0+\gamma$, $e^++e^-\to e^++e^-+\pi^0$, and $e^++e^-\to\pi^++\pi^-$ are calculated. The photon spectrum in the reaction $e^++e^-\to\pi^++\pi^-+\gamma$ is also calculated. Consideration is given to some of the possible effects of strong interactions.

* Supported in part by the U. S. Atomic Energy Commission. Most of this work was done while the author was a National Science Foundation Predoctoral Fellow at the University of Chicago; a version was submitted as a thesis to the faculty of the University of Chicago.

JB10. Photon Asymmetry in Bremstrahlung of Transversely Polarized Electrons. E. SOBOLAK AND P. STEHLE, *University of Pittsburgh.*—There is a left-right asymmetry in the emission of photons by transversely polarized electrons analogous to the left-right asymmetry in Mott scattering. The magnitude of this effect has been calculated in Born approximation, where it appears in the matrix elements of order Z^3e^5. Principal contributions come from Feynman diagrams with the photon emitted before or after both Coulomb interactions. The diagram with the photon emitted between the two Coulomb interactions contributes asymmetric terms $(v/c)^2$ relative to the others, and involves integrals which are much more difficult to evaluate and which have been neglected. It appears impractical to integrate the resulting cross section over electron momentum analytically. The results for forward electron momentum are evaluated in detail. The dominant terms in the asymmetry are proportional to $(p\text{-}s)$, where p-s is the momentum charge of the electron.

JB11. Corrections to Hyperfine Structure in Hydrogen.* MORTON M. STERNHEIM, *Columbia University.*—The α^2m/M corrections to the ratio of the hyperfine structure (hfs) of the $1s$ and $2s$ states of atomic hydrogen have been evaluated using the Bethe-Salpeter equation. The theoretical value for the ground state hfs, which apparently disagrees with the measured frequency,[1] depends upon proton form factors and is very laborious to compute for terms smaller than α^2(hfs) or $\alpha^2(m/M)$(hfs). The ratio is much simpler to calculate and does not depend upon nucleon structure effects. All the α^2m/M terms may in fact be found by adding the proton's nonrelativistic kinetic energy $p^2/2M$ and the effects of its Dirac and Pauli moments to the Dirac equation for the electron. In units of 10^{-6}, they contribute -0.13 to $R=(8\nu_{2s}/\nu_{1s})-1$. The total theoretical value for R is 34.44 ± 0.02, in good agreement with the experimental value 34.49 ± 0.06.

* This work was started during the tenure of a National Science Foundation Predoctoral Fellowship and completed with the support of the theoretical physics contract of the U. S. Atomic Energy Commission.
[1] C. K. Iddings and P. M. Platzman, Phys. Rev. 113, 192 (1959); 115, 919 (1959); A. Layzer and D. Zwanziger (private communication).

JB12. Method of Ostragradsky in Nonrelativistic Electrodynamics.* M. SCHWARTZ AND RALPH SCHILLER,† *Syracuse University.*—The structure independent electron theory of Kramers is a nonrelativistic model for a charged particle in interaction with its own and an external electromagnetic field.

We have investigated this model in the same electric dipole approximation as Kramers did in his original work. We have found it possible to formulate Kramers' problem anew by means of a technique due to Ostragradsky which is appropriate for Lagrangians which contain time derivatives of an order greater than one. However, not all the canonical variables of the theory are independent, as is evidenced by the special relations (constraints) amongst these variables. A theory with constraints may be treated by introducing modified Poisson brackets (commutators) due to Dirac. With these modifications we have shown that the theory may be given a consistent canonical form. Similar constraints appear in Kramers' formulation, but he did not deal explicitly with this problem. We have also investigated the influence of boundary values and initial conditions on the dynamical equations of motion, and on the reduction of the canonical variables to an independent set.

* Research supported by Wright Air Development Center.
† On leave of absence from Stevens Institute of Technology.

JB13. Electromagnetic Model for Charged Mesons. E. J. STERNGLASS, *Westinghouse Research Laboratories.*—The relativistic electron-pair model for the π^0 meson[1] is extended to describe the charged π mesons. When the magnetic moments of the particles forming the π^0 are oriented parallel, a third electron may be bound by spin-spin and spin-orbit interactions in an orbit of $\frac{1}{2}\hbar$ relative to the precessing perehelion frame K_p defined by the π^0 core.[1] The intrinsic spin of the orbital electron is cancelled by the precessional momentum $\hbar/2$ of K_p resulting in a total angular momentum zero and Bose statistics. The total energy is essentially that of the π^0 core, $(2/\alpha)m_0c^2 = 274\ m_0c^2$, since the relativistic precession limits the magnetic binding energy of the added electron to a value of order m_0c^2. The ground-state orbit has a radius equal to the π-meson Compton wavelength, as required by the known range of nuclear forces. Since the forces between the orbital electron and the core are relatively weak, the orbital electron may be shared between mesons of adjacent nucleons, providing a physical interpretation for the exchange character of nuclear forces. If the π-meson structure loses an angular momentum $\hbar/2$, magnetic binding increases by $\frac{1}{2}(1/\alpha)m_0c^2$. This results in a tightly bound, weakly interacting system of spin $\hbar/2$ and mass $\frac{1}{2}(1/\alpha)m_0 = 205.5m_0$ suggestive of the μ meson.

[1] E. J. Sternglass, Bull. Am. Phys. Soc. 6, 80 (1961).

TUESDAY AFTERNOON AT 2:00

Adams-Hamilton Room

(WALTER GORDY presiding)

Spins, IV

K1. Electron Spin Resonance of γ-Irradiated Single Crystals of α-Amino Isobutyric Acid, Isobutyramide, and *DL* Valine.† HOWARD SHIELDS† AND WALTER GORDY, *Duke University.*—The electron spin resonances of γ-irradiated single crystals of α-amino isobutyric acid $(CH_3)_2C(NH_2)COOH$, isobutyramide $(CH_3)_2CHC(NH_2)OH$, and *DL* valine $(CH_3)_2CHCH(NH_2)COOH$ have been observed at room temperature. The first two gave the septet patterns characteristic of 6 protons with equal and very nearly isotropic couplings of 23 gauss. The g factor observed for both is only slightly anisotropic and is close to that for the free electron spin, 2.0023. It is concluded that the free radical is $(CH_3)_2CCOOH$ for isobutyric acid and $(CH_3)_2CC(NH_2)OH$ for isobutyramide. The pattern for *DL* valine is incompletely resolved for most orientations, but for H perpendicular to the flat surface of the crystal a septet pattern is observed. This pattern, apparently caused by 6 equivalent protons of 23-gauss coupling, has a triplet substructure which is probably caused by N^{14} coupling of 9 gauss. The free radical is believed to be $(CH_3)_2CCH(NH_2)COOH$.

* Supported by the Office of Scientific Research, U. S. Air Force.
† Now in the Department of Physics, Wake Forest College.

K2. Electron Spin Resonance of H Atoms Produced by γ Irradiation of Substances at 4.2°K.* HARVEY N. REXROAD† AND WALTER GORDY, *Duke University.*—ESR has been observed in several substances which were γ irradiated directly in the microwave cavity at 4.2°K. For dosages less than 10^6 r, strong doublets of H atoms were observed from HF and H_2O with spacings of 506 gauss and linewidths of about a gauss. No H atoms were detected for the same dosage in the related substances HCl and H_2S. Although resonance of H atoms in irradiated H_2O has been previously detected,[1] we have observed an anomaly not reported. The lower field component of the H doublet in γ-irradiated H_2O at 4.2°K was found to be many times stronger than the upper one, an effect thought to arise from an interaction of the H with an unidentified free radical having a broad resonance which overlaps the lower component and enhances its relaxation.[2] No such anomaly was observed for the D component in irradiated D_2O, but surprisingly in this sample (D above 99%) the lower component of H was observed to be an order of magnitude stronger than the D components.

* Supported by the Office of Scientific Research, U. S. Air Force.
† Now at West Virginia University.
[1] L. H. Piette, R. C. Rempel, H. E. Weaver, and J. M. Flournoy, J. Chem. Phys. 30, 1623 (1959).
[2] A similar phenomenon discovered for As-doped Si by Honig and Combrisson is treated by G. Feher and E. A. Gere, Phys. Rev. 114, 1245 (1959).

K3. Electron Spin Resonance Studies on an Irradiated Single Crystal of Deuterated DL-Tartaric Acid.* D. V. G. L. NARASIMHA RAO AND WALTER GORDY, *Duke University.*—The ESR spectra of an irradiated single crystal of DL-tartaric acid grown from water is found to be quite complex, but the spectra of a deuterated single crystal could be analyzed and the nature of the free radical ascertained. Measurements were made at 9 and at 23 kMc/sec. For some orientations of the crystal in the external magnetic field an unresolved doublet with weak satellite lines separated by 5 gauss at 9 kMc/sec and 13 gauss at 23 kMc/sec was observed. These satellite lines evidently arise from second-order transitions[1] and are very similar to those already reported by us for a single crystal of urea oxalate. From the analysis we suggest that the free radical is probably,

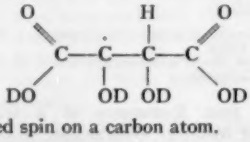

with the unpaired spin on a carbon atom.

* Supported by the Office of Scientific Research, U. S. Air Force.
[1] I. Miyagawa and W. Gordy, J. Chem. Phys. 32, 255 (1960).

K4. Comparisons of the ESR of γ-Irradiated Proteins with that of Proportional Mixtures of their Amino Acid Constituents.* RAYMOND PATTEN AND WALTER GORDY, *Duke University.*—The electron spin resonance of a number of proteins has been compared with that of proportional mechanical mixtures of their amino acid constituents, both at 77°K and at 300°K. The proetins include bovine albumin, ovalbumin, chymotrypsinogen, edistin, gliadin, lysozyme, and zein. Generally, the proteins give broad, unresolved ESR patterns similar to those of their mixed constituents when irradiated and observed at 77°K. When warmed to 300°K the proteins give patterns more noticeably different from those of their constituent amino acid mixtures and more like those found in a number of other proteins irradiated and observed at room temperature. The results support the thesis that at room temperature radiation damage to proteins does not occur proportionally in all the different amino acid residue, but occurs selectively in certain residue. Also, it appears that as the temperature is raised, unpaired electrons produced in different parts of the protein at 77°K tend to migrate to the more favored sites.

* Supported by the Office of Scientific Research, U. S. Air Force.

K5. Electron Spin Resonance of Gamma-Irradiated Single Crystals of Acetylalanine, Chloroacetylalanine, and Acetyl *L*-Glutamic Acid.* MIKIO KATAYAMA AND WALTER GORDY, *Duke University.*—Single crystals of acetyl-, and chloroacetyl-, *d,l*-alanine, and acetyl *L*-glutamic acid have been gamma irradiated and the electron spin resonance of the radiation induced free radicals observed for various orientations in the magnetic field. The spectra of the former two crystals are quartets of intensity ratio 1:3:3:1. The free radical for each is shown to have the form

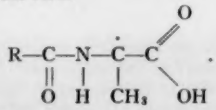

The ESR of acetyl-*L*-glutamic acid is somewhat complicated and changes with time. Its analysis is still incomplete.

* Supported by the U. S. Army Research Office.

K6. Electron Spin Resonance of γ-Irradiated Polypeptides.* RUSSELL DREW† AND WALTER GORDY, *Duke University.*—Electron spin resonance has been observed in 19 γ-irradiated synthetic polypeptides, including poly-glycine, poly-*L*-alanine, poly-*L*-valine, poly-*L*-leucine, poly-*L*-phenylalanine, poly-*L*-proline, poly-*L*-glutamic acid, poly-*L*-aspartic acid, and poly-*L*-tyrosine. Studies have been made on powdered samples at 77°K and 300°K. The effects of air or oxygen on the resonances have been observed. The various ESR patterns and oxygen effects are compared with those for native proteins. Unlike the proteins, the synthetic polypeptides were found to give characteristically different ESR patterns when irradiated, except that poly-glycine and poly-sarcosine gave similar doublets. Of the polypeptides so far investigated, none of which contained sulfur, the ESR pattern of poly-glycine (or poly-sarcosine) is the only one which is strikingly similar to that found in a variety of proteins. We are planning more detailed studies on oriented samples of certain of these polypeptides and are attempting to obtain some polypeptides which contain sulfur.

* Supported by the Office of Scientific Research, U. S. Air Force and by the Army Research Office.
† Lieutenant, U. S. Navy. Supported by the U. S. Naval Postgraduate School, Monterey, California.

K7. Electron Spin Resonance of a Gamma-Irradiated Single Crystal of *N*-acetyl Methionine.* ERNESTO CIPOLLINI AND WALTER GORDY, *Duke University.*—The ESR of a γ-irradiated single crystal of *N*-acetyl methionine has been investigated at 9 kMc/sec. Patterns from two chemically different free radicals were observed. The free radical giving the more intense pattern has principal g values 2.008, 2.022, and 2.071 and a nearly isotropic doublet splitting of 9 gauss. This free radical is believed to be

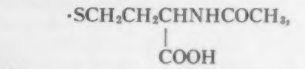

which is similar in form to that found for *L*-cystine dihydrochloride[1] in which the unpaired electron is mainly on the S. The second free radical has principal g values 2.0023, 2.0025, and 2.0045 and a nearly isotropic and equal coupling by two protons of 10.5 gauss. It is believed to have the form

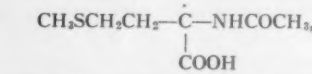

in which the spin density is concentrated on a C.

* Supported by the Office of Scientific Research, U. S. Air Force.
[1] Y. Kurita and W. Gordy, J. Chem. Phys. 34, 282 (1961).

K8. A Cyclotron Resonance Study of Low-Pressure Acetylene-Oxygen Flames, Containing Traces of Chlorine.* P. J. PADLEY AND E. M. BULEWICZ, *Duke University* (introduced by Walter Gordy).—The reaction zones of acetylene flames contain anomalously high concentrations of free electrons—up to a factor of 10^5 above equilibrium. At reduced pressure these concentrations can conveniently be measured by the method of cyclotron resonance. When traces of chlorine gas (of the order of 1% of the total gas) are added, a reduction in the electron concentration is observed, which can be attributed to the formation of the Cl^- ion. The flame gases normally contain about 10% of the H_2 and H atoms, and the total chlorine is distributed between HCl and Cl, in accordance with the balanced reaction $Cl+H_2 \rightarrow HCl+H$; Cl^- can then be formed by two distinct mechanisms: (1) $HCl+e \rightarrow H+Cl^-$, or (2) $Cl+e+X \rightarrow Cl^-+X$ where X is a third body. The two mechanisms lead to widely different values of $[Cl^-]/[e]$, with different dependence on the flame temperature and composition. It was shown that the experimental results are consistent only with mechanism (1), in agreement with earlier work on the formation of the Cl^- ion in gaseous discharges.

* Supported by the Office of Scientific Research, U. S. Air Force, and by a grant from the California Research Corporation.

K9. Correlation of Anomalous Line-Reversal Measurements of Temperature with Excess Electron Concentrations in Acetylene-Oxygen Flames.* E. M. BULEWICZ AND P. J. PADLEY, *Duke University* (introduced by Walter Gordy).—Line-reversal measurements, made on the spectral lines of various metal additives, in the reaction zone of premixed hydrocarbon-oxygen-diluent flames often give rise to temperatures considerably above those expected on the basis of full thermodynamic equilibrium of the burnt gases. Line intensities of the Fe 4050 A (nonresonance) group [produced by additon of $Fe(CO)_5$] were measured as a function of preburned flame gas composition (λ varying from 0.35 to 2.6) in acetylene-oxygen mixtures burning at 10–30 mm pressure. The technique of cyclotron resonance was used to measure, in these same flames, the anomalously high electron concentrations known to exist in the reaction zone—for these purposes, convenient absorption was found to take place, with 48-kMc/sec radiation, at a magnetic field strength of 17 000 gauss. When quenching is taken into consideration, a good correlation between these two effects can be obtained, even when the preburned gases are suitably diluted with argon or hydrogen, or when the pressure is varied from 10 mm Hg to 1 atm. A scheme is proposed to account for these observations.

* Supported by the Office of Scientific Research, U. S. Air Force.

TUESDAY AFTERNOON AT 2:00

Continental Room

(K. L. DUNNING presiding)

Nuclear Reactions, IV

KA1. Level Structure of Na^{24} from the (d,p) Reaction.* C. DAUM,† *The University of Michigan.*—The level structure of Na^{24} up to an excitation of approximately 8 Mev has been obtained using the magnetic-analysis instrumentation associated with the Michigan 42-in. cyclotron by observing the energy and angular distributions of the proton groups in the reaction $Na^{23}(d,p)Na^{24}$ at a deuteron energy of 7.8 Mev. Although the spectrum is in good agreement with earlier work,[1] some new levels have been found, and values of l_n have been obtained for levels not previously resolved. The interpretation of the level scheme of Na^{24}, an odd-odd nucleus, will be discussed in terms of the rotational model.

* This work was supported in part by the U. S. Atomic Energy Commission.
† On leave from the Institute for Nuclear Physics Research, Amsterdam, The Netherlands.
[1] A. Sperduto and W. W. Buechner, Phys. Rev. **88**, 574 (1952); A. W. Dalton, G. Parry, and H. D. Scott, (to be published); and F. A. El Bedewi and M. A. El Wahab, Nuclear Phys. **21**, 49 (1960).

KA2. Level Structure of the Magnesium Isotopes.* W. C. PARKINSON, *The University of Michigan.*—The spectra of the three isotopes Mg^{25}, Mg^{26}, and Mg^{27} have been obtained to an excitation energy of approximately 6 Mev by means of the (d,p) reaction using the magnetic analysis system associated with the Michigan 42-in. cyclotron at a deuteron energy of 7.8 Mev. Measurements of the angular distributions of the proton groups and of the reduced widths determine the parity and in some cases the spins of the levels. The interpretation of the level structure of Mg^{26} in terms of the rotational model is well known.[1] Mg^{27}, also an even-odd nucleus, will be discussed in the light of the data available.

* Supported in part by the U. S. Atomic Energy Commission.
[1] Litherland *et al.*, Can. J. Phys. **36**, 378 (1958).

KA3. Level Structure of Al^{28} from the (d,p) Reaction.* R. S. TICKLE AND K. T. HECHT, *The University of Michigan.*—The properties of a number of the energy levels below 7 Mev in the nucleus Al^{28} have been investigated using the reaction Al^{27} (d,p) Al^{28} at an incident deuteron energy of 7.8 Mev. Angular distributions have been measured between the laboratory angles 0° and 90° using the magnetic-analysis instrumentation associated with the Michigan 42-in. cyclotron. Where applicable, l values have been determined. A summary of the presently available information on the level structure of Al^{28}, an odd-odd nucleus, will be presented, including comments on its theoretical interpretation.

* Supported in part by the U. S. Atomic Energy Commission.

KA4. Level Structure of P^{32} from the (d,p) Reaction.* T. HOLTEBEKK,† *The University of Michigan.*—The energy spectrum and the angular distributions of the proton groups leading to excited levels in P^{32} up to approximately 5 Mev have been measured using the magnetic analysis instrumentation associated with the Michigan 42-in. cyclotron. The data are in good agreement with earlier measurements.[1] A level previously unreported is found at an excitation energy of 1.51 Mev, and several l values not previously reported have been determined. The interpretation of the level scheme of P^{32}, an odd-odd nucleus, will be discussed.

* This work supported in part by the U. S. Atomic Energy Commission.
† On leave from the University of Oslo, Norway.
[1] D. Paraino, C. H. Paris, and W. W. Buechner, Phys. Rev. **119**, 732 (1960); W. C. Parkinson, Phys. Rev. **110**, 485 (1958); A. W. Dalton, S. Hinds, and G. Parry, Proc. Phys. Soc. (London) **A70**, 586 (1957).

KA5. Level Structure of S^{33} and S^{35} from the (d,p) Reaction.* JOACHIM JÄNECKE,† *The University of Michigan.*—The spectra for S^{33} and S^{35} have been obtained at 30° by means of the (d,p) reaction using the magnetic-analysis instrumentation associated with the Michigan 42-in. cyclotron. Targets of CdS were bombarded with 7.8-Mev deuterons. The results are in good agreement with the earlier work of Endt and Paris.[1] Angular distributions of the proton groups and relative reduced widths have been determined for levels up to about 5-Mev excitation and extend earlier measurements.[2] The level schemes of S^{33} and S^{35}, both even-odd nuclei, will be discussed.

* This work was supported in part by the U. S. Atomic Energy Commission.
† On leave from Max-Planck Institute, Heidelberg.
[1] P. M. Endt and C. H. Paris, Phys. Rev. **110**, 89 (1958).
[2] T. R. Holt and T. N. Marsham, Proc. Phys. Soc. (London) **A66**, 467 (1953); and R. Middleton (private communication).

KA6. Deuteron Elastic Scattering Cross Sections.* JOHN BARDWICK, R. S. TICKLE, AND W. C. PARKINSON, *The University of Michigan.*—The deuteron differential elastic scattering cross-sections for a variety of elements have been measured using the 7.8-Mev deuteron beam of the Michigan 42-in. cyclotron. Measurements were made at angles from 30° to 95° and in some cases from 0 to 95°. Results for Be, Mg, Al, Cl, S, Ni, and Au will be compared with the theoretical results obtained at Oak Ridge.[1]

* This work was supported in part by the U. S. Atomic Energy Commission.
[1] G. R. Satchler (private communication).

KA7. Elastic Scattering of Protons by Argon-36.* C. C. KIM† AND A. C. L. BARNARD,‡ *State University of Iowa.*—Absolute differential cross sections for the elastic scattering of protons by A^{36} have been measured for laboratory proton energies from 1.0 to 1.8 Mev at a center-of-mass angle of 155.4°. The cross sections are equal to the Rutherford value except in an anomalous region near $E_p = 1.494$ Mev, corresponding to a level in K^{37} with 3.34-Mev excitation. Cross sections were measured as a function of energy at angles $\theta_{cm} = 90.0°$, 125.3°, and 160.1°, and an angular distribution was taken at the resonance energy. The data were analyzed using dispersion theory and $j\pi = \frac{1}{2}$ was assigned to the K^{37} state.

* Supported in part by the U. S. Atomic Energy Commission.
† Now at the University of Southern California, Los Angeles, California.
‡ Now at Rice University, Houston, Texas.

KA8. Neutron Yield Anomaly Near Threshold for the Reaction $Cl^{37}(p,n)A^{37*}$ 1.46 Mev.† A. C. L. BARNARD, G. S. MANI, AND P. D. FORSYTH, *Rice University.*—A sodium chloride target (~100 kev thick to 2 Mev protons) was bombarded with protons in the energy range $1.6 < E_p < 4.1$ Mev, and yields of neutrons averaged over an energy interval equal to the target thickness were measured. The yields of neutrons from the reaction $Cl^{37}(p,n)$ leaving A^{37} in its first excited state ($E_x = 1.46$ Mev) were separated from the yields of neutrons to the A^{37} ground state by using sphere counters.[1] The averaged yield of excited-state neutrons shows broad maxima near thresholds very similar to those reported in the yield of ground-state neutrons.[2]

† Supported in part by the U. S. Atomic Energy Commission.
[1] R. Bramblett, R. I. Ewing, and T. W. Bonner, Nuclear Instr. & Methods **9**, 1 (1960).
[2] G. S. Mani, A. C. L. Barnard, T. A. Tombrello, and D. A. A. S. N. Rao, Bull. Am. Phys. Soc. **6**, 38 (1961).

KA9. Level Structure of A^{41} from the $A^{40}(d,p)A^{41}$ Reaction.* E. KASHY, A. M. HOOGENBOOM,† AND W. W. BUECHNER, *M.I.T.*—The energy-level structure of A^{41} has been investigated by bombarding argon gas with 7.5-Mev deuterons using the M. I. T.-O. N. R. Van de Graaff accelerator, and measuring the energy spectrum and angular distribution of the reaction protons. The argon target was contained in a small rotating gas cell with thin Formvar windows. Thirty-four levels were observed up to 5.1-Mev excitation energy, including a low-lying level at 0.171 Mev. Results of the stripping analysis will be shown, and shell-model description of some of the levels will be discussed.

* This work has been supported in part by the U. S. Atomic Energy Commission, the Office of Naval Research, and the U. S. Air Force Office of Scientific Research.
† Now at Philips' Gloeilampenfabrieken, Institute for Nuclear Research, Amsterdam, Holland.

KA10. Reaction Cross Sections for Several Nuclides with 10-Mev Protons.* J. WING AND J. R. HUIZENGA, *Argonne National Laboratory.*—Excitation functions for the reactions $Cr^{52}(p,n)Mn^{52g+52m}$, $Cu^{63}(p,n)Zn^{63}$, $Cu^{65}(p,n)Zn^{65}$, $Ag^{107}(p,n)Cd^{107}$, $Ag^{107}(p,n)Cd^{109}$, $Cd^{111}(p,n)In^{111}$, $Cd^{114}(p,n)In^{114g+114m}$, and $La^{139}(p,n)Ce^{139}$ have been measured by the stacked-foil technique with protons from the Argonne cyclotron of 10.6-Mev initial energy. The (p,n) cross sections are a good estimate of the total reaction cross sections at the lower energies and for Ag, Cd, and La targets this is true for proton energies up to about 10 Mev. For other targets, cross sections of competing reactions such as (p,p') and (p,α) are added to the (p,n) cross sections in obtaining the total reaction cross sections. The experimental reaction cross sections will be compared with those obtained from optical model calculations with parameters that fit proton elastic scattering and polarization measurements. Our (p,n) cross sections on the copper isotopes at 9.85 Mev are considerably smaller than those recently reported[1]; for example, 550 mb for Cu^{63} compared to 700 mb.

* Based on work performed under the auspices of the U. S. Atomic Energy Commission.
[1] R. D. Albert and L. F. Hansen, Phys. Rev. Letters 6, 13 (1961).

KA11. Energy Levels of Cr^{52}.* R. R. WILSON, A. A. BARTLETT, J. J. KRAUSHAAR, J. D. MCCULLEN, AND ROBERT A. RISTENEN, *University of Colorado.*—The Cr^{52} energy levels have been investigated by studying the decay of Mn^{52} with a $\sqrt{2}\pi$ double-focusing beta-ray spectrometer and with sodium-iodide scintillation counters in coincidence. The spectrometer studies using both internal and external conversion indicated the energies of the three principal gamma rays to be 1432.4 ± 1.2, 934.3 ± 1.1, and 743.3 ± 0.8 kev. The scintillation studies indicated that the following gamma rays are in coincidence with the 1.43-Mev transition: 0.93 (70%), 0.74 (70%), 1.33 (5%), and 1.26 Mev (5%) along with 0.51 Mev (50%) annihilation quanta. Other weak transitions are as yet uncertain. The 1.33-Mev gamma ray appears to be a transition from the 2.77- to the 1.43-Mev levels and the 1.26-Mev gamma ray a transition from a new level at 3.62 Mev to the 2.37-Mev level. The results of the beta-ray spectrometer intensity studies are consistent with those of the scintillation studies.

* Supported in part by the U. S. Atomic Energy Commission and the National Science Foundation.

KA12. Inelastic Scattering of Protons at 40 Mev. I.* NORTON M. HINTZ, L. L. LEE, JR., AND TANNIE STOVALL, *University of Minnesota.*—A 40-in. radius, 180-deg, double-focusing magnetic spectrometer has been constructed to study reaction products from 10-, 40-, and 68-Mev protons from the Minnesota Linear Accelerator. A brief description of the design and preliminary performance data for the spectrometer will be presented. To facilitate data taking, a 10-unit scintillation detector has been installed in the focal plane. Twenty momentum intervals can be observed simultaneously by placing absorbers over half of each scintillator and observing the pulse height in each detector. The data are recorded in a fast, transistorized 20-channel discriminator.[1] Data will be shown for angular distributions of inelastic proton scattering to the first excited states of C^{12} ($Q=-4.43$ Mev), and Mg^{24} ($Q=-1.37$ Mev).

* Supported in part by the U. S. Atomic Energy Commission.
[1] Designed by Dr. C. J. Candy.

KA13. Inelastic Scattering of Protons at 40 Mev. II.* L. L. LEE, JR., NORTON M. HINTZ, C. D. KAVALOSKI, AND TANNIE STOVALL, *University of Minnesota.*—A program has been initiated to study the inelastic excitation of low-lying states in various nuclei, using the 40-in. magnetic spectrometer and multichannel detector described in the previous abstract. Data will be presented for the angular distributions of the first 2+ state and the strongly excited 3− octupole vibrational state in Ni^{58}, Ni^{60}, Fe^{56}, and other isotopes now being studied. These angular distributions show that the Blair inelastic-diffraction scattering approximation[1] is not valid for protons. The results seem to confirm the recent suggestion of Kromminga and McCarthy[2] that the small-angle behavior of the inelastic cross section might reveal the parity of the state.

* Supported in part by the U. S. Atomic Energy Commission.
[1] J. S. Blair, Phys. Rev. 115, 928 (1959).
[2] A. J. Kromminga and I. E. McCarthy, Phys. Rev. Letters 6, 62 (1961).

TUESDAY AFTERNOON AT 2:00

Cotillion Room, South

(J. E. EVANS presiding)

Cold-Neutron Scattering and Solid-State Physics

L1. Neutron Optics Research Facility at Livermore Pool Type Reactor.* W. C. DICKINSON, L. PASSELL, AND O. HALPERN,† *Lawrence Radiation Laboratory, Livermore.*—The experimental facility for the performance of high-precision neutron optics experiments is described. The first experiment completed was a precision determination of the neutron-proton coherent scattering amplitude by mirror reflection. Sources of error in neutron optics measurements are discussed, including influence of incoherent scattering on reflectivity, effect of angular beam spread on average angle of reflection, effect of vapor or air above a reflecting liquid surface on the effective index of refraction, attenuation of the beam by vapor, and effect of neutron-electron interaction. The plans for measurement of several other neutron coherent scattering amplitudes are discussed. Such data are important in the understanding of nuclear phenomena and magnetic neutron scattering, and for an improved measurement of the neutron-electron interaction. A new comparison method for measuring scattering amplitudes is described, using liquids with indices of refraction greater than unity so that there is no total reflection. This

means that a precise knowledge of the long-wavelength neutron spectrum is not necessary. Also described is an experiment to confirm the predicted effect of incoherent scattering and/or absorption on the reflectivity.

* Work done under auspices of the U. S. Atomic Energy Commission.
† Consultant to Lawrence Radiation Laboratory, Livermore.

L2. Renninger Scattering in Single-Crystal Neutron Diffraction.* R. M. Moon, *Lincoln Laboratory,*† and C. G. Shull, *M.I.T.*—Intensity variations as great as 50% have been observed in strong neutron diffraction peaks from single crystals of iron arising from Renninger scattering,[1] i.e., simultaneous Bragg reflection from two or more sets of planes. These variations are observed by rotating the crystal about an axis normal to a primary set of reflecting planes. When the geometry is such that Bragg reflection is possible from another set of planes, the intensity of the primary reflection increases or decreases by an amount which is strongly dependent on the sample geometry. An approximate theory, valid in the limit of low extinction and negligible absorption, gives fair agreement with the magnitude of the observed variations. Charts giving the azimuthal angles at which simultaneous reflections occur for a given primary reflection are in preparation for the body-centered and face-centered cubic lattices. Experimental procedures for avoiding or minimizing this effect are suggested.

* Research supported by National Science Foundation.
† Operated with the support of the U. S. Army, Navy, and Air Force.
[1] M. Renninger, Z. Physik **106**, 141 (1937).

L3. Design of Rotating Shutters for Cold-Neutron Experiments.* K. Otnes and H. Palevsky, *Brookhaven National Laboratory.*—New and more refined cold-neutron experiments are made possible through the development of high-flux reactors. In general these experiments require an incident beam of monochromatic cold neutrons, and a scheme for measuring the energy of the scattered neutrons. In preparation for performing such experiments at the new high-flux Brookhaven reactor we have been comparing various rotating-shutter devices that perform the above functions. Expressions for transmission, burst time, and velocity resolution have been obtained. These allow a comparison of the various systems to be made. The method of calculation and the results in terms of working curves for aid in design consideration will be presented.

* Work carried out under the auspices of the U. S. Atomic Energy Commission.

L4. Crystal Dynamics of Sodium by Neutron Spectrometry. A. D. B. Woods, B. N. Brockhouse, and R. H. March, *Chalk River Laboratories,* and Raymond Bowers,* *Cornell University.*—The frequency/wave number dispersion relations for the lattice vibrations in bcc sodium at 90°K have been measured for the $[00\zeta]$, $[\zeta\zeta 0]$, $[\zeta\zeta\zeta]$, $[\zeta\zeta 1]$ and $[\frac{1}{2}\frac{1}{2}\zeta]$ symmetric directions, as well as at several general positions in reciprocal space. Frequencies of some special modes (units 10^{12} cps) are: [0,0,1], 3.58±0.05 (*L* and *T* degenerate by symmetry); $[\frac{1}{4},\frac{1}{4},\frac{1}{4}]$, 2.89±0.05 (also degenerate); $[\frac{1}{4},\frac{1}{4},0]L$, 3.80±0.1; $[\frac{1}{4},\frac{1}{4},0]T_1$, 0.90±0.04; $[\frac{1}{4},\frac{1}{4},0]T_2$, 2.56±0.05. The results agree fairly well with basic calculations by Toya.[1] Fourier analysis indicates that, for a Born-von Kármán-type fit to the data, forces out to at least fourth neighbors are required. At higher temperatures (210°K and 296°K) the neutron groups show broadening qualitatively similar to that observed in lead [Bull. Am. Phys. Soc. **5**, 39, 199 (1960)], suggesting very short lifetimes for phonons at these temperatures. At 296°K frequencies of the above special modes are: [0,0,1], 3.28±0.1; $[\frac{1}{4},\frac{1}{4},\frac{1}{4}]$, 2.72±0.06; $[\frac{1}{4},\frac{1}{4},0]L$, 3.68±0.1; $[\frac{1}{4},\frac{1}{4},0]T_1$, 0.91±0.06; $[\frac{1}{4},\frac{1}{4},0]T_2$, 2.30±0.05.

* Part of this work supported by U. S. Atomic Energy Commission.
[1] T. Toya, J. Research Inst. Catalysis Hokkaido Univ. **6**, 183 (1958).

L5. Calculation of Intensity Variations in Crystalline Bragg Scattering Due to Secondary Scattering.* R. I. Schermer, *M.I.T.*† (introduced by G. Brownell).—Sharp variations in intensity diffracted by single crystals have been observed by a number of experimenters, and have been attributed to secondary or multiple Bragg scattering in the crystal. Several authors have shown how the secondary planes responsible for the individual variations may be indexed. Renninger[1] has exhibited the intensity calculation for the case of one secondary beam, with both primary and secondary beams transmitted through the crystal, and with no absorption. The introduction of absorption, or of reflected beams, complicates the problem. Here, the equations are derived for *n* beams moving in arbitrary directions in a large slab of absorbing crystal, using the same mosaic model as is usually applied to the treatment of secondary extinction. The equations are solved by Laplace transform methods, in an approximation in which interaction between the secondary beams is neglected. The system properties are discussed in terms of an electrical analog. Results will be presented for the variation of the effect with thickness and system parameters, and for the shape of the observed variations.

* Work supported by the Rockefeller Foundation and the U. S. Atomic Energy Commission.
† Current address: Brookhaven National Labor .tory, Upton, New York.
[1] M. Renninger, Z. Physik **106**, 141 (1937).

L6. Proton Motion in Hydrogenous Compounds by Slow-Neutron Scattering Cross Sections.* J. J. Rush, T. I. Taylor, and W. W. Havens, *Columbia University and Brookhaven National Laboratory.*—Slow-neutron cross sections have been obtained from 0.0007 to 2 ev for several hydrogenous polycrystalline compounds to extend the measurements previously reported.[1] Cross-section vs temperature curves for NH_4Cl and NH_4I have been obtained from −80° to +23°C at a neutron energy of 0.001 ev. In this temperature range these compounds undergo several crystal phase changes. A sudden increase in cross section is observed for NH_4I at ∼−5°C, which is considered to be due to a first-order phase transition above which the ammonium ion is relatively free to rotate around a single axis. Curves of scattering cross section per proton vs neutron wavelength for NH_4I above and below the transition give slopes in the long wavelength region of 11 *b*/A-*H* and 6*b*/A-*H*,[1] indicating much greater freedom of motion for the ammonium ion in the high-temperature phase. Cross-section data will also be presented for KH_2PO_4, NH_4ClO_4, and $(NH_4)2CrO_4$. The slope of the *KDP* curve at long wavelengths (1 *b*/A-*H*) indicates extremely tight binding for the protons in this compound. The cross section of NH_4ClO_4, however, is consistent with a freedom of motion for the ammonium ion similar to that in NH_4I.

* Supported in part by the U. S. Atomic Energy Commission.
[1] J. J. Rush, T. I. Taylor, and W. W. Havens, Jr., Phys. Rev. Letters **5**, 507 (1960).

L7. Scattering of Cold Neutrons by Ammonia and Ammonium Halides.* H. Palevsky, V. W. Myers, and V. M. Brajovic,† *Brookhaven National Laboratory.*—The spectra of beryllium-filtered pile neutrons scattered at 90° have been measured for NH_4F, NH_4Cl, NH_4Br, NH_4I, and NH_3 gas. At 20°C NH_4F, NH_4Cl, and NH_4Br each exhibit two sharp peaks in an energy range of 20–100 mv, while NH_4I and NH_3 show only a broad distribution of neutrons. At −25°C NH_4I has two peaks similar to those observed in the other halides at room temperature. The energy of high-energy transitions agree with frequencies obtained from the combination bands in infrared experiments and yield the characteristic frequency of the torsional oscillation of the NH_4^+ ion in the field of its neighbors.[1] The lower energy peaks most likely represent the optical vibration frequency of the ammonium ion, which cannot be observed by infra-absorption techniques. A detailed comparison of the parameters obtained from the neutron

measurements with those obtained by other means will be presented.

* Work carried out under the auspices of the U. S. Atomic Energy Commission.
† Guest scientist from Institute of Boris Kidric, Belgrade, Yugoslavia.
[1] E. L. Wagner and D. F. Hornig, J. Chem. Phys. 18, 296 (1950).

L8. Scattering of Cold Neutrons in Organic Compounds.* V. W. MYERS, M. J. COTTER, AND H. PALEVSKY, *Brookhaven National Laboratory.*—The scattering spectra of 5-mv neutrons have been measured in several hydrogenous organic compounds. At 20°C, liquid benzene has two high-energy peaks at neutron energies of approximately 50 and 90 mv. These energy levels are consistent with Raman spectra observations, and are interpreted as vibrations in the benzene ring. These high-energy peaks in benzene are superposed on a very broad distribution which has a maximum at an energy of about 12 mv. This low-energy distribution may be due to the effects of hindered rotations of the molecules and intermolecular vibrations. At −25°C, solid benzene exhibits a low-energy spectrum similar to that of the liquid. At 20°C, polyethylene, cellulose acetate, nylon, and the alcohols have very broad single resonances in the neutron energy range 10–30 mv.

* Work carried out under the auspices of the U. S. Atomic Energy Commission.

L9. Scattering of Cold Neutrons by Liquid Tin.* H. R. MUETHER,† Y. WAKUTA,‡ AND R. L. STEARNS,§ *Brookhaven National Laboratory.*—The spectrum of beryllium-filtered neutrons scattered at 90° by thin samples of liquid tin has been measured using the Brookhaven slow-chopper apparatus. The spectrum shape shows a diffusive-type broadening of the incident spectrum similar to that previously observed in liquid lead. The broadening increases with temperature, and this variation gives an activation energy of 2000 cal/mole, approximately half the value obtained from macroscopic diffusion measurements. A broad peak of inelastically scattered neutrons is also observed at energy gains of approximately 15 mv. Polycrystalline solid sample shows a sharper peak at this same energy, consistent with the Debye temperature of tin. These results indicate that the liquid-tin atom dwells for a time in the field of its neighbors before making a diffusive jump.

* Work carried out under the auspices of the U. S. Atomic Energy Commission.
† Permanent address: State University of New York, Long Island Center.
‡ I. A. E. A. Fellow from University of Kyushu, Japan.
§ Permanent address: Vassar College.

L10. Neutron Scattering by Low-Temperature H_2O.† W. L. WHITTEMORE AND A. W. MCREYNOLDS, *General Dynamics Corporation.*—The scattering of neutrons by H_2O at temperatures down to 4°K has been investigated as part of a study of water structure. The total scattering cross section of H_2O at 21°, 77°, 268°, and 278°K was determined for $0.0005 < E < 0.1$ ev. The time of flight distributions of neutrons scattered by H_2O arranged in appropriate geometrical shapes have been studied for water temperatures of 4°, 21°, and 300°K. The spectrum for 21°K is depressed in the region around 0.06 and 0.021 ev, corresponding to reported energy levels for liquid H_2O.[1,2] There is no structure in the spectrum corresponding to levels reported at 0.008, 0.005, and 0.0005 ev.[2] The total cross-section measurements for H_2O at 21° and 77°K give no evidence of structure in the vicinity of any of these levels. At low energies, the cross section decreases with decreasing temperature, an indication of the scarcity of low-lying energy levels. The neutron spectra from 4°K and 21°K H_2O indicate that neutrons fail to thermalize completely to these low temperatures, further indicating the lack of important low-lying energy levels in solid H_2O.

† This work supported by the Atomic Energy Commission.
[1] B. N. Brockhouse, Acta Cryst. 10, 827 (1957).
[2] D. J. Hughes, H. Palevsky, W. Klen, and E. Tunkelo, Phys. Rev. 119, 872 (1960).

L11. Structure and Dynamics of Liquid Hydrogen by Neutron Scattering.* A. W. MCREYNOLDS AND W. L. WHITTEMORE, *General Atomic Division.*—In the very low energy range 0–0.010 ev, scattering interactions of neutrons with hydrogen are particularly sensitive to the details of bonding. Two types of measurements have been made on H_2O and liquid H_2 at temperatures from 4°K to 20°K to determine the energy distribution of initially fast neutrons from an electron linear accelerator, after multiple collisions, and to determine the total scattering cross section as a function of energy from 0.0001 to 0.1 ev. The neutron energy spectrum from liquid parahydrogen approaches more nearly than the ice spectrum to the equilibrium distribution for 20°K, corresponding to $kT = 0.0017$ ev. It shows a relatively sharp break in scattering properties at about 0.010 ev, above which there is indication of energy levels. This is confirmed by total cross-section measurements which also show that, in contrast to other hydrogenous materials, there is a definite transition point at 0.010 ev, below which behavior is similar to gaseous parahydrogen, and above which the cross section rises steeply, indicating a threshold for energy level excitations dependent on intermolecular forces and spin correlation.

* Supported in part by the U. S. Atomic Energy Commission.

L12. Neutron Scattering by Conduction Electrons as a Probe of the Superconductivity Energy Gap.* WILLIAM H. LUPTON† AND RICHARD A. FERRELL, *University of Maryland.*—A consideration of the inelastic scattering of neutrons by the conduction electrons in a metal reveals a cross section that is peaked in the forward direction due to the interaction of the neutron magnetic moment with the electronic currents. A phenomenological treatment shows that the cross section is related to the frequency and wave number-dependent conductivity. A degenerate electron gas is used as a model for the normal state of a metal. In a superconductor an electron must receive enough energy to surmount the energy gap, hence the small angle cross section is reduced. The ratio of the cross sections in the superconducting and normal states has been estimated from the conductivity reported by Glover and Tinkham. The scattering by the nuclei of the crystal lattice is also analyzed since it would be an important competing process in a proposed experiment.

* Supported by the Office of Naval Research and the Air Force Office of Scientific Research, ARDC.
† Now at the U. S. Naval Research Laboratory.

L13. Fluctuation-Dissipation Relations for Neutron Diffraction. RICHARD L. BECKER, *Oak Ridge National Laboratory.*—Fluctuation-dissipation (FD) relations are relations between responses of driven systems and their equilibrium fluctuations. Usually the system is considered in interaction with an external field (signal generator). By using perturbation theory, one may generalize to situations in which the reaction on the driving system must be included. The scattering of a neutron wave packet by a fluid initially in equilibrium is treated, using the Fermi pseudopotential and the van Hove statistical space-time correlation function $G(\mathbf{r},t)$. The relevant response functions, $d^2\sigma/d\Omega dE$ and the time-dependent local particle density in the fluid are expressed most directly in terms of both ReG and $\hbar^{-1}ImG$. We regard such expressions as primitive FD relations. A systematic presentation is given of integral representations of ReG in terms of $\hbar^{-1}ImG$ and of their converses. These statistical relations are valid for any system in equilibrium and are independent of considerations of driving the system. Although ImG equals zero in the classical limit, $\hbar^{-1}ImG$ does not. On eliminating $\hbar^{-1}ImG$ in favor of ReG by means of one of the statistical relations, the responses may be expressed in terms of ReG alone, which corresponds to the usual form of FD relations.

L14. Temperature Measurements in High-Temperature Gases Using Thermal Neutron Scattering. PATRICK DOHERTY, RONALD BARR, RICHARD BOEDEKER, ROBERT DELANEY, DONALD MANSON, AND A. H. WEBER, *Saint Louis University.*—The feasibility of developing a neutron thermometer is discussed theoretically and experimentally. Neutrons in a collimated beam from the thermal column of a reactor are allowed to impinge on a volume element of a high-temperature gas. They are scattered in such a manner that at a given angle their energy distribution depends on the average ion temperature of the volume element and is independent of the ionization. An analysis of this energy distribution can be made by looking at the transmission of the scattered neutrons through cadmium foils. Results of an experiment using an oxyhydrogen flame as the scatterer will be given.

TUESDAY AFTERNOON AT 2:00

Sheraton Hall

(M. M. SHAPIRO presiding)

Cosmic Rays and Space

LA1. Primary Cosmic-Ray Spectrum in 1958.* HUGH R. ANDERSON, *California Institute of Technology and Jet Propulsion Laboratory.*—In 1958 our Laboratory made a latitude survey of cosmic-ray intensity using integrating ionization chambers and sounding balloons. Thirty-eight simultaneous pairs of balloon flights were launched. The rate of ionization was successfully measured as a function of atmospheric depth at a base station and simultaneously from a roving station at twenty-nine different latitudes between 87°N and 79°S geomagnetic latitude. A primary differential rigidity spectrum over the latitude sensitive region has been calculated from these data using geomagnetic theory and an assumed charge spectrum. The integral flux of nuclei with rigidity >16 Bev may be obtained from our data by assuming that the spectrum has a constant slope at all higher rigidities. By combining this result with the derived differential spectra the integral flux of primary nuclei with rigidity >0.6 Bev has been computed. It is found that $N(>0.6$ Bev) equals 0.11 nuclei/cm² sec sr, in 1958.

* Assisted by the joint program of the Office of Naval Research and the U. S. Atomic Energy Commission.

LA2. Flux and Energy Spectra of Primary Cosmic-Ray Protons from 70 to 400 Mev.* ROCHUS VOGT, *University of Chicago.*—During August and September, 1960 three Skyhook balloon flights were carried out from Fort Churchill, Manitoba at altitudes of 125 000 ft. The energy spectrum of the vertically incident protons was determined through the measurement of the particle energy loss and range in lead. It was found that the flux of low-energy protons rises with decreasing energy between 75 and 400 Mev. The particle flux and energy spectra will be presented, and the implications of these results on cosmic-ray modulation mechanisms will be discussed. On September 8 additional protons of solar origin were observed which probably originated in the solar flare of September 3 and remained trapped in interplanetary space.

* Research supported in part by the Office of Scientific Research, U. S. Air Force, the National Science Foundation, and the Office of Naval Research, U. S. Navy.

LA3. Solar Protons and α Particles from the September 3, 1960 Flare.* S. BISWAS,† PHYLLIS FREIER, AND W. STEIN, *University of Minnesota.*—A class 3+ solar flare started at 0040 UT on September 3, 1960, and reached maximum intensity at 0110 UT. The average proton differential energy spectrum from 0930–1700 UT on September 3rd has been measured in the energy interval 250–800 Mev. Expressing $dN/dE = k \cdot E^{-\gamma}$, γ is approximately 2 from 250–400 Mev and increases to approximately 3 at higher energies. The proton cutoff energy has been measured and is 250±15 Mev. This corresponds to a magnetic rigidity of 0.72 Bev at Minneapolis. The sudden commencement of the magnetic storm following this flare occurred at 0230 UT on September 4th. After this time, protons of energy <250 Mev were also observed. We are measuring the proton spectrum in the energy interval 80–800 Mev from 1700–2320 UT on September 4th. The solar α-particle differential energy spectra at these two times have also been measured. For α particles $\gamma = 3$ in the energy interval 100–200 Mev/nucleon. Before the magnetic storm the ratio of the flux of protons to the flux of α particles in the rigidity region 0.88–1.3 Bev is $J_p^0/J_\alpha^0 = (3700$ particles/m²·sec·sr)/(120 particles/m²·sec·sr) = 31±8.

* This work was supported by the joint program of the Office of Naval Research and the U. S. Atomic Energy Commission.
† On leave from Tata Institute of Fundamental Research, Bombay.

LA4. Polarization of Cosmic-Ray Mu Mesons Underground and at Sea Level.* H. V. BRADT AND G. W. CLARK, *M.I.T.*—The polarization of cosmic-ray mu mesons that come to rest in a brass absorber has been measured at sea level with less than 20 g/cm² of material above the absorber and underground with about 3700 g/cm² of rock cover. The polarization was determined from the degree of asymmetry in the distribution of directions of decay electrons. Approximately 200 000 decay events were observed at each site, and the ratio of polarizations at the underground and sea-level sites P_u/P_s was found to be 0.98±0.18. A determination of the absolute polarizations from the observed effect yielded $P_u = P_s = 0.26 \pm 0.03$, where the scattering of the decay electrons in the brass absorber was not taken into account. According to the theory of Hayakawa, the measured polarization depends, in part, upon the proportion of K mesons among the parents of stopped muons. Assuming no anomalous depolarization of the muons in the rock, one concludes, therefore, that the measured results impose an upper limit on the K/π production ratio at the primary energies defined by the 3700 g/cm² of cover at the underground site. These energies are, on the average, above that presently available from machines.

* This work is supported in part by funds provided by the U. S. Atomic Energy Commission, the Office of Naval Research, and the U. S. Air Force Office of Scientific Research.

LA5. Effective Directional Sensitivity of Cosmic-Ray Neutron Monitors. SERGE M. LAPOINTE, *Université de Montréal,* AND D. C. ROSE, *National Research Council.*—The direction of maximum sensitivity of a neutron monitor is calculated

numerically for a set of points on the same geomagnetic meridian but extending in latitude from the equator to the pole. This leads to two master curves, one for the longitude and the other for the latitude of this direction. From these curves this direction is obtained in geographic coordinates for some twenty cosmic-ray stations. The method of calculation is described taking into account atmospheric absorption and the energy spectrum of the incident particles. The aperture of the sensitive cone, or source width, also is calculated. Finally the accuracy of the results is discussed and the application of the concept of effective direction is described.

LA6. Secondary Cosmic-Ray Photons below Cascade Energy.* K. A. ANDERSON, *University of California, Berkeley.*—On several occasions during 1958 and 1959 scintillation spectrometers have been included in balloon-borne apparatus designed to study auroral zone x-ray effects. Incidental to these observations the counting rates in the crystal due to photons in equilibrium with the primary cosmic-ray beam have been obtained over the energy interval 30 to 300 kev. The maximum intensity of these photons occurs at 100 g cm^{-2} depth and is approximately 22 cm^{-2} sec^{-1} as compared with a charged particle flux of 1.9 cm^{-2} sec^{-1}. The differential energy spectrum of these photons is quite flat varying roughly as E^{-1}. These flights attained atmospheric depths of 6.5 g cm^{-2} and estimates of the photon flux at zero depth can be made by extrapolation. The photon albedo of the atmosphere is thus found to be about 8 cm^{-2} sec^{-1} above 30 kev. The origin of these photons is believed to be mainly in the electromagnetic cascade. Their great abundance is due to the long absorption length in the 30- to 300-kev region where the dominant interaction with matter is the Compton process.

* Supported by the U. S. Office of Naval Research.

LA7. Evidence for Storage of Solar Cosmic Rays within the Magnetic Configuration Responsible for a Forbush Decrease. H. CARMICHAEL AND J. F. STELJES, *Atomic Energy of Canada Limited.*—Three major solar flare and radio noise outbursts in rapid succession, associated with a large sunspot, occurred on November 10, 11, and 12, 1960, starting at 1000, 0304, and 1320 UT, respectively. Solar cosmic radiation generated in the third of these outbursts produced a conspicuous increase in sea-level neutron monitors. At Deep River, Ontario, the increase started slowly at 1342 UT and was declining at 1900 UT when a sudden enhancement occurred followed by some rapid fluctuations. There was no significant solar activity at this time, some 5 hr after the start of the flare. About half an hour later a sharp (Forbush) decrease of the intensity of galactic cosmic radiation occurred. Sudden-commencement magnetic storms had begun at 1348 and 1844 UT. It is reasoned that these storms and the Forbush decrease were produced by an expanding plasma cloud from the flares of November 10 and 11 and that the sunspot field entrained in the cloud formed a magnetic bottle[1] attached to the sun in which high-energy particles injected by the flare of November 12 were trapped and were being stored. As the plasma front passed the earth, the monitor suddenly sampled a higher flux due to the trapped solar cosmic-ray particles.

[1] Thomas Gold, J. Geophys. Research 64, 1665–1674 (1959).

LA8. Interplanetary Magnetic Fields as Derived from Cosmic-Ray Observations.* K. G. MCCRACKEN, *M.I.T.* (introduced by Frank Scherb).—During 1959 and 1960 there were six occasions on which a large solar flare produced relativistic cosmic rays which were detected at the earth. The time behavior and isotropy of the six events were markedly different, and will be shown to impose limits on the magnetic field configurations in the inner solar system, being consistent with a theoretical model proposed by Gold, Piddington, and others. For example, the flare effects occurring after cosmic-ray production near the western solar limb exhibited rapid rise times, and marked anisotropy, while, when the parent flare was further to the east, the rise times were long, and the radiation relatively isotropic. While these above facts yield information on the magnetic configurations between the sun and the earth, the decay of the flare effect is determined by the magnetic field regime in the solar system as a whole. It will be shown that the dimensions and properties of the fields inferred from the solar and cosmic-ray events prior to the flare effects yield satisfactory explanations for the various types of decaying phases which were observed.

* Sponsored by the World Wide Research Scientists Project on the International Co-operation Administration of the U. S. Government.

LA9. An Investigation in High-Energy Gamma-Ray Astronomy.*† THOMAS L. CLINE,‡ *M.I.T.*—A study of the 100-Mev photon component of cosmic radiation was carried out by use of a balloon-borne scintillation-Čerenkov counter telescope. A directional search for primary photons yielded a negative result; an upper limit of the isotropic primary photon intensity was set at 3×10^{-3} cm^{-2} sec^{-1} sr^{-1}, and of the intensity from the galactic plane at 1.2×10^{-2} cm^{-2} sec^{-1} sr^{-1}. Assuming the current galactic model, a limit on the steady-state antiproton creation rate was set at a value slightly below that required by the cosmological model. Possible point sources of photons were investigated; an upper limit of the flux from the direction of Cygnus-A was set at 7×10^{-4} cm^{-2} sec^{-1}. Other results will be discussed.

* This work was supported in part by the U. S. Atomic Energy Commission and by the Office of Naval Research.
† Abstracted from a thesis submitted to the Department of Physics in partial fulfillment of the requirements for the degree of Ph.D.
‡ Now at National Aeronautics and Space Administration's Goddard Space Flight Center.

LA10. Stimulated Emission of Synchrotron Radiation from Jupiter. PAUL J. KELLOG, *University of Minnesota.*—Jupiter is an amazingly powerful radio source, and the mechanism of the radio emission is thought to be synchrotron or cyclotron emission from electrons trapped in a radiation belt.[1] This interpretation requires either a very large number of relativistic electrons or a large magnetic field. We consider whether stimulated emission of such synchrotron radiation may be important. If the radio source has five times the area of Jupiter's disk, then the observed power flux corresponds to an occupation number of the order of 1000 radio photons per quantum state at a wavelength of 68 cm. It is possible then, that stimulated emission is 1000 times more important than spontaneous emission. If spontaneous emission dominates, then radio emission in a direction in which the gradient of magnetic field vanishes is enhanced, and the geometry of the source will be changed. This and other consequences of the assumption of predominant stimulated emission will be discussed.

[1] G. B. Field, J. Geophys. Research 65, 1661 (1960).

LA11. Space Erosion of the Grant Meteorite. DAVID E. FISHER, *Cornell University.*—An upper limit to the erosion of iron meteorites in space is calculated, based on the cosmic exposure age of the Grant meteorite and on the measured depth variation of cosmogenic neon-21 in this meteorite. A value for E_{max} of 10^{-8} cm/yr is found. The analysis does not differentiate between erosion due to interplanetary gas, dust, or ions. Suitability of the Grant meteorite for this analysis, and previous estimates of erosion rates and of interplanetary dust will be discussed.

TUESDAY AFTERNOON AT 2:00

National Bureau of Standards, East Building

(L. MARTON presiding)

Electron Physics

M1. Electrical Conduction and Breakdown in High-Pressure (0.25-300 mm) Rare Gases. R. FORMAN, *Union Carbide Corporation.*—The current voltage characteristics of high-pressure (0.25–300 mm) inert-gas diodes have been measured. Unexpected phenomena have been observed and some of the general results can be summarized as (1) the current vs voltage characteristics of argon and xenon-filled diodes at gas pressures above 1 mm, do not obey a space-charge law if the cathode temperature is above 2400°K; (2) the current vs voltage characteristics of helium-filled diodes, however, do obey the space-charge relations at all filament temperatures available with present cathode materials; (3) unusual early breakdown phenomena were observed. An attempt will be made to explain these data qualitatively by postulating the existence of thermally generated xenon or argon ions at the operating temperatures.

M2. Electron Guns for Low-Energy Scattering Experiments. C. E. KUYATT AND J. AROL SIMPSON, *National Bureau of Standards.*—For a planned experiment on differential inelastic electron scattering in gases, the need arose for an electron beam of the following characteristics: energy 200 to 1000 ev, current at least 30 microamperes, cross section 1 mm, angular divergence less than 5 milliradians. Since energy-resolved cross sections are desired the energy spread of the beam must be as narrow as practical. At these energies the requirements are contradictory. The highly collimated fine-focus beams of electron microscope or cathode-ray tube guns have insufficient current while space-charge limited guns of the Pierce type have sufficient current but are neither fine enough focus nor well enough collimated. Furthermore, many guns have energy spreads far above thermal. Guns of both types were tested for (1) current density and collimation and (2) energy spread. The first was determined by measuring the current through a 0.3 mm hole 240 mm from the gun anode; the second by a retarding field analyser. The best gun tested was a two stage device derived from electron microscope practice. The energy spread was only slightly beam-current sensitive and close to thermal. All oxide-cathode guns gave significantly poorer results than pure metal. Both the energy spread and the mean energy of beams from oxide cathodes, at least in our vacuum system, are very current-dependent and far from thermal.

M3. Combined Theories of Elastic and Inelastic Electron Scattering in Metals. H. A. FOWLER, *National Bureau of Standards.*—The characteristic-loss spectra of electrons scattered by transmission through metal foils are regarded as ideal examples of plural scattering. However, no satisfactory model exists in the literature to explain the angular dependence of these spectra. Competing models of the pure-elastic scattering process are the coherent diffraction theory of Bethe and von Laue, and the incoherent diffusion theory of Molière, Lenz, and Leonhard. Competing models of the plural, diffuse, inelastic process have been based on two different types of cross-section: the narrow, highly peaked type of Lenz and Leonhard, and the broad type considered by Ferrell, proportional to $\theta_E/\theta_E^2+\theta^2$. A new combined model is proposed, in which the pure-elastic process is coherent diffraction, and the plural inelastic process has a cross-section of the Ferrell type. A representation in terms of linear integral operators is suggested. Critical features of the new model are (1) the dependence of the pure-elastic angular distribution on thickness, (2) the angular spreading of the successive discrete-loss peaks, and (3) the Poisson statistical distribution of electrons among the discrete-loss peaks.

M4. Plural Inelastic Scattering of Electrons in Aluminum at 20 kev. L. MARTON, J. AROL SIMPSON, H. A. FOWLER, AND N. SWANSON, *National Bureau of Standards.*—Experimental observations of the angular dependence of characteristic-loss spectra have been made with an incident beam of 1–1.5 mrad half-width. These are compared with the theoretical model of the preceding paper. (1) The angular width of the elastic peak does not increase appreciably with specimen thickness, between 500 and 1800 A. (2) The angular spreading of the successive discrete-loss peaks is accurately described by a folding operation with the Ferrell type of differential cross section. Both the half-width and the long tails of this cross section agree well with experiment. (3) The integrated angular distributions of the elastic and discrete-loss peaks compare accurately with Poisson-distribution functions of argument range 0.75–2.4. On combining these arguments with foil thickness measurements by a Fizeau-Tolansky interferometer, a value of mean free path in the 8 to 900-A range is obtained for 20-kev electrons. This is in agreement with the previously reported value of Blackstock, Ritchie, and Birkhoff,[1] when differences in the experimental method are considered.

[1] A. W. Blackstock, R. H. Ritchie, and R. D. Birkhoff, Phys. Rev. 100, 1078 (1955).

M5. Polarization of Photoelectrons from Magnetized Nickel.* R. L. LONG, VERNON W. HUGHES, AND J. S. GREENBERG, *Yale University,* AND I. AMES AND R. L. CHRISTENSEN, *IBM Research Laboratories.*—An attempt has been made to produce a beam of transversely polarized electrons by photoemission from a high-purity single crystal of nickel. The crystal was magnetized along the 111 direction by a permanent magnet, and the electrons were emitted from the 110 face. An electronic getter-ion vacuum pump provided a pressure of about 5×10^{-8} mm of Hg. The light source was a mercury UV lamp[1] which produced primarily the 1850 A and 2537 A lines of Hg. By use of a filter, it was found that essentially all of the photoelectrons were produced by the 1850 A line. The photoelectrons were accelerated to 140 kv by an electrostatic accelerator to give a current of about 10^{-10} amp. A cylindrical electrostatic field was used to energy analyze the beam, which then entered a Mott scattering polarization analyzer.[2] The electrons were scattered by an 83 μg/cm^2 gold target. The scattering asymmetry was measured and the polarization was calculated according to the methods of Greenberg *et al.*[2] No polarization has been found, whereas, a polarization of 10% would have been observed. Further experiments are planned with better vacuum conditions and with other selected wavelength lines.

* This research has been supported in part by the National Aeronautics and Space Administration.

[1] Pen-Ray Model 11SC-2, made by Black Light Eastern Corporation.

[2] J. S. Greenberg, D. P. Malone, R. L. Gluckstern, and V. M. Hughes, Phys. Rev. 120, 1393 (1960).

M6. Electron Emission from Metals at Temperatures Near Their Melting Points. H. F. KAISER, *U. S. Naval Research Laboratory.*—In a previous paper[1] the possibility of obtaining high current density electron emission from various pure metals and carbon operated at temperatures through and

above their melting points was explored. Possible durable operation under pulsed conditions at emission current densities exceeding 100 amp/cm² was indicated by a study of vaporization characteristics for a few metals. In this paper, this topic is extended with a study of a possible further increase of emission by the space charge neutralization brought about by metal vapor ions produced in the extraction process. Experimental results with equipment produced to date will be described.

[1] H. F. Kaiser, Bull. Am. Phys. Soc. **5**, 281 (1960); and NRL Quarterly on Nuclear Science and Technology, July, 1960, pp. 18–27.

M7. Optical Emission of Irradiated Ag and Al Foils. E. T. ARAKAWA, A. L. FRANK, R. D. BIRKHOFF, AND R. H. RITCHIE, *Oak Ridge National Laboratory.**—Light emitted by thin foils of Ag and Al during irradiation by 40- to 115-kev electrons has been analyzed with a vacuum ultraviolet spectrometer having an EMI 6256B photomultiplier and conventional dc current amplifier as detector. Spectra were obtained between 1700 A and 6000 A at 30° from the foil normal for Al foils of thicknesses 125 A, 250 A, 375 A, and 500 A, and Ag foils of thicknesses 1200 A, 1600 A, 2000 A, and 2400 A. The peak at 3400 A in Ag, ascribed to plasma radiation by Brown[1] and Steinmann,[2] was investigated for the foils and energies stated above. For Al a continuum was found which increased in intensity as the wavelength decreased. Comparison will be made between the latter and a generalization of the Frank-Ginsberg transition radiation theory as formulated by Ritchie and Eldridge.[3]

* Operated by Union Carbide Corporation for the U. S. Atomic Energy Commission.
[1] R. W. Brown, P. Wessel, and E. P. Trounson, Phys. Rev. Letters **5**, 472 (1960).
[2] W. Steinmann, Phys. Rev. Letters **5**, 470 (1960).
[3] R. H. Ritchie and H. B. Eldridge, Bull. Am. Phys. Soc. Ser. II **4**, 384 (1959).

M8. Electroluminescence of Thin ZnS Films. W. A. THORNTON, *Westinghouse Lamp Division.*—The ac electroluminescence of thin ZnS:Cu,Cl films is like that of powder phosphors. The major difference is that strong asymmetry in the films causes light emission only during the half-cycle of the applied voltage when the transparent tin oxide electrode, upon which the film is formed, is negative. The other (aluminum) electrode plays no part since an intermediate insulating layer has no effect. The resistive current component in the films is, however, symmetrical with voltage polarity, as are both light and current in powder phosphors; this implies that the electrodes are never involved and that current and light emission are controlled by internal junctions in both phosphor films and powders. Direct current, as well as instantaneous ac current (resistive), in these films is proportional to $[\exp(V/V')-1]$, where V' is a constant. If either voltage half-cycle is clipped (or eliminated) by a rectifier, the light emission is reduced (or eliminated). Direct voltage bias, added to the alternating voltage, has the same effect although in this case the rms voltage is constant; the effect of the sign of the dc bias voltage indicates that the ionization process occurs during one half-cycle (with no light emission), and that the resulting light emission occurs on the following half-cycle.

M9. Material and Enclosure Effects on the Threshold for Pulsations in Induced Fluorescence R. W. HELLWARTH, *Hughes Research Laboratories.*—The nature of the pulsations in the induced fluorescence from a "three-level" crystal excited between two parallel reflecting plates has been estimated[1] for the case where interference effects may be neglected. In this same case, the threshold level of exciting (pump) radiation, measured by the pump transition rate w_0 at threshold, is found to depend on the anisotropy of the crystal absorption coefficient for the fluorescent transition $\alpha(\theta,\nu)$ and on the anisotropy of the plate reflectivity $R(\theta)$, as well as on the fluorescent ion concentration and maximum reflectivity. If τ is the natural lifetime of the fluorescent state, and n_1 and n_2 are the lower and upper fluorescent level populations at the point where the material gain just balances the losses in an optimum direction, then one finds for w_0 that $w_0\tau n_1 = n_2 \int d\Omega g(\theta)[1-t(\theta)g(\theta)]^{-\frac{1}{2}} / \int d\Omega g(\theta)$. We have assumed for simplicity that α and R are only functions of the angle θ measured from the direction of highest gain, and $g(\theta) \equiv \alpha(\theta,0)/\alpha(0,0)$; $t(\theta) \equiv [1-R(0)]/[1-R(\theta)]$. The results of numerical calculations of w_0 under various conditions and corrections for systems involving more than three levels will be given. Possibilities for control and variation of pulsations will be discussed.

[1] R. W. Hellwarth, Phys. Rev. Letters **6**, 9 (1961).

M10. Brillouin Flow in Relativistic Beams. P. B. ULRICH AND D. C. DEPACKH, *U. S. Naval Research Laboratory.*—A solution in closed form for Brillouin flow under relativistic conditions in a cylindrical geometry has been found in the limit of low beam temperature. Curves and formulas will be presented relating density, magnetic field, energy, and tangential velocity throughout the beam. It will be shown that the forward component of velocity is constant to all orders in the radius, that the beam exhibits a depression in central density due to diamagnetism, and that the central electrons in the beam of maximum perveance have an upper energy limit of approximately 200 kev.

M11. Eddy Current Instability of an Electron Beam in a Conducting Tube. D. C. DEPACKH, *U. S. Naval Research Laboratory.*—An intense electron beam confined by external focusing within a shielding tube of finite conductivity should exhibit an instability resulting from partial penetration of the beam field into the tube. This instability is analogous to the instability predicted by Rosenbluth[1] for a beam penetrating a plasma. Its growth rate is approximately proportional to the square of the electron momentum, the square of the ratio of beam diameter to tube diameter, and the reciprocal time constant of decay of tangential currents in the tube for a beam in equilibrium between space charge and focusing forces.

[1] M. N. Rosenbluth, Phys. Fluids **3**, 932 (1969).

M12. Electron Trajectories in Axially Symmetric Magnetic Fields.* R. F. STETSON, B. N. A. LAMBORN, AND D. L. LAFFERTY, *University of Florida.*—The behavior of electron beams of variable energies injected into an axially symmetric magnetic field is investigated. In the experiments, the beams are injected in the $r-\theta$ plane; with suitable choice of radial field gradient, the electron beam can be made to spiral inward from the injection radius and to reflect off some finite inner radius. With the proper choice of beam energy, the path traversed by the beam can be made very large.

* Supported in part by the U. S. Atomic Energy Commission.

M13. Electron Beam Interactions with a Plasma.* D. L. LAFFERTY AND B. N. A. LAMBORN, *University of Florida.*—The system has been analyzed in terms of collective variables and is described by a set of coupled, nonlinear differential equations relating the Fourier components of the charge densities of the two sub-systems. The general equations will be discussed and solutions obtained for several special cases.

* Supported in part by the U. S. Atomic Energy Commission.

M14. Longitudinal Oscillations in a System of Charged Particle Streams.* B. N. A. LAMBORN AND D. L. LAFFERTY, *University of Florida.*—A system of n streams of particles, each containing particles of one charge, mass, and translational velocity except for thermal variations, is investigated using collective coordinates. The total system is assumed to be charge neutralized. An equation of motion is derived for each stream relative to its center of mass. The corresponding dispersion relation of the system is obtained and discussed.

* Supported in part by the U. S. Atomic Energy Commission.

TUESDAY AFTERNOON AT 2:00
Cotillion Room, North
(J. G. DAUNT presiding)

Cryogenics

MA1. Effect of Dissolved Gases on Some Superconducting Properties of Niobium. WARREN DESORBO AND GLENN E. NICHOLS, *General Electric Research Laboratory.*—Studies have been made on the superconducting resistance transitions characteristics, in a longitudinal magnetic field, of wire specimens of niobium containing various dissolved gases, i.e., oxygen, nitrogen, hydrogen, and deuterium. Before the addition of the gases, the wires, made from an electron beam melted stock, were annealed and "degassed" in a high vacuum ($1<1\times10^{-6}$ mm of Hg) and high temperatures (1800–2000°K). For a specimen with a resistance ratio equal to ~500, $T_c=$ 9.465°K, whereas, prior to the thermal treatment, $T_c=$ 9.668°K. These are in good agreement with T_c values recently reported.[1,2] The initial slope of the critical magnetic field, $(\partial H_c/\partial T)_i$, is 530 oe/deg after the thermal treatment, and 1140 oe/deg prior to it. Oxygen has the largest effect on T_c and on the non-continuous behavior of the transition. The addition of small amounts decreases T_c and increases $(\partial H_c/\partial T)_i$, e.g., for a specimen containing 1.4 at. %, $T_c=5.840$°K, $(\partial H_c/\partial T)_i=$ 5000 oe/deg. The addition of oxygen in larger amounts increases T_c again while $(\partial H_c/\partial T)_i$ decreases. Some consequences of this will be discussed. The cryostat which renders temperatures reproducible to 1 millidegree will be described.

[1] G. von Minnigerode, Z. Physik **154**, 442 (1959).
[2] A. Calverley (private communication).

MA2. Change in Young's Modulus between Normal and Superconducting Indium.* DWIJENDRA BHATTACHARYA AND EDWARD A. STERN, *University of Maryland.*—Recent measurements[1,2] have shown that the lattice specific heat of indium in the superconducting state is roughly 20% less than that of the normal state below 0.7°K, while the change in the lattice Debye temperature as determined from elastic constants at 1.4°K is less than one part in 6×10^3. To further study this apparent paradox, changes in the Young's modulus of a polycrystalline indium bar between the normal and superconducting states is studied in more detail down to about 1.0°K with a sensitivity of better than one part in 10^5.

* Research supported by U. S. Signal Corp.
[1] C. A. Bryant and P. H. Keesom, Phys. Rev. Letters **4**, 460 (1960).
[2] B. S. Chandrasekhar and J. A. Rayne, Phys. Rev. Letters **6**, 3 (1961).

MA3. Current Distributions In Thin Superconducting Films. PAUL M. MARCUS, *IBM, Yorktown Heights.*—Detailed solutions have been obtained for current distributions within, and the magnetic fields in and around, a superconducting film of rectangular cross section carrying a steady current when the London constitutive equation for a superconductor is satisfied. The problem has been attacked through the inhomogeneous linear integral equation over the cross section for the current density. By power series expansion in the thickness coordinate, the problem is reduced to a series of coupled integral equations in one coordinate, which are then solved by systematic approximation by sets of linear equations. The cases of interest consider films of thickness t comparable to the penetration depth λ and widths w up to 500 λ or more. The current distributions are then fairly uniform through the thickness, but very sharply peaked at the edges, and fall off slowly toward a minimum value at the center; the ratio of the center value to the edge value varies approximately as $1/(wt)^{\frac{1}{2}}$ and is 0.075 for $w=500\,\lambda$, $t=\lambda$. The effects of a ground plane of external magnetic fields, and of nonlocal constitutive equations are also being studied.

MA4. Deviations from the Law of Corresponding States in the Theory of Superconductivity. JAMES C. SWIHART, *IBM Research Center.*—The BCS[1] integral equation has been studied for various nonseparable interactions $V_{kk'}=V(|\epsilon_k-\epsilon_{k'}|)$. Numerical solutions have been obtained on an IBM 704 for the energy-gap function $\Delta_k(T)$ for a square well potential $V(x)$ which is attractive for $x<\frac{1}{2}\theta_D$, repulsive for $\frac{1}{2}\theta_D<x<x_1$, and zero for $x>x_1$. The cutoff x_1 is arbitrarily taken between θ_D and $2\theta_D$. The ratio $\eta=2\Delta_{kF}/kT_c$ is rather insensitive to the various parameters for several cases tried, giving nearly the original BCS value of 3.5. This shows that the BCS theory does give the law of corresponding states. In one case, to simulate Pb or Hg, a potential was taken with the repulsive part equal to the average Coulomb interaction, while the attractive part was chosen to give a T_c of 7.3° with $\theta_D=70$°. For this strong coupling case, η was raised to 4.01. This solution gives for the jump in the specific heat at T_c the value 1.51 compared to 1.40 for BCS.

[1] J. Bardeen, L. N. Cooper, and J. R. Schrieffer, Phys. Rev. **108**, 1175 (1957).

MA5. Superconducting Film Geometry with Strong Critical Current Asymmetry. H. H. EDWARDS AND V. L. NEWHOUSE, *General Electric Research Laboratory.*—It is shown that film critical current, defined as the maximum current for which the film shows no resistance, can be strongly increased in one direction and strongly decreased in the order by the field from two current-carrying wires placed parallel to the film edges. The increase in critical current is shown to be associated with a mutual cancellation of the normal magnetic fields created by the wire currents and the film current. This cancellation occurs when the film current is uniformly distributed. This fact causes a uniform current distribution to occur. Experimental evidence is presented that the symmetrical increase of critical current due to the proximity of a superconducting "shield" plane[1] is the result of the same mechanism. Fields normal to the film surface also may be largely responsible for the broad current-induced transition[2] of flat "unshielded" films. With mutually opposed wire currents, the variation of critical current with wire current exhibits a significant hysteresis.

[1] V. L. Newhouse, J. W. Bremer, and H. H. Edwards, Proc. Inst. Radio Engrs. 1395 (1960).
[2] J. W. Bremer and V. L. Newhouse, Phys. Rev. **116**, 309 (1959).

MA6. Magnetic Field Dependence of the Superconducting Energy Gap and Penetration Depth. D. H. DOUGLASS, JR., *Lincoln Laboratory.**—Gor'kov[1] has recently derived the Ginzburg-Landau[2] (GL) phenomenological equations of superconductivity from the microscopic theory in the region where $T_c-T\ll T_c$ and $\xi\ll\lambda(T)$, where ξ is the coherence length and $\lambda(T)$ is the penetration depth. He showed that the order parameter ψ of the GL theory is directly proportional to the energy gap. In the GL theory, ψ is a function of temperature and field, and is identified with the penetration depth. Thus, the field dependence of the energy gap and penetration depth can be obtained by solving the GL equations for $\psi(H)$. This has been done for a superconducting plate. The results show that the maximum effect occurs for thin specimens. For very thin plates, $[\lambda(T,0)/\lambda(T,H)]^2=1-(H/H_c)^2$, $[\epsilon(T,H)/\epsilon(T,0)]^2=1-(H/H_c)^2$, where ϵ is the energy gap and H_c is the critical field of the plate.

* Operated with support from the U. S. Army, Navy, and Air Force.
[1] L. P. Gor'kov, J. Exptl. Theoret. Phys. (U.S.S.R.) **36**, 1918 (1959); Soviet Phys.—JETP **9**, 1364 (1959).
[2] V. L. Ginzburg and L. D. Landau, J. Exptl. Theoret. Phys. (U.S.S.R.) **20**, 1064 (1950).

MA7. Kapitza Boundary Resistance between Normal and Superconducting Tin and Liquid Helium.* J. I. GITTLEMAN, *RCA Laboratories.*—Measurements of the Kapitza boundary resistance between liquid helium and tin have been made in the temperature range from 1.4°K to 2.0°K. The Kapitza resistance was found to vary as T^{-3} in this range, as would be expected from the work of Khalatnikov and Little. A 9% increase was noted when the tin was in the superconducting state as when it was normal. This is contrary to measurements reported by Challis for lead, which showed that the Kapitza resistance in the same temperature range was nearly three times larger for lead in the superconducting state than in the normal state. Although the reason for the difference between the results for lead and tin is not known, it is probably related to the fact that the Debye temperature of tin is much higher than for lead. Thus, in lead the lattice dominates the thermal properties, whereas in tin the electrons contribute strongly. Measurements on indium, which has a Debye temperature slightly higher than that of lead, have also been made. The Kapitza resistance in the normal state measures slightly less than in the superconducting state.

* Sponsored by U. S. Air Force, Wright Air Development Division.

MA8. Free Precession Measurements in Solid He^3.* J. M. GOODKIND AND W. M. FAIRBANK, *Stanford University.*—Measurements of T_1, T_2, and susceptibility have been continued with a different sample container. The earlier results[1] have been reproduced with the exception of T_1 in the β phase at 1.37°K. At this point, T_1 has been found to be immeasurably long (longer than 24 hours). The susceptibility has been measured as a function of pressure at 1.4°K from a pressure of 900 to 1600 lb/in^2. The variation of the volume susceptibility over this pressure range agrees, within an experimental error of five per cent of the total change, with the variation in density as extrapolated from the measurements of Grilly and Mills at the melting line. This information, combined with the $1/T$ temperature dependence of the susceptibility in this region and earlier normalization in the liquid and the gas, establishes that the susceptibility is obeying a classical Curie law in this region. T_2 measurements above 1°K are inconsistent with the exchange energy predicted by Bernardes and Primakoff and indicated by the susceptibility below 0.2°K on the basis of simple exchange narrowing theory. The T_2 measurements are being extended to lower temperatures to check this result in the region of the susceptibility anomaly.

* Supported in part by the Office of Ordnance Research and the National Science Foundation.
[1] J. M. Goodkind and W. M. Fairbank, *Helium Three* (Ohio State University Press, Columbus, 1960), p. 52.

MA9. Susceptibility of Liquid He^3 and He^3-He^4 Solutions.* E. D. ADAMS AND W. M. FAIRBANK, *Stanford University.*—Fairbank, Ard, and Walters[1] have reported a temperature dependence of the susceptibility of pure liquid He^3 under its saturated vapor pressure between 0.13°K and 2.1°K. Their results indicate that the susceptibility has the qualitative behavior of an ideal-gas model, but with a degeneracy temperature of 0.45°K, an order of magnitude lower than the ideal-gas model. Low, Rorschach, and Schwetman[2] have recently reported results on 95% He^3 between 1.2°K and 2.0°K which depart from the Curie law more rapidly than the earlier results[1] on pure He^3, extrapolating to a degeneracy temperature of 0.9°K. We have remeasured the susceptibility of pure He^3 from 0.06°K to 2.0°K, using a He^3 refrigerator for maintaining temperature equilibrium between 0.5°K and 1.2°K, and find it agrees with the results of Fairbank, Ard, and Walters.[1] Measurements are in progress on the susceptibility of He^3-He^4 solutions to determine if the discrepancy is due to the presence of He^4 in He^3. The latest results will be reported.

* Supported in part by the Office of Ordnance Research and the National Science Foundation.
[1] W. M. Fairbank, W. B. Ard, and G. K. Walters, Phys. Rev. 95, 566 (1954).
[2] F. S. Low, H. E. Rorschach, Jr., and H. A. Schwetman, *Helium Three* (Ohio State University Press, Columbus, 1960), p. 29.

MA10. Optical Observation of Flow in Liquid Helium.* R. MESERVEY, *Yale University.*—An optical method has been developed to measure the surface contour of a thin layer ($\approx 10^{-2}$ cm) of liquid helium on a horizontal substrate (minimum detectable change in elevation $\approx 5\times 10^{-6}$ cm). From the two fluid equations, the pressure, velocity, and temperature fields can be calculated. Using this technique, critical velocities for the onset of additional frictional forces in internal convection were obtained from 1.1 to 2.0°K. Turbulence and shock effects were observed. Also, the curvature of a thin layer of steadily rotating helium was measured at Reynold's numbers as low as 20, and found to be that of a normal viscous liquid.

* Supported by the National Science Foundation and the U. S. Army Office of Ordnance Research.

MA11. Thermodynamic Behavior of Liquid Helium Three in Its Possible Superfluid Phase.* TOSHIO SODA AND R. VASUDEVAN, *University of California, Berkeley and La Jolla.*—The thermodynamic behavior of liquid He^3 in its possible superfluid phase is investigated by extending the method of Brueckner *et al.*[1] The values of the energy gap and free energy for a given system for different pure azimuthal modes, for $l=2$ interaction state which is predominant, are calculated for different temperatures using numerical integrations. The pure mode $l=2$, $m=0$ gives lower energy gap values than the other two modes for all temperatures. The free energy for the $l=2$, $m=2$ mode and $m=1$ are very close to each other and the $m=0$ mode always leads to higher free energy. The mixing of different modes is investigated near the critical temperature and it is found that $l=2$, $m=2$ pure mode is the lowest free energy state. All linear combinations in which $m=0$, ± 1 and ± 2 are symmetrically mixed lead to the free energy corresponding to the $m=0$ mode. The combination in which $l=2$, $m=2$, $m=1$, and $m=0$ only are mixed leads to that of the pure mode $l=2$, $m=2$. The corerlation lengths are analyzed. The specific heat and entropy of the system are calculated for $l=1$, $m=2$ case.

* Research supported in part by the U. S. Atomic Energy Commission, Office of Naval Research, and Office of Scientific Research.
[1] K. A. Brueckner, T. Soda, P. W. Anderson, and P. Morel, Phys. Rev. 118, 1442 (1960).

TUESDAY AFTERNOON AT 2:00

Burgundy Room

(G. A. SNOW presiding)

Theory, IV: Properties and Interactions of Elementary Particles

MB1. Magnetic Moments of Mu-Mesonic Atoms.* KENNETH W. FORD, *Brandeis University;* VERNON W. HUGHES, *Yale University,* AND JOHN G. WILLS,† *Los Alamos Scientific Laboratory.*—The magnetic moment of a negative muon bound in the field of a nucleus is slightly less than the moment of a free muon. This binding correction to the moment has been

calculated accurately for a number of nuclei, using realistic nuclear charge distributions. Polarization of the nucleus and of the atomic electrons by the muon also gives rise to significant corrections to the muon moment. Precise determinations of the magnetic moment of heavy mu-mesonic atoms afford, in principle, a way of testing for possible structure of the muon. However, uncertainty in the nuclear magnetic dipole polarizability renders this test rather insensitive. Alternatively, the measurements would provide experimental values of nuclear and electronic polarizability.

* Supported by the U. S. Atomic Energy Commission and by the National Science Foundation.
† Now at the University of Washington.

MB2. Decay of Bound Muons. ROBERT W. HUFF, *Carnegie Institute of Technology*, R. H. DALITZ, *University of Chicago*, AND KENNETH SMITH, *Argonne National Laboratory*.—The present calculation of the decay rate of a negative muon bound to an atomic nucleus is part of an attempt to resolve the discrepancy between the experimental rates[1] and recent approximate calculations[2,3] of that rate. This calculation avoids most of the approximations of the earlier calculations by using correct relativistic wave functions, corresponding to an extended charge distribution, for both the moun and the final electron. The resulting radial integrals are then performed and combined by electronic computer to give the energy spectrum of the final electron, as well as, the total decay rate for several elements including iron, lead, and antimony.

[1] D. D. Yovanovitch, Phys. Rev. **117**, 1580 (1960).
[2] H. Überall, Phys. Rev. **119**, 365 (1960).
[3] V. Gilinsky and J. Mathews, Phys. Rev. **120**, 1450 (1960).

MB3. The Mass of the Muon Neutrino.* J. N. BAHCALL AND R. B. CURTIS, *Indiana University*.—We have assumed that the mass of the muon neutrino γ_ν is nonzero, and have calculated the theoretical effects of this assumption on: (1) Polarization of muons emitted in pion and kaon decays; (2) Muon-electron branching ratios in pion and kaon decays; (3) Electron spectrum from muon decay; (4) Polarization of electrons emitted in muon decay; (5) Muon lifetime. We have restricted ourselves to free processes and have assumed a V-A interaction for most but not all of our calculations. We shall discuss in detail experimental and theoretical aspects of the electron spectrum from isotropic muon decay, since the slope of this spectrum near the endpoint energy of the electrons is sensitive to the mass of γ_ν. We also mention that the data of Dudziak *et al.*[1] on the endpoint energy of electrons from muon decay may be combined with the recent x-ray measurements of the mass of the muon to set a probable upper limit on the mass of γ_ν equal to six electron masses.

* Supported in part by the National Science Foundation.
[1] W. Dudziak, R. Sagane, and J. Vedder, Phys. Rev. **114**, 336 (1959).

MB4. Observability of the Signs of Interaction Coupling Constants.* D. B. LICHTENBERG, *Michigan State University*.—Criteria given by Kobzarev and Okun,[1] and independently by the author,[2] for the observability of the signs of coupling constants, are applied to strong and weak interactions. For an often considered strong interaction Lagrangian containing eight coupling constants, only four relative signs are observable.[1,2] However, if weak interactions are considered simultaneously, it follows quite simply from the criteria that additional relative signs are observable. This means it is possible to determine certain relative signs from experiments involving the decay of strongly interacting particles, as pointed out by Feldman, Matthews, and Salam.[3] The observability of the signs of the coupling constants of certain meson-meson interactions will also be discussed.

* Work supported in part by a grant from the National Science Foundation.
[1] I. Yu. Kobzarev and L. B. Okun, J. Exptl. Theoret. Phys. **30**, 210 (1960); Soviet Phys.—JETP **12**, 150 (1961).
[2] D. B. Lichtenberg, Ann. Phys. (to be published) see especially Sec. II; also D. B. Lichtenberg (unpublished).
[3] G. Feldman, P. T. Matthews, and A. Salam, Phys. Rev. **121**, 302 (1961).

MB5. Invalidity of the Rafael Analysis for Moderate Energy NN Scattering.* RICHARD YODER AND PETER SIGNELL, *Pennsylvania State University*.—A modified effective range expansion by Rafael[1] has recently been used by Noyes[2] and others[3] to argue that a potential or boundary-value model could not satisfy the nucleon-nucleon scattering data in the 0–300 Mev region, and hence, one had no choice but to use a dispersion-theoretic approach. Rafael introduced the origin-shifted expansion for the $^1S_0$ phase shift, $k\cot(\delta+k\bar{r})=A_0+A_1k^2+A_2k^4+\cdots$, intended to be valid in the 0–300 Mev region. It was supposed that choosing $\bar{r}$ such that $A_1=0$ would make the series weakly energy dependent, justifying a termination of the series with A_2k^4. We have tested the Rafael series with reasonable potentials and found that it does not converge sufficiently to truncate it. Furthermore, comparison of the truncated series with the usual effective range expansion produced negative shape parameters where direct calculation produced positive shape parameters. We conclude that the Rafael analysis can not be used to reject potential and boundary-value models.

* This work was supported in part by the U. S. Atomic Energy Commission.
[1] R. B. Raphael, Phys. Rev. **102**, 905 (1956).
[2] H. P. Noyes, University of California Radiation Lab. Rept. UCRL 5521-T, March 1959, and International Conference on Nuclear Forces and the New Nucleon Problem, University College, London, July, 1959 (to be published).
[3] M. H. MacGregor, M. J. Moravcsik, and H. P. Noyes, University of California Radiation Report, UCRL 5582-T, May 1959.

MB6. Hyperon-Nucleon Scattering. C. DULLEMOND, *University of Rochester*, AND J. J. DE SWART, *Enrico Fermi Institute*.—From the rather well-known nucleon-nucleon potentials, one can construct the hyperon-nucleon potentials if one assumes a universal pion-baryon coupling.[1] For the $T=1$ nucleon-nucleon potential we choose the Bryan potential,[2] and for the $T=0$ nucleon-nucleon potential we choose the Gartenhaus $T=0$ potential.[3] At several different energies above and below the threshold for the reaction $\Lambda+N\rightarrow\Sigma+N$, we have solved the Schrödinger equation for $T=\frac{1}{2}$ and $T=\frac{3}{2}$ for J values up to $J=5$. This allows us to predict all the relevant experimental parameters for reactions of the type $Y+N\rightarrow Y+N$.

[1] D. B. Lichtenberg and M. H. Ross, Phys. Rev. **103**, 1131 (1956).
[2] R. A. Bryan, Nuovo cimento **16**, 895 (1960).
[3] S. Gartenhaus, Phys. Rev. **100**, 900 (1955).

MB7. Λ-Nucleon Potential and Hyper Fragments. J. J. DE SWART, *Enrico Fermi Institute*, AND C. DULLEMOND, *University of Rochester*.—A shape-independent relation connecting the volume integral $\bar{V}$ of an effective two-body central potential with the low-energy scattering parameters is derived. For the Λ-nucleon potential, rather accurate volume integrals are obtained by Downs and Dalitz,[1] from an analysis of the hyper fragments. Using the hyperon-nucleon potentials as described in the preceding abstract, we have calculated the low-energy scattering parameters for the Λ-nucleon system. Using the shape-independent relation, we obtain the corresponding "volume integrals" $\bar{V}$. Using the range parameter $b=1.4843f$, we obtain $\bar{V}_s=369$ Mev f^3 and $\bar{V}_p=-63$ Mev f^3. Downs and Dalitz[1] obtain $\bar{V}_s=(386\pm39)$ Mev f^3 and $\bar{V}_p=(174\pm21)$ Mev f^3. The results will be discussed.

[1] B. W. Downs and R. H. Dalitz, Phys. Rev. **114**, 593 (1959).

MB8. Statistical Theory of Y-$\bar{Y}$ Production via P-$\bar{P}$ Annihilation.* J. S. KOVACS, *Michigan State University*.—On the basis of the statistical model, the observed cross sections for the production of Y-$\bar{Y}$ pairs in P-$\bar{P}$ annihilation at 1 and 1.25 Bev are compared with the total cross section for annihilation to K-mesons at these energies and to the cross section for annihilation to two pions. A relation is thus obtained between the characteristic volumes associated with the K, π, and Y.

Cross sections for other final states and for annihilations at other energies are obtained on this basis.

* Supported in part by a grant from the National Science Foundation.

MB9. Production of $\bar{\Lambda}\Lambda$ Pairs in $\bar{p}p$ Collisions.* GEORGE C. SUMMERFIELD, *Michigan State University* (introduced by D. B. Lichtenberg).—A calculation of the energy dependence and angular distribution of $\bar{\Lambda}\Lambda$ pairs produced in $\bar{p}p$ annihilation is carried out. This is done considering the $\bar{\Lambda}\Lambda$ production to arise from a nondiagonal potential in the Hamiltonian. The $\bar{p}p$ interaction is taken as an optical potential adjusted to agree with experimental values of the inelastic total cross section and the elastic angular cross section.[1] The nondiagonal potential is considered to arise from a single K exchange and its range is taken as the kaon Compton wavelength. However, for simplicity in the calculation, the shape of the potential is taken to be a square well. The depth of the nondiagonal potential is adjusted to agree with an experimental determination of the total cross section,[2] and both the angular and energy dependence of the interaction are determined. The $\bar{\Lambda}\Lambda$ interaction is taken to be zero as there is no experimental evidence on which to base such an interaction. Results will be compared with experiment.

* Work supported in part by the National Science Foundation.
[1] Armenteros *et al.*, "Antiproton-proton cross sections at 1.0, 1.25, and 2.0 Bev" (unpublished) UCRL-8851.
[2] J. Button *et al.*, Phys. Rev. Letters **4**, 530 (1960).

MB10. Global Symmetry and the Pion-Hyperon Interaction in the Final State.* JUSTIN C. HUANG† AND JULIUS S. KOVACS, *Michigan State University.*—The implications of the assumption of Global Symmetry in the final-state πY interaction in the process $\pi^- + P \rightarrow K + Y + \pi$ are studied. All interactions among the final state particles excpet for the πY interactions were neglected. The branching ratios at various energies and the kaon momentum spectrum at a total center of mass energy of 16 m_π were calculated and compared with the corresponding results using a purely statistical model (neglecting any final state interaction). The results, in general, indicate that the experiments considered here would not give a very strong test of Global Symmetry.

* Supported in part by a grant from the National Science Foundation.
† National Science Foundation Cooperative Fellow.

MB11. On the Conservation of Isotopic Spin J. C. PATI, *California Institute of Technology.*—The mass differences within iostropic multiplets seem to require rather unnatural corrections due to the electromagnetism. Furthermore, in the framework of a strict $|\vec{\Delta I}| = \frac{1}{2}$-weak interaction, the observed rate of $K^+ \rightarrow \pi^+ + \pi^0$ seems to be much faster than normally expected due to electromagnetic corrections. These lead one to examine the possible existence of a new class of isotropic spin-violating interactions other than electromagnetism. In the present context, it is only of interest if the strength of these interactions is intermediate between those of electromagnetic and strong interactions. The observed conservation laws in different processes would require that these interactions should conserve parity and strangeness. Specific examples of such interactions, their compatibility with the present experiments, and verifiable consequences will be discussed. If such interactions exist, it would appear that each type of elementary particle-interaction possesses a partner with similar conservation properties, but slightly different strength. This seems to be the case in the strong and weak interactions. In the former the pion and the K-meson interactions, while in the latter the $\Delta S = 0$ and the $|\Delta S| = 1$-interactions seem to form the partners. There may be an analogous isotopic spin violating partner of electromagnetism.

MB12. "De Divina Proportione" in the Physical World. NICHOLAS Efremov.—The universal significance of the rules of "divinae proportiones" can be clearly demonstrated on the many patterns observable in the physical world. The application of these rules of "divinae proportiones" in combination with the rules of sequential series can explain many phenomena and particularly the sequence of the chemical elements in the rare gases and triplet element groups in the *P.S.* of chemical elements, such as: He-Ne-A-Fe-Kr-Ru-Xe-Os-Rn, or such sequence of the atomic numbers: 2, 10, 18, 26, 36, 44, 54, 76, 86. The atomic number proportions between successive pairs of these elements, e.g.: He:Ne = 2:10 = 0.2, Ne:A = 10:18 = 0.555, Fe:Kr = 0.722, Kr:Ru = 0.818, Ru:Xe = 0.814, Xe:Os = 0.710, Os:Rn = 0.883 cna be expressed by the coefficients 0.2, 0.555, 0.722, etc. The mean value of the coefficients in this series is 0.672. This mean coefficient is close to 0.667—the coefficient expressing the simplest proportion in the "proportio divina" series, which is 2:3 = 0.667. It is noteworthy that the regularity of the series of so-called "magic numbers" (e.g., 50, 82, 126) can be explained on the basis of the same rules. It is clear that coefficients expressing the proportions between successive pairs of these magic numbers, such as 50:82 = 0.609 or 82:126 = 0.650 approximate those which occur in "proportio divina" series.

WEDNESDAY MORNING AT 10:30

Adams-Hamilton Room

(R. S. MULLIKEN presiding)

Molecules

N1. Centrifugal Stretching and Stark Effect of $CClF_3$.* R. C. JOHNSON, T. L. WEATHERLY, AND QUITMAN WILLIAMS, *Georgia Institute of Technology.*—A recent investigation[1] on CCl_3F yielded a negative value for D_{JJ} which varied with J. Centrifugal stretching of $CCl^{35}F_3$ was examined because of bonding similar to CCl_3F. The $J = 1 \rightarrow 2$ through $4 \rightarrow 5$ transitions were measured. Absorption lines for $J = 2 \rightarrow 3$ and $3 \rightarrow 4$ have been reported[2] previously; however, the $2 \rightarrow 3$ data are believed to be slightly in error. Present data yield $B_0 = 3335.60$ Mc, $eQq = -78.07$ Mc, $D_{JJ} = +0.58$ kc and $D_{JK} = +1.99$ kc; neither distortion constant exhibited J dependence. A Taylor's expansion of energy illustrates that distortion coefficients are constants by definition; contrary behavior should be accounted for by considering higher-order terms. The CCl_3F data[1] are inconsistent even when second-order terms are considered. Agreement between calculated and measured distortion constants is fair for several XYZ_3 molecules. Exceptions are $CHCl_3$ and $CFCl_3$, the only molecules involving three identical nuclei with spin 3/2. Stark effect measurements for $J = 1 \rightarrow 2$ yielded a dipole moment of 0.499 ± 0.002 debye.

* Supported in part by the Office of Naval Research and the National Science Foundation.
[1] M. W. Long, Q. Williams, and T. L. Weatherly, J. Chem. Phys. **33**, 508 (1960).
[2] D. K. Coles and R. H. Hughes, Natl. Bur. Standards (U. S.), Circ. No. **518**, 9 (1952).

N2. Rotational Magnetic Moments of LiH and LiD.* THOMAS R. LAWRENCE, CHARLES H. ANDERSON, AND NORMAN F. RAMSEY, *Harvard University.*—The rotational magnetic moments of LiH and LiD were measured in a molecular beam magnetic resonance experiment. The values obtained are $\mu_R/J=-0.640\pm0.005$ nuclear magneton for LiH and $\mu_R/J=-0.267\pm0.005$ nuclear magneton for LiD. These are average values over all the rotational and vibrational states. The full width at half-height of the resonance curves is about 140 kc for LiH and 80 kc for LiD with an intrinsic linewidth of about 40 kc for the rf coil. The magnitude of the electric dipole moment calculated from these values of the magnetic moments is 5.7 ± 0.4 debye which agrees with the more precise determination by Wharton *et al.*[1] in a molecular beam electric resonance experiment. The sign of the electric dipole moment is found to be that corresponding to a plus charge on Li and a negative charge on H as expected theoretically[2] but not previously determined experimentally.

* Supported in part by the Office of Naval Research.
[1] Lennard Wharton, L. Peter Gold, and William Klemperer, J. Chem. Phys. **33**, 1255 (1960).
[2] R. P. Hurst, James Miller, and F. A. Matsen, J. Chem. Phys. **26**, 1092 (1957).

N3. Large Rotational Magnetic Moment of NO.* SUNNEY I. CHAN AND MILTON R. BAKER, *Harvard University.*—A recently constructed molecular beam magnetic-resonance apparatus designed primarily for the study of $^2\Sigma$ molecules has been modified for the investigation of paramagnetic molecules and gaseous free radicals. Our initial studies have been of the Zeeman effect of the $^2\pi_{\frac{1}{2}}$ state of the molecule NO. The rf resonance spectrum observed in a magnetic field of 210.0 gauss consists of a doublet, whose center of gravity corresponds to an average magnetic moment of $0.0263\,\mu_0$ and whose splitting corresponds approximately to $0.002\,\mu_0$. These results are in agreement with those reported by Mizushima, Cox, and Gordy.[1] However, a large number of molecular rotational states contribute to our spectrum. A perturbation treatment due to Van Vleck gives an average magnetic moment of $0.0281\,\mu_0\times[1-(\frac{1}{2})/J(J+1)]$ for each rotational state and satisfactorily accounts for the gross features of the spectrum. The magnitude of the doublet separation, however, has not been satisfactorily explained. This work is presently being extended over a wide range of magnetic fields.

* Work supported by the National Science Foundation and by the joint program of the Office of Naval Research and the U. S. Atomic Energy Commission.
[1] M. Mizushima, J. T. Cox, and W. Gordy, Phys. Rev. **98**, 1034 (1955).

N4. Interaction of Coriolis Forces and Internal Rotation in Symmetric Rotor Molecules.* VICTOR W. LAURIE, *Stanford University.*—Through the effect of the internal angular momentum on rotational microwave spectra, it has been possible over the past few years to obtain precise values for the potential barriers hindering internal rotational in a large number of molecules. Unfortunately, the selection rules for symmetric rotor molecules generally permit observation of only rather indirect effects of internal rotation and the determination of barrier heights is much more difficult. It will be shown, however, that for the case of molecules in excited degenerate vibrational states, the presence of vibrational angular momentum allows a more direct determination of the internal rotation barrier. The "*l*-type doubling" may be thought of as a pseudo-asymmetry which allows internal rotation to directly split rotational transitions.

* Supported in part by the National Science Foundation.

N5. Triplet-Singlet Luminescence from Methylated Benzenes in the Crystalline State and in Rigid Glass Solutions.* H. SPONER AND Y. KANDA,† *Duke University* (introduced by H. Sponer).—In continuation of earlier studies triplet-singlet emission of the following methylated benzenes will be reported in their solid phases: mesitylene, durene, hexamethylbenzene. The spectra were obtained in rigid EPA solutions at 77°K, and in the crystalline state at 77°K and at 4°K. Two different spectra were found for mesitylene and durene crystals at shorter wavelengths, one representing the genuine triplet-singlet emission of the substance, and the other at longer wavelengths belonging to the lowest phosphorescence of an oxydation product. Hexamethylbenzene crystal exhibits only one spectrum at any temperature. No solution spectrum was obtained of the last substance because of its poor solubility. For an interpretation of the observations, various physical and photochemical processes will be discussed taking place in these crystals upon light illumination.

* Supported by the National Science Foundation.
† Present address: Chemistry Department, Science Faculty, Kyushu University, Fukuoka, Japan.

N6. Phosphorescence Lifetime Studies in Methylated Benzenes at Low Temperatures.* D. OLNESS AND H. SPONER, *Duke University* (introduced by H. Sponer).—Triplet-singlet decay curves from several methylated benzenes have been studied in the crystalline phase at temperatures of 4.2°K and higher, and for comparison in rigid glass solutions at 77°K. The decay from true dilute solutions was found to follow an exponential law, while that from the crystals was always non-exponential. In general, the later portions of all of these decay curves were nearly exponential. When the mean half-life measured in these later portions was plotted as a function of temperature, the lifetime decreased with increasing temperature as $\log 1/T$, throughout the temperature region studied. Various interpretations concerning the causes of the non-exponential decay and the change in general shape of the decay curves with temperature will be discussed.

* Supported by the Office of Ordnance Research.

N7. De-excitation of Molecular Vibration by Collision. ERNEST BAUER AND F. W. CUMMINGS, *Aeronutronic.*—We have calculated the reaction rate for a vibrationally excited diatomic molecule to be de-excited by collision with another atom or molecule, the second particle carrying away the excess vibrational energy as kinetic energy. The quantum mechanical perturbed stationary state method is used in the "Modified Wave Number" approximation, and anharmonicity in the vibrational motion is taken into account both in the choice of vibrational wave functions (Morse functions) and in the interaction potential. The calculation is applied to the reaction

$$N_2(a^1\pi_g;v)+N_2(X)\Longrightarrow N_2(a^1\pi_g;v'<v)+N_2(X)+\text{kinetic energy}$$

for the vibrational transitions $v=5$ to $v'=4, 3, 2, 1, 0$, and for $v=2$ to $v'=0$ and $v=1$ to $v'=0$, for the temperature range 300–6000°K. The results show clearly that in a situation of this kind the collisional de-excitation of the molecular vibration proceeds in steps $v-v'=\delta v=1$, rather than $\delta v>1$.

N8. Energy and Character of the Lowest Excited Singlet State of Acetaldehyde.* K. K. INNES AND L. E. GIDDINGS, JR., *Vanderbilt University.*—Low dispersion absorption spectra of CH_3CHO vapor at 300°K and at 523°K were recorded photoelectrically between 2300 and 3500 A. (Maximum absorption, 2970 A.) All bands were found to be equally sensitive to temperature. It is concluded that all important bands originate from the lowest vibrational level of the ground electronic state. The origin of the transition is therefore at energies at least as low as that of the longest wavelength (weakest) band observed, that is, near 28 700 cm^{-1}. It then follows from available measurements that the vibrational assignments are entirely

analogous to those recently made for the corresponding transition of the isoelectronic molecule, HCOF. In particular, the prominent upper-state frequencies are those of the CO stretching mode and of the out-of-plane mode of the CCHO skeleton. The skeleton is evidently nonplanar in the excited electronic state. Further evidence that the origin is near 3483 A is found in an emission spectrum[1] which extends to wavelengths as low as 3500 A.

* Supported by the Office of Ordnance Research with funds provided by the Advanced Research Projects Agency.

[1] G. W. Robinson, J. Chem. Phys. 22, 1147 (1954).

WEDNESDAY MORNING AT 9:30

Continental Room

(B. COHEN presiding)

Nuclear Reactions, V

NA1. $(p,p'\gamma)$ Spectra for Ni^{58}, Ni^{60}, and Ni^{62}.* P. N. TREHAN AND D. M. VAN PATTER, *Bartol Research Foundation.*—Isotopically enriched targets of Ni^{58}(99.9%), Ni^{60}(99.8%), and Ni^{62}(98.0%) on 8-mil Au backings were bombarded by protons with $E_p = 3.4$–5.2 Mev, and γ-ray spectra with $E_\gamma > 0.6$ Mev were investigated. In the case of Ni^{58}, only γ rays of 1.01 and 1.45 Mev ($\pm 1\%$) were seen. Gamma-rays of 0.83, 0.95, 1.33, 1.79, 2.16, and 2.28 (weak) Mev ($\pm 1\%$) were observed from Ni^{60}. The branching ratio of the second $2+$ level of Ni^{60} at 2.16 Mev has been measured as 0.14 ± 0.02, which differs from earlier radio activity measurements. In the case of Ni^{62}, γ rays of 0.88, 1.17, 1.73, 2.05 (weak) and 2.30 Mev ($\pm 1\%$) were observed. The branching ratio for the 2.05-Mev level is estimated as 0.06 ± 0.015. The observation of a prominent 2.30-Mev γ ray appears to eliminate the possibility of $0+$ for the 2.30-Mev level of Ni^{62}. Knowledge of the level schemes of these nickel isotopes indicates that all the γ rays listed should be assigned to the $(p,p'\gamma)$ reaction. The excitation curves for some prominent γ rays of Ni^{60} and Ni^{62} have been measured.

* Supported by the U. S. Air Force through the Air Force Office of Scientific Research of the Air Research Development Command.

NA2. Deuteron Spectra from the $Ni^{64}(p,d)Ni^{63}$ Reaction. C. B. FULMER, C. D. GOODMAN, AND J. B. BALL, *Oak Ridge National Laboratory.**—Deuteron spectra from (p,d) reactions induced by 22-Mev protons on Ni^{64} were measured experimentally. Two distinct shapes of angular distributions are observed for the deuteron groups from reactions that result in $\lesssim 5$-Mev excitation of the residual nucleus. In the manner previously discussed[1] we conclude that the two kinds of angular distributions correspond to angular momentum changes of one and three units, respectively; we classify the states accordingly. Peaks that result in less than ~ 2.5-Mev excitation of the residual nucleus are characterized by $l = 1$. The first $l = 3$ peak occurs at $Q = -10.8$ Mev (3.4-Mev excitation of the residual nucleus). By comparison with (p,d) spectra from Fe isotopes[1] this level is assigned to the pickup of an $f_{7/2}$ neutron. No evidence for a peak near the ground state corresponding to the pickup of an $f_{\frac{1}{2}}$ neutron is observed. The results are consistent with neutron-bound states in a spheroidal potential as calculated, for example, by Nilsson. This indicates that the Ni^{64} nucleus has a prolate deformation.

* Operated for the U. S. Atomic Energy Commission by Union Carbide Corporation.

[1] Ball, Goodman, and Fulmer, Bull. Am. Phys. Soc. 6, 47 (1960).

NA3. The (α,He^3) Reaction on Fe^{56}, Ni^{58}, Ni^{60}, and Zn^{64}.* T. H. BRAID, J. L. YNTEMA, B. ZEIDMAN, AND H. W. BROEK, *Argonne National Laboratory.*—We have observed the $X^A(\alpha,He^3)X^{(A+1)}$ reaction from targets of Fe^{56}, Ni^{58}, Ni^{60}, and Zn^{64} when bombarded with 43-Mev α particles from the 60-in. cyclotron. The reaction products were detected by a pair of surface-barrier solid-state counters arranged to measure dE and E. The resolution in dE was sufficient to distinguish the He^3 particles from the inelastically scattered α particles. A pulse multiplier was used to select particles of the correct $mZ^2 \approx dE \times E$. In each of these targets we observe two strong groups. In the case of $Zn^{64}(\alpha He^3)Zn^{65}$, the group corresponding to the more negative Q value is approximately twice as intense as the other. We have measured the angular distributions for this target from 20° to 42° in the laboratory system. The distributions are peaked in the forward direction.

* Work performed under the auspices of the U. S. Atomic Energy Commission.

NA4. The $Cu^{65}(d,He^3)Ni^{64}$ and $Ni^{60}(d,He^3)Co^{59}$ Reactions.* J. L. YNTEMA, B. ZEIDMAN, T. H. BRAID, AND H. W. BROEK, *Argonne National Laboratory.*—The (d,He^3) reactions have been observed in targets of Cu^{65} and Ni^{60} bombarded by 21.6-Mev deuterons from the 60-in. cyclotron. The detection system was that used in the preceding abstract. We observe He^3 groups corresponding to the ground state and first excited state of Ni^{64} and the ground state of Co^{59}. We have measured the angular distribution for both targets from 14° to 32° in the laboratory system. The angular distribution of the peak corresponding to the Ni^{64} ground state shows a maximum at 27° and a very sharp rise at small angles while the peak corresponding to the Co^{59} ground state shows a maximim at about 23° and falls off slowly towards small angles. The oscillations in the angular distribution are less pronounced than in (d,t) reactions on nuclei in this region.

* Work performed under the auspices of the U. S. Atomic Energy Commission.

NA5. Inelastic Scattering of α-Particles by Ni^{60} and Co^{59}.* H. W. BROEK, T. H. BRAID, J. L. YNTEMA, AND B. ZEIDMAN, *Argonne National Laboratory.*—The α-particle spectrum from the bombardment of Ni^{60} by 43-Mev α-particles has been obtained over the angular range from 12° to 42°. A solid-state counter was used to detect the particles. The resolution width was approximately 1%, primarily because of the energy spread of the incident particles. In addition to the 1.33-Mev 2^+ state and the 4.1-Mev 3^- state, groups were observed at approximately 2.4 Mev, 3.2 Mev, 5.2 Mev, 6.4 Mev, and 7.3 Mev. The angular distribution of the 5.2-Mev group shows minima at about 28° and 38° and is widely different from those of the elastic scattering, the first exicted state, and the 3^- state. An assignment of 4^+ appears to be the most likely one for this group. In the inelastic scattering from Co^{59}, an $l = 2$ transition was observed at an excitation of approximately 1.3 Mev and a transition with an odd l value to a state at about 3.9 Mev.

* Work performed under the auspices of the U. S. Atomic Energy Commission.

NA6. Coulomb Excitation of Levels in Se^{77}. R. L. ROBINSON, F. K. MCGOWAN, AND P. H. STELSON, *Oak Ridge National Laboratory.*—Levels at 242±6 (doublet), 440±4, and 515±6 kev have been Coulomb excited with α particles of variable energies ranging from 2.1 to 8.0 Mev. The $B(E2)$'s for excitation of these levels are (1.9±0.2), (2.6±0.2), and (0.10±0.02) $\times 10^{-48} e^2$ cm^4, respectively. It is interesting to note that the sum of these $B(E2)$'s is very nearly equal to the average $B(E2)$ value for excitation of the first 2+ levels of Se^{76} and Se^{78}. Besides the three ground-state transitions, gamma rays with energies 87, 161, 203, and 283 kev were observed. Excitation curves of the 87- and 161-kev transitions have the same shape as that of the 242-kev transitions. Coincidence studies revealed that the 203-kev gamma ray, which deexcites the 440-kev level, is in coincidence with a 242-kev gamma ray but not the 87-kev gamma ray. This provides new evidence for the previously suggested level doublet at 242 kev.[1] The angular distributions of the 203-, 242-, and 440-kev gamma rays have been measured to obtain information on spin and multipolarity assignments.

[1] *Nuclear Data Sheets*, National Academy of Sciences, National Research Council, Washington, D. C.

NA7. Cross Sections for the (p,n) Reaction on Heavy Elements. J. P. SCHIFFER,* *Argonne National Laboratory*, AND G. A. JONES, *Atomic Energy Research Establishment, Harwell.*—The A.E.R.E. tandem Van de Graaff accelerator has been used to bombard thick targets of nineteen elements ranging from atomic weight 138 to 238 with protons of 4–10 Mev. The energies were restricted to be sufficiently low such that neutron emission was the primary mode of decay for the compound nucleus. The neutron yields divided by an integral of the barrier penetrability and stopping power yield a quantity closely related to the proton strength function. This quantity was found to remain constant within ±20%, which was approximately the experimental error for the targets studied, with the exception of U and Th. In these latter cases the results are approximately consistent if it is assumed that fission is an important mode of decay of the compound nucleus.

* Work performed while at A.E.R.E. as a John Simon Guggenheim Fellow.

NA8. Cross Sections for the (p,n) Reaction at 9.85 Mev. G. A. JONES, *Atomic Energy Research Establishment, Harwell*, AND J. P. SCHIFFER,* *Argonne National Laboratory.*—The A.E.R.E. tandem Van de Graaff accelerator has been used to bombard thin targets of Al, Co, Cu, Fe, Ni, Ag, and Sn with 9.85-Mev protons. A BF_3 "long counter" was used to detect the neutrons produced. The cross sections measured when combined with charged particle reaction cross sections have been compared with optical model predictions of the total reaction cross section,[1] and were found to be in better agreement than previous results.[2] The angular distributions showed slight forward peaking and corrections for this were included in the results. The cross sections were measured as 320 mb for Cu^{63}, 550 mb for Cu^{65}. The results are believed to be accurate to ±12%.

* Work performed while at A.E.R.E. as a John Simon Guggenheim Fellow.
[1] V. Meyer and N. M. Hintz, Phys. Rev. Letters **5**, 207 (1960).
[2] R. D. Albert and L. F. Hansen, Phys. Rev. Letters **6**, 13 (1961).

NA9. Optical Resonance Phenomena. KARL WILDERMUTH, *Florida State University and Oak Ridge National Laboratory*, AND R. L. CAROVILLANO, *Boston College.**—The purpose of this work is to discuss the physical reasons for expecting the appearance of optical giant resonances to be a very general feature of nuclear reactions. Giant resonances should occur not only in the scattering of nucleons on nuclei, but also in the scattering of composite particles on nuclei and in certain reaction channels of a compound nucleus decay. The main ingredient in our discussion is that the indistinguishability of the nucleons has the effect of prolonging the lifetime of the nuclear clusters to times of order 10^{-20} to 10^{-22} sec.

* Oak Ridge Institute of Nuclear Studies Summer Research Participant, 1960.

NA10. A Simple Interpretation of Back-Angle Maxima.* N. S. WALL, *M.I.T.*—In a variety of reactions involving incident particles which are strongly absorbed in nuclei pronounced backward maxima have been observed in the angular distributions of the reaction products. Typical of these reactions are intermediate energy (α,p)[1,2] and (d,p)[3] reactions. Utilizing Blair's[4] approach of representing the scattering of particles in terms of a Fraunhofer diffraction analysis we have considered reactions to take place by the emission of waves from the back hemisphere (the absorbing surface) of the nucleus. In reality this is only a representation of a realistic distorted wave analysis of nuclear reactions, but serves to establish a simple, physical picture for the process. It should be pointed out that this approach is different from both the reflection phenomenon of Bulter, Austern, and Pearson and the heavy particle stripping analysis of Owen and Madansky. Qualitative and quantitative comparison with experiment will be made, and the shortcomings of the analysis will be discussed.

* This work was supported in part by the U. S. Atomic Energy Commission.
[1] Klein, Cindro, Swenson, and Wall, Nuclear Phys. **16**, 374, (1960).
[2] Nonaka *et al.*, J. Phys. Soc. Japan (to be published).
[3] Elwyn, Kane, Ofer, and Wilkinson, Phys. Rev. **116**, 1490 (1959).
[4] J. S. Blair, Phys. Rev. **115**, 928 (1959).

NA11. Fine Structure in the Energy Spectra of (d,α) Reactions in Heavy Elements.* JAMES B. MEAD AND SERGIO MICHELETTI, *University of Pittsburgh.*—High resolution energy spectra of (d,α) reactions initiated by 15-Mev deuterons have been measured for several heavy elements in the Pb region. A gas-ionization chamber and solid-state detector have been used to obtain the energy spectra with a resolution of about 2%. A group of strongly excited levels showing forward peaking have been found at a few Mev excitation. The energy of these fine structure levels is consistant with a mechanism describing (d,α) reactions as a two-particle pick-up from shell model single particle states.[1] An attempt has been made to explain the observed relative intensities. Angular distributions and improved resolution studies using a magnetic spectrometer are being undertaken.

* Work done in the Sarah Mellon Scaife Radiation Laboratory and assisted by the joint program of the Office of Naval Research and the U. S. Atomic Energy Commission and N.S.F.
[1] James B. Mead and B. L. Cohen, Bull. Am. Phys. Soc. **6**, 49 (1961).

NA12. Nuclear Resonance Effects in Coulomb Excitation.* T. A. GRIFFY, *Rice University*, AND L. C. BIEDENHARN, *Duke University.*—The changes in the Coulomb excitation process due to nuclear interactions in the incident and exit channels are calculated using first-order perturbation theory for the electromagnetic interaction and the Wigner Eisenbud formalism for the nuclear interaction. In particular, resonances in the elastic scattering channel cause modifications of the radial integrals which occur in the expression for the Coulomb excitation cross section. Explicitly, the radial integrals for an $E2$ transition become

$$I(l,l+m)=\int_R^\infty dr r^{-3}[\cos\delta_l F_l(\eta_1,k_1r)+\sin\delta_l G_l(\eta_1,k_1r)]\cdot[\cos\delta_{l+m}F_{l+m}(\eta_2,k_2r)+\sin\delta_{l+m}G_{l+m}(\eta_2,k_2r)],$$

with a similar expression for other multipole orders. The predictions of this theory are compared with the results of Temmer and Heydenburg for the reaction $Na^{23}(p,p',\gamma)$. It is shown that the anomaly at $E_p=870$ kev can be explained by taking into account the resonance in the elastic scattering of the proton. A discussion of the applications of the present calculation to

determining phase shifts (including relative phases) and other nuclear parameters will be given.

* Work supported by the U. S. Atomic Energy Commission, the National Aeronautics and Space Administration, and the Research Corporation.

NA13. Coulomb-Distorted (d,p) Angular Distributions as a Function of Bombarding Energy.* D. W. MILLER, *Indiana University*, H. E. WEGNER, AND W. S. HALL, *Los Alamos Scientific Laboratory*.—Measurements of the angular distributions of six proton groups from the $Pb^{206}(d,p)Pb^{207}$ reaction have been performed at 12.5 and 14 Mev. dE/dx and E counters were employed for mass separation and energy measurement. The states resolved in Pb^{207} correspond to neutron capture with orbital angular momentum transfers of 1, 2, 4, and 6. These angular distributions will be compared with published results by Stokes at Los Alamos (8.30 and 9.05 Mev), McEllistrem *et al.*, at Indiana (10.8 Mev), and Cohen *et al.*, at Pittsburgh (15 Mev). Of most interest is the ground-state reaction (representing p-neutron capture) which shows the greatest angular strucure. As the deuteron energy is decreased, the forward peaks in the ground-state angular distribution are quickly attenuated, but do not shift angular positions markedly. Some results will be shown of distorted-wave stripping calculations of these angular distributions obtained with the code developed by W. Tobocman and adapted for the Los Alamos computers by Blair Swartz and L. S. Rodberg.

* Work supported by the U. S. Atomic Energy Commission.

WEDNESDAY MORNING AT 10:30

Cotillion Room, South

(J. A. HARVEY presiding)

Neutron Spectroscopy

P1. Resonance Parameters for the 130-ev Level in Co^{60}.* A. P. JAIN,† H. PALEVSKY, R. E. CHRIEN, AND H. BOLOTIN, *Brookhaven National Laboratory*.—Accurate determinations of the resonance parameters of the 130-ev resonance level in Co^{60} have been made from neutron transmission data using the BNL fast chopper and 1024 time-of-flight analyzer. Extreme care was taken in the preparation of samples ($CoSO_4$ in D_2O) and in the determination of sample thicknesses. Thin and thick samples of 0.569×10^{20}, 3.53×10^{20}, and 7.20×10^{20} atoms/cm^2, respectively, were used and the results of preliminary area analysis yielded the following "best fit" parameters: $E_0=130.2$ ev, $2g\Gamma n=(6.00\pm0.13)$ ev, $\Gamma=(5.15\pm0.25)$ ev. These results are consistent only with the spin assignment $J=4$, and excludes the $J=3$ possibility. This is to be compared with the previously reported work[1] which was unable to distinguish between the two spin possibilities. Direct measurements of the intensity of of the capture γ rays are being made, which will allow an accurate determination of $\Gamma\gamma$, and the related resonance absorption integral.

* Work carried out under the auspices of the U. S. Atomic Energy Commission.
† Predoctoral Fellow from Cornell University.
[1] F. G. P. Seidl *et al.*, Phys. Rev. 95, 493 (1954).

P2. Fluctuations in Partial Radiation Widths of U^{239}.* H. E. JACKSON AND L. M. BOLLINGER, *Argonne National Laboratory*.—The distribution of partial widths Γ_{ij} of high-energy radiative transitions from nuclear states of the same spin and parity excited by s-wave neutron capture has recently been extensively studied. The reported results for U^{239}, which indicated that Γ_{ij} fluctuates only about 11% from the mean, are in strong disagreement with the large fluctuations observed for other nuclides. To determine whether the difference is real or instrumental, the Argonne fast chopper was used to measure the relative probabilities for transitions of approximately 4 Mev from levels formed by neutron capture in the 6.7-, 21-, 37-, and 61-ev resonances of U^{238}. The probabilities were determined from pulse-height spectra of a single large (8×6 in.) NaI(Tl) scintillator. A qualitative examination of our data gives two results of particular interest. First, assuming that only one line is present in the neighborhood of 4.06 Mev, as was done by the Brookhaven group, we obtain relative intensities of 1.37 ± 0.05, 1.17 ± 0.05, 0.75 ± 0.05, and 0.72 ± 0.05 for the above resonances, values which exhibit much greater fluctuations than the previously reported intensities of 1.13 ± 0.04, 1.02 ± 0.05, 1.03 ± 0.04, and 0.79 ± 0.05 for the same resonances. Second, our spectra are well enough resolved to reveal the presence of three lines between 3.8 and 4.2 Mev.

* Work performed under the auspices of the U. S. Atomic Energy Commission.

P3. Distribution of Partial Radiation Widths.* L. M. BOLLINGER, R. E. COTÉ, AND J. P. MARION, *Argonne National Laboratory*.—Important improvements in the available experimental equipment have made it seem worth while to repeat and extend the previously reported measurements[1] on the partial widths for the high-energy $E1$ transitions from states formed by neutron capture in resonances of Se^{77}, W^{183}, Pt^{195}, and Hg^{199}. In the new measurements, the Argonne fast chopper was operated with a neutron time-of-flight resolution of 0.08 μsec/m, the γ-ray spectrometer was a single 8×6 in. NaI(Tl) scintillator, and the spectra were recorded in a 3-variable magnetic-tape recording pulse-height analyzer. The high quality of the pulse-height spectra made it feasible to deduce, by least-squares curve fitting, the relative widths for high-energy transitions to several low-energy states in each nuclide. Widths were obtained for 3 $E1$ transitions from each of 3 initial states of Se^{78}, for 2 transitions from 5 states of W^{184}, for 3 transitions from 7 states of Pt^{196}, and for 2 transitions from 3 states of Hg^{200}—a total of 46 widths. In agreement with our previous results and in contradiction to those of several other groups, the data for each of the nuclides studies are consistent with a χ^2 distribution with one degree of freedom.

* Work performed under the auspices of the U. S. Atomic Energy Commission.
[1] L. M. Bollinger, R. E. Coté, and T. J. Kennett, Phys. Rev. Letters 3, 376 (1959).

P4. Neutron Radiative Capture Measurements. R. C. BLOCK, F. C. VON DER LAGE, AND L. W. WESTON, *Oak Ridge National Laboratory*.—Additional neutron radiative capture measurements have been carried out with the 28-in.-diam spherical liquid scintillation detector[1] installed at the 11.5-m flight path of the ORNL fast chopper. The radiative capture cross sections of ~30 naturally abundant elements in the atomic weight range $90<A<200$ have been measured from ~200 to 6000 ev with a resolution of 0.17 μsec/m. These cross sections agree to within 20–25% with the reported Van de Graaff results[2] in the 6000-ev region. Capture measurements

have also been made upon thin samples of Co to obtain the radiation width of the 132-ev resonance; this width is determined to be (0.67±0.15) ev.

[1] R. C. Block, Bull. Am. Phys. Soc. **4**, 474 (1959).
[2] Gibbons, Macklin, Miller, and Neiler, Phys. Rev. (to be published).

P5. Measurements with Polarized Neutrons and Polarized Target Nuclei.* V. L. SAILOR, H. MARSHAK, F. J. SHORE, C. A. REYNOLDS, AND H. POSTMA, *Brookhaven National Laboratory.*—Equipment for measurements with polarized, monochromatic neutrons and polarized target nuclei has been completed and preliminary transmission measurements have been made on Ho and In targets. The system consists of a neutron crystal spectrometer, and a cryostat for cooling the target located on the spectrometer "arm." Monochromatic, polarized neutrons in the energy range from 0.06 to ~10 ev are obtained by Bragg reflection from a magnetized 94% cobalt—6% iron single crystal. Guide fields serve to maintain the beam polarization and to rotate the direction of polarization from the vertical to the horizontal before entering the target. The neutron beam enters the cold target through a re-entrant tube in the cryostat. The cryostat consists of a large liquid nitrogen Dewar, a liquid helium bath, and a two-stage magnetic refrigerator. The refrigerator is designed to produce target temperatures in the range of 0.01°K, so that, when necessary, the "brute force" method can be used for producing the nuclear polarization. The various solenoids and magnets used for the two stages of adiabatic demagnetization, and for the nuclear polarization are submerged in the liquid nitrogen bath. During the cooling cycle approximately 10 kw are dissipated in the liquid nitrogen.

* Work performed under contract with U. S. Atomic Energy Commission.

P6. Transmission of Polarized Neutrons Through a Sample of Polarized ^{165}Ho Nuclei.* H. POSTMA, H. MARSHAK, V. L. SAILOR, F. J. SHORE, AND C. A. REYNOLDS, *Brookhaven National Laboratory.*—A polycrystalline sample of holmium ethyl sulphate is cooled down to 1.0°K in the cryostat which is described in the previous abstract. The ^{165}Ho nuclei (spin $\frac{7}{2}$) are polarized with the aid of an external magnetic field (Rose-Gorter method). The spin Hamiltonian as proposed by Bleaney and Baker is used for calculating the degree of nuclear polarization along the direction of the applied magnetic field. The nuclear polarization for the polycrystalline sample at 1.0°K is calculated to be 0.15. The nuclei are expected to be polarized in the hemisphere of the positive direction of the applied magnetic field, because of the positive value of Ar[2]. In order to reduce possible interactions between the Ho^{3+} ions the applied magnetic field was made large, e.g., 10.4 kilooersted. The relative difference $(T^+-T^-)/(T^++T^-)$ in transmission with the neutrons polarized parallel (T^+) or polarized antiparallel (T^-) with respect to the applied magnetic field is measured for the 3.96-ev resonance to be 2.9±0.1%. Hence the spin of the compound nucleus at the 3.96-ev resonance is $I-\frac{1}{2}=3$. Preliminary measurements for the 12.8 ev resonance indicate spin 3 for this resonance also. Depolarization of the neutron beam due to the polycrystalline sample was measured for an energy of 0.073 ev.

* Work performed under contract with U. S. Atomic Energy Commission.

P7. Spin States of Neutron Resonances in Gd^{155} and Gd^{157}. A. STOLOVY, *U. S. Naval Research Laboratory.*—By observing the interaction of polarized resonance neutrons with a polarized target,[1] the spin states associated with resonances in gadolinium are being studied. The resonances in Gd^{155} at 2.10 ev and 2.57 ev were found to have different spin states in spite of their identical radiation widths.[2] In view of the small magnetic moments of the gadolinium isotopes,[3] the size of the effects observed indicates strong hyperfine coupling, with an effective field at the nucleus of about 1.4×10^8 gauss. The direction has not been established yet, but by implication, it is negative. This would make $J=1$ for the 2.01-ev level and $J=2$ for the 2.57-ev level. Data taken at 0.09 ev indicate that the 0.031 ev resonance in Gd^{157}, which predominates,[2] has the same spin state as the 2.01-ev resonance in Gd^{155}.

[1] A. Stolovy, Phys. Rev. **118**, 211 (1960).
[2] H. B. Møller, F. J. Shore, and V. L. Sailor, Nuclear Sci. and Eng. **8**, 183 (1960).
[3] N. I. Kaliteevskii, M. P. Chaika, I. Kh. Pacheva, and E. E. Fradkin, J. Exptl. Theoret. Phys. (U.S.S.R.) **37**, 882 (1959); English translation JETP **37**, 629 (1960).

P8. Analysis of the Pu^{241} Total Neutron Cross Section.* O. D. SIMPSON AND M. S. MOORE, *Phillips Petroleum Company, Idaho Falls.*—Transmission measurements of 81% enriched Pu^{241} samples were made with the MTR fast chopper from 0.02 ev to 2 kev. The data below 12 ev have been analyzed using the multilevel formula of Reich and Moore, assuming the resonance asymmetries are due to interference in a small number of fission channels. The analysis is interpreted as evidence that there is a spin-state dependence of the size of the fission widths. The data are well described by the parameters in Table I.

TABLE I.

Level (λ)	E_λ (ev)	$g\Gamma^0_{\lambda n}$ (10^{-3} ev)	$\Gamma_{\lambda f1}$ (10^{-3} ev)	$\Gamma_{\lambda f2}$ (10^{-3} ev)	$\Gamma_{\lambda\gamma}$ (10^{-3} ev)	Relative signs $(\Gamma_{\lambda n}\Gamma_{\lambda f i})^{1/2}$
1	−0.160	0.0725	0	60	40	+
2	0.264	0.101	0	72	40	−
3	4.28	0.255	0	45	40	−
4	4.56	0.194	190	0	40	+
5	5.91	1.020	1350	0	40	+
6	6.94	0.218	0	85	40	+
7	8.60	0.268	0	70	40	+
8	9.56	0.035	0	100	40	−
9	10.20	0.400	1000	0	40	−

* Work performed under the auspices of the U. S. Atomic Energy Commission.

P9. Improved Li^6-Loaded Glass Scintillator for Neutron Detection. G. G. SLAUGHTER AND F. W. K. FIRK,* *Oak Ridge National Laboratory,* AND R. J. GINTHER, *Naval Research Laboratory.*—A cerium activated, Li^6-loaded, glass scintillator of improved scintillation efficiency and Li^6 content has been developed and used for detecting neutrons with energies from 1 ev to 80 kev by time-of-flight techniques. The following properties of a Li^6 glass scintillator were determined: (1) an efficiency of 30% for detecting 1 kev neutrons, (2) a resolution of 18% for the $Li^6(n,\alpha)T$ peak, and (3) a time resolution $\lesssim5\times10^{-9}$ sec using a "fast-slow" coincidence system. The neutron spectrum from the reaction $Li^7(p,n)Be^7$ has been measured using the ORNL pulsed Van de Graaff and the associated nanosecond time-of-flight equipment. The neutron energies extended from 5 to 80 kev. Total neutron cross section results up to 5 kev demonstrate the use of the detector with a fast-chopper neutron spectrometer. Lithium- and boron-loaded glass scintillators have been compared and it is concluded that lithium glass is, in general, the more suitable for neutron detection.

* Now visiting O.R.N.L. from A.E.R.E., Harwell, England.

P10. Interference between Radiative Transitions.* R. E. COTÉ AND L. M. BOLLINGER, *Argonne National Laboratory.*—Interference between neutron scattering[1] resonances and between the fission[2] components of neutron resonances has been shown to exist, but heretofore measurement of the radiative capture associated with neutron resonances has shown no such effect. It has been argued that this lack of interference is the natural result of the many channel processes associated with radiative de-excitation of the compound nucleus formed by the capture of a neutron, and that if a single radiative transition could be studied interference would be observed. The present

measurements show that this is indeed true. A study of the intensity of the 7.92-Mev transition of Pt^{196} throughout the region of energy dominated by the two resonances at 11.9 and 19.6 ev shows a distinct departure from the intensity expected on the basis of two noninterfering resonances. Moreover, preliminary computations indicate that the data are consistent with a single-channel process. These studies were carried out with the Argonne fast chopper in conjunction with a 6×8 in. NaI(Tl) scintillator and a pulse analyzer which stores the relevant pulse heights and time differences on magnetic tape.

* Work performed under the auspices of the U. S. Atomic Energy Commission.

[1] L. M. Bollinger, D. A. Dahlberg, R. R. Palmer, and G. E. Thomas, Phys. Rev. 100, 126 (1955).

[2] R. E. Coté and L. M. Bollinger, Bull. Am. Phys. Soc. I, 328 (1956).

WEDNESDAY MORNING AT 9:45

Sheraton Hall

(J. A. VAN ALLEN presiding)

Invited Paper

PA1. Recovery and Study of Nuclear Emulsions from Orbiting Satellites. HERMAN YAGODA, *Air Force Cambridge Research Laboratories.* (30 min.)

Cosmic-Ray Studies with Satellites

PA2. Star-Producing Radiations in Emulsions Recovered from Polar Orbits. R. FILZ AND HERMAN YAGODA, *AF Cambridge Research Laboratories.*—An Ilford G5 block 10×15 cm weighing 774 g launched into a polar orbit on December 7, 1960, received a total trans-atmospheric exposure of 3.124 days during a period of quiescent solar activity. The instrument capsule recovered from Discoverer satellite No. 18 made 48 orbits around the earth with apogees of 688 km and perigees of 232 km. The minimum absorber path over the emulsions was 1.9 g cm^{-2}. Preliminary estimates of stars with $N_h \geqslant 3$ indicate an accumulation of ~20 000 cc^{-1} which is about twice greater than that anticipated from counter data and emulsions flown in rockets from sites whose geomagnetic latitudes extended between the equator and the polar regions. The slope of the star spectra indicate a component of low-energy star-producing radiation which may originate in the fringes of the lower Van Allen belt, or low-energy protons arriving in the polar regions.

PA3. Low-Energy Heavy Primary Component Recorded in Emulsions Recovered from Polar Satellite Orbits. K. FUKUI AND HERMAN YAGODA, *AF Cambridge Research Laboratories.*—The emulsion block recovered from Discoverer No. 18 is being studied for the tracks of heavy nuclei $Z \geqslant 6$ which stop by ionization in the recording medium. A preliminary estimate of 10.9±1.5 cc^{-1} corresponds to a rate of 7.95±1.8 cc^{-1} day^{-1} on the basis of flight duration over latitudes ⩾50°N and S. In a balloon flight at 140 000-ft elevation launched at Minnesota July 29, 1960, the emulsions recorded 7.84±2.3 heavy primary thindown tracks cc^{-1} day^{-1} indicating that the flux does not increase appreciably at geomagnetic latitudes >55°N or S. On the Discoverer No. 17 satellite, which was launched into a 3+solar flare on November 12, 1960, the emulsions were severely underdeveloped to a point permitting recognition of terminating heavy primaries. These are estimated at 13±3 cc^{-1} day^{-1} suggesting that the flux of slow heavy primaries remains essentially unaltered during a major solar flare.

PA4. Air Masses and Effective Solid Angles Traversed by Cosmic Radiation at Satellite Elevations. JOHN T. A. ELY, *AF Cambridge Research Laboratories* (introduced by Herman Yagoda).—To correlate cosmic-ray counting data from high-altitude satellites and probes with balloon measurements made near the top of the atmosphere, a knowledge of the effective solid angle $\omega(H,L)$ for radiation crossing the atmosphere with a mean free path L and a zenith direction θ must be known. To calculate $m(H,\theta)$ up to 700 km, line integrals were made using the atmospheric densities from the ARDC Model Atmosphere (1959) based on satellite retardation. The integrals in the expression

$$\omega(H,L) = 2\pi \int_0^{\theta_{\max}} \left[\sum_{jkn} a_{jkn} (X_j)^n \exp(-X_k) \right] \sin\theta d\theta,$$

where $X_i = m(H,\theta)/L_i$, have been evaluated on the 709 computer for values of L between 10 and 120 g cm^{-2}. The flat earth assumption of the gross transformation and gold integral is not employed in the calculation of $\omega(H,L)$. Application of these parameters for normalizing cosmic-ray measurements at varying altitudes above a circular earth will be described.

PA5. Explorer VII Observations of Solar Cosmic Rays, November 12-23, 1960. J. A. VAN ALLEN, *State University of Iowa.*—The time history of the incidence of solar cosmic rays, their absolute intensities, and the latitude dependence of their arrival have been studied for the period November 12–23, 1960. Representative preliminary data on the absolute omnidirectional intensity J_0 of protons (E>30 Mev) plus alpha particles (E>120 Mev) are given in Table I. The time integral of J_0 for the period November 12–16 was ~10^9 cm^{-2}. The latitude dependence will be described and discussed.

TABLE I.

U.T.	Long.	Lat.	Alt.	$(cm^2\ sec)^{-1}$
2330/12 Nov.	−59.4	+44.4	878 km	21 000
0356/13 Nov.	+112.5	−48.1	619	11 000
0230/14 Nov.	−102.9	+46.7	886	1 250
2130/15 Nov.	+135.2	−44.3	802	13 000
0240/18 Nov.	−102.6	+50.4	897	98
0130/21 Nov.	−90.3	+50.4	881	980
0042/23 Nov.	−89.0	+50.4	849	10

PA6. Tritium in Recovered Satellite Material. E. L. FIREMAN, J. DEFELICE, AND D. TILLES, *Smithsonian Astrophysical Observatory.*—The radioactive isotope tritium (12.4 year half-life) was measured in iron and in lead from the Discoverer XVII satellite. This satellite was exposed to the solar flare of November 12, 1960. The tritium content of the iron was 50±3 decays/kg min, and of two lead samples was 7.5±0.2 and 24.0±0.5 decays/kg min. The tritium production rate averaged over the 50 hr that the satellite was in orbit was 150 000 tritons/kg min in the iron, and 23 000 and 75 000

tritons/kg min in the lead samples. The largest tritium production rate measured in iron meteorites or in the iron phase of stony meteorites is 300 tritons/kg min. The iron from the Discoverer XVII contained over 500 times more tritium than would be expected from the action of cosmic rays. The ratio of tritium to argon-37 production is 2500 in the Discoverer XVII iron compared to a ratio of 40 in iron targets bombarded by 160-Mev protons and a ratio of 15 in iron targets bombarded by 1 Bev protons. The large tritium content probably results from tritium in the flare itself.

PA7. Argon-37 in Recovered Satellite Material. D. TILLES, J. DEFELICE, AND E. L. FIREMAN, *Smithsonian Astrophysical Observatory.*—The amount of the radioactive isotope argon-37 (34 day half-life) was measured in iron and in lead from the Discoverer XVII satellite and in iron from the Discoverer XVIII satellite. Both were in polar orbits; the Discoverer XVII was exposed to the solar flare of November 12, 1960 while in orbit. At the time of recovery, iron in the Discoverer XVII satellite contained 2.5 ± 0.3 argon-37 decays/kg min corresponding to an average production rate of 58 ± 7 argon-37 atoms/kg min. In the Discoverer XVIII satellite the argon-37 production was less than 10 argon-37 atoms/kg min in iron covered by only 0.5 g/cm² of shileding. The argon-37 production rate in the iron meteorite Aroos was 23 atoms/kg min which is lower than the rate observed in the iron from Discoverer XVII but higher than that of Discoverer XVIII. The argon-37 production rate in the lead of Discoverer XVII was 4 atoms/kg min or less. The results indicate that the flare produced an appreciable amount of argon-37 in iron but not in lead.

PA8. Argon-37 Produced in Stainless Steel from Discoverer XVII and XVIII and Its Relation to Meteorites.* R. W. STOENNER AND R. DAVIS, JR., *Brookhaven National Laboratory.*—Argon-37 production rates were obtained on pieces of stainless-steel battery case carried by Discoverer XVII and XVIII. During the flight of Discoverer XVII a solar flare of Importance 3+ occurred, with associated increases in cosmic-ray neutron intensities.[1] The argon-37 activities observed were as follows: Discoverer XVII, 3.2 ± 0.4 dis/min^{-1} kg^{-1}; Discoverer XVIII, 1.1 ± 0.3 dis/min^{-1} kg^{-1}. The latter value approximates that expected from the normal cosmic-ray proton intensity outside the earth's atmosphere. The greater argon-37 activity found in Discoverer XVII results from solar flare protons. Argon-37 is a high-energy spallation product with a threshold of about 200 Mev. From the production cross section as a function of the energy, and the observed argon-37 in Discoverer XVII, the high-energy flare proton intensities can be evaluated. The results obtained can be related to argon activities observed in meteorites.

* Research performed under the auspices of the U. S. Atomic Energy Commission.

[1] M. A. Pomerantz, S. P. Duggal, and K. Nagashima, Phys. Rev. Letters 6, 123 (1961).

PA9. Radioactivity Produced in AgBr Emulsion Block Carried on Discoverer 17.* J. T. WASSON, P. J. DREVINSKY, AND M. I. KALKSTEIN, *Air Force Cambridge Research Laboratories.*—Scintillation-spectroscopy measurements on an emulsion block (containing 330 g Ag) from Discoverer 17, which was flown during a period of high solar cosmic-ray activity on November 12, 1960, reveal a gamma-ray spectrum attributable to 8.4-day Ag^{108}. The disintegration rate, corrected to a probable production time of 2100 UT, November 12, 1960, is 14 dis/sec. If one assumes a (p,pn) cross section of 100 mb, this corresponds to a total dosage within the emulsion of about 1.6×10^{8} protons/cm². An attempt to measure the gamma spectrum of 40-day Ag^{105} was unsuccessful, allowing the assignment of an upper limit on the disintegration rate of 1 dis/sec at the time of production. A search for 1.3-year Cd^{109} is under way.

* Supported in part by the U. S. Atomic Energy Commission.

PA10. Induced Radioactivities in Pb Carried on Discoverer XVII.* R. W. DODSON, G. FRIEDLANDER, J. HUDIS, AND O. A. SCHAEFFER, *Brookhaven National Laboratory.*—A sheet of lead ballast 7 g/cm² thick carried in the nose cone of Discoverer XVII was obtained. From one portion of the entire thickness of the lead a bismuth fraction was isolated and examined for x rays resulting from electron capture decay of Bi^{205} (14 day) and Bi^{206} (6 day). A small but real counting rate was observed whose decay was compatible with a 14-day half-life. Extrapolating back to the time of recovery the activity would correspond to 0.5 dpm of Bi^{205}/g of Pb. From the known excitation functions of the p,xn reactions on lead isotopes one can conclude that this Bi^{205} activity resulted largely from protons of between 50 and 100 Mev. Bi, Hg, and Tl were isolated from a surface sample 1 g/cm² thick. The measurements on the thallium fraction indicated less than 0.06 dis/min of Tl^{202}/g of Pb at time of recovery. The mercury fraction showed a β activity compatible with 0.004 dis/min of Hg^{203}/g of Pb at time of recovery. The bismuth samples are being counted by x-γ coincidences. The implications of these results with respect to the intensity and spectrum of the solar flare protons will be discussed.

* Research performed under the auspices of the U. S. Atomic Energy Commission.

WEDNESDAY MORNING AT 10:00

National Bureau of Standards, East Building

(F. N. FRENKIEL presiding)

Fluid Dynamics

Q1. Simplified Approach to Non-Newtonian Fluid Flows in Channels and Pipes. CHIEH C. CHANG, *Aerospace Corporation,* AND P. RAMANAIAH,* *University of Minnesota.*—The laminar channel and pipe flows of an incompressible, non-Newtonian fluid for the steady state are studied. According to an approximation of the rheological relation of the non-Newtonian fluids suggested by the authors, the viscosity variation with velocity gradient can be represented by a power law for moderate velocity gradients, whereas at high and low values of the velocity gradient the viscosity coefficient remains constant equal to μ_∞ and μ_0, respectively. Expressions for the velocity in different regions are obtained. A practical example is given and is compared with an equivalent Newtonian flow problem.

* Supported by U. S. Atomic Energy Commission and the National Institutes of Health.

Q2. Stability of Spiral Flow. H. A. SNYDER, *University of Chicago.*—The hydrodynamic stability of flow between rotating coaxial cylinders with a superposed axial pressure gradient has been studied experimentally. The apparatus is designed to

fulfill the assumptions used in deriving existing theories. The stability curve of the critical Taylor number T vs axial Reynolds number R has been determined to an accuracy of 1% up to $R=250$. It is shown that this curve has a linear slope of $\Delta T/\Delta R=58$ at $R=0$. At flow rates greater than $R=20$ the curve is nearly linear with a slope of $\Delta T/\Delta R=109$. There are measurable and physically significant departures from this curve of up to 8% in T. The Taylor cell widths and their speed of propagation at marginal stability have been measured for $R\leq 100$. A rough determination of the boundaries in the T,R-plane between various stable normal modes of secondary flow has been made. The results are compared with calculations by S. Chandrasekhar and by R. DiPrima.

Q3. On Simulation Studies of Motion of Bodies in Ionized Atmosphere.* K. P. CHOPRA, *Polytechnic Institute of Brooklyn.*—The principle of dimensional similitude is applied to the laboratory model studies of the motion of bodies in an ionized atmosphere pervaded by a magnetic field. The correspondence relationships of the various characteristic physical parameters in the actual and laboratory scale are obtained. It is shown that the scaling relationships satisfy the conditions of electrodynamic, magnetohydrodynamic and aerodynamic similitude. These relationships indicate that it is not necessary to obtain atmospheric densities in the laboratory. By adopting a suitable scaling factor it should be possible to simulate flight conditions corresponding to upper atmosphere of the earth. Details of a suggested experimental arrangement in a hypersonic wind tunnel are described.

* Supported by U. S. Air Force Office of Scientific Research.

Q4. Fall of Small Particles or Heavy Molecules Through the Upper Atmosphere.* H. L. DAVIS AND JOHN R. BANISTER, *Sandia Laboratory.*—We have computed the passage of small particles or heavy molecules through the upper atmosphere, taking account of both the fall rate and diffusion. For this calculation, which is carried out on a IBM 704 computer, we have assumed that the atmosphere is stagnant, isothermal, and has an exponential dependence of density upon the height. Using a fall rate expression derived from the steady state distribution and the usual diffusion coefficient, we find that the material injected in arbitrary profile is soon transposed into a profile which remains unchanged as the material passes down through the atmosphere. The descent rate of this profile is that of the fall rate of the particles at the maximum concentration, while the characteristic dimension of the profile is related to the e-fold distance. The behavior indicated by the 704 calculations is not unexpected and may be anticipated using qualitative arguments. Use of these qualitative arguments also allows a powerful generalization of the specific calculations. An approximate argument indicates that passing through a turbulent layer would not seriously affect the later distribution of material.

* This work performed under the auspices of the U. S. Atomic Energy Commission.

Q5. Neutral Shock Wave Structure. S. ZIERING AND F. EK, *Allied Research Associates.*—The bimodal method of Mott-Smith[1] and the two-fluid approach of Glansdorff[2] have been extensively modified to yield a description of neutral shock waves spanning the domain from weak to infinitely strong shocks. The results, in contrast with the bimodal or two-fluid approach, are substantially in agreement with the Navier Stokes analysis for weak shocks ($M<1.2$). There is also good agreement with the experimental results of Anderson and Hornig[3] as well as Sherman and Talbot.[4]

[1] H. M. Mott-Smith, Phys. Rev. **82**, 885 (1951).
[2] P. Glansdorff, "The thickness of shock waves by the two-fluid model theory extended to rarefied gases," abstracts of the Second International Symposium on Rarefied Gas Dynamics, Berkeley, California, (1960).
[3] W. H. Anderson and D. F. Hornig, Mol. Phys. **2**, 49 (1959).
[4] F. S. Sherman and L. Talbot, *Rarefied Gas Dynamics* (Pergamon Press, New York, 1960).

Q6. Calculations of Four Shock Intersections. W. R. SMITH, *Lehigh University.*—The perfect gas flow parameters associated with the two-dimensional stationary flow configuration of four plane shock waves intersecting at a point have been calculated using a Royal McBee LGP-30 computer for a gas specific heat ratio $\gamma=1.4$. Four shock configurations arise from the mutual reflection of an initial pair of shock waves of arbitrary strengths. The ratio of one initial shock strength to the other used in the calculations ranged from 1 to 100 in terms of the pressure ratios across each of the initial shocks, and the strength of the weaker wave ranged between 1.1 and 100. Calculations were made at 10° intervals over the entire range of incidence for which the four shock configuration was possible. The weak solution for the configuration was entirely machine calculated along with its extreme angle. The sonic angles were calculated by graphical interpolation. Solutions for other than the weak solution were found graphically from machine calculated shock polars. A new family of solutions has been discovered which exists for certain ranges of initial unequal shock strengths and angles.

Q7. Effect of Boundary-Layer Growth in a Shock Tube on Shock Reflection from a Closed End.* GEORGE RUDINGER, *Cornell Aeronautical Laboratory.*—The pressure behind the primary shock wave increases slightly with time because of boundary-layer growth.[1] It is shwon that this rise is considerably magnified by the reflected shock. Analysis of the interaction of the latter with the boundary layer yields information on the shock configuration,[2] but the combined effect of the waves produced by the growing boundary layer along the entire shock tube must be considered to obtain the conditions in the gas behind the reflected shock. The flow field behind the incident shock is computed on the basis of the theory of Mirels and Braun,[3] modified to allow for the effects of a nonideal shock-tube diaphragm. Standard wave-diagram procedures are simplified to compute the pressure rise behind the reflected shock without having to prepare a complete wave diagram. Experimental observations of the pressure rise, obtained for shock pressure ratios up to about 4.5, are in good agreement with the computed results.

* Work supported by the Office of Naval Research through Project SQUID.
[1] R. J. Emrich and D. B. Wheeler, Jr., Phys. Fluids **1**, 14 (1958).
[2] H. Mark, Natl. Advisory Comm. Aeronaut. Tech. Mem. 1418 (1958).
[3] H. Mirels and W. H. Braun, Natl. Advisory Comm. Aeronaut. Tech. Notes 4021 (1957).

Q8. Experimental Study of the Flow Field in a MAST of Large Radius Ratio. J. C. KECK, F. FISHMAN, AND H. E. PETSCHEK, *Avco-Everett Research Laboratory.*—The magnetic annular shock tube, MAST, is among the most promising devices for producing high-temperature high-velocity plasmas. In analyzing the performance of this device, the assumption of one-dimensional flow has been made.[1] This leads to the paradox that while the dynamic pressure across the shock wave is independent of radius r the magnetic pressure across the driving current interface decreases as $1/r^2$ and thus the two cannot balance. In an effort to establish the true pattern of the flow, measurements are being carried out in shock tubes with various radius ratios utilizing optical, electrostatic, and magnetic probes. The initial measurements have been conducted in a MAST having an inner radius of 1 in. and an outer radius of 3 in. It has been ascertained that in such a device, the current interface has the form of a paraboloid of revolution with the inner edge leading the outer by 2.5 in. The velocity of the current interface is such that the dynamic and magnet pressures balance at the inner radius. Efforts to detect the shock wave preceding the current interface have been unsuccessful, although the possibility of a detachment distance less than 1 cm has not been ruled out. The above observations can be

explained and the shape of the current interface calculated by matching a Newtonian pressure distribution to the magnetic pressure distribution. We would like to emphasize that these observations for a MAST of large radius ratio do not imply that a similar situation will exist in a MAST radius ratio near unity such as that used by Patrick[2] in the production of collisionless shocks. The study of the flow in such a MAST is currently in progress.

[1] N. H. Kemp and H. E. Petschek, Phys. Fluids **2**, 599 (1960).
[2] R. M. Patrick, Phys. Fluids **2**, 589 (1960).

Q9. Gun Technique for Low Pressure Shock Hydrodynamics.* JAMES J. BILLINGS AND F. STANLEY MINSHALL, *Los Alamos Scientific Laboratory.*—Shock waves with pressures less than 60 kb can be produced in metals by detonating explosives, but with difficulty. The conservation of mass and momentum upon impact of two flat pieces of metal of the same material permits such shock waves to be produced in metals by a gun in which the projectile speed can be varied. Some data have already been reported by others.[1] This paper reports the results of a series of experiments designed to test a gun to be used for equation-of-state measurements. Free surface motion was examined by a combined pin and capacitor technique. For 1020 steel the Hugoniot elastic wave velocity obtained for pressures of about 50 kb and less varies by as much as 5% above and below the value of 6 mm/μsec for higher pressures obtained by detonating explosives. The sound velocity of the target metal was 6 mm/μsec. Gun velocity at times of impact seems to have been about 10^{-4} mm/μsec and with essentially zero acceleration. Maximum projectile tilt was about 0.04 μsec/in.

* Work performed under auspices of U. S. Atomic Energy Commission.
[1] L. E. Gourley, Jr., "Shock-wave compression of iron and bismuth" (thesis), University of Texas (1959).

Q10. Some Experiments With the Liquid Driven Shock Tube. E. TERNER, *Armour Research Foundation.*—The shock tube, containing liquid in the driver section, is equipped with heating elements such that the liquid can be heated under pressure. In the present design, experiments can be carried out in a temperature range up to 500°F and under pressures up to 1000 psi. Pressure gages and thermocouples are provided at stations along the tube. The driven section, containing air or an inert gas at some suitable pressure, is separated from the driver by a special glass diaphragm. If the liquid is heated under pressure above its normal boiling point, it will undergo a phase transition at decompression due to diaphragm breakage. Ordinarily a two-phase jet will discharge into the driven section. In the present run of experiments this jetting effect, as well as the advance of the boiling front into the liquid at decompression, have been recorded with a Fastax motion camera. Further the propagation of subsequent reflections of the decompression pulse has been recorded in the liquid; rise of pressure due to vapor accumulation in the driven chamber has been determined together with the density variations in the jet discharge into the driven chamber. The experiments have been carried out with water as well as some organic liquids, and it is shown that the tube can serve as a research tool.

WEDNESDAY MORNING AT 10:15

Cotillion Room, North

(J. W. BEAMS presiding)

Invited Paper

QA1. Interactions between Dislocations in Crystals of Silver Halides. J. W. MITCHELL, *University of Virginia.* (30 min.)

General Solid-State Physics, I

QA2. On the Energy of Formation of Vacancies in Crystals.* HENRI AMAR, *Franklin Institute Laboratories and Temple University.*—In order to justify indirectly measured values of the energy of formation of a vacancy, experimenters frequently quote the quantum mechanical calculation of this quantity by HSB (Huntington,[1] Seitz,[2] and Brooks[3] who showed that the 1.8 ev of HSB should be corrected and reduced to 1 ev). In the HSB work, this formation energy is the algebraic sum of about ten different and relatively large contributions. A discussion of the basic assumptions and approximations of HSD is here undertaken, and after some criticism of a general nature (Brooks and other authors expressed similar criticisms), specific contributions (such as Fermi energy, electrostatic self-energy) are singled out and recalculated. This quantitative analysis clearly shows that the uncertainty in some of the items approaches or exceeds the final result. The conclusion is that, while the HSB method is qualitatively illuminating, the quantitative results are of little value in validating experimentally measured parameters.

* Work supported by the U. S. Atomic Energy Commission.
[1] H. B. Huntington, Phys. Rev. **61**, 325 (1942).
[2] H. B. Huntington and F. Seitz, Phys. Rev. **61**, 315 (1942).
[3] H. Brooks, Trans. Am. Soc. Metals **47**, 1 ff. (1955).

QA3. Growth of Graphite Single Crystals and Aluminum Oxide Whiskers.* P. J. BRYANT AND S. L. LEVY, *Midwest Research Institute.*—A 2500°C furnace with unuaual temperature stability was designed and constructed for the production of graphite single crystals. A tungsten heater was employed. By the combined use of carbonized cotton for electrical insulation and lamp black for thermal insulation, it was possible to achieve a temperature of 2500°C with an input power of less than 1.5 kw. The low thermal loss feature contributes to the high temperature stability. Details of the furnace design will be discussed. During the production of graphite single crystals by the thermal decomposition of aluminum carbide[1] serendipity prevailed so that in addition graphite crystals grew by deposition from a vapor phase, and α-phase aluminum oxide whiskers were deposited. These whiskers grew to a length of 4 cm while maintaining a uniform cross section of less than 10 μ.

* This research was supported by the U. S. Air Force, monitored by the Materials Laboratory, Wright Air Development Center, Wright-Patterson Air Force Base, Ohio.
[1] L. M. Foster, G. Long, and H. C. Stumpf, Am. Mineralogist **43**, 285–296 (1958).

QA4. Lattice Vibrations of Zincblende Structure Crystals.* HARVEY KAPLAN AND JOHN J. SULLIVAN, *Syracuse University.*

—We report here a calculation of the lattice vibration spectrum of zincblende structure crystals in symmetry directions in the Brillouin zone, using the shell model previously used by Cochran *et al.*[1,2] to study germanium and alkali halide crystals. The parameters of the model (shell and core charges, shell springs and short range force constants) are adjusted to fit the elastic, piezoelectric and high and low frequency dielectric constants. Care is taken to ensure that the model corresponds to zero pressure in equilibrium. The zincblende structure differs from the alkali halides in that the polarizabilities affect the elastic consant C_{44}. A comparison calculation using the Born and Huang model, which includes long-range but not short-range polarization effects, reveals the same instability for short wave lengths in the ⟨100⟩ directions as was found earlier for the alkali halides.[2] Our work will be compared with a calculation of Merten[3] which used a rigid ion model.

* Supported in part by the U. S. Air Force Office of Scientific Research.
[1] W. Cochran, Proc. Roy. Soc. (London) **A253**, 260 (1959).
[2] A. D. B. Woods, W. Cochran, and B. N. Brockhouse, Phys. Rev. **119**, 980 (1960).
[3] L. Merten, Z. Naturforsch. **13A**, 662, 1067 (1958).

QA5. Dislocations in Silver Chloride Crystals.* MAX G. MILLER AND LAWRENCE SLIFKIN, *University of North Carolina.*—Dislocations in silver chloride have been studied utilizing two distinct experimental techniques: (a) Dislocations in the interior of crystals have been decorated by forming internal print-out, using the Haynes Shockley technique; (b) Tensile experiments, using a "hard" tensile machine have been performed to determine the effect of impurities, defects inducted by quenching, and internal print-out on the plastic properties of AgCl. The relative contrast of dislocation decoration has been found to be extremely dependent on impurity content. At the time of writing, no evidence has been found for pile-ups or Frank-Read sources of dislocations in strained AgCl, although bowed out loops have been observed. In copper-doped crystls, the presence or absence of strain aging has been found to be dependent upon whether the impurity is in the divalent or monovalent state. Crystals containing decorated dislocations have been tested in tension and show a slight increase in initial yield point. Further similar experiments are in progress. Quenching experiments indicate that defects thus produced increase the yield point markedly and also decrease the rate of work hardening.

* Supported in part by the U. S. Army Office of Ordnance Research and the U. S. Air Force Office of Scientific Research.

QA6. Point Defect Trapping in Crystal Growth. W. W. WEBB, *Union Carbide Metals Company.*—The problem of whether appreciable nonequilibrium concentrations of point defects can be trapped in crystals during near-equilibrium growth has been considered. A semiquantitative treatment based on the established theory of near-equilibrium growth on vicinal surfaces indicates that either a supersaturation or undersaturation of point defects may result from near-equilibrium growth. A dimensionless parameter D_v/Rd, where D_v is the diffusion coefficient for point defects, R is the growth rate, and d is the effective interface thickness, describes most of the relevant features of the growth conditions. At temperatures well below the crystal melting temperature large supersaturations may be trapped, but near the melting point only small undersaturations may be retained. The effects of growth-trapped point defects on subsequent dislocation climb appear to be significant in solution-grown crystals, in metal whiskers, in some vapor-grown crystals, and possibly in melt-grown crystals.

QA7. Calculation of Intensity Variations in Crystalline Bragg Scattering Due to Secondary Scattering.* R. I. SCHERMER,† *M.I.T.* (introduced by G. Brownell).—Sharp variations in intensity diffracted by single crystals have been observed by a number of experimenters, and have been attributed to secondary, or multiple, Bragg scattering in the crystal. Several authors have shown how the secondary planes responsible for the individual variations may be indexed. Renninger[1] has exhibited the intensity calculation for the case of one secondary beam, with both primary and secondary beams transmitted through the crystal and with no absorption. The introduction of absorption, or of reflected beams, complicates the problem. Here, the equations are derived for n beams moving in arbitrary directions in a large slab of absorbing crystal, using the same mosaic model as is usually applied to the treatment of secondary extinction. The equations are solved by Laplace-transform methods, in an approximation in which interaction between the secondary beams is neglected. The system properties are discussed in terms of an electrical analogue. Results will be presented for the variation of the effect with thickness and system parameters, and for the shape of the observed variations.

* Work supported by the Rockefeller Foundation and the U. S. Atomic Energy Commission.
† Current address: Brookhaven National Laboratory, Upton, New York.
[1] M. Renninger, Z. Physik **106**, 141 (1937).

QA8. Proposed Spin Arrangement in β MnS.* F. KEFFER, *University of Pittsburgh.*—In β MnS each anion is surrounded tetrahedrally by four magnetic cations. Any state with the four spins summing to zero will have lowest near-neighbor antiferromagnetic superexchange energy. Absence of inversion symmetry allows a Moriya coupling[1] of the form $\mathbf{D}_{ij}\cdot\mathbf{S}_i\times\mathbf{S}_j$, with symmetry requiring $\mathbf{D}_{ij}$ normal to the plane defined by i, j, and the anion. The lowest energy arrangement consistent with translation symmetry is then $\mathbf{S}_1=-\mathbf{S}_2$ and both orthogonal to $\mathbf{S}_3=-\mathbf{S}_4$. (In crystals considered heretofore, the Moriya energy produces only a slight canting.) The observed powder neutron diffraction pattern has been interpreted as indicating ordering of the third kind with spins normal to the ordering axis[2]; this arrangement however does not have minimum dipolar energy.[3] The present proposed arrangement leads to the same diffraction pattern, and the Moriya energy easily overbalances the dipolar. Neutron diffraction in MnS_2 indicates an arrangement with minimum dipolar energy.[3] This is not surprising since the pyrite structure allows no Moriya coupling.

* Supported by the U. S. Air Force Office of Scientific Research.
[1] T. Moriya, Phys. Rev. **120**, 91 (1960).
[2] J. M. Hastings, L. M. Corliss, and N. Elliott, Phys. Rev. **104**, 924 (1956); **115**, 13 (1959).
[3] F. Keffer and W. O'Sullivan, Phys. Rev. **108**, 637 (1957).

QA9. Anisotropic Superexchange Interaction in β MnS.* J. J. PEARSON, *University of Pittsburgh.*—The suggestion in the previous abstract of a Moriya interaction in β MnS led to the present detailed calculation. Whereas Moriya's work utilized Anderson's new theory of superexchange and was confined to ions with one electron in the 3*d* shell, this calculation was performed with more customary superexchange methods and for a half-filled 3*d* shell. The unperturbed state was taken to consist of two Mn^{++} ions toegther with their common S^{--} nearest neighbor, each in a tetrahedral crystal field. The perturbing Hamiltonian contained the electronic spin-orbit interaction and the Coulomb interaction between electrons on neighboring ions. The mechanism involved going from the ground state to an excited crystal field state on one Mn^{++} ion by the spin-orbit effect, then back to the ground state by superexchange between the Mn's. The direction of the **D** vector was found to be perpendicular to the plane of the three ions, and its magnitude of the order of a superecxhange integral times the spin-orbit parameter over a crystal field splitting energy. The existence of the effect depends importantly upon π overlap between the Mn and S orbitals.

* Supported by the U. S. Air Force Office of Scientific Research.

QA10. Low Temperature Photoconductivity of Additively Colored KCl.* R. L. WILD, *University of California, Riverside.*—The spectral photoresponse of additively colored KCl at 10°K reflects the absorption structure found by Luty.[1] The product of quantum yield and carrier range is nearly constant in the L_1 and L_2 band (3.6 and 4.2 ev) but drops sharply in the K and F region. This suggests that the K band (as well as the F) results from excitations to states below the bottom of the conduction band. Partial saturation of photoconductivity vs electric field yielded carrier range estimates near 10^{-6} cm²/v. This plus Luty's result of optical absorption proportional to F-band absorption yields 0.04 for quantum yield, indicating competing processes. The F center (or closely associated centers) is the main trap for heavily colored cyrstals with a trapping cross section $\cong 10^{-14}$ cm², but shallow traps become dominant in lightly colored crystals. For these shallow traps the product of concentration and cross section is 1000–4000 cm^{-1} which suggests large cross section or very high concentration. Illumination fills these shallow traps and produces enhanced photosensitivity in the infrared.

* This work was done at the University of Illinois, supported in part by the National Science Foundation and the Air Force Office of Scientific Research.

[1] F. Luty, "Höhere Anregungszustände von Farbzentren," Color Centers in Alkali Halides Symposium, Corvallis, Oregon (1959).

QA11. Hypersonic Resonance of Quartz at 3500 Mc. ELLEN S. STEWART AND JAMES L. STEWART, *U. S. Navy Electronics Laboratory.*—The resonance of X-cut quartz crystals 0.1 mm thick at the odd harmonics between 2950 Mc and 3600 Mc at room temperature has been observed. The crystal, of 1.0-cm diam, is in the gap of a reentrant cylindrical cavity. The mechanical resonance of the piezoelectric quartz is observed by its reaction on the electrical resonance of the cavity. Since only the odd harmonics have been observed and since they appear to be simple resonances, it is concluded that these crystals are excited in pure thickness modes in contrast to the complex excitation of many undesired modes of an X-cut quartz crystal at lower frequencies. The velocity of sound in the quartz, computed from the resonant frequencies and the thickness, is 5.39×10^5 cm/sec, about 5% less than low frequency values. The Q is approximately 3000, in good agreement with that predicted from the quartz absorption extrapolated from the data of Bömmel and Dransfeld[1] using a frequency square dependence. Hypersonic radiation into water has been detected by the damping of the quartz resonance and the specific acoustic impedance has been measured.

[1] H. Bömmel and K. Dransfeld, Phys. Rev. Letters **2**, 298 (1959).

QA12. Role of Surfaces in Plastic Flow of Rock-Salt Single Crystals. S. MENDELSON, *Columbia University.*—By a suitable technique it is possible to activate dislocation sources in the center of a large surface of NaCl crystals. A refined birefringence and sensitive etch pit method were used to make direct observations of dislocations as they move towards opposite edges of the crystal. Sharp slip steps were observed on the surface of well prepared small crystals. Dislocation pileups were not found against the nascent surface but were found against an ozonized surface. It was found that the initially active sources lie close to or on the surface. Ozonization of NaCl surfaces for short periods restricts the action of surface sources, and for longer times provides barriers to the egress of dislocations. The Suzuki effect (formation of a work-hardened surface layer) was also studied in NaCl. It was found to depend upon the existence of a multiplicity of surface sources such as is produced by polishing on wet silk. In the absence of this, the "Suzuki effect" is not found. Cross-slip of screw dislocations at the surface under the image force is found to be greater when the specimen is polished during or after the formation of glide bands. This effect is proposed as the likely mechanism to explain the "Joffe effect" when atmospheric variables are eliminated.

WEDNESDAY MORNING AT 9:30

Burgundy Room

(L. H. THOMAS presiding)

Theory, V: Atomic, Molecular, and General Theory

QB1. The Faraday Effect in O_2. J. FINKEL, *U. S. Naval Ordnance Laboratory,* AND E. A. STERN, *University of Maryland.*—The anomalous Faraday dispersion of O_2 in the visible, near-ultraviolet, and near-infrared spectral regions was shown to be due to the interaction of the spin magnetic moment of the O_2 molecule with the magnetic field of the light wave.[1] An alternate derivation of this result will be given which shows in a simpler and more transparent way how the spin magnetic moment enters into the problem. Using appropriate dispersion relations[2] it is shown that the Verdet constant of O_2 contains in addition to the usual terms a frequency-independent term originating from the spins. The latter is calculated numerically. The results obtained with this method are in complete agreement with those of Hougen.[1]

[1] J. T. Hougen, J. Chem. Phys. **32**, 1122 (1960).
[2] B. S. Gourary, J. Appl. Phys. **28**, 283 (1957); H. S. Bennett and E. A. Stern, Bull. Am. Phys. Soc. Ser. II **5**, 279 (1960).

QB2. Numerical Calculations of Some Shielding Constants. JAMES N. PINKERTON AND CHARLES H. ANDERSON, *Harvard University.*—By using the values of several recently measured spin-rotational constants,[1] we have been able on the basis of Ramsey's formula,[2] given by

$$\sigma=\frac{e^2}{3mc^2}\left[\int p\frac{(\mathbf{r})}{r}d\tau-\Sigma_i\frac{z_i}{a_i}+\frac{h}{2\mu N^2 g_1 M}C_1 I\right],$$

to predict in a number of molecules the proton shielding constants and the fluorine chemical shifts. Methods for evaluating $\int[p(\mathbf{r})d\tau/r]$ the above formula will be presented. Combining such an evaluation of the integral with the measured C_1 gives results in agreement with experiment. These will be discussed in particular for HCN, HCl, HBr, HI, HF, SF_6, and CF_4. The method can be extended to molecules containing other nuclei.

[1] M. R. Baker, S. I. Chan, J. H. Leavitt, and H. M. Nelson (private communications).
[2] N. F. Ramsey, Phys. Rev. **78**, 699 (1950).

QB3. Potential Model Scattering of Electrons by Atoms and the Existence of Negative Ions. F. B. MALIK* AND E. TREFFTZ, *Max Planck Institut für Physik und Astrophysik, Munich.*—The low-energy scattering of electrons by different neutral atoms has been treated by assuming that the atomic wave functions remain unchanged even in the presence of the

scattered particle and by neglecting the exchange between the scattered electron and bound electrons. The potential term in the differential equation of the scattered particle is exactly the atomic potential of the neutral atom and is approximated by analytical expressions yielding the potential scattering equation. The variational treatment of Hulthén and Kohn and related treatments are applied to solve this equation for Hartree atoms and for the s-partial wave. The scattering by He, C, and N is treated explicitly and the results for He indicate that in this way one may get some good results without going into the great complexity of many-body problem. It has further been pointed out that the study of scattering by neutral atoms near zero energy under this model may serve as a possible means of investigating the existence of different negative ions and their number of bound states. It seems from this point of view that He^- C^- and N^- may exist and that each has only one bound state.

* Now at Princeton and with Pakistan Atomic Energy Commission.

QB4. Exchange Interaction and Heisenberg's Spin Hamiltonian.* TADASHI ARAI, *Argonne National Laboratory.*—Use of the Heisenberg spin operator for magnetic problems has been criticized by Slater[1] since the expression $-\frac{1}{2}\Sigma J_{kl} \times(1+S_k\cdot S_l)$ is valid only if orthogonal atomic orbitals are used. In this case, however, the exchange integrals J_{kl} are positive and it is not possible to explain antiferromagnetism. On the other hand, use of nonorthogonal orbitals gives divergence in both the denominator and the numerator of the energy expression. Therefore, it is unjustified to derive the Heisenberg operatore by omitting higher permutations. By the use of representation matrices of the permutation group, we can expand the energy matrix such that $E=\Sigma_P J(P)U(P)$ and show that all the coefficients $J(P)$ are bounded and determined uniquely. This means that the expansion is mathematically valid even though nonorthogonal orbitals are used. Furthermore, we shall show that the nonorthogonality catastrophe does not appear and values of the coefficients can be evaluated even if we omit higher permutations. Then we find the Heisenberg operator as the first-order approximation of the expansion.

* Based on work performed under the auspices of the U. S. Atomic Energy Commission.
[1] J. C. Slater, Revs. Modern Phys. 25, 199 (1953).

QB5. Generalized Bloch Equations. G. M. VOLKOFF AND S. D. JOG, *University of British Columbia.*—A unified general discussion using density-matrix formalism is given for the methods previously proposed for setting up generalized Bloch equations $d\mathbf{r}/dt=\mathbf{r}\times\boldsymbol{\Omega}$ in the absence of relaxation for special degenerate[1,2] and nondegenerate[3] cases of systems of nuclei of spin I subjected to given magnetic and electric fields. The interrelationship between the three methods is established and explicit expressions are obtained for $\boldsymbol{\Omega}$ in terms of the Hamiltonian, and for $\mathbf{r}$ in terms of suitable linear combinations of macroscopic quantities (magnetization, quadrupole moment density, etc.) describing the system.

[1] M. Bloom, E. L. Hahn, and B. Herzog, Phys. Rev. 97, 1699 (1955).
[2] F. Lurçat, J. phys. radium 19, 713 (1958).
[3] M. Bloom, L. B. Robinson, and G. M. Volkoff, Can. J. Phys. 36, 1286 (1958).

QB6. Minimum Principle for Multichannel Scattering Problems.* LEONARD ROSENBERG AND LARRY SPRUCH, *New York University.*—We have previously introduced a variational technique for obtaining a rigorous bound on the phase shift for the general one-channel scattering problem.[1] The method has now been extended to the case of an arbitrary number N of open channels. It was convenient to use the (real, symmetric) reactance matrix K in the parametrization of the scattering process. A straightforward generalization of the previous work gives a minimum principle for (a,Ka), where a is a real, but otherwise arbitrary $(N\times 1)$ matrix. The scattering problem considered is such that in each channel there is a radius beyond which the interaction between the two groups of particles associated with that channel reduces to a solvable two-body potential. This corresponds to the assumption made in the Wigner-Eisenbud theory of nuclear reactions. For low and moderate scattering energies it is expected that the cutoff radius can be made large enough, even for atomic scattering, such that meaningful results can be obtained with a reasonable amount of labor.

* Sponsored by the AFCRL, the OOR, and the Office of Naval Research.
[1] L. Rosenberg and L. Spruch, Phys. Rev. 120, 474 (1960), and an article to be published.

QB7. Constitutive Relations for Systems in Bound States. FREDERICK R. INNES, *Air Force Cambridge Research Laboratories.*—These relations connect the energy and other parameters of systems in bound states. They may be derived from the zero expectation values of commutators of certain system operators with an appropriate energy expression. The virial theorem in its quantum-mechanical form is one example. The number of independent relations must be limited by the system characteristics, for example, the number of configurations taken into account. The use of these relations is indicated for the improvement or simplification of many sorts of computations, in particular, of self-consistent field and variational calculations on bound-state systems generally. If the wave functions are separated and the operators expanded in separated form, the relations reduce to equations between the radial integrals of the system. It is possible that these methods can be extended to the study of a more general class of stationary states than that considered here.

QB8. The Order of Levels of Symmetric Hamiltonians. MELVIN M. SAFFREN, *General Electric Research Laboratory.*—Suppose each eigenvalue of a symmetric Hamiltonian to be labeled with a symmetry index. The index identifies an irreducible representation of the group of the Hamiltonian so that an eigenvalue bears the index of the irreducible manifold to which its associated eigenfunctions belong. Then, as will be shown, it turns out that for Hamiltonians whose group is of a particular type the relative position of an eigenvalue in the spectrum depends, in part, upon its symmetry index alone. In other words, again, theorems regarding the order of levels of certain symmtric Hamiltonians can be proved, the results of such theorems being dependent solely upon the group of the Hamiltonian. Such theorems will be illustrated by three particular cases: one electron in a cubic field, one electron in a body-centered periodic potential, and one electron in a face-centered periodic potential. As an application of these theorems, their bearing upon the pseudopotential method of Phillips and Kleinman will be discussed.

QB9. Lower Bounds for Eigenvalues of the Schrödinger Equation. II. N. W. BAZLEY, *National Bureau of Standards* AND D. W. FOX, *Applied Physics Laboratory, The Johns Hopkins University* (introduced by J. P. Vinti).—We give another procedure for lower bounds to eigenvalues of the Schrödinger equation related to that given in A.M.S. Notices 6, 839 (1959) and Bull. Am. Phys. Soc. Ser. II 6, 43 (1961). Let H be a Hamiltonian, Hermitian in the inner product $(\varphi,\psi)=\int\varphi\psi^*d\tau$, and denote the lowest eigenvalues and corresponding eigenfunctions of H by E_i and ψ_i, $i=1, 2, \cdots$. Let H^o be another Hamiltonian such that $(H^o\psi,\psi)\leq(H\psi,\psi)$ and for which $H^o\psi_i{}^o=E_i{}^o\psi_i{}^o$ has known eigenvalues $E_i{}^o$ and eigenfunctions $\psi_i{}^o$. Then $E_i{}^o\leq E_i$, $i=1, 2, \cdots$. We introduce the Hamiltonians $H^{n,o}$ defined by

$$H^{n,o}\psi=\sum_{j=1}^{n}(\psi,\psi_j{}^o)E_j{}^o\psi_j{}^o + E_{n+1}{}^o\Big[\psi-\sum_{j=1}^{n}(\psi,\psi_j{}^o)\psi_j{}^o\Big],\quad n=1, 2, \cdots,$$

These satisfy $(H^{n,0}\psi,\psi)\leq(H^{n+1}\psi,\psi)\leq(H\psi,\psi)$. Let $p_1, p_2, \cdots, p_k$ be arbitrary vectors, and introduce vector spaces with inner products $[\varphi,\psi]_n$ given by $[\varphi,\psi]_n=(\{H-H^{n,0}\}\varphi,\psi)$. Denote the projection of ψ on the span of $p_1, p_2, \cdots, p_k$ in these vector spaces by $P^{n,k}\psi$ and define $H^{n,k}=H^{n,0}+\{H-H^{n,0}\}P^{n,k}$. Then $(H^{n,k}\psi,\psi)\leq(H\psi,\psi)$. The equation $H^{n,k}\psi=E\psi$ has ordered eigenvalues $E_i^{n,k}$ with eigenfunctions $\psi_i^{n,k}$ which give lower bounds, $E_i^{n,k}\leq E_i$, $i=1, 2, 3 \cdots$. The $E_i^{n,k}$ and $\psi_i^{n,k}$ are found from an algebraic problem involving the matrix elements

$$(\{H-H^0\}p_j, \psi_i^0), \quad (\{H-H^{n,0}\}p_j, p_s) \quad \text{and} \quad (\{H-H^{n,0}\}p_t, \{H-H^{n,0}\}p_s),$$

where $j=1, \cdots, n$; $s, t=1, \cdots, k$.

QB10. Quasi-Classical Transformation Theory.* RALPH SCHILLER,† *Syracuse University.*—The approximate WKB solutions to Schrödinger's equation are usually given as functions of our ordinary space-time variables. There is however a general statement of the WKB approximation due to Van Vleck (1928), hereafter called the quasi-classical theory, which is invariant under canonical transformations. We have found the laws of transformation of these approximate wave functions and operators. For infinitesimal transformations of wave functions, the canonical group is the unitary group of quantum mechanics. In bound-state problems we have found configuration space variables such that the WKB wave functions are continuous in the entire range of the configuration space. In terms of these variables we have found classical representations of creation and destruction operators. The corresponding WKB wave functions for some dynamical problems turn out to be exact solutions of a similarly transformed Schrödinger equation. This is significant for it shows that by classical methods one can construct exact solutions of the Schrödinger equation. The existence of these wave functions does not imply quantization, which arises only after suitable boundary conditions have been imposed on the wave functions.

* Research supported by Wright Air Development Center.
† On leave from Stevens Institute of Technology.

QB11. A Possible Mechanism for the Quantum Mechanical Liouville Equation. GEORGE J. YEVICK, *Stevens Institute of Technology* AND JEROME K. PERCUS, *New York University.*—We should like to ascertain the "mechanism" for the diffusion-like behavior of the probability density in phase space characterizing quantum-mechanical motion. If we consider a system of identical particles and treat it as fluid using fluid-density coordinates and a velocity potential, we obtain after a suitable Jacobian transformation, a Hamiltonian which yields the Bohm-type equations. If now we abstract from this fluid a single particle, there results a coupled system of particle and fluid. Next we make a canonical transformation such that in the absence of the fluid field the particle obeys the classical equations of motion. In the new equations of motion, the particle can initially have a nonquantum-mechanical distribution in phase space. It is conjectured that such a distribution goes over rapidly into the quantum mechanical distribution which is due to the background fluid. We have demonstrated this to be true in the special case of a free-particle wave packet. In the foregoing, we must eliminate field coordinates and momenta, thereby reducing the over-all Liouville equation to a positive-density Liouville equation for a single quantum-mechanical particle.

QB12. A Model of a Photon. CHESTER J. MARCINKOWSKI, *Polytechnic Institute of Brooklyn.*—A photon is constructed from a source-free solution of Maxwell's equations. The photon consists of a modal superposition of cylindrical waves at the electron-rest frequency ω_e of the creating particle and propagating in varying directions to produce a finite photon length. Upon this carrier frequency is superimposed a photon modulation frequency ω_p with $(\omega_p/\omega_e)^2\ll 1$. A photon of wavelength λ_p has a needle-shaped structure with a length $\sim\lambda_p(\lambda_p/\lambda_e)$ in the direction of its motion and a diameter of an electron wavelength $\lambda_e\sim 10^{-10}$ cm. The photon travels with a velocity $v\simeq c$ with transverse fields approximately linearly polarized ($v<c$). The photon field resembles a plane wave with phase fronts propagating at the phase velocity $u=c^2/v$ and decaying as $1/r^3$ in the transverse direction. The arbitrary phase of the carrier frequency ω_e provides a hidden variable. This photon has an energy $\hbar\omega_p$, a linear momentum $\hbar\omega_p/c$, and a vanishing angular momentum. By changing carriers to a nucleon rest frequency $\omega_n(\omega_e\rightarrow\omega_n, \lambda_e\rightarrow\lambda_n)$, this model may also represent a neutrino.

WEDNESDAY AFTERNOON AT 2:00

Adams-Hamilton Room

Optical and X-Ray Physics; Astrophysics

R1. Measurements on HeI Line Broadening in a Plasma. W. B. JOHNSON, *Linde Company.*—Measurements have been made on the broadening of a number of lines of neutral helium as a function of electron density. The experiment has been carried out using the plasma produced by a continuous electric arc operating in pure helium at 200 amp and at atmospheric pressure. Temperatures were determined from a comparison of theoretical and observed line intensities of the 3888 A and 5875 A spectral lines with the densities being determined from the Saha equation at the observed temperature. Line profiles have been determined along with the resultant data on shifts and half-widths as a function of electron density in the range between 10^{16} and 10^{17} electrons/cm^3 with the temperature varying from 16 000° to 20 000°K. Lines which have been studied have mainly been the more narrow lines of the helium spectrum, namely the 6678, 5875, 5047, 5015, 4713, 4120, 3964, and 3888 A lines. As one would expect, these narrow lines are those with relatively low lying upper states which are perturbed to a lesser degree than higher states.

R2. Spectral Line Intensity and Electron Density Measurements in Flame Gases Containing Metal Vapors.* FRITZ W. HOFMANN AND HEDWIG KOHN, *Duke University.*—In premixed high-temperature flames (2500°–2760°K) the dependence of the degree of ionization of alkali and alkaline earth atoms on their density distorts the intensity-density curves for the atomic resonance lines of these elements. This distortion was removed by admixing an amount of a second easily ionizable element which suffices to hold the electron concentration, and hence the degree of ionization, constant over the range of metal concentrations required to obtain the low- and high-density asymptotes of the intensity-density curve. Cross sections for collisional broadening of the measured spectral lines were determined from the point of intersection of these

asymptotes. The underlying assumption of thermally equilibrated ionization in a flame zone a few mm above the primary reaction zone was verified, for one and for a mixture of two alkalis, by electron density measurements by microwave attenuation. For the alkaline earths, ionic resonance line intensities were measured in addition to atomic resonance lines and electron densities, thus permitting a direct experimental determination of the Saha equilibrium constants.

* Supported in part by the Office of Naval Research.

R3. Effect of Temperature on Infrared Absorption of Solid LiH and LiD.* R. H. MISHO AND D. J. MONTGOMERY, *Michigan State University.*—Infrared absorption spectra of thin films of LiH(~97% Li^7, 100% H^1) and LiD(~97% Li^7, ~96% H^2) evaporated on KBr plates were obtained in the range 12.5μ–25μ from 100°K to 400°K in a specially constructed cryostat-oven. The chamber containing the specimen was maintained under vacuum continuously during preparation and observation of the films. At room temperature, the primary feature of the spectrum for each material is a broad peak at 17.0μ for LiH and at 22.5μ for LiD, in agreement with results reported earlier.[1] At high temperatures, the peaks flatten to such an extent that it is difficult to establish definitely the existence of a shift. At low temperatures, the peaks become deeper and narrower, and the position of the minimum transmission shifts by only a few tenths of a micron, an amount much smaller than expected by analogy with results on alkali halides.[2] In view of the unexpected nature of the shifts, the experiment is being repeated with different substrates.

* This research was supported by the U. S. Air Force through the Air Force Office of Scientific Research (ARDC), and by the U. S. Atomic Energy Commission through the Metallurgy and Materials Branch of the Division of Research.
[1] W. B. Zimmerman and D. J. Montgomery, Phys. Rev. 120, 405 (1960).
[2] M. Hass, Phys. Rev. 119, 633 (1960).

R4. Intensity Dependence of the Soft X-ray Continuous Spectrum on Take-off Angle.* T. J. PETERSON, JR., AND D. H. TOMBOULIAN, *Cornell University.*—The variation of relative intensities as a function of angle of observation over the 80- to 180-A wavelength region has been investigated in continuation of the general line of study previously reported.[1] Mg, Mn, and Ag have been used as targets for the incident electron beam at energies of 675 ev, 1200 ev, and 1500 ev, respectively; and the spectrum has been observed at angles of 95°, 110°, and 135° measured from the forward direction of electron motion. The experimental results in the case of a Mg target can be directly compared with the numerical calculations of the Sommerfeld theory.[2] The results for Mn and Ag will be discussed in the light of the predictions for Mg.

* Supported in part by the Office of Ordnance Research, U. S. Army.
[1] T. J. Peterson, Jr. and D. H. Tomboulian, Bull. Am. Phys. Soc. 4, 263 419 (1959).
[2] P. Kirkpatrick and L. Weidmann, Phys. Rev. 67, 321 (1945).

R5. Photon Absorption by Valence Electrons in Chromium.* H. KROGER AND D. H. TOMBOULIAN, *Cornell University.*—The absorption of Cr foils was investigated on the low energy side of the $M_{2,3}$ edge (43.4 ev). Observations indicate the presence of secondary absorption peaks at the following incident photon energies expressed in ev: 22.0, 24.0, 25.8, 27.0, 30.1, 35.3, 39.5. The spectrum of the source which was a capillary discharge in argon, consisted of closely spaced high-intensity radiations. This circumstance increases the danger of order contamination and leads to difficulties in connection with the determination of relative intensities. For these reasons, the values of the first three peaks listed above must be regarded as less reliable. The peaks at 22.0 and 25.6 ev may be identified with secondary maxima observed on the high energy side of the $M_{2,3}$ edge. The 22.0 ev peak also agrees with the characteristic electron loss value of 21.8 ev. The fluctuations in the absorption are superimposed on a background which becomes more transparent with increasing energy. Over the 20–40 ev range the absorption coefficient decreases by a factor of 3.5. This change agrees with previous observations.[1] The present data do not reveal conclusively the onset of transmission at the predicted plasmon energy of 25 ev.

* Supported by the Office of Ordnance Research, U. S. Army.
[1] N. N. Axelrod and M. P. Givens, Phys. Rev. 120, 1205 (1960).

R6. Gas Absorption Cell in the Soft X-Ray Region.* D. L. EDERER, D. J. BAKER, AND D. E. BEDO, *Cornell University.*—For the determination of gas absorption coefficients, it is preferable to confine the gas in a cell, rather than utilize the spectrograph chamber itself. With a cell, higher values of the pressure may be used, the pressure may be controlled reliably and the attenuation can be measured as a function of cell pressure, thus providing an accurate means for evaluating the cross section. Also, the use of a cell minimizes the possibility of contaminating the gas and of disturbing the operation of the source and detector. The cell to be described consists of a 2½ in. long stainless steel chamber with windows (¾ in. in diam) made of two 500 A layers of Zapon backed up by a fine mesh screen (500/in.). Typical windows readily withstand pressure differences of 40 mm of Hg without leaking. At 180 A, each window gives rise to an attenuation of about 10. Preliminary tests have been made with the cell in conjunction with grazing and normal incidence vacuum spectrographs. Instrumental details involving the mounting of the cell and the scheme used for pressure measurements will be presented along with sample measurements of absorption at 180 A utilizing a Be-Cu photomultiplier as a detector.

* Research supported by the Office of Naval Research.

R7. Demountable X-ray Tube for Secondary Excitation of Intense Characteristic Spectra between 1 and 10 A.* ROBERT J. LIEFELD, *Cornell University.*—A 5-kw tube has been constructed to excite x-ray emission spectra by fluorescence for registration with a luminous two-crystal vacuum spectrometer.[1] The tube design features a water-cooled copper anode, two helically wound tungsten ribbon filaments, a beryllium window (1 in. diam×0.002 in. thick), and a continuous evacuation system. Glass-metal construction is used with indium wire gaskets in demountable joints. Efficient irradiation of prospective secondary sources is achieved by the high transmission of the beryllium window, the positioning of secondary sources adjacent to the window, an anode-to-window separation of less than 1 in., and pre-assembly evaporation onto the anode of a material which has several intense lines of slightly higher energy than the level to be excited in the secondary source. The $K\beta_1$ line from chlorine atoms in KCl has been recorded using this tube and quartz crystals having a resolving power of ~10 000. A line peak intensity of 100 counts/sec was obtained against an off-line background of 0.1 counts/sec, with silver on the anode, 20 kv, and 200 ma.

* Supported by the U. S. Air Force.
[1] Prepared by R. Deslattes, to be reported.

R8. The *M* Emission Spectrum of the Transition Metals Zr, Nb, Mo, and Ru. J. E. HOLLIDAY, *United States Steel Corporation.*—The *M* emission spectra of Zr, Nb, Mo, and Ru were first investigated by Siegbahn.[1] We have reinvestigated these spectra using improved detection methods, vacuum and surface preparation. The spectrometer and detector have been described elsewhere.[2] The x-ray chamber was pumped to a vacuum of 8×10^{-6} mm of Hg before the spectrum was recorded. The targets were etched and polished before being placed in the x-ray chamber. They were then cleaned by ion bombardment using argon at a pressure of 5 μ and −400 to −500 v on the target. The $M_{IV,V}$ $N_{II,III}$, M_{III} $M_{IV,V}$, and M_{II} M_{IV}, emission lines and the $M_{IV,V}$ emission bands were investigated. By dipole selection rules the $M_{IV,V}$ emission

band gives a measure of the density of states with p symmetry. The intensity of the $M_{IV,V}$ emission band and the lack of any for the $M_{II,III}$ emission band for Zr, Nb, and Mo indicates that some of the 4d electrons are in a hybridized band with p symmetry. There appears to be a double maximum in the $M_{IV,V}$ emission band. The separation between the two peaks and the band width increases with atomic number.

[1] M. Siegbahn and T. Magusson, Z. Physik **88**, 559 (1934).
[2] J. E. Holliday, Rev. Sci. Instr. **31**, 891 (1960).

R9. On the Dynamics of Spiral Galaxies. HOWARD GREYBER,* *Geophysics Corporation of America.*—Recent radio astronomy research by F. D. Drake[1] at NRAO and F. J. Kerr in Australia has revealed considerable detail on the internal structure of our galaxy. A new theoretical model for the steady state dynamics of a spiral galaxy is described, based on the remarkably small central core observed and on an assumed general dipole magnetic field for the galaxy. The model predicts the very thin galactic gas disk observed and an essentially continuous production of spiral arms. Comparison with other concepts of galactic dynamics will be discussed.

* Present address: Institute of Mathematical Sciences, New York University.
[1] F. D. Drake, 1959 Annual Report, National Radio Astronomy Observatory.

R10. Adiabatic Exponents Associated With Supernova Explosions. A. G. W. CAMERON, *Chalk River Laboratories.*—One cause of supernova explosions is believed to be the onset of hydrostatic instability in massive stars when the temperature and density at the center become large enough. Dyson has shown that this requires the adiabatic exponent $\Gamma_1 = d \log P / d \log \rho$ to be less than $\frac{4}{3}$ throughout an appreciable fraction of the stellar interior. Values of the adiabatic exponent have been calculated for generalized matter consisting of radiation, electrons of both charge, and nuclei in statistical equilibrium. In parts of the star where radiation pressure greatly predominates, $\Gamma_1 < \frac{4}{3}$ at quite low temperatures (5×10^8 °K) owing to the creation of electron pairs. If the radiation and gas pressure are comparable, $\Gamma_1 < \frac{4}{3}$ for $T > 5 \times 10^9$ °K, owing to the endothermic conversion of Fe to He. In an adiabatic compression from this condition, Γ_1 stays less than $\frac{4}{3}$ until the density becomes nearly 10^{12} g/cm^3; here the electron capture rates are fast compared to free fall rates. At this point a great deal of Fe is still present in equilibrium and much of the He has been transformed into nucleons. These calculations support the hypothesis that degenerate neutron stars are formed as remnants of explosions of this kind.

R11. Supernova Instability,* STIRLING A. COLGATE, WILLIAM H. GRASBERGER, AND RICHARD H. WHITE, *Lawrence Radiation Laboratory, Livermore.*—We have been using a Lagrangian hydrodynamics machine code to investigate the conditions immediately prior to and during the unstable collapse of a supernova star. An initial polytropic stellar density-temperature distribution is chosen that is just stable to the collapse from the iron-helium transformation.[1] The lack of perfect initial equilibrium is observed as very weak sound waves oscillating through the star. The programmed removal of a small fraction of the energy content of each mass zone mocks up a quasi-static stellar evolution. Upon reaching instability, the star collapses and dynamically over-shoots its new equilibrium configuration reaching peak densities of 10^{11} g/cc and 7-Mev temperature. In the return to equilibrium a shock wave is propagated radially outwards that ejects a fraction of the mass of the star. We are repeating these calculations including the additional specific heat of relativistic degeneracy and the helium breakup into neutrons and protons as implied by the above density and temperature.

* This work was done under the auspices of the U. S. Atomic Energy Commission.
[1] E. M. Burbidge, G. R. Burbidge, W. A. Fowler, and F. Hoyle, Revs. Modern Phys. **29**, 547 (1957).

Invited Paper

R12. Statistical Theory of Critical Opalescence. M. S. GREEN, *National Bureau of Standards.* (30 min.)

WEDNESDAY AFTERNOON AT 2:00

Continental Room

(L. G. ELLIOTT presiding)

Nuclear Reactions, VI: Heavy-Ion Reactions

RA1. Recoil Method for Measuring Lifetime of Excited States Produced in Heavy Ion Reactions.* I. F. WRIGHT, *University of Wisconsin.*—In this method the recoils are stopped in a plate placed at a distance behind a thin target. Because of the large momentum of the incoming heavy ion and the smaller momentum of the product particles the recoil nuclei all travel forward with velocities that have a small spread about the mean. Since these nuclei are stopped approximately 10^{-12} sec after reaching the plate, essentially all γ rays emitted from states with lifetimes $\sim$ or $> 10^{-11}$ sec are emitted from nuclei recoiling freely or from nuclei at rest. For reactions caused by 40 Mev O^{16} ions incident on light nuclei the energies of these two groups of γ rays differ by $\sim 5\%$ at 0° in the laboratory system. Measurements of γ-ray spectra using a sodium iodide crystal placed at either 0° or 160° show that the numbers in these two groups can be determined from the differences between spectra for different distances between target and stopping plate. Preliminary measurements on a 350 kev γ ray attributed to $B^{10}(O^{16},\alpha p)Ne^{21*}$ show that the lifetime of the first excited state of Ne^{21} (or, possibly, the combined lifetimes of this and higher states producing γ rays in cascade) is $\sim 10^{-11}$ sec.

* Work supported by the U. S. Atomic Energy Commission and the Wisconsin Alumni Research Foundation.

RA2. Elastic Scattering of N^{14} by Mg^{24}. A. ZUCKER, *Oak Ridge National Laboratory.**—The differential cross section for elastic scattering of N^{14} by Mg^{24} at 28.2 Mev (lab) was measured from 30° to 118° c.m. The target was isotopically enriched to 99.7% Mg^{24}, about 45 μg/cm^2 thick, evaporated on a thin carbon film. Elastically scattered nitrogen ions as well as the recoil Mg ions were counted in two Si barrier counters in coincidence to eliminate contributions from transfer reactions and inelastic scattering. The value of σ/σ_c has an initial maximum around 50° c.m., becomes unity at 65°, and decreases monotonically to 0.04 at 118°. The experimental

data fit a Blair model calculation from about 65° to 80° c.m. provided one includes the effect of beam energy spread. A value of $r_0=1.5$ f gives the best agreement with the data. The results of a rainbow model calculation also fit the data well, from 85° to 118° c.m. The pertinent parameters are $\theta_r=87.5°$ and $q=0.168$, leading to a value of $r_0=1.57$ f and a nuclear surface thickness $\Delta R=1.1$ f.

* Operated for the U. S. Atomic Energy Commission by Union Carbide Corporation.

RA3. Alpha Particles from N^{14} Bombardment of O^{16}. M. L. HALBERT, *Oak Ridge National Laboratory.**—The energy spectrum and angular distribution of alpha particles emitted during bombardment of a thin copper oxide target by 28-Mev N^{14} ions has been studied with a silicon surface-barrier counter having a sensitive region 0.6 mm deep at 500 v bias. Spectra were obtained at 12 angles from 0° to 160° and covered a range of alpha energies from 3 Mev to the maximum possible energy (33 Mev for 0°). The proton contamination which was present up to 9 Mev at full bias was eliminated by reducing the barrier depth. The spectra were analyzed in terms of the statistical model; parameters describing the level density will be given. The angular distributions for alphas corresponding to the same excitation energy in the residual nucleus are peaked forward and backward with a minimum at 90°. With the improved resolution now possible the isolated peaks in the forward direction noted earlier on the evaporation continuum were found to have a width of about 0.4 Mev. The true widths are probably much smaller than 0.4 Mev because the energy spread of the incident beam and the target thickness are sufficient to broaden a sharp emission line by this amount. Information on the energy variation of these peaks with angle and bombarding energy will be presented.

* Operated for the U. S. Atomic Energy Commission by Union Carbide Corporation.

RA4. Neutron Transfer Reaction $B^{10}(N^{14},N^{13})B^{11}$. KENNETH S. TOTH, *Oak Ridge National Laboratory.**—The angular distribution of N^{13} particles produced in the reaction $B^{10}\times(N^{14},N^{13})B^{11}$ has been investigated for angles ranging from 4° to 19.5° in the laboratory system with 28-Mev N^{14} ions accelerated in the Oak Ridge 63-in. cyclotron. Circular strips of aluminum foil placed at a known distance from the target and each encompassing a known angular increment were used to stop the radioactive N^{13} (10 min). Range curves for N^{13} particles emitted at various angles were determined and these indicated that most of the N^{13} nuclei originated from transfers leaving both products in their ground states. The differential cross section was found to peak at about 17° c.m. The angular distribution when replotted as $d\sigma/dR_{\min}$ vs $R_{\min}$ (where $R_{\min}$ is the distance of closest approach for a classical trajectory) peaked at an $R_{\min}$ of ~9.2 f corresponding to an r_0 of ~2.0 f.

* Operated for the U. S. Atomic Energy Commission by Union Carbide Corporation.

RA5. Proton Transfer Reaction $B^{10}(N^{14},O^{15})Be^9$. E. NEWMAN, *Oak Ridge National Laboratory.**—The differential cross section for the proton transfer reaction $B^{10}(N^{14},O^{15})Be^9$ has been investigated for the case in which the resulting nuclei are both left in the ground state. The energy of the incident N^{14} was 27.9 Mev and the Q value for the reaction is +0.77 Mev. The angular distributions were followed from 20° to 155° in the center of mass. The cross section was seen to rise to a peak value of approximately 8 mb/sr at ~30° and then to drop monotonically. The total cross section is about 4 mb. A detection system was used in which both the scattered O^{15} and the recoil Be^9 were counted in coincidence by silicon diode barrier detectors.[1] This method together with the reaction kinematics served to suppress the otherwise overwhelming effect of elastic scattering. The observed distribution when plotted as $d\sigma/dR_{\min}$ vs $R_{\min}$ yields a value of 10 f as the most probable separation for transfer, which corresponds to a value of $r_0=2.2$ f. A comparison of the experimental results with tunneling theory is made.

* Operated for the U. S. Atomic Energy Commission by Union Carbide Corporation.
[1] M. L. Halbert and A. Zucker, Phys. Rev. 115, 1635 (1959).

RA6. Alpha Particles Emitted in the Bombardment of Au^{197} and Bi^{209} by C^{12}, N^{14}, and O^{16} Projectiles. I. Direct Processes.* H. C. BRITT AND A. R. QUINTON, *Yale University.*—Angular distributions, energy spectra, and absolute cross sections have been measured for alpha particles emitted in the bombardment of Au^{197} and Bi^{209} by C^{12}, N^{14}, and O^{16} projectiles with energies of 10.5 Mev/nucleon. Measurements have also been made for the C+Bi reaction at energies of 8.7 and 7.1 Mev/nucleon. It was found that from the angular distributions and energy spectra it was possible to separate the contributions from direct and evaporation processes. The direct alpha particles are sharply forward peaked, with broad energy spectra peaked near the beam velocity. No target dependence is observed but the results are dependent on the projectile and its velocity. These data suggest that the principal direct process involved is breakup of the projectile in a nuclear surface interaction. A simple model leads to reasonable values of the most probable interaction distances. The absolute cross sections for direct alpha production at bombarding energies of 10.5 Mev/nucleon are 0.55±0.10 b for the oxygen and nitrogen induced reactions, and 0.85±0.15 b for the carbon induced reactions. The cross section decreases rapidly with decreasing bombarding energy to a value of 0.18±0.05 b for the case of C+Bi at 7.1 Mev/nucleon.

* Work supported by the U. S. Atomic Energy Commission.

RA7. Alpha Particles Emitted in the Bombardment of Au^{197} and Bi^{209} by C^{12}, N^{14}, and O^{16} Projectiles. II. Evaporation Processes.* A. R. QUINTON AND H. C. BRITT, *Yale University.*—From the data taken at backward angles for the reactions described in the previous abstract, energy spectra and absolute cross sections have been determined for alpha particles emitted in evaporation processes. It is found that the ratio of the evaporation cross section to the calculated total reaction cross section[1] is an exponentially increasing function of the initial excitation energy of the compound system. This ratio increases from 0.01 to 0.10 as the excitation energy increases from 50 to 135 Mev. The energy spectra peak at the Coulomb barrier energy is determined from optical model calculations.[2] The shapes of the spectra can be fitted by an expression of the form $\exp(-E_\alpha/T)$ and show that the temperature T is proportional to the square root of the excitation energy of the residual nucleus. Use of the level density formula $\rho(E)\sim\exp 2(aE)^{\frac{1}{2}}$ yields a value for the parameter $a=22\pm2$ Mev^{-1}.

* Work supported by the U. S. Atomic Energy Commission.
[1] T. D. Thomas, Phys. Rev. 116, 703 (1959).
[2] G. Igo, Phys. Rev. 115, 1665 (1959).

RA8. Inelastic Excitations in Heavy Ion Reactions.* D. J. WILLIAMS, A. M. SMITH, G. GARVEY, AND F. E. STEIGERT, *Yale University.*—Inelastic excitations in the reactions (C^{12},C^{12}), (C^{12},O^{16}), (O^{16},O^{16}), (N^{14},C^{12}), (N^{14},N^{14}), and (O^{16},Ar^{40}) have been observed at the Yale University heavy ion accelerator. The incident energy was 10 Mev per nucleon. The angles observed ran from 5° to 12° laboratory. A junction counter was used to provide the energy resolution required. The pulse heights were sorted with a 400 channel analyzer. The angular distributions exhibit the oscillations usually characteristic of diffraction calculations. Some of the excitations appear to be out of phase with the elastic scattering angular distribution in agreement with the rule of even parity transitions being out of phase and odd parity transitions being in phase with the

elastic scattering. These excitations appear to be quite large, approaching the magnitude of the elastic peak around 10° laboratory. Absolute cross sections will be given.

* This work was supported in part by the U. S. Atomic Energy Commission.

RA9. Bombardment of Ar^{40} with 160 Mev O^{16} Ions.* J. G. KELLEY,† A. M. SMITH, F. E. STEIGERT, AND W. W. WATSON, *Yale University.*—A target of Ar^{40} was bombarded with 10-Mev/ArO^{16} ions from the Yale heavy ion accelerator. The elastic scattering cross section was measured as a function of angle from 2° to 18° (laboratory) in 15-min intervals. The use of solid-state detectors permitted separation of the inelastic spectrum from the ground state group. Reaction products were also observed using the apparatus of Anderson *et al.*[1] between the angles of 8° and 77° in approximately 5° intervals. Evidence of both two- and three-body breakup were obtained. Alpha-particle type nuclei would appear to be favored. The carbon and neon yields are greater than those of nitrogen and fluorine, respectively.

* This work was supported in part by the U. S. Atomic Energy Commission.
† Now at Raytheon Company, Wayland, Massachusetts.
[1] C. E. Anderson, A. R. Quinton, and W. J. Knox, Phys. Rev. Letters 3, 557 (1959).

RA10. Resonances in Heavy Ion Inelastic Scattering. E. ALMQVIST AND J. A. KUEHNER, *Chalk River Laboratories.*—The inelastic scattering of heavy ions from light elements is being studied. Events are identified by detecting both the scattered and recoil particles in coincidence using solid state counters. Excitation curves for $C^{12}(C^{12},C^{12})C^{12*}$ (4.43 Mev) between $E_{CM}=8$ to 13 Mev show sharp structure with differential cross sections averaging 1.5 mb/sr at both 90° and 120°; $C^{12}(O^{16},O^{16})C^{12*}$ (4.43) between $E_{CM}=11$ to 15 Mev shows less prominent structure and cross sections rising to 0.7 mb/sr. These magnitudes are similar to those observed by Halbert and Zucker[1] for $C^{12}(N^{14},N^{14})C^{12*}$ (4.43) and much greater than for $C^{12}(N^{14},C^{12})N^{14*}$. This fact may be related to the observation of quasi-molecular states in carbon interactions[2–4] and particularly to the suggestion of Vogt and McManus[5] that easy deformability and excitation of vibrational modes of the incident ions play important roles.

[1] M. L. Halbert and A. Zucker, Phys. Rev. 121, 236 (1961).
[2] D. A. Bromley, J. A. Kuehner, and E. Almqvist, Phys. Rev. Letters 4, 365 (1960).
[3] E. Almqvist, D. A. Bromley, and J. A. Kuehner, Phys. Rev. Letters 4, 515 (1960).
[4] J. A. Kuehner and E. Almqvist, Bull. Am. Phys. Soc. Ser. II, 6,1 (1961).
[5] E. Vogt and H. McManus, Phys. Rev. Letters 4, 535 (1960).

RA11. Heavy Fragment Studies.* D. A. BROMLEY, M. SACHS, AND C. E. ANDERSON,† *Yale University.*—Heavy ion induced reactions on light targets have been shown to be characterized by significant yields of nuclear fragments ranging from isotopes of H and He to masses only slightly less than that of the equivalent compound system.[1] To obtain detailed information on the reaction mechanism involved, an improved higher resolution $dE/dx \times E$ particle identification system has been developed for study of the energy spectra and production cross sections for these fragments. This system is capable of resolving individual isotopes of fragments up to oxygen for independent study. Experiments have been carried out in which the energy spectra for oxygen, nitrogen, carbon, and boron fragments from 168 Mev O^{16} bombardment of Al^{27} and C^{13}, and from 126 Mev C^{12} bombardment of C^{12} have been examined at several angles of observation. In these preliminary measurements no attempt was made to resolve the individual isotopes of a particular element. The spectra obtained show residual fine structure which in some cases may be identified with particular excited levels of the nuclei involved; gross structure effects are also present.

* This work performed under the auspices of the U. S. Atomic Energy Commission.
† Now at the Applied Physics Laboratory, Johns Hopkins University, Baltimore, Maryland.
[1] C. E. Anderson, W. J. J. Knox, A. R. Quinton, and G. E. Bach, Phys. Rev. Letters 3, 557 (1959).

RA12. Charged-Particle Spectra from Heavy-Ion Bombardment.* HARRY H. HECKMAN, DONALD V. REAMES, AND WILLIAM G. SIMON, *Lawrence Radiation Laboratory.*—The energy spectra of charged particles ($Z=1$, 2, and 3) emitted at 0° from targets of Al, Ni, Ag, and Au when bombarded by O^{16} nuclei ($T_{max}=160$ Mev) are under investigation. Light interaction products produced in the targets and emitted in the forward direction enter radially a magnetic field 22 in. in diam. The momentum-analyzed secondary particles are detected by nuclear emulsions placed along the circumference of the magnet. Preliminary analyses of the Au data show that the spectra reach maxima at about $14Z$ Mev and extend to much higher energies. From Au, protons, deuterons, tritons, and α particles in excess of 50 Mev have been detected. Energetic fragments from the interaction of O^{16} ions with Al nuclei are more abundant, and attain higher energies, than those from Au. For example, from Al, p, d, and t have ali been observed with kinetic energies greater than 65 Mev, while He^4 and He^3 in excess of 100 Mev also are produced.

* This work was performed under the auspices of the U. S. Atomic Energy Commission.

RA13. Neutron-Deficient Alpha Emitters of Holmium.* RONALD D. MACFARLANE AND ROGER D. GRIFFIOEN, *Lawrence Radiation Laboratory.*—Bombardment of neodymium isotopes with N^{14} ions (65–130 Mev) using the Berkeley heavy ion accelerator has resulted in the discovery of five new alpha-emitting isotopes of holmium. Their decay characteristics are:

Isotope	E_α (Mev)	Half-life	Alpha branching ratio
Ho^{152}	4.48	31 sec	~0.1
Ho^{150}	4.40	64 sec	~0.1
Ho^{150}	4.34	187 sec	~0.005
Ho^{151}	4.12	5.6 min	0.017
Ho^{155}	3.96	16.5 min	0.0078

Mass assignments were determined by excitation functions using enriched $Nd^{142,4,8}$ targets and in three cases substantiated by identification of alpha-decaying daughters ($Dy^{151,3}$,Tb^{149}). None of these holmium alpha emitters appear to have a hindered alpha decay.

* This work was performed under the auspices of the U. S. Atomic Energy Commission.

RA14. Difference in the Transfer of a Neutron from N^{14} to Pb^{207} and to Pb^{208}.* T. L. WATTS AND J. A. MCINTYRE, *Yale University.*—The N^{13} nuclei created by bombardment of Pb^{207} and Pb^{208} targets by a beam of N^{14} nuclei were detected and their energy spectrum at different scattering angles obtained by means of stacked foils. At a laboratory bombarding energy of about 120 Mev on Pb^{207} and an angle of scatter corresponding to a classical distance of closest approach equal to the sum of the radii of N^{14} and Pb^{207}, the neutron is almost always transferred to the higher levels of the residual Pb^{208}. In a similar bombardment of Pb^{208} the neutron is transferred from the N^{14} to the ground state and excited states of the residual Pb^{209}, the transfer occurring at the same Q values as in the bombardment of Pb^{207}.

* Supported by U. S. Atomic Energy Commission.

WEDNESDAY AFTERNOON AT 2:00

Sheraton Hall

(L. L. FOLDY presiding)

Invited Paper

S1. New Results on the Structure of Nucleons. ROBERT HOFSTADTER, *Stanford University.* (30 min.)

Nucleonic Structure and Scattering

S2. New Information about the Electromagnetic Structure of the Neutron. C. DE VRIES* AND ROBERT HOFSTADTER, *Stanford University,* AND ROBERT HERMAN, *Research Laboratories General Motors Corporation.*—Inelastic electron-deuteron scattering experiments have been made at values of the momentum transfer q, ranging from $q^2=8.5$ f^{-2} to $q^2=21$ f^{-2}. Absolute peak cross sections for the deuteron are obtained by comparison measurements on the proton, employing absolute cross sections for the proton.[1] Meson exchange effects have been neglected. The modified Jankus theory, incorporating the Dirac (F_{1N},F_{1P}) and Pauli (F_{2N},F_{2P}) form factors of the neutron and proton, has been applied. Combining data taken at different energies and angles but at the same q value, absolute values of F_{1N} and F_{2N} are obtained. Inherent in the analysis are four possible choices of these form factors. All choices indicate that the charge distribution of the neutron is not identically zero. The arguments given in the accompanying paper favor one of the four possible cases as the natural choice.

* On leave of absence from Institute of Nuclear Research, Amsterdam, Holland.
[1] F. Bumiller, M. Croissiaux, and R. Hofstadter, Phys. Rev. Letters 5, 261 (1960).

S3. Electromagnetic Form Factors of the Proton and Neutron. ROBERT HERMAN, *Research Laboratories General Motors Corporation,* AND ROBERT HOFSTADTER, *Stanford University.*—The new information on the electromagnetic form factors of the neutron,[1] taken together with the split form factors of the proton[2] form a consistent body of data from which the structure of the proton and neutron can be deduced. Using the idea that the proton and neutron correspond to two orientations of the z component of the isotopic spin of the nucleon we have developed four basic isotopic form factors, namely, F_{1S}, F_{1V}, F_{2S}, and F_{2V}. Taking sums and differences of the basic isotopic form factors one can obtain proton and neutron charge distributions. The latter prove to be consistent with known experimental facts including the rms radii of the two fundamental particles. The neutron appears to have a positive outer fringe of charge. We have developed also the density distributions of the magnetic moments of the proton and neutron, which again are consistent with known experimental facts.

[1] C. De Vries, R. Hofstadter, and Robert Herman (preceding abstract).
[2] R. Hofstadter, F. Bumiller, and M. Croissiaux, Phys. Rev. Letters 5, 263 (1960).

S4. Small Angle Polarizations and Cross Sections at 146 Mev.* D. J. STEINBERG, J. N. PALMIERI, AND A. M. CORMACK, *Harvard University.*—Polarization and cross sections at 146 Mev have been measured in the angular range 2°–11° for beryllium, carbon, and aluminum, and from 3½° to 10° and 3½° to 7° for iron and tantalum, respectively. Careful alignment of the apparatus and continual monitoring of the incident beam position permitted the polarizations to be measured to ±0.01. By utilizing a telescope with angular resolution of ½° full width, and with multiple air scattering, background, and random coincidences experimentally eliminated, the relative cross sections were measured to ±0.7% and the absolute cross sections to ±2%. The polarizations tend smoothly toward zero at the smallest angles, and the values in the interference region are about the same from element to element except for tantalum whose values are approximately half as great. The absolute cross sections for carbon are higher by about 20% than the Harwell results, and are in consequent agreement with the values suggested by Wilson.[1]

* Supported by the joint program of the Office of Naval Research and the U. S. Atomic Energy Commission.
[1] Richard Wilson, Phys. Rev. 114, 260 (1959).

S5. Neutron-Proton Coherent Scattering Amplitude.* L. PASSELL, W. C. DICKINSON, W. BARTOLINI, AND O. HALPERN,† *Lawrence Radiation Laboratory.*—The neutron-proton coherent scattering amplitude has been measured by two independent but related methods. The first method, developed originally by Burgy *et al.*,[1] involves determining the angles which give the same intensity of neutron reflection from a series of four liquid hydrocarbons with hydrogen-to-carbon ratios of 1.4, 1.5, 1.6, and 1.7. This method determines the hydrogen scattering amplitude in terms of the accurately known carbon scattering amplitude and is capable of very high precision. The second method involves comparison of the intensities reflected from water and dodecene ($C_{12}H_{24}$). This gives the hydrogen scattering amplitude in terms of the carbon and oxygen scattering amplitudes. The preliminary result of our first experiment is $a_C/|a_H|=1.773\pm0.005$, compared to 1.753 ± 0.005 obtained previously.[1] Possible explanations for the discrepancy are discussed. When our value is combined with the value for the carbon scattering amplitude $a_C=(6.62\pm0.02)\times10^{-13}$ cm we find for the hydrogen scattering amplitude $a_H=(-3.73\pm0.02)\times10^{-13}$ cm. Assuming $a_O/a_C=0.879\pm0.005$, the second experiment gives $a_C/|a_H|=1.78\pm0.01$, in good agreement with the first result.

* Work done under auspices of the U. S. Atomic Energy Commission.
† Consultant to Lawrence Radiation Laboratory.
[1] M. T. Burgy, G. R. Ringo, and D. J. Hughes, Phys. Rev. 84, 1160 (1951).

S6. *p-n*, *p-p*, and *p-d* Triple Scattering Parameters at 140 Mev: I. Experimental Method.* R. A. HOFFMAN, J. LEFRANÇOIS, E. H. THORNDIKE, AND RICHARD WILSON, *Harvard University.*—A liquid deuterium target is bombarded by a 140-Mev polarized proton beam. Scatterings off the quasi-free neutrons are used to measure the proton-neutron triple scattering parameters, scatterings off the quasi-free protons give the proton-proton parameters, and elastic scatterings off the deuteron give the *p-d* parameters. The polarization of the scattered proton is analyzed by a third scattering on carbon, by previously described techniques.[1] The *p-n* events are identified by detection of the recoil neutron in time coincidence with the triply scattered proton; the *p-p* events are distinguished by detection of a recoil proton; the *p-d* elastic events are separated by energy analysis of the triply scattered proton. The counting arrangement used enables all three measurements to be made concurrently. Results will be presented and experimental errors discussed.

* Supported by the joint program of the Office of Naval Research and the U. S. Atomic Energy Commission.
[1] E. H. Thorndike, J. Lefrançois, and Richard Wilson, Phys. Rev. 120, 1819 (1960).

S7. p-n, p-p, and p-d Triple Scattering Parameters at 140 Mev: II. Analysis of Results. J. LEFRANÇOIS, R. A. HOFFMAN, E. H. THORNDIKE, AND RICHARD WILSON. *Harvard University.*—The p-p and p-n parameters measured using quasi-free target particles are related to those for free p-p and p-n scattering by the spectator model. This model assumes that the incident proton interacts with only one particle in the deuteron, the momentum of the remaining (spectator) particle being unchanged. Theoretical calculations by Everett[1] show that, if the distinction between spectator and struck particle is unambiguous, corrections to this theory are small compared to our experimental errors. The angular and energy distribution predicted by the spectator model have been investigated with a computer program. The variation in momentum of the target particle, subject to the constraints of target and counter size, causes a variation in the correlation angle between the scattered and struck particle in the laboratory system (typically $\pm 5°$), in the incident energy in the system where the target particle is at rest (± 10 Mev), and in the center of mass scattering angle ($\pm 5°$). These three variations are strongly correlated. The p-d elastic triple scattering parameters are analyzed in simple impulse approximation, and related to the free p-n and p-p scattering amplitudes. A comparison will be made of our results with free p-p parameters and with semiphenomenological predictions.

[1] A. Everett, Ph.D. thesis, Harvard University, 1960 (unpublished), and private communication.

WEDNESDAY AFTERNOON AT 2:00

National Bureau of Standards, East Building

(D. W. KERST presiding)

Plasma, I

SA1. Dynamics of Ionized Gases.* THOMAS H. DUPREE, *M.I.T.* (introduced by D. J. Rose).—Ionized gas dynamics is discussed in terms of two coupled equations for the one- and two-particle distribution functions. The equations have been obtained previously by multiple integration of the Liouville equation and a formal expansion in the specific volume. The two-particle equation is solved for a multi-component plasma in terms of two operators which depend on the one-particle functions. It is shown that these operators have a simple interpretation and lend an easy insight into the correlation mechanism. If one neglects the time dependence of the one-particle functions which occur in the operators, then the operators can be obtained explicitly. This procedure is shown to be valid for plasmas with "smooth" velocity distributions and no large inhomogeneities. When velocity instabilities exist, the correlation function is subject to growing oscillation. The ultimate effect of this instability is not clear.

* This work was supported in part by the U. S. Army Signal Corps, the Air Force Office of Scientific Research, and the Office of Naval Research.

SA2. Boltzmann Equation for a Plasma.* ARNOLD H. KRITZ AND DAVID MINTZER, *Yale University.*—A derivation of the Boltzmann equation for a plasma from the BBGKY equation has been considered. It is demonstrated that the internal electric field is due to interactions of uncorrelated electrons; whereas, the collision term represents the effect of velocity correlation of two electrons. If the velocity dependent correlation function is assumed negligible, then $\partial H_0/\partial t = 0$; i.e., the disorder of the plasma is fixed, and the system can not proceed from its initial state to equilibrium. The plasma equilibrium correlation function is derived using the Born and Green method.[1]

* Supported by the Office of Naval Research.
[1] Born and Green, *General Kinetic Theory of Liquids* (Cambridge University Press, New York, 1949).

SA3. H-Theorem and Variational Principles for Plasmas.* JOEL L. LEBOWITZ AND E. MORRIS,† *Yeshiva University.*—The distribution functions $f^i(\mathbf{r},\boldsymbol{\xi})$ of the components of an ionized plasma are generally assumed to obey a Fokker-Planck type equation. This equation like the Boltzmann equation, from which it can be "derived,"[1] is quadratic in the distribution functions. Unlike the Boltzmann equation, however, the distribution functions do not enter symmetrically here and it becomes somewhat complicated to prove the H theorem for these equations. We have carried through the proof and find that the rate of entropy production due to collisions is proportional to $\Sigma \int d\xi \int d\eta \{(\eta-\xi)\times[\nabla \ln f^i(\xi)/m_i - \nabla \ln f^j(\eta)/m_j]\}^2$ which is positive and vanishes only for the case of Maxwellian distributions. The extension of the H theorem for more general equations of this form and the use of some variational principles for obtaining solutions of these equations will also be discussed.

* Supported in part by the Air Force Office of Scientific Research and by the Atomic Energy Commission.
† Now at Aldermaston, England.
[1] H. Grad, NYO-7980, New York University.

SA4. Collision Frequency of a Plasma as a Function of Applied ac Frequency.* S. YOSHIKAWA, *M.I.T.*—The Coulomb collision frequency, ν_c, was calculated by means of the time-dependent Fokker-Planck equation derived from the $6N$-dimensional Liouville equation. The collision frequency was found to depend on the frequency, ω, of the applied external field. The first-order approximation leads to the result previously obtained by Ginsburg[1] in dc external field. The frequency dependence is contained only inside the Coulomb logarithm,[2] Λ, which is replaced by $\Lambda\omega_p/\omega$ whenever ω exceeds the plasma frequency, ω_p. This result can be interpreted as a decrease of the effective radius of the Debye sphere. Before an electron can travel a distance v_0/ω (v_0 = average velocity of the electron) the external field reverses its sign; hence the lesser of v_0/ω and the Debye length v_0/ω_p should enter as the cutoff of the Coulomb interaction. The former becomes shorter, if $\omega > \omega_p$. The result follows.

* This work was supported in part by the U. S. Army Signal Corps, the U. S. Air Force Office of Scientific Research, and the Office of Naval Research.
[1] V. L. Ginsburg, J. Phys. (U.S.S.R.) **8**, 253 (1944).
[2] L. Spitzer, Jr., *Physics of Fully Ionized Gases* (Interscience Publishers, Inc., New York, 1956), p. 73.

SA5. Instability of the Double Sheath.* FRANCIS F. CHEN, *Princeton University.*—Space-charge limited electron emission from an infinite plane immersed in an infinite plasma has been computed for the case λ (ion-neutral mfp) $\gg h$ (Debye length). In contrast to previous work,[1] this problem is independent of the details of creation of the plasma, as long as the plasma

parameters are specified, and contains only the two lengths λ and h. In the case $V \geq kT_e$, where V is the potential difference between plasma and emitter, it is reasonable to assume that the ion flux I_+ to the emitter is $n_0(kT_e/M)^{\frac{1}{2}}$. The solution then becomes very simple, the relation between V and the emitted current, I_e, being given analytically. I_e rises with V but approaches $(M/m)^{\frac{1}{2}}I_+$ asymptotically at high V. Also I_e is proportional to n_0, which means that a hot cathode discharge will be unstable under fluctuations in emission. This may explain low-frequency fluctuations observed in a reflex arc by the author and in mercury discharges by others.[2] This theory also predicts the behavior of an emitting probe in a strong magnetic field.

* Work performed under auspices of U. S. Atomic Energy Commission.
[1] I. Langmuir, Phys. Rev. **33**, 954 (1929).
[2] F. W. Crawford (unpublished).

SA6. Interaction of Relativistic Electron Beams with a Quasi-Neutral Plasma.* N. CHRISTOFILOS, *Lawrence Radiation Laboratory, Livermore.*—The interaction of finite size electron beams with high frequency electromagnetic waves in the presence of a quasineutral plasma has been studied. The effect of the finite beam size, with a smooth variation of the density, is that normal mode solutions satisfying the boundary conditions require that the curl of the electric field is finite throughout the region of the beam, resulting in coupling the unstable longitudinal mode with a stable transverse mode. The dispersion relation is a second order differential equation which has been examined in the two particular cases of a cylindrical beam and a finite slab of streaming electrons. In both cases a Maxwellian transverse velocity distribution is assumed resulting in a self-consistent solution of the density distribution transversely to the stream. The solutions of the equation yield harmonic oscillations which are stable under certain sets of parameters. If the variation of the beam density is neglected the equation assumes the familiar form of the dispersion relation of the two-stream instability. Possible application of this problem in the Astron E layer will be discussed.

* Work performed under the auspices of the U. S. Atomic Energy Commission.

SA7. Thermalization of Fast Ion Groups in a Plasma. HERBERT C. KRANZER, *Adelphi College* (introduced by R. D. Richtmyer).—The process of thermalization of a single fast ion injected into a plasma in equilibrium was studied by Kranzer.[1] The procedure used was numerical integration of the fully linearized Fokker-Planck equation with time-independent coefficients corresponding to an undisturbed plasma. In some proposed thermonuclear reactors, however, a whole group of ions, few in number but high in energy, would be injected. These ions would continuously transfer energy to the plasma during thermalization, significantly altering the coefficients in the Fokker-Planck equation. Accordingly, the computations of Kranzer have been repeated with two modifications. First, the initial ion distribution is taken as Maxwellian rather than as a delta function. Second, the plasma ions and electrons are allowed (separately) to increase in temperature as the injected ions cool down; the total energy of the system remains constant. In general, the mean time of thermalization for a group of fast ions is found to be longer than for a single ion at the same temperature.

[1] H. C. Kranzer, Phys. Fluids **4**, 214 (1961).

SA8. Effect of Collisions on Landau Damping of Plasma Oscillations. PHILIP M. PLATZMAN AND S. J. BUCHSBAUM, *Bell Telephone Laboratories.*—The effect of collisions on the Landau damping of a one-dimensional longitudinal plasma oscillation in the absence of a magnetic field is analyzed. It is found that in a steady state, collisions (no matter how few in number) affect the velocity distribution of the trapped electrons and thus play a major role in determining the Landau damping. We find that when the damping is small ($Imk \ll Rek$), it is reduced from its collisionless value by a factor $\nu^2/(\nu^2+\Omega^2)$ where ν is the electron collision frequency for momentum transfer and $\Omega^2 = zEk/m$ is the frequency of oscillations of a trapped electron in the approximately parabolic potential trough of the wave.

SA9. Magnetic Confinement of a Maxwellian Plasma. GEORGE SCHMIDT,* *Stevens Institute of Technology,* AND DAVID FINKELSTEIN, *Stevens Institute of Technology, New York University, and Yeshiva University.*—Can a "high beta" plasma whose interior is Maxwellian be completely confined by a static magnetic field? Self-consistent solutions are sought for a collisionless stationary Maxwellian plasma occupying a region in space with no internal magnetic field, separated by a boundary layer from a region of uniform magnetic field and vanishing plasma. If particles trapped in the boundary layer are excluded the problem is uniquely determined by the self-consistent equations. It is found that such a solution does exist and the distribution function at any point is a truncated Maxwellian distribution. The addition of trapped particles results in a new class of solutions.

* Supported by the U. S. Atomic Energy Commission.

SA10. Equilibria and Stabilities of Slightly Asymmetric Plasma Columns.* T. OHKAWA† AND D. W. KERST, *General Dynamics Corporation.*—When the equilibria and the stabilities of plasma columns which are cylindrically symmetric and surrounded by conducting walls are considered, the so-called singular surface where $krB_\theta + mB_\theta$ vanishes plays an important role by separating the plasma column into two separate regions. However, if the degeneracy due to the symmetry is removed, the singular surface disappears and the finite number of singular lines which might be called magnetic axes appear. The symmetric equilibria, which could be reached continuously from asymmetric ones by diminishing asymmetric boundary conditions, have the common property that the pressure gradient vanishes on the surface. The behavior of the characteristic differential equations for stability calculations is quite different for these equilibria. Several examples of the equilibria and the stability criteria will be discussed.

* Research on controlled thermonuclear reactions is a joint program carried out by General Atomic and the Texas Atomic Energy Research Foundation.
† On leave from the University of Tokyo.

SA11. Particle Diffusion Across a Magnetic Field. JOSEPH SLEPIAN, *Pittsburgh, Pa.*—Lyman Spitzer, Jr.,[1] is surprised that R. A. Ellis *et al.*[2] experimentally verify the conclusion of my Letter[3] explaining that $\rho\mathbf{v}\cdot\nabla\mathbf{v}$ should not be omitted from the equation for a hot completely ionized plasma within a conducting container which can accept only electrons and an equal charge of positive ions. He cites a number of theoretical references which led him to the opposite belief. The first of these is to J. L. Johnson *et al.*[4] who write for their first equation $\nabla P = \mathbf{j}\times\mathbf{B}$ when it should have been $\rho\mathbf{v}\cdot\nabla\mathbf{v} + \nabla P = \mathbf{j}\times\mathbf{B}$. A second reference is to J. L. Johnson[5] who makes the same mistake again. A third reference is to I. B. Bernstein *et al.*[6] who state that references 4 and 5 are theoretically sound except for certain low-frequency ion waves. The remaining references are not immediately available to me except that one of D. Bohm's which is empirical and contradicts the assumption of $\rho\mathbf{v}\cdot\nabla\mathbf{v}$ being negligible.

[1] L. Spitzer, Jr., Phys. Fluids **3**, 659 (1960).
[2] R. A. Ellis, Jr., L. P. Goldberg, and J. G. Gorman, Phys. Fluids **3**, 468 (1960).
[3] J. Slepian, Phys. Fluids **3**, 490 (1960).
[4] J. L. Johnson, C. R. Oberman, R. M. Kulsrud, and F. A. Frieman, Phys. Fluids **1**, 281 (1958).
[5] J. L. Johnson, Phys. Fluids **3**, 658 (1960).
[6] I. B. Bernstein, E. A. Frieman, R. M. Kulsrud, and M. N. Rosenbluth, Phys. Fluids **3**, 136 (1960).

WEDNESDAY AFTERNOON AT 2:00

Cotillion Room, South

(M. GOLDHABER presiding)

Strange Particles

T1. Charge Exchange Production of Antineutrons and Antineutron Annihilation in Hydrogen.* C. K. HINRICHS, B. J. MOYER, P. M. OGDEN, AND J. A. POIRIER, *Lawrence Radiation Laboratory, Berkeley.*—A separated beam of 1.63 Bev/c antiprotons was directed into the 72-in. hydrogen bubble chamber where three charge exchange reactions were studied: (1) $\bar{p}+p\rightarrow\bar{n}+n$; (2) $\bar{p}+p\rightarrow\bar{n}+n+\pi^0$; (3) $\bar{p}+p\rightarrow\bar{n}+p+\pi^-$. The cross section obtained for (1) plus (2) was 7.9 ± 0.5 mb. That found for (3) was 1.0 ± 0.3 mb implying a similar value for reaction (2). The angular differential cross section for (1) was strongly peaked forward with a value at 0 degrees of 5.5 ± 1.0 mb/sr. However, the 12% contamination from (2) was included. There were antineutrons from (1) and (2) annihilated in the chamber yielding an annihilation cross section of 44.6 ± 5.2 mb. The ratio of the number of annihilations containing five charged pions to those containing three charged pions, and the momentum distribution of the pions have been compared to predictions of the statistical model. This model used the covariant phase space integrals of Srivastava and Sudarshan and the branching ratios given by Pais. Reasonable agreement was obtained for a volume five times that of a sphere with a radius of one pion compton wave length.

* Supported by the U. S. Atomic Energy Commission.

T2. Reaction $\pi^-+p\rightarrow\Lambda+\theta$ From Threshold to 870 Mev.* L. BERTANZA, P. L. CONNOLLY, B. B. CULWICK, F. R. EISLER, T. W. MORRIS, R. B. PALMER, A. G. PRODELL, AND N. P. SAMIOS, *Brookhaven National Laboratory.*—The Brookhaven National Laboratory's 20-in. liquid hydrogen bubble chamber was exposed to negative pion beams of 770-, 790-, 835-, and 870-Mev kinetic energy. 10 000 pictures were taken at 770-Mev kinetic energy and 50 000 pictures at each of the other energies, with approximately 30 tracks per pictures. Thus far we have obtained 200 events at 790 Mev and expect 400 to 500 events at both 835 and 870 Mev. Total and differential cross sections as well as the Λ polarizations will be presented and discussed in the light of the rapid variation of the $\Lambda+\theta$ cross section in this energy interval.

* Work performed under the auspices of the U. S. Atomic Energy Commission.

T3. Production of the $\Lambda\pi$ Resonance by 1.15 Bev/c K^- Mesons.* R. P. ELY, S. Y. FUNG, G. GIDAL, Y. L. PAN, W. M. POWELL, AND H. WHITE, *Lawrence Radiation Laboratory, Berkeley.*—We have studied the reactions $K^-+P\rightarrow\Lambda+\pi^++\pi^-$ and $K^-+N\rightarrow\Lambda^0+\pi^0+\pi^-$ produced by the interactions of 1.15 Bev/c K^- mesons in the Berkeley 30-in. propane bubble chamber, and observe the production of the $\Lambda\pi$ resonance[1] (Y^*) in both the charged and neutral modes. The resonance parameters from a preliminary sample are $E_0=130\pm8$ Mev, $\Gamma=25\pm10$ Mev where E_0 is the peak resonance energy and Γ is the half-width at half-maximum. Results based on 150 events of $K^-+P\rightarrow Y^{*\pm}+\pi^\mp$ and 90 events of $K^-+N\rightarrow Y^{*0}+\pi^0$ will be presented including production cross sections, resonance parameters, and decay angular distributions of the Y^*.

* This work was done under the auspices of the U. S. Atomic Energy Commission.
[1] M. Alston, L. W. Alvarez, P. Eberhard, M. L. Good, W. Graziano, H. K. Ticho, and S. G. Wojcicki, Phys. Rev. Letters 5, 520 (1960

T4. Production of Hyperfragments from K^- Capture in Nuclear Emulsion.* O. SKJEGGESTAD, R. G. AMMAR,† N. CRAYTON, R. LEVI-SETTI AND M. RAYMUND, *University of Chicago,* AND D. ABELEDO AND L. CHOY, *Northwestern University.*—We studied 436 K^--capture stars emitting mesic hyperfragments (*HF*) in an attempt to underatand the mechanism of their production. Of these, 390 were found in a stack of standard *K*5 and *L*4 emulsion (EFINS-NU collaboration[1]), and 46 were in a stack of *K*5 2*X* diluted emulsion. In addition, about 120 K^- stars yielding Li^8 fragments were considered. A separation between captures in light and heavy elements has been achieved making use of the prong-range cutoff arising from the Coulomb barrier of Ag and Br. Lower limits for *HF* emission from light elements are 50, 70, 80, and 80% for $_\Lambda H$, $_\Lambda He$, $_\Lambda Li$, and Li^8. The range distributions on ~60 $_\Lambda Li$ and ~100 Li^8 tracks are indistinguishable. Analogous results are obtained for the range distribution of ~150 $_\Lambda He$ and of ~500 stable prongs of range $<150\,\mu$ (mostly α particles). The *HF* momentum was found to point preferentially opposite to that of the associated π or fast proton. Various hypothesis for the *HF* production mechanism will be discussed.

* Research supported by the U. S. Air Force Office of Scientific Research.
† Now at Northwestern University.
[1] R. G. Ammar, R. Levi-Setti, S. Limentani, P. E. Schlein, W. E. Slater, and P. H. Steinberg. Nuovo cimento 13, 1456 (1959); 15, 181 (1960) and December 15, 1960.

T5. K^+-Proton Interactions Below 100 Mev.* T. STUBBS, S. GOLDHABER, H. BRADNER, W. CHINOWSKY,† G. GOLDHABER, W. LEE, AND T. O'HALLORAN, *Lawrence Radiation Laboratory, Berkeley,* AND W. SLATER, D. STORK, AND H. K. TICHO, *University of California, Los Angeles.*—The LRL 15 in. hydrogen-deuterium bubble chamber was exposed to an electromagnetically separated beam of K^+ mesons at various energies. The experimental arrangement and partial results of this work have been previously reported[1] on K^+ proton scattering in the energy range 5 to 85 Mev. The angular distribution of 700 events analyzed to date is well fitted with pure *S*-wave nuclear scattering and constructive coulomb interference. This verifies the previous result of Kycia *et al.*[2] that the K^+-P potential is repulsive. The total path length of K^+-meson track, as a function of energy, is being evaluated to permit a determination of the total cross-section, which will be reported.

* Work supported in part by the U. S. Atomic Energy Commission.
† On leave from Brookhaven National Laboratory.
[1] Proceedings of the 1960 Annual International Conference of High Energy Physics at Rochester, p. 451.
[2] T. F. Kycia, L. T. Kerth, and R. G. Baender, Phys. Rev. 118, 553 (1960).

T6. (Abstract withdrawn.)

T7. K^- Interactions in Hydrogen at 1.15 Bev/c.* MARGARET ALSTON, L. W. ALVAREZ, P. EBERHARD,† M. L. GOOD,‡ W. GRAZIANO, H. K. TICHO,§ AND S. G. WOJCICKI, *Lawrence Radiation Laboratory, Berkeley.*—The study of K^--p interactions at 1.15 Bev/c in the Berkeley hydrogen bubble chamber has been continued. In addition to the $\Lambda\pi^+\pi^-$ events already published,[1] about 600 other hyperon-production events have been observed. In both $\Sigma^+\pi^-$ and $\Sigma^-\pi^+$ production there is a backward peaking in the angular distribution of the hyperon. From the $\Sigma+2\pi$ production events we find that the branching ratio

$$(Y^*_{I=1} \to \Sigma+\pi)/(Y^*_{I=1} \to \Lambda+\pi)$$

is small and consistent with zero. Total cross sections for all the hyperon-producing channels will be presented.

* Work done under the auspices of the U. S. Atomic Energy Commission.
† Presently at Laboratoire de Physique Atomique, College de France.
‡ Presently at University of Wisconsin.
§ Presently at University of California at Los Angeles.
[1] M. Alston, L. W. Alvarez, P. Eberhard, M. L. Good, W. Graziano, H. K. Ticho, and S. G. Wojcicki, Phys. Rev. Letters **5**, 520 (1960).

T8. Evidence for Low Rates of Electronic Decays of Hyperons.* WILLIAM E. HUMPHREY, JANOS KIRZ, AND ARTHUR H. ROSENFELD, *Lawrence Radiation Laboratory, Berkeley,* AND JACK LEITNER, *Syracuse University.*—We have examined for leptonic decay $\sim$6000 Σ^-, $\sim$2500 Σ^+, and $\sim$1400 Λ particles produced in the Berkeley 15-in. hydrogen bubble chamber by K^- captures.[1] We sought decay tracks with a momentum of $\lesssim$100 Mev/c leaving a Σ, and noncoplanar Λ decays. Thus our efficiency for detecting $\Sigma \to e^-$ is $\sim$1/3 and for $\Lambda \to e^-$ $\sim$80%. No Σ^- nor new $\Lambda \to e$ events have been positively identified. Three Σ^- candidates have been found,[2] one of which had a 50-Mev/c electron leaving the decay vertex. According to the most naive form of the Universal Fermi Interaction,[3] we should have seen $\sim$110 $\Sigma^- \to e^-$ and $\sim$18 $\Lambda \to e^-$. Hence rates of leptonic decays of hyperons seem lower by a little more than an order of magnitude than those predicted. This discrepancy resembles the well-known suppression of K leptonic decays, compared to $\pi \to \mu+\nu$.

* Work sponsored by the U. S. Atomic Energy Commission.
[1] This includes a smaller sample already reported in which one $\Lambda \to e$ was found. See P. Nordin, J. Orear, L. Reed, A. H. Rosenfeld, F. T. Solmitz, H. D. Taft, and R. D. Tripp, Phys. Rev. Letters **1**, 380 (1958); J. Leitner, P. Nordin, A. H. Rosenfeld, F. T. Solmitz, and R. D. Tripp, *ibid.* **3**, 186 (1959).
[2] Some of these are probably not electronic decays. Two decay tracks have not been positively identified as electrons.
[3] R. P. Feynmann and M. Gell-Mann, Phys. Rev. **109**, 193 (1958).

T9. Measurements on Dalitz Pairs Produced in Nuclear Emulsions by 5.4-Bev π^--Mesons and 6.3-Bev Protons. P. L. JAIN AND H. C. GLAHE, *University of Buffalo.*—We have observed about 20 electron-positron pairs from the Dalitz decay mode ($\pi^0 \to \gamma+e^++e^-$) in approximately 3000 stars found by area scanning in Ilford G-5 and K plates which were exposed to 5.4-Bev π^--meson[1] and 6.3-Bev proton beams. The distance s of the origin of the pair from the point of interaction was measured by two different methods and in each case the results were in good agreement. The angular distribution of the opening angles of the $e^\pm$ pairs from the Dalitz decay mode has a peak consistent with that observed in more than 100 $e^\pm$ pairs from the normal decay mode ($\pi^0 \to 2\gamma$). Preliminary results on the lifetime of the π^0 meson estimated from the observed distances, s, will be presented.

[1] We are grateful to Professor J. J. Lord, University of Washington, for the 5.4-Bev π^- developed plates.

T10. Antiproton Annihilation in Deuterium.* W. CHINOWSKY† AND E. SEGRÈ, *University of California, Berkeley.*—The annihilation of antiprotons at rest in deuterium is being studied. With the LRL 15-in. deuterium-filled bubble chamber exposed to a highly separated $\bar{P}$ beam, there resulted one annihilation in $\sim$15 pictures with a background flux of the order of four tracks per picture. A total of 45 000 pictures was obtained and $\sim$15% of these have been scanned to date. Based on the 492 annihilation events in this partial sample, we find a ratio of proton annihilations to neutron annihilations 1.34 ± 0.12. Consider the annihilation on a mixture of equal number of neutrons and protons, neglecting the fact that they are bound in deuterons. Assume also, that the probability of annihilation into a given state of n pions is independent of I spin. Pais[1] has then shown that the ratio of the number of annihilations on protons to the number of annihilations on neutrons should be very close to 1.4. This agrees with observation. If the annihilation occurred only in $I=1$, the ratio would be 1; if in $I=0$, there would be no annihilation on neutrons. The average number of charged prongs in the proton annihilations is 3.09 ± 0.08; in the neutron annihilations it is 3.09 ± 0.09. Only 3 K_1^0 decays have been observed, implying a K-meson production in these stars of the order of 2%.

* Supported by the U. S. Atomic Energy Commission.
† On leave from Brookhaven National Laboratory.
[1] A. Pais, Ann. of Phys. **9**, 548 (1960).

T11. Sign of the Nuclear Potential for Σ Hyperons.* H. E. FISK AND D. J. PROWSE, *University of California at Los Angeles.*—Search has been continued for elastic collisions of Σ^+ and Σ^- hyperons with bound emulsion nucleons. Together with other data available on this process, the results obtained have been analyzed on the basis of a very simple model designed to give the sign of the nuclear potential which the Σ hyperons experience in the nucleus. Indications from this analysis are that the potential is attractive, in agreement with previous results[1] from other types of experiments.

* Supported in part by the U. S. Atomic Energy Commission.
[1] For instance: I. E. McCarthy and D. J. Prowse, Nuclear Phys. **17**, 96 (1960).

WEDNESDAY AFTERNOON AT 2:00

Cotillion Room, North

(J. W. MITCHELL presiding)

General Solid-State Physics, II

TA1. Structure Constants for a Cubic Crystal.* HERBERT KURSS, *Polytechnic Institute of Brooklyn.*—In the cavity approach of Kohn-Rostoker-Korringa for computing the band structure of a cubic crystal of spherically symmetric scatterers a key item is the calculation of certain lattice sums which are referred to as structure constants. Formulas for the evaluation

of these lattice sums are derived by judicious applications of the Poisson transform. This Poisson transform approach provides a useful alternative to the Laplace transform approach of P. P. Ewald.

* This work was supported by the U. S. Signal Corps.

TA2. Analysis of Crystal Faceting as a Linear Programming Problem. W. W. MULLINS AND R. F. SEKERKA.—The determination of the minimum free energy that an infinite planar surface can achieve by faceting (breaking up into orientations other than the one originally present) is formulated as a linear programming (LP) problem. By appealing to the dual theorem of the LP theory, the minimum is found in terms of a construction carried out on the Gibbs-Wulff equilibrium form. The construction also gives the orientations present on the faceted surface. A Γ plot is constructed, representing the minimum energy attainable by faceting as a function of orientation. Certain previous results due to Herring are reinterpreted by comparing the Γ plot with the ordinary polar plot of free energy (γ plot).

TA3. Band Structure of Solid Argon.* ROBERT S. KNOX, *University of Rochester*, AND FRANCO BASSANI, *Argonne National Laboratory*.—The OPW method, as modified by Bassani and Celli,[1] has been used to compute the lowest-lying conduction states in (fcc) solid argon at the symmetry points Γ, X, L, and K. The $3s$ and $3p$ valence bands have been treated by simple tight binding theory. The potential consists of a sum of effective atomic potentials, where a free electron-like expression is used for the exchange contribution.[2] The lowest conduction state appears to be Γ_1, lying 12.4 ev above the highest valence state (Γ_{15}). The reliability of the potential used will be discussed, and the results of the computation will be compared with present experimental and theoretical knowledge of the electronic structure of the solid rare gases.

* Based on work performed under the auspices of the U. S. Atomic Energy Commission and supported in part by the U. S. Air Force Office of Scientific Research.
[1] F. Bassani and V. Celli, J. Phys. Chem. Solids (to be published).
[2] R. Casella, Phys. Rev. **104**, 1260 (1956); J. C. Slater, Phys. Rev. **81**, 385 (1951).

TA4. High-Temperature Limits and Temperature Dependence of the Debye Characteristic Temperatures for the Thermodynamic Functions of a Solid.* MARIO TOSI AND FAUSTO FUMI,† *Argonne National Laboratory*.—The well-known Thirring expansions for the thermal and vibrational energy of a nonmetal, and the Thirring-like expansion for its entropy, provide a direct analytical proof for the explicit temperature dependence of the Debye characteristic temperature appropriate to a given thermodynamic function in the temperature range of validity of these expansions ($T>80$°K for a solid with a maximum vibrational frequency of 10^{13} sec^{-1}), and they demonstrate the difference between the Debye characteristic temperatures for the entropy, the heat capacity, and the thermal energy at high temperatures. The explicit temperature dependence of the Debye characteristic temperature for a given thermodynamic function can be established analytically also at low temperatures, where only long-wave acoustic modes are thermally excited.

* Based on work performed under the auspices of the U. S. Atomic Energy Commission.
† On leave of absence from the University of Pavia, Italy.

TA5. On the Hildebrand and Mie-Grüneisen Approximations to the Equation of State of Cubic Solids.* FAUSTO FUMI† AND MARIO TOSI, *Argonne National Laboratory*.—An analysis is made of the conditions under which the equation of state of a cubic nonmetal under hydrostatic pressure reduces to the forms given by the Hildebrand or Mie-Grüneisen approximations, which are commonly used to investigate the volume dependence of the lattice energy with the help of empirical data. The analysis is based upon the restrictions that the validity of these approximations imposes on the dependence of the thermodynamic functions of the solid on its temperature and volume, and consists of a search for temperature ranges where these restrictions are satisfied in the quasi-harmonic approximation. The analysis shows, in particular, that at moderate temperatures above the Debye characteristic temperature for the heat capacity at high temperatures, the equation of state has the form given by the Hildebrand approximation for the vibrational energy, while in the low temperature T^3 region of the heat capacity it has the form given by the thermal formulation of the Mie-Grüneisen approximation.

* Based on work performed under the auspices of the U. S. Atomic Energy Commission.
† On leave of absence from the University of Pavia, Italy.

TA6. Approximation Functions for the Frequency Distribution and Specific Heat of Lattice Vibrations.* R. A. SACK,† *University of Chicago* (introduced by C. C. J. Roothaan).—In a three-dimensional lattice the distribution of vibrational frequencies ω as a function of $X=(\omega/\omega_L)^2$, where ω_L is the upper limit of the spectrum, can be expressed as $(X-X^2)^{\frac{1}{2}}\varphi(X)$ where $\varphi(X)$ is regular at both limits. Any expression of $\varphi(X)$ is best carried out in terms of Chebyshev polynomials, S_n. The dependence of the specific heat C_v on temperature corresponding to S_n has been tabulated for n up to 7. The higher terms contribute little to C_v at high or moderate temperatures; at low temperatures power series are most appropriate. The coefficients of the Chebyshev expansion are easily calculated from either theoretically computed moments or from measured values of C_v.

* Work assisted in part by the Wright Patterson Air Force Base Dayton, Ohio, and in part by a grant from the National Science Foundation.
† Permanent address: Royal Technical College, Salford, England.

TA7. Theory on Lattice Thermal Conductivity. JOHN H. HENKEL, *University of Georgia*.—Lattice thermal conduction is explained first, using a linear chain of identical atoms in which each atom moves about its mean position in a potential field because of all the atoms at rest in their mean positions. Thermal conduction is introduced using perturbing second degree potentials (not third degree). This model leads to the results that thermal conduction is proportional to the first power of the inverse temperature for relatively high temperatures and decreases exponentially for low temperatures. The extension to a three-dimensional lattice is easily made and quantitative results are easily obtained. This model is an Einstein type model and is useful only at relatively high temperatures. A Debye type model is then introduced.

TA8. Classical Scattering by Repulsive Potentials and Irradiation Effects in Solids.* E. M. BARODY, *Battelle Memorial Institute*.—Earlier approximations[1] are extended with greater emphasis on analytic methods. Certain cross sections for scattering by a repulsive interatomic potential $V(r)$ are expressed in terms of the distance of closest approach in a head-on collision c and $\gamma=-(d\ln V/d\ln r)_c$. The differential cross section for 180° scattering is $\sigma(\pi)=(c/2I_0)^2$, where I_0 is an integral determined by $V(r)$ and c. For a simple exponential potential and large γ, $I_0=1+(\ln 4)/\gamma-1.368/\gamma^2+3.41/\gamma^3+\cdots$. The focusing parameter for collisions in a linear chain of identical atoms with separation S is $\Lambda=(\theta_{i+1}/\theta_i)=(SI_0/c)-1$. Application to the ⟨110⟩ chains in copper gives slightly *less* focusing than found in machine calculations[2] on a three-dimensional model. The difference may arise from the effect of neighboring chains.

* Supported by the Aeronautical Research Laboratories, Wright Air Development Division.
[1] E. M. Baroody, Bull. Am. Phys. Soc. **5**, 340 (1960).
[2] J. B. Gibson, A. N. Goland, M. Milgram, and G. H. Vineyard, Phys. Rev. **120**, 1229 (1960).

TA9. Activation Energies of Monocrystalline Boron.* R. A. BRUNGS AND V. P. JACOBSMEYER, *Saint Louis University.*—The thermal and optical activation energies were measured for five samples of the β-rhombohedral polymorph of boron.[1] Three samples were monocrystalline, one a double crystal, and the last was nearly polycrystalline. The dimensions of the samples were approximately 4×1×0.8 mm, with a density of 2.33 g/cm³. The activation energies are:

Crystal direction	Thermal band gap (ev)	Optical band (ev)
[010]	1.27±0.03	1.35±0.08
[101]	1.28±0.03	1.33±0.05
parallel to (101)	1.35±0.03	1.32±0.05

The optical band gap of the nearly polycrystalline sample was found to be 1.53±0.06 ev. These measurements will be compared with previous experimental results.

* Supported in part by Office of Ordnance Research.
[1] The bulk boron was obtained from U. S. Army Signal Rseearch and Development Laboratory, Fort Monmouth, New Jersey.

TA10. Resistance of Shocked Solids and Deduction of Shock Temperatures.* BERNIE ALDER AND RICHARD GROVER, *Lawrence Radiation Laboratory, Livermore.*—Methods have been developed to measure the resistivity of a material at a given shock pressure and several temperatures by a variation of the initial temperature. If a minimum of three initial temperatures are used, it is then possible from the resistivity data to deduce approximately the energy gap and the temperature at the given condition. Application to iodine has shown the energy gap is consistent with static measurements and that the temperature is also consistent with the value calculated from Hugoniot data by means of Gruneisen theory. However, in order to test such a theory critically, more extensive data is required to determine the temperature accurately.

* Supported by the U. S. Atomic Energy Commission.

TA11. Some Measured Properties of a Dynamic Hard Sphere Model. GEORGE H. GILMER, *University of Virginia,* AND DAVID TURNBULL, *General Electric Research Laboratory.*—Methods have been developed for measuring the "pressure" and some other properties of the two-dimensional dynamic hard sphere model described by Turnbull and Cormia.[1] The pressure, velocity distribution, radial distribution function, and self diffusion coefficient have been measured as functions of density, using polyethylene spheres. Where comparison is possible the results are in good agreement with the results of the Monte Carlo calculations for a hard sphere system. The model exhibits a first order fluid → crystal transition. The self-diffusion coefficient in the fluid is in fair agreement with the Longuet-Higgins-Pople relation at intermediate densities but falls considerably below this relation at the highest densities.

[1] D. Turnbull and R. L. Cormia, J. Appl. Phys. 31, 674 (1960).

TA12. Carrier Concentration Variation in Organic Solids. HERBERT METTE AND WAYNE R. WENGER, *U. S. Army Signal Laboratory.*—A ferrocene derivative has been discovered which permits the arbitrary variation of the number of conduction carriers by orders of magnitude by means of "controlled" partial polymerization. This material may serve as a model substance for investigating the conduction mechanism and sources of electrons in organic and metallo-organic solids. Analogous to the behavior of inorganic semiconductors with increasing doping, the $\log\rho$ vs $1/T$ curves are broken lines with activation energies of 2.1 ev, corresponding to the pure, and 0.6 ev, corresponding to the polymerized material, with the break shifting to higher temperatures with increasing polymerization. The resistivities were between 10^6 and 10^{13} ohm cm. Assuming an equal order of magnitude for all mobilities, the curves indicate that an increase of 0.6-ev carriers at each temperature is accompanied by a corresponding decrease in the concentration of 2.1-ev carriers. As a result of these findings and the infrared studies, it is tentatively concluded that the source of free carriers is identical with or related to those bonds that polymerize first. The material studied was polycrystalline 1.1′-dibenzoyl ferrocene which is very stable and slightly volatile up to its melting point of 102°C.

TA13. Comparison of Shear Coefficients with Single Relaxation Theory for Diphenyl Hexachloride. D. O. MILES, *Lockheed Missiles and Space Division.*—A pure sinusoidal shear is applied to a sample of diphenyl hexachloride at several temperatures in the frequency range 10–10³ cps. The shear rigidity and shear viscosity are obtained as functions of frequency at each temperature. Comparison at low frequencies with static measurements by others is within experimental error. The experimental data are fitted with excellent agreement to single relaxation theory. The significance of this agreement is discussed in light of evidence that compressional effects in the same liquid occur over a distribution of relaxation times. Although a difference in the distribution functions of relaxation times for shear and compressional processes has been previously observed by ultrasonic measurements in some liquids, no theoretical explanation has appeared. An attempt is made to explain the difference in distribution functions using the Debye-Frenkel rearrangement theory. The theory leads us to conclude that diphenyl hexachloride, as other liquids, has a distribution of relaxation times for shear as well as for compressional processes, but the distribution for shear is too narrow to detect experimentally. The temperature dependence of the high frequency shear rigidity is also obtained, and the expected plateau is observed at the glass transition.

WEDNESDAY AFTERNOON AT 2:00

Burgundy Room

(C. W. UFFORD presiding)

Theory, V; Nuclear Reactions

TB1. Interaction Moments in the Light Nuclei. CARL WERNTZ, *University of Wisconsin.*—The phenomenological interaction moment operators of Austern and Sachs[1] have been used to calculate corrections to cross sections for mangetic dipole capture of thermal neutrons by the proton, the dueteron, and He^3. It has been found that these interaction moment operators yield a consistent explanation of the three capture cross sections as well as the deuteron and triton magnetic moments if (a) D-state probabilities ~4% are taken for the ground states of H^2, H^3, He^3, and He^4, and (b) spin-orbit forces are taken to be negligible.

[1] N. Austern and R. G. Sachs, Phys. Rev. 82, 710 (1951).

TB2. Calculation of Inelastic Neutron Scattering from Zirconium-90 and Niobium-93. D. T. GOLDMAN, *Knolls Atomic Power Laboratory.**—The Hauser-Feshbach theory for

the inelastic scattering of neutrons has been generalized to include spin-orbit penetrabilities. Formulas for the total and differential scattering cross sections will be presented. The extended theory has been used to calculate the cross section for the sacttering of neutrons from Zr^{90} and Nb^{93}. The penetrabilities, T_l^j were calculated from an optical potential whose parameters were chosen so that the total and elastic cross sections were given correctly. The differential cross section and strength functions were also examined. The sensitivity of the calculated quantities to variations of the parameters has been investigated. The calculated cross section for the neutron excitation of Zr^{90} as function of energy has been compared with available experimental data. In the absence of complete data on branching ratios, no exact comparison can be made but general agreement between calculated and experimental values has been noted in the energy range of 2.8–3.7 Mev, and poorer agreement for a neutron energy of less than 2.8 Mev. The Nb^{93} results were in good agreement with experimental values up to an incident energy of 1.25 Mev, the limit of the available data. It was possible to discern a difference in calculated results depending upon the choice of spins and parities.

* Operated by the General Electric Company for the U. S. Atomic Energy Commission.

TB3. Elastic and Inelastic Scattering of Neutrons by Al^{27}. C. R. LUBITZ AND D. T. GOLDMAN, *Knolls Atomic Power Laboratory.**—Calculations similar to those of the preceding abstract[1] have been carried out for Al^{27}. With optical potential parameters that fit the elastic scattering and total cross sections at various energies, it is possible to fit the 4.4 Mev (n,n') data of Weddell[2] for the 0.84, 1.01, 2.21, 2.98, and 3.00 Mev levels, using the spin assignments suggested by the rotational collective model.[3] The only discrepancy is a predicted strong excitation of the (assumed) $\frac{5}{2}+$ level at 2.73 Mev, contrary to the low experimental cross section. This may represent a class of transitions $(j_i=j_f)$ for which the statistical theory (Hauser-Feshbach) characteristically overestimates transitions rates, probably due to its neglect of all quantum numbers (selection rules) but spin and parity.

* Operated by the General Electric Company for the U. S. Atomic Energy Commission.
[1] D. T. Goldman (preceding abstract).
[2] J. B. Weddell, Phys. Rev. **104**, 1069 (1956).
[3] Almqvist, Bromley, Gove and Litherland, Nuclear Phys. **19**, 1 (1960).

TB4. Effects of Angular Momentum in Compound Nucleus Reactions.* T. DARRAH THOMAS, *Brookhaven National Laboratory.*—The statistical theory of nuclear reactions is used to calculate the rate with which a nucleus with excitation energy E_i and angular momentum J will emit a neutron, proton, or alpha particle to leave a residual nucleus with excitation energy E_f and angular momentum j. Two different approximations to the density of states are considered: $\omega=C\exp[2(aE)^{\frac{1}{2}}]$ and $\omega=C'\exp(E/T)$, where C, C', T, and a are constants and E is the excitation energy. For large moments of inertia and $\omega=C\exp[2(aE)^{\frac{1}{2}}]$, Γ, the width for particle emission, and ϵ, the average kinetic energy of the emitted particle, both decrease with increasing J. The lower the initial excitation, the more pronounced the effect. For small moments of inertia or $\omega=C'\exp(E/T)$, both Γ and ϵ increase with J. The average value of the spin change, $j-J$, depends only slightly on which state density expression is assumed, but strongly on the moment of inertia. Approximate expressions are presented for the variation with J of Γ and $\bar{\epsilon}$. There are two principal effects of angular momentum on the competition between different kinds of particles. To first order, high angular momentum favors the emission of the particle that carries off the least energy. To second order, it favors the particle that carries off the most angular momentum.

* Research performed under the auspices of the U. S. Atomic Energy Commission.

TB5. The Spin-Orbit Interaction in Deuteron Stripping.* W. TOBOCMAN,† *Case Institute of Technology,* AND W. R. GIBBS, *Rice University.*—Calculations have been carried out using spin-orbit optical model wave functions in the distorted wave Born approximation. A sizeable polarization is predicted for the case of the neutron being captured with zero angular momentum. The dependence of the polarization and cross section on the proton and deuteron spin-orbit interaction is also examined. It is seen that polarizations as large as those observed[1] may easily be obtained with the assumption of a spin-orbit potential.

* Supported in part by the National Science Foundation.
† On leave of absence from Rice University.
[1] J. C. Hensel and W. C. Parkinson, Phys. Rev. **110**, 128 (1958).

TB6. Two-Particle Stripping Calculations.* D. E. BILHORN, *Rice University,* AND W. TOBOCMAN,† *Case Institute of Technology.*—The usual plane wave Born approximation treatments of the two-nucleon stripping reaction assume that the (three or four) nucleons in the incident particle are all in a relative s state. We know that this is not realistic. By generalizing the theory[1] we may use a more realistic wave function for the incident particle and study the effects on the angular distribution of the emergent particle. We present expressions for the (He^3,p) and (t,p) reactions leading to final nuclei in which the two captured particles are in the p shell. Comparison with experiments will be discussed.

* Supported by the National Science Foundation.
† On leave of absence from Rice University.
[1] W. Tobocman (to be published).

TB7. Mechanism for the $He^3(d,\gamma)Li^5$ Reaction.* T. A. TOMBRELLO AND G. C. PHILLIPS, *Rice University.*—A simple rearrangement calculation is made for the capture reaction $He^3(d,\gamma)Li^5$. The mechanism proposed is that of a resonant E-1 capture process proceeding through the $S_{\frac{1}{2}}$ partial wave and a strong nonresonant E-1 capture proceeding through the $S_{\frac{3}{2}}$ partial wave. The sum of these two contributions yields an excitation curve that is compared with the experimental results of Blair *et al.*[1] A further result of this calculation is the energy distribution of protons coming from the break-up of the $P_{\frac{3}{2}}$ state of Li^5 that is formed by this capture reaction.

* Supported in part by the U. S. Atomic Energy Commission.
[1] J. M. Blair, N. M. Hintz, and D. M. Van Patter, Phys. Rev. **96**, 1023 (1954).

TB8. Elastic Scattering by Bound Nuclei. G. T. TRAMMELL, *Oak Ridge National Laboratory.*—A slightly modified formula of Lamb[1] gives the elastic scattering amplitude for the resonant scattering of a particle by a nucleus which is bound in a crystal. The effect of the binding is represented by the factor $\langle\chi_{n0}|\exp[-i(\mathbf{k}_f-\mathbf{k}_0)\cdot\mathbf{r}]|\chi_{n0}\rangle$ if the level width is much larger than a mean intermediate energy transfer to the crystal (the nucleus doesn't move much during collision), and by $\langle\chi_{n0}|\exp(-i\mathbf{k}_f\cdot\mathbf{r})|\chi_{n0}\rangle\langle\chi_{n0}|\exp(+i\mathbf{k}_0\cdot\mathbf{r})|\chi_{n0}\rangle$ in the opposite extreme (Mössbauer) (the nucleus executes several oscillations during the collision) χ_{n0} is the initial (and the final) crystal wave function, $\mathbf{r}$ the nuclear position, $\mathbf{k}_0$ and $\mathbf{k}_f$ the initial and final wave vectors. Resonant scattering of slow neutrons usually represents a case intermediate between the extremes and will be discussed. A generalization of Lamb's formula for slow neutrons is derived:

$$f=(M+m)M^{-1}\sum_n a(k_n')\langle\chi_{n0}|\exp(-i\mathbf{k}_f\cdot\mathbf{r})|\varphi_n\rangle \times\langle\varphi_n|\exp(i\mathbf{k}_0\cdot\mathbf{r})|\chi_{n0}\rangle.$$

Where the φ_n are crystal wave functions with the nuclear mass increased to $M+m$, $a(k_n')$ is the free particles scattering length for c.m. energy $k_0^2(2m)^{-1}-\epsilon_n'+\epsilon_{n0}$. This leads to the Fermi

result for potential scattering and the Lamb result for the resonance scattering.

[1] W. E. Lamb, Phys. Rev. 55, 190 (1939).

TB9. Alpha-Deuteron Model of the Li^6 Nucleus and the $Be^9(Li^6,\alpha)$ B^{11} Reaction. M. L. RUSTGI,* *National Research Council, Ottawa.*—A calculation of the angular distribution of the particles emitted in the $Be^9(Li^6,\alpha)B^{11}$ reaction is made on the assumption that it is a stripping reaction. An alpha-deuteron model of the Li^6 nucleus is assumed. Moreover, the Coulomb effects of the interacting particles are neglected and the nuclear interaction between the outgoing particles is not taken into account. Comparison between the derived formula and the experimental data of Leigh and Blair[1] on the differential cross section for the $Be^9(Li^6,\alpha)B^{11}$ reaction will be presented.

* National Research Council Postdoctorate Fellow, 1960–1961.
[1] J. J. Leigh and J. M. Blair, Phys. Rev. 121, 246 (1961).

TB10. Forces between Two Nuclei.* HUBERT REEVES, *Université de Montréal.*—The experimental reaction cross sections for collisions between various "heavy ions" (C^{12}, N^{14}, O^{16}, F^{19}) has been analyzed. Far enough above the Coulomb barrier the asymptotic formula $\sigma = R^2$ yields interaction radii (R) roughly equal to the sum of the radii of the colliding nuclei. However, in the region below the Coublomb barrier the cross sections in all cases fall much too rapidly to be accounted for in terms of purely attractive (Wood-Saxon type) complex potentials. To match the experimental results one has to decrease progressively the interaction radii to almost unrealistic values, no matter what values were given to the other usual parameters. An analysis of these numerical results indicates that the inclusion of a repulsive core, followed by an attractive shell would get rid of such difficulties. It has already been pointed out[1] that the rearrangement of nucleonic orbits which would accompany such a reaction might well give rise to a repulsive force, as in, the case of molecules.

* Work performed under the auspices of the Atomic Energy of Canada, Chalk River, Ontario.
[1] R. E. Peierls, at the Kingston meeting.

TB11. Elastic Scattering of Heavy Nuclei.* J. S. MCINTOSH, S. C. PARK, AND G. H. RAWITSCHER, *Yale University.*—Attempts to calculate the small angle elastic scattering of heavy nuclei by heavy nuclei at low energies, previously reported[1] for N^{14} on N^{14}, have been extended to the case of $O^{16}-C^{12}$ and $N^{14}-C^{12}$. As suggested by G. Breit, a potential energy derived from the known nucleon-nucleus scattering is employed for large internuclear distances. Absorption renders the scattering rather insensitive to the exact form of interaction energy assumed for small internuclear distances. Good agreement with the experimental results of Bromley *et al.*[2] for $O^{16}-C^{12}$ at $E_{c.m.}=11.57$ Mev in the angular range θ_{cm} up to 70° can be obtained, and the assumptions involved will be discussed. As a result, inferences on the single nucleon reduced width can be made.

* Supported by the U. S. Atomic Energy Commission and by the Office of Ordnance Research, U. S. Army.
[1] J. S. McIntosh, S. C. Park, and G. H. Rawitscher, *Reactions between Complex Nuclei*, edited by A. Zucker, E. C. Halbert, and F. T. Howard (John Wiley & Sons, Inc., New York, 1960), p. 127.
[2] D. A. Bromley, J. A. Kuehner, and E. Almqvist, reference 1, p. 151.

TB12. Tests of Accuracy of Nucleon Transfer Calculations.* Y. NISHIDA AND G. H. HERLING, *Yale University.*—The one-dimensional model of the nucleon transfer mechanism for which exact solutions are possible[1] has been used to estimate the accuracy of tunneling calculations employing the "energy matrix" approximation.[2] Since a translation of the three-dimensional case with small accelerations to the one-dimensional model with sudden reversal of motion is not possible, alternative parametrizations have been used and a partial analysis of differences in results of various calculations has been made. Classical mechanics is used for the motion of heavy aggregates. If the transition probability is kept the same by adjusting the distance of closest approach, the ratio of the exact to the energy matrix value in the asymmetric model for $N^{14}(N^{14},N^{13})N^{15}$ is ~0.87 at 15 Mev incident energy. Other reactions and conditions of comparison will be discussed.

* Supported by U. S. Atomic Energy Commission and by the Office of Ordnance Research, U. S. Army.
[1] G. Breit, *Reactions between Complex Nuclei*, edited by A. Zucker, E. C. Halbert, and F. T. Howard (John Wiley & Sons, Inc., New York, 1960), paper A-1.
[2] G. Breit and M. E. Ebel, Phys. Rev. 103, 679 (1956); G. Breit, "Theory of resonance reactions and allied topics," in *Handbuch der Physik* (Springer-Verlag, Berlin, 1959), Vol. 41, esp. pp. 375–378.

TB13. Effective Interaction in Direct Reactions. N. C. FRANCIS, D. T. GOLDMAN, AND C. R. LUBITZ, *Knolls Atomic Power Laboratory.**—Although many nuclear reactions require direct interaction for their explanation, the theory is not developed sufficiently to permit unique calculations. The distorted wave Born approximation has been used with surface, finite, and zero range interactions. For reactions in the nuclear surface, many body aspects of the problem are absent and approximate quantitative features of the effective interaction can be discussed. We assume: (1) Nucleons other than the colliding pair may be neglected during the collision. (2) A variational method with bound state trial functions can be used to estimate the dependence of the t matrix on the energy and relative momenta, initial and final, of a pair of nucleons. When the target nucleon has a binding energy of about 7 Mev and the incident nucleon has low energy (about 1 Mev), a zero range effective interaction may be used. We also include velocity dependent corrections to this δ-function interaction. When the incident energy is increased to 7 Mev, and the interacting pair are neutrons, the effective interaction is strong and nonlocal with a large effective radius of interaction.

* Operated by the General Electric Company for the U. S. Atomic Energy Commission.

WEDNESDAY EVENING AT 7:00

Sheraton-Park Hotel

(FREDERICK SEITZ presiding)

Banquet of The American Physical Society

After-dinner talk: **Some Thoughts on Atomic-Energy Research.** G. T. SEABORG, *Chairman, U. S. Atomic Energy Commission.*

THURSDAY MORNING AT 9:30

Cotillion Room, South

(P. KUSCH presiding)

General Physics; Masers

U1. Determination of Focusing Properties of Solar Collectors by an Integral Formula. PAUL MAZUR, *Avco.*—An analytical procedure has been derived for determining the distribution of energy at the focal plane of a mirror such as is used in a solar collector system. The method is a general one that permits any shape of emitting and reflecting surfaces, and is an analytical equivalent of the conventional ray-tracing procedure of geometrical optics. The advantage provided is that the calculation of intensity of collected radiation at a given point can be performed on a digital computer in less than a minute whereas one man-week is required for graphical ray-tracing. The solution takes the form of an exact double integral which gives directly the irradiance by reflection at any given point for an arbitrary Lambert surface emitting at least partially to an arbitrary reflecting surface. The double integral has been programmed on a digital computer to evaluate the performance of solar collectors. Reflected energy distributions will be presented for various distorted collectors.

U2. Spherical Analogues of the Gaussian. ERNST BREITENBERGER, *University of South Carolina.*—The plane gaussian probability distribution arises as the unique solution in a variety of problems. When the analogous problems are formulated on the sphere, however, hteir solutions become quite different. Thus, a gaussian population is the only one in the plane for which the center of mass of a sample, and hence the center of least (polar) moment of inertia, yields a maximum likelihood estimate of location. On the sphere, in sharp contrast, use of the center of mass leads to the distribution $\exp\{\kappa\cos\theta\}$, use of the moment of inertia to $\exp\{-\frac{1}{2}\kappa\sin^2\theta \times[1+2\sin^2(\phi-\mu)]\}$, where κ, λ, and μ are free parameters. Both these distributions reduce to plane gaussians when κ is large and positive, but the second one appears as a closer analog because it contains the three parameters which one should expect rather than a single one; it may find its practical uses in research on rock magnetism where the simple $\exp\{\kappa\cos\theta\}$ is not always adequate.

U3. Ripples and Waves on Deep Water. R. D. EDGE, *University of South Carolina.*—The profile, particle motion, velocity, and viscous decay of ripples and waves of short wavelength have been investigated using electrical and optical methods. Stokes'[1] calculated profile is followed to within 10% down to 8-cm wavelength, and Crapper's[2] profile to within 8% for very short wavelengths, although the ripples sometimes have flatter crests than predicted. Stokes' estimate of maximum slope remains good below 8-cm wavelength when modified for surface tension. For ripples, the maximum inclination obtainable ($<40°$ to the horizontal) is less than Crapper suggests, possibly because of the initial extermely rapid viscous decay. The particle motion is correctly predicted for the liquid body, and for a clean surface, but a grease film renders the surface inextensible for short ripples, and at about 6-cm wavelength a longitudinal elastic surface wave persists in this film supported by the motion of the water underneath. Wilton's[3] theory was found to give a good estimate for waveforms in the anomalous region where surface tension and gravity forces are comparable; one new profile was also found.

[1] G. G. Stokes, Mathematical and Physical Papers, Cambridge (1880).
[2] G. D. Crapper, J. Fluid Mech. 2, 532 (1957).
[3] J. R. Wilton, Phil. Mag. (6), 29, 688 (1915).

U4. Re-Evaluation of the Atomic Constants. J. A. BEARDEN, JOHN S. THOMSEN, AND WILLIAM C. SAUDER, *Johns Hopkins University.*—New experimental data and theoretical studies since 1955 indicate the need for a completely new least-squares readjustment of the best values for the atomic constants. In the x-ray field, several important new developments have occurred, e.g., Ulmer's study of the "h/e exepriments" and Cohen's analysis of errors in certain λ_g/λ_s measurements. Among the experiments producing critical changes in the constants are the redetermination of the gyromagnetic ratio of the proton by Bender and Driscoll and the chemical measurement of the Faraday by Craig, Hoffman, Law, and Hamer. The precision of the present data now requires a more careful consideration of the acceleration of gravity and the determination of the absolute values of electrical standards. In these areas important new work has been completed. The effects of the various changes on a re-evaluation will be discussed.

U5. Nuclear Depolarization as an ENDOR Mechanism. E. C. MCIRVINE, JOHN LAMBE, NEAL LAURANCE, AND R. W. TERHUNE, *Ford Motor Company.*—A mechanism of electron-nuclear double resonance (ENDOR) is described wherein an EPR signal serves to detect the removal of a dynamic nuclear polarization.[1] Since the application of auxiliary rf power at some transition frequency Δ of the nuclear system removes this polarization, nuclear transition frequencies may be sensitively detected. The mechanism applies in the case of an EPR line inhomogeneously broadened by the presence of a magnetic nuclear species. The application of microwave power at a frequency ω on one side of such a line not only saturates the allowed electron spin transitions in the spin packet at ω, but also causes forbidden transitions flipping both electron and nuclear spins. The saturation of the electron spin packets at $\omega-\Delta$ and $\omega+\Delta$ is limited by the principle of detailed balance for the nuclear spin population, which sets up a steady state dynamic nuclear polarization. The application of rf at the nuclear transition frequency Δ removes this nuclear polarization and changes the EPR signal. This mechanism is consistent with experimental results on "distant" Al^{27} nuclei in ruby (nuclei having negligible hyperfine interaction with the chromium ion).

[1] A. Abragam and W. G. Proctor, Compt. rend. **246**, 2253 (1958).

U6. ENDOR in Dilute Ruby. JOHN LAMBE, NEAL LAURANCE, AND E. C. MCIRVINE, *Ford Motor Company.*—ENDOR experiments have been carried out in dilute ruby (0.01% Cr) at 4.2°K. In this material ENDOR lines are observed which can be assigned to Al^{27} nuclei near the Cr^{3+} sites. The mechanism whereby these nuclei are observed is probably the "packet shifting" ENDOR described by Feher[1] as opposed to the depolarization ENDOR which also occurs in ruby. The speed of response of the ENDOR effects is used in distinguishing these different mechanisms. The "packet shifting" ENDOR should have a response time corresponding to the electron T_1, the depolarization effect corresponding to the nuclear T_1. The ENDOR measurements were made while transitions corresponding to $S_z+\frac{1}{2}\rightarrow+\frac{3}{2}$ or $-\frac{1}{2}\rightarrow+\frac{1}{2}$ were saturated. A given transition yields of the order of 100 ENDOR lines. The spectrum is not yet completely analyzed but some features are clear. A major point is the large variation in nuclear quardrupole splitting of the Al^{27} nuclei. Splittings

vary from 260 kc to 500 kc compared with the normal splitting of 360 kc. This presumably is a measure of the distortion in the crystalline electric field near the Cr^{3+}.

[1] G. Feher, Phys. Rev. **103**, 834 (1956).

U7. Possible Use of $\overline{F_2}$ Centers in LiF as a RASER. MOHAN LAL NARCHAL AND WILLIAM A. BARKER, *Saint Louis University.*—The paramagnetic resonance absorption spectrum of $\overline{F_2}$ centers produced at liquid N_2 temperatures by the x-radiation of LiF has been extensively studied by Woodruff and Kanzig.[1] A detailed theoretical analysis of the population distribution of this system has been made by the method of partial distributions[2] in which we assume that one or another of the paramagnetic transitions is saturated by a microwave pump of $f_p = 9.5$ kMc/sec or 30 kMc/sec. In several cases we find population inversion among levels designated by different values of m_I but the same value of m_s. The material appears to be suitable for RASER action. As a result of the magnitude and anisotropy of the hyperfine structure, the proposed amplifier should have a signal frequency in the range between about 100 and 1000 Mc/sec.

[1] T. O. Woodruff and W. Kanzig, Phys. and Chem. of Solids **5**, 268 (1958).
[2] J. D. Keating, L. Follis, and W. A. Barker, Bull. Am. Phys. Soc. Ser. II, **6**, 68 (1961).

U8. Optics of Radiation from Optical Masers. JENNY E. ROSENTHAL, *Bramley Consultants.*—Many interesting problems are connected with the in-phase radiation from optical masers, such as described by Maiman. The method previously suggested for transmitting information assumed that the cross section of a coherent beam with a wavefront planar at emission could be magnified by an optical system with the following conditions being satisfied: The radiation stays coherent and the wavefront at the locus of the counter part of the original source is planar. The validity of this premise is discussed and in particular the conditions imposed on an optical system so that a coherent parallel beam of area A and divergence angle α can be transformed into a beam of area f^2A, $f>1$, and divergence angle α/f. The problem is complicated by the high-energy density of the light beam since the photon density in the ruby is comparable to the impurity density in high-resistance silicon. With the available maser output power, the electrical intensity calculated from Poynting's equation may exceed 2 kv/cm. This would severely perturb the energy band scheme of the medium used in the optical system and cast doubt on the applicability of the first order dispersion theory.

U9. A Zero-Field *X*-Band Maser Spectrometer. N. MCAVOY, M. R. KAGAN, AND VW. T. TOWNSEND, *Melpar, Inc.*—An *x*-band paramagnetic resonance spectrometer using a maser as either an oscillator or detector has been constructed. A zero-field maser using Fe^{3+} doped Al_2O_3,[1] is employed. Theoretical and experimental evaluations will be given comparing the sensitivities of a conventional spectrometer with a maser-type spectrometer. This theoretical treatment will include a four-part circulator, with oscillator-detector combinations. The design problems introduced by using detectors and sources with less than the blackbody noise will also be discussed.

[1] J. E. King and R. W. Terhune, J. Appl. Phys. **30**, 1844 (1959).

Invited Paper

U10. The Atomic-Hydrogen Maser. NORMAN F. RAMSEY, *Harvard University.* (30 min.)

THURSDAY MORNING AT 9:30

Cotillion Room, North

(A. H. SNELL presiding)

Invited Papers

UA1. Neutron Experiments with a Tandem Electrostatic Accelerator. H. H. BARSCHALL, *University of Wisconsin.* (30 min.)

UA2. Influence of the Indistinguishability of the Nucleons on the Structure of the Nuclei. KARL WILDERMUTH, *Florida State University.* (30 min.)

UA3. Distorted-Wave Theory of Direct Nuclear Reactions. G. R. SATCHLER, *Oak Ridge National Laboratory.* (30 min.)

UA4. A Detailed Study of the Recoil Ions from the Beta Decay of He^6. C. H. JOHNSON, *Oak Ridge National Laboratory.* (30 min.)

THURSDAY MORNING AT 9:30

Sheraton Hall

(FREDERICK SEITZ presiding)

Invited Papers

V1. The Past and Future of Dispersion Theory. M. L. GOLDBERGER, *Princeton University.* (40 min.)

V2. Tritium Geophysics. W. F. LIBBY, *University of California, Los Angeles.* (40 min.)

V3. Superconductivity in High Magnetic Fields at High Current Densities. J. E. KUNZLER, *Bell Telephone Laboratories.* (30 min.)

V4. Transition Temperatures of Superconductors. B. T. MATTHIAS, *Bell Telephone Laboratories.* (30 min.)

THURSDAY MORNING AT 9:30

National Bureau of Standards, East Building

(N. CHRISTOFILOS presiding)

Plasma, II

VA1. Radio Emission by Plasma Oscillations in Non-uniform Plasmas. DEREK A. TIDMAN AND GEORGE H. WEISS, *University of Maryland.*—We consider a longitudinal electric plane wave unpinging on a small density fluctuation in a plasma, and calculate to first order in perturbation theory, the consequent radio emission. This procedure can be carried through either by using moment equations[1] which neglect third order moments or by starting directly from the Boltzmann equation and making a far-field approximation. The results are qualitatively identical. It is shown that a spherically symmetric density fluctuation shows a dipole radiation pattern.

[1] D. A. Tidman, Phys. Rev. 117, 366 (1960).

VA2. Interaction between a Radiowave and a Plasma in the Presence of a Uniform Magnetic Field.* TOYOKI KOGA, *Engineering Center, University of Southern California.*—On account of the imposed magnetic field, the effect of movements of ions is not to be neglected. Considering a plausible model of plasmas where molecules are partly ionized, Boltzmann-type equations for electrons and ions are proposed. By introducing "generalized moments" of the distribution functions, it is easy[1] to solve the equations obtaining the conductivity of a plasma to an oscillating electric field. There are seven frequencies which characterize the phenomena: (i) Larmor's frequencies of electrons and of ions, (ii) frequency of radiowave, (iii) plasma frequency and a similar frequency defined with respect to ions, (iv) collision frequencies of electrons and of ions. As special cases, Alfvén's hydromagnetic wave and Margenau's conductivity are included in the theory.

* Supported by the U. S. Air Force, the Office of Scientific Research and the Office of Naval Research.

[1] The method is similar to what was used in the papers presented by the author at the 1st and 2nd annual meetings of Division of Plasma Physics, A.P.S.

VA3. Collisionless Electrostatic Shock.* CHARLES W. HARTMAN AND STIRLING A. COLGATE, *Lawrence Radiation Laboratory, Livermore,* AND PAUL J. KELLOGG, *University of Minnesota.*—The formation of a shock wave in cold, collisionless plasma with no magnetic field is machine computed for a one-dimensional sheet-charge model with mass ratio 10. The noninteracting initial condition is represented by two cold interpenetrating plasma streams. Purely electrostatic interaction of the two stream instability type proceeds first through electron-electron interaction producing waves of dominant wavelength (v_0/f_{pe})(v_0=streaming velocity) which grow (in several electron plasma periods) to saturation potentials comparable with the electron streaming energy. Subsequent ion-electron waves $[\lambda \simeq (v_0/f_{pi})]$ grow in several ion plasma periods to potential comparable to the ion streaming energy. All fields appear to fluctuate at about f_{pe}, and the interaction after 4 ion wavelengths is strong enough to slow the original ion streams to ½ their original velocity and randomized their velocity to a width equal to ½ the peak separation. The electron energy is random and equal to ½ the ion energy.

* This work was done under the auspices of the U. S. Atomic Energy Commission.

VA4. Plasma Cavitation. RICHARD L. MOORE, *Richard L. Moore Consultants.*—In previous work, a condition of dynamic equilibrium for a cylindrical, fully ionized plasma confined by a surface magnetic pressure was found to give a gaussian density distribution centered at the origin if the magnetic pressure at the surface (mks units) $HB/2 \geq M\omega^2/2\pi$, where M is the lineal mass density, ω is the angular velocity. If this condition is violated, the condition of dynamic equilibrium gives an annular density distribution described as

$$\rho(r_m)\{r/r_m\}^{c_2/RT} \exp\{-(r^2-r_m^2)/2\sigma^2\} \cdot r_m$$

is the radius of maximum density,

$$c_2 \text{ is } -(\pi\mu/M)[\{H(r_0)\}^2+\{H(r_i)\}^2],$$

and σ^2 is

$$MRT[r_i^{-2}-r_0^{-2}][\pi\mu\{H^2(r_0)r_i^{-2}+H^2(r_i)r_0^{-2}\} - M\omega^2\{r_i^{-2}-r_0^{-2}\}]^{-1},$$

where r_i is the radius of the hole on the axis and r_0 is the radius of the outside surface of the plasma. Qualitative comparison will be made with recent plasma experiments[1] in which the plasma has been observed to develop a noncentral mass distribution.

[1] V. Josephson, M. Dazey, and R. Wuerker, Phys. Rev. Letters 5, 416 (1960); A. Kolb and N. Rostoker, Bull. Am. Phys. Soc. 6, 203 (1961).

VA5. Air Core Plasma Betatron Coil Design. A. G. RUBIN AND R. P. MEISTER, *Williamson Development Corp., Inc.,* AND M. A. LEVINE, *Air Force Cambridge Research Laboratories.*—The air core plasma betatron imposes the following conditions on the magnetic field coils: extremely low inductance precise field shaping, small dimensions, and for high-magnetic fields, considerable strength. Several novel designs have evolved to meet these requirements. The energy source for the plasma betatron is a capacitor bank. This type of single shot operation requires that the betatron magnetic field be frequency-independent over a considerable frequency range; in the case considered from about 30 Mc to 0.3 Mc. Methods of minimizing variations in current distribution in a skin effect dominated coil are considered. The additional problem of distributed capacity and its frequency-sensitive effect on the coil currents is treated. Field shapes and the necessary coils were designed using an analog plotting tank and the extension of these techniques to other novel field shapes with one turn coils will be discussed.

VA6. Electric Field Measurements in a Rotating Plasma.* D. A. BAKER AND J. E. HAMMEL, *Los Alamos Scientific Laboratory.*—Electrostatic probe measurements were made of the voltage distribution as a function of radius on the midplane of Ixion, the Los Alamos rotating plasma device. During the time after the initial current pulse has been drawn and plasma rotation established, the electrostatic probe shows that the electric field near the wall (anode) is small. The major portion of the voltage appears inside the active plasma volume, implying electric fields $\geq$800 v/cm and drift velocities $\geq 8.6\times10^6$ cm/sec, corresponding to deuteron drift energies of at least 75 ev under normal operating conditions. During the "waiting period" between application of the voltage to the weakly ionized gas and the onset of the initial pulse of charging current, it was found that no quiescent electron sheath exists at the anode. There are indications of an unstable sheath which rapidly forms and disintegrates during the waiting period.

* Work performed under the auspices of the U. S. Atomic Energy Commission.

VA7. Energy Losses and Ultraviolet Radiation in Ixion.* J. E. HAMMEL AND D. A. BAKER, *Los Alamos Scientific Laboratory.*—It has been observed in rotating plasma experiments, that the rotational velocity of the plasma will not exceed a certain critical limit.[1] The hypothesis has been advanced that the plasma is only partially ionized and that its rotation is impeded through ion-neutral and electron-neutral interactions. This paper reports experiments with Ixion (the Los Alamos rotating plasma experiment) which show that a large portion of the plasma is fully ionized and, therefore, that losses through collisions with neutrals in this portion of the plasma are unimportant. The interaction by which the angular momentum of the rotating ions is lost probably occurs near the outer boundary of the plasma. Studies of the radiation from the discharge were made with a vacuum uv monochromator, an infrared bolometer, a uv pinhole camera and a photo-cell. The results of these experiments indicate a large energy loss in hard ultraviolet radiation from contaminants in the deuterium plasma. Over the duration of plasma rotation this loss accounts, within a factor of approximately two, for all of the plasma energy.

* Work performed under the auspices of the U. S. Atomic Energy Commission.
[1] See for example, D. A. Baker and J. E. Hammel, Bull. Am. Phys. Soc. **5**, 341 (1960).

VA8. Connected Plasma Containing Regions—Tuck's Cusp Bridge.* D. W. KERST AND T. OHKAWA,† *General Atomic Division.*—Regions of differing field strength along a magnetic tube of flux have isotropic velocity distributions and the same particle density and perpendicular pressure if the low-field region distribution is isotropic. The inverse is not true. This is demonstrated by solution of the Vlasov equation yielding $f(v,\mu)$, μ being the invariant magnetic moment. Applied to Tuck's[1] "bridges" connecting two cusps to eliminate leaks, this shows that since density and pressure are the same in the bridge as in the plasma within the cusps, than $\beta \ll 1$ is possible in the bridge composed of the extension of the cusp sheath. Greatly simplified structure is possible with straight multipole producing wires having close-spaced jackets which give mechanical stability, stability against inflation, and high field in the bridge. Flute instability is avoided because the close-spacing determines $\delta \int d_l/B$. Mirror coil point cusps or twists can terminate long multipole cusps. Shear by twists or windings can be used to improve stability.

* This work supported by General Atomic and Texas Atomic Energy Research Foundation.
† On leave from the University of Tokyo.
[1] J. L. Tuck, Nature **187**, 863 (1960).

VA9. Behavior of Plasma in Rotating Mirror and Cusp Magnetic Geometries.* JOHN R. BANISTER AND RICHARD D. JONES, *Sandia Laboratory.*—An experimental survey of the behavior of plasmas in rotating mirror and cusp magnetic geometries has been conducted using argon, helium, and hydrogen. This was accomplished by placing three orthogonal pairs of coils about a sphere containing the low pressure gas. These coils could be arranged to generate either magnetic mirrors or magnetic cusps. The pairs of coils were attached to three individual capacitors equipped with spark gap switches, which could be fired at different times through a delay system to achieve various phase relations of the ringing discharges. The observational technique was exclusively optical, using a Beckman-Whitley framing camera. By using the rotating mirror geometry, it was found that the argon was apparently initially assembled at the sphere center, but then swelled back against the diminishing magnetic fields. No such assemblage was observed with hydrogen and helium, presumably because of the higher speed of sound in these gases. It was also noticed that the assemblage was less complete with argon when a cusp geometry was used.

* This work was performed under the auspices of the U. S. Atomic Energy Commission.

VA10. Effect of Metallic Walls on Confinement of Plasma in a Mirror Machine.* W. A. PERKINS AND R. F. POST, *Lawrence Radiation Laboratory, Livermore.*—A hydrogen plasma is injected, captured, and heated in a mirror machine by adiabatic magnetic compression, producing a plasma with high (25 kev) electron temperature. Escaping plasma electrons are monitored by scintillators protruding radially and axially into the vacuum chamber. A velocity-space plasma instability[1] occurs under certain conditions of density and compression ratio when there is no metallic coating on the inner walls of the glass vacuum chamber. Under identical conditions with the metallic coating, the end energy flux increased by a factor of two while the radial energy flux decreased by a factor of 20 with a marked change in its variation with time, indicating a decrease in the velocity-space instability. Further investigation showed that a higher initial density near the axis was achieved with the metallic coating present. The higher initial density meant that collisions could smooth out the anisotropic velocity distribution and thereby inhibit the instability. Indeed when the amount of injected plasma was decreased, the radial probe signal increased in magnitude and returned to a time behavior characteristic of no metallic coating. A few explanations will be discussed.

* Work performed under the auspices of the U. S. Atomic Energy Commission.
[1] R. F. Post and W. A. Perkins, Phys. Rev. Letters **6**, 85 (1961).

VA11. Cyclotron Instabilities in a Bounded Plasma. P. B. BURT* AND E. G. HARRIS, *The University of Tennessee.*—The longitudinal oscillations of an infinite plasma in a uniform magnetic field have been investigated previously by Harris[1] for very anisotropic velocity distributions. Unstable modes were found to occur if $\omega_{pe}^2 > \omega_{ce}^2$, where ω_{pe} is the electron plasma frequency and ω_{ce} is the electron cyclotron frequency. A similar investigation has been carried out for a finite, cylindrical shell of plasma in a uniform magnetic field, with ions moving initially in Larmor orbits and stationary electrons. The dispersion relation obtained for the longitudinal oscillations is solved for ω, the frequency of the perturbation, in the limit of short wavelength disturbances along the axis of the shell. Approximate conditions for instability are obtained which are similar to the result found by Harris.[1] In addition, it is found that the real parts of the unstable frequencies occur at multiples of the ion cyclotron frequency.

* National Science Foundation Predoctoral Fellow.
[1] E. G. Harris, Phys. Rev. Letters **2**, 34 (1959).

THURSDAY MORNING AT 9:30

Continental Room

(ALLEN SACHS presiding)

Muons and Pions

W1. Quenching of the Depolarization of Muons in Semiconductors by Application of Longitudinal Magnetic Fields.* R. PREPOST AND A. M. SACHS, *Columbia University,* AND G. FEHER, *University of California, LaJolla.*—Experiments on the depolarization of positive muons in silicon and germanium[1] have been extended. Measurements have been made of the

asymmetry of the decay positrons from polarized muons stopping in samples with various impurity concentrations, between room and liquid nitrogen temperatures, in longitudinal magnetic fields. For the sample of phosphorous-doped n-type silicon with 4×10^{13} free electrons/cm^3, a field of approximately 1000 gauss quenched half the muon depolarization at room temperature. At liquid nitrogen temperature, half the depolarization in the same sample is quenched by a field of less than 100 gauss, consistent with the idea of a substantially reduced number of formations of muonium shallow donors. The sample of silicon with 2×10^{16} free electrons/cm^3, which also depolarizes muons, does not show this reduction in longitudinal field necessary to quench the depolarization at liquid nitrogen temperatures.

* Supported by joint contract of the U. S. Atomic Energy Commission and the Office of Naval Research.
[1] G. Feher, R. Prepost, and A. M. Sachs, Phys. Rev. Letters **5**, 515 (1960).

W2. Measurement of Muon Absorption Rate $\mu^-+C^{12}\rightarrow B^{12}+\nu$.* E. J. Maier, B. Bloch, R. Edelstein, and R. T. Siegel, *Carnegie Institute of Technology.*—The reaction rate above has been measured by counter techniques with cyclotron produced muons. A beam of 45 Mev muons was stopped in a 4×4×2-in. thick plastic scintillant ($CH_{1.10}$). The number of muons decaying in this counter was monitored by the μ-e decays, and the number captured to bound states of B^{12} was measured by detecting the 20-msec β decay of B^{12}. Correction was made for failure to detect electrons due to the finite energy threshold of the counter. Numerical results will be presented.

* This research was supported in part by the U. S. Atomic Energy Commission.

W3. Measurement of the High-Energy End of the μ-Meson Spectrum $K\mu_3$ Decay.* E. Loh, A. Boyarski, L. Q. Niemela, and D. Ritson, *M.I.T.*, S. Ozaki, *Brookhaven National Laboratory*, and R. Weinstein, *Northwestern University.*—The ranges of particles resulting from K^+ decay have been measured by means of a system of hodoscopes. One hundred thousand K^+ decays were examined yielding 106 μ-e tracks with the muon having an energy between 134 and 115 Mev. Fifty-one out of the 106 tracks have one or two associated γ rays. The measured relative abundance of $K\mu_3$ in the energy region mentioned above is $0.68\pm0.07\%$. The relative abundance of $K\mu_3$ obtained by this experiment together with that obtained by Talor *et al.*[1] will be compared with the calculations of Gatto[2] and Bernstein.[3]

* This work is supported in part by the U. S. Atomic Energy Commission, the Office of Naval Research, and the U. S. Air Force Office of Scientific Research.
[1] S. Taylor, G. Harris, J. Orear, J. Lee, and P. Baumel, Phys. Rev. **114**, 359 (1959).
[2] R. Gatto, Phys. Rev. **111**, 1426 (1958).
[3] J. Bernstein and S. Weinberg, Phys. Rev. Letters **5**, 481 (1960).

W4. Momentum Dependence of the Asymmetry in Muon Decay.* Kenneth M. Crowe and Hans Kruger, *Lawrence Radiation Laboratory, Berkeley.*—Positive muons from the Berkeley 184-in. synchrocyclotron were stopped in various material and the momentum dependence of the asymmetry of positrons from their decay measured with a magnetic spectrometer. The parameters of the polarized muon spectrum, determined by least-squares fitting the theoretical form of the asymmetry to its measured values, are $\rho=0.774\pm0.042$, $\delta=0.782\pm0.031$, and $|\xi|\geq R|\xi|=0.848\pm0.036$ for an unrestricted local μ-decay interaction with $\eta\ll1$. Here R is the effective muon-beam polarization. These values of the parameters include radiative corrections and corrections for bremsstrahlung and all instrumental effects. When the local μ-decay interaction is restricted to $g_T=-g_T'$, these values of ρ and δ imply $|\xi|=0.989\pm0.014$. Thus the average muon-beam polarization during this experiment was $R=0.857\pm0.024$.

* This work was done under the auspices of the U. S. Atomic Energy Commission.

W5. Scattering Cross Sections of Mu Mesons by the Extended Nucleus of Bromine.* G. H. Rawitscher, *Yale University.*—Recent measurements[1] of the scattering of μ^+ mesons in nuclear emulsions were compared[1] with calculations based on the assumption that μ^+ mesons are heavy positrons, and good agreement was found. Differential μ^+ and μ^- scattering cross sections, calculated for the comparison mentioned above, will be presented. The ratio v/c lies between 0.2 and 0.7. The dependence of the cross section σ on the atomic number Z and transfer momentum q will be compared for μ^+ and μ^- mesons. The plot of σ vs q is fairly insensitive to v/c for $\mu_N{}^+$ and not for μ^-. For the latter the plot of $\sigma/\sigma_{\text{point}}$ vs q is useful in the comparison of different Z at the same v/c, enabling one to extrapolate to $Z=47$ (silver) from values for $Z=80$ and 48 available in the literature.

* This research was supported by the U. S. Air Force, monitored by the Air Force Office of Scientific Research of the Air Research and Development Command.
[1] P. Connolly, J. G. McEwen, and J. Orear, *Proceedings of the Tenth Annual International Rochester Conference on High Energy Physics, 1960* (Interscience Publishers, Inc., New York, 1960), p. 796.

W6. Atomic Processes Involving Antimuonium; Possible Method of Detecting Antimuonium.* Vernon W. Hughes, *Yale University.*—Recently there has been considerable speculation about an interaction coupling muonium M and antimuonium $\overline{M}$.[1] Muonium can be produced by stopping positive muons in argon gas,[2] and, if an interaction coupling M to $\overline{M}$ exists, a certain fraction of the decays will occur from the $\overline{M}$ component of the wavefunction. The presence of the argon Ar atoms inhibits the development of the $\overline{M}$ component of the wavefunction due to the different electrostatic interactions of M and $\overline{M}$ in elastic collisions with Ar. The μ^- from $\overline{M}$ can be captured by an Ar atom or the e^+ can annihilate with an electron in an Ar atom, and the rates of these processes in the high-pressure Ar gas are much greater than the muon decay rate. The characteristic feature of $\overline{M}$ disappearance wihch is probably most easy to detect experimentally is the $2p\rightarrow1s$ argon mu mesonic x ray.

* This research has been supported in part by the Air Force Office of Scientific Research.
[1] B. Pontecorvo, J. Exptl. Theoret. Phys. **33**, 549 (1957); preprints and private communications from S. Glashow, G. Feinberg, and S. Weinberg; Proceedings of 1960 Rochester Conference.
[2] V. M. Hughes, D. McColm, R. Prepost, and K. Ziock, Phys. Rev. Letters **5**, 63 (1960).

W7. Single Pion Production in π^--Proton Collisions at 0.90 and 1.1 Bev.* D. K. Robinson, B. Munir,† E. Pickup,‡ and E. O. Salant, *Brookhaven National Laboratory.*—About 1600 two-prong events produced by 1.1 Bev π^- mesons in the Berkeley 10-in. hydrogen bubble chamber, and a similar number produced by 0.9 Bev negative pions in the Brookhaven 20-in. liquid hydrogen chamber have been measured. All positive secondaries have been identified visually from the ionization density of the tracks, and the events have been kinematically analyzed and calssified as elastic, single pion production, and multiple pion production. The single pion production events are of two types, neutron reactions ($\pi^-+p\rightarrow\pi^-+\pi^++n$) and proton reactions ($\pi^-+p\rightarrow\pi^-+\pi^0+n$). At 0.9 Bev the center-of-mass angular distribution of the protons is strongly peaked backward, while the neutrons have an almost symmetric distribution. However, at 1.1 Bev, the nucleons from both proton and neutron reactions exhibit strong backward peaking. The momentum distribution of the protons and neutrons at both energies have low energy groups in disagreement with the predictions of the statistical and the standard isobar theories of pion production. The significance of these results with reference to nucleon isobar and pion-pion interactions will be discussed.

* Work performed under the auspices of the U. S. Atomic Energy Commission.
† On leave of absence from the Florida State University, Tallahassee, Florida.
‡ On leave of absence from the National Research Council, Ottawa, Ontario, Canada.

W8. Elastic Scattering and Single Pion Production in 2 Bev *P-P* Interactions. W. FICKINGER, *Yale University*, AND E. PICKUP, D. K. ROBINSON, AND E. O. SALANT, *Brookhaven National Laboratory*.—The 20-in. hydrogen bubble chamber of the BNL Bubble Chamber Group was exposed to a well-collimated beam of 2 Bev protons. A total of 4000 two-prong events has been measured. Analyses of one fourth of these data yield the following partial cross sections: elastic 18.7 ± 1.3 mb, single π^+ 15.1 ± 0.9 mb, single π^0 3.7 ± 0.4 mb, multiple meson 7.7 ± 0.6, and π^+D 0.09 ± 0.07 mb. With the inclusion of the four-prong ($pp-$) events, cross section 3.2 ± 0.2 mb, the total cross section is 48.5 ± 1.7 mb. A sample of 600 elastic scatterings has been examined for possible polarization effects due to an initial 4° scattering of the beam by a carbon target in the cosmotron. The resulting quotient $(R-L)/(R+L)$ is 0.01 ± 0.06. The single π^+ production events show a strong peak at 150 Mev (half-width 40 Mev) in the π^+P Q values, clear evidence of the $\pi^+P_{\frac{3}{2}}$, $\frac{3}{2}$ resonance. Final analyses of all events will be presented, including angular distributions of isobar productions and decays.

W9. Multiple Pion Production in *P-P* Collisions at 2 Bev.* E. PICKUP,† D. K. ROBINSON, AND E. O. SALANT, *Brookhaven National Laboratory*.—In an exposure of the Brookhaven 20-in. liquid hydrogen bubble chamber in a 2 Bev proton beam at the cosmotron, about 57 000 interactions were photographed. 7.2% of the interactions gave four charged secondary particles, representing mostly double and triple pion production events of the types (a) $\pi^+\pi^-PP$, (b) $\pi^+\pi^-\pi^+PN$, (c) $\pi^+\pi^-\pi^0PP$, (d) $\pi^+\pi^-\pi^+D$, and also some $PP\pi^0$ events with Dalitz electron pairs. 980 of these four-prong events have been measured, using a digitized microscope system. From the kinematic analysis completed to date (about 300 events), the relative frequency of the reactions mentioned is (a)/(b)/(c)/(d) $=227/31/16/3$, these numbers being actual numbers of events classified. Additional results of the kinematic analysis, with differential cross sections, will be given, and the detailed behavior of these reactions will be discussed.

* Work performed under the auspices of the U. S. Atomic Energy Commission.
† On leave of absence from the National Research Council, Ottawa, Ontario, Canada.

W10. Deuterons in *P-P* Collisions at 2.0 Bev.* B. SECHI ZORN, *Brookhaven National Laboratory* (introduced by E. O. Salant).—The formation of deuterons in p-p collisions at 2 Bev is being studied in the BNL 20-in. hydrogen bubble chamber. The deuterons were identified by bubble-density vs momentum measurements. The reactious studied were (1) $p+p\rightarrow D+\pi^+$, and (3) $p+p\rightarrow D+n\pi$, where $n>1$ and the pions are charged or neutral. A preliminary value for the total cross section for the reactions with deuterons produced is 0.20 ± 0.05 mb. This value is in good agreement with the calculation of Hagedorn for $p-p$ collisions at 2.3 Bev.[1] At present the ratio of cross sections for reaction (1) to that for reaction (2) is ~0.1. This ratio, however, does not seem to agree with the calculation of Hagedorn.

* Work performed under the auspices of the U. S. Atomic Energy Commission.
[1] R. Hagedorn, Phys. Rev. Letters 5, 278 (1960).

THURSDAY MORNING AT 9:30

Burgundy Room

(E. E. LOEBNER presiding)

Semiconductors, I

WA1. Equilibrium Concentration of Impurities in a Semiconductor Adjacent to a Gas Phase from Thermodynamic Data. KURT LEHOVEC, *Sprague Electric Company*.—The equilibrium concentration of impurities can be calculated using vapor pressure data and the phase diagram of the binary system semiconductor-impurity metal. The calculation is based on a thermodynamic cycle involving the impurities (a) in the semiconductor, (b) in the gas phase outside the semiconductor, (c) in the gas phase above the liquidus of the impurity metal-semiconductor binary system, (d) in the liquidus, and (e) in the semiconductor in equilibrium with the liquidus. Since the vapor pressure of impurities adjacent to the semiconductor at the diffusion temperature is usually smaller than that pertaining to the liquidus, it is necessary to dilute the liquidus in a metal experiment to obtain the appropriate vapor pressure. However, this dilution must be done without affecting the binary system metal-semiconductor, e.g., by considering a liquidus containing two impurity isotopes, one of which has a partial vapor pressure equal to the impurity vapor pressure adjacent to the semiconductor. Vapor pressure data pertaining to the liquidus line do not seem available to test our results. Experimental work to obtain pertinent data is in progress.

WA2. Faraday Ellipticity in Semiconductors as a Function of the Energy Dependent Relaxation Time.* J. K. FURDYNA AND M. E. BRODWIN, *Northwestern University*.—The theory of Faraday ellipticity in semiconductors, developed previously under the assumption of constant relaxation time τ[1], is presently extended to include the dependence of τ on energy. For $\omega^2\tau^2\ll1$, $\mu^2B^2\ll1$, and small losses, the ellipticity becomes

$$E=\left(\frac{\mu_0}{\epsilon}\right)^{\frac{1}{2}}t\sigma\mu B\omega\langle\tau\rangle\left(\frac{\langle\tau^3\rangle}{\langle\tau^2\rangle\langle\tau\rangle}-\frac{1}{4}\frac{\omega_p^2}{\omega^2}\right),$$

where the angular brackets denote Maxwellian averages, μ_0 is the permeability of free space, ϵ the static dielectric constant, t sample thickness, σ dc conductivity, μ Hall mobility, B magnetic field, ω frequency of the electromagnetic wave, and ω_p^2 equals $\sigma/\langle\tau\rangle\epsilon$. The value of ellipticity and the condition for change of sign thus depend strongly on the type of scattering. Effects of the energy-dependence of τ on the Faraday ellipticity will also be discussed for other ranges of μB, $\omega\tau$, and the dielectric loss. Comparison with the available experimental values[1] shows that the agreement between theory and experiment is significantly improved when the energy-dependence of τ is taken into account.

* Supported by the Advanced Research Projects Agency of the U. S. Department of Defense.
[1] J. K. Furdyna and S. Broersma, Phys. Rev. 120, 1995 (1960).

WA3. Hall Mobility of the Small Polaron. L. FRIEDMAN AND T. HOLSTEIN, *University of Pittsburgh*.—In insulators of sufficiently narrow conduction-bandwidth, an excess electron tends to get trapped at atomic sites by self-induced lattice distortion. Thermal vibrations give rise to jumps between two such sites by causing momentary coincidences of electronic

energies, thereby allowing the electronic-overlap jump mechanism to become operative. A modification of the elementary jump probability by an applied magnetic field occurs for those events in which the energies of three sites are simultaneously coincident. The effect arises from the interference between the amplitude for the first-order jump between two sites and that for a second-order jump involving intermediate occupancy of the third site. For $H=0$, the two amplitudes are 90° out of phase and do not interfere; for $H=0$, the phase difference is altered by an amount proportional to the magnetic flux enclosed by the triangle defined by the site centroids. The resulting Hall mobility is found to be greater than or comparable to the normal value, according to whether or not the three sites are mutually nearest neighbors.

WA4. Resistivity of Diamond at Room Temperature. J. A. ELMGREN AND D. E. HUDSON,* *Iowa State University.*—The resistivity of diamond (Type I or Type IIa) is usually quoted as 10^{14}–10^{16} ohm cm, but very little reliable experimental work is reported to support the values. Measurements of the rate of decay of persistent polarization of diamond in the dark have been made by a counting experiment. The method is one which measures primarily the bulk resistivity rather than surface effects. The results lead to the conclusion that the diamonds under investigation have bulk resistivities of the order of 10^{19} ohm cm or higher, at 25°C. Resistivities of this order are in more reasonable agreement with theoretical calculations based on the activation energies of imperfection systems observed by optical absorption techniques.

* Contribution No. 996. Work was performed in the Ames Laboratory of the U. S. Atomic Energy Commission.

WA5. Semiconducting Stress Transducers Utilizing the Transverse and Shear Piezoresistance Effects. W. G. PFANN AND R. N. THURSTON, *Bell Telephone Laboratories.*—Principles of a varied group of new semiconducting, piezoresistive stress and strain transducers are outlined. These devices have in common the utilization of the transverse or shear piezoresistive effect. One group of devices consists of gauges in the form of a thin rectangular sheet which is bonded to the best piece, and whose resistance change can be expressed as a simple function of the principal stresses in the test piece. Two special gauges in this group are described. In one, the resistance change is proportional to the sum of the principal biaxial stresses for any orientation of the gauge on the test piece. In the other, the resistance change is proportional only to longitudinal stress components, being independent of transverse stress components. Also described are: a four-terminal gauge for complete determination of biaxial stresses, full-bridge gauges made from a single crystal, load cells of low compliance, new torque transducers, and diffusion techniques for making some of the foregoing. The devices are illustrated in terms of germanium and silicon, but extension to other semiconductors is straightforward.

WA6. Dependence of Impact Ionization Breakdown Field on Impurity Concentration. A. L. MCWHORTER, *Lincoln Laboratory.**—In impact ionization of impurities in Ge, the breakdown field is found experimentally[1] to increase linearly with the (majority) impurity concentration for densities above about 10^{16}/cm^3, whereas existing theory[2] predicts only a square-root dependence. This discrepancy can apparently be resolved by taking into account the inelastic scattering due to electronic excitation of neutral impurities in addition to the usual neutral impurity elastic scattering. Since lattice losses are a negligible drag on the electrons at the high fields encountered, the situation is quite analogous to htat in hydrogen gas, where the controlling factor in the ionization rate normally is the number of excitations per ionization, both theory and experiment giving for this ratio the form $A\exp(Bp/E)$, where p is the pressure.[3] Assuming the simple hydrogenic model for donors, and scaling the experimental data for hydrogen accordingly, both the correct magnitude for the breakdown field and the linear dependence on concentration ("pressure") are obtained.

* Operated with support from the U. S. Army, Navy, and Air Force.
[1] N. Sclar and E. Burstein, J. Phys. Chem. Solids **2**, 1 (1957), and E. I. Abaulina-Zavaritskaya, Soviet Phys.—JETP **9**, 953 (1959).
[2] V. A. Chuenkov, Soviet Phys.—Solid State **2**, 734 (1960).
[3] W. P. Allis and S. C. Brown, Phys. Rev. **87**, 419 (1953).

WA7. Effect of Hydrogen on the Displacement Process in Ge.* J. A. NABER AND H. M. JAMES, *Purdue University.*—The threshold for production of displaced atoms by electron bombardment of Ge has been placed at 360 kev. However, it is found that less energetic electrons do produce very similar effects. It occurred to us that these "below threshold" effects might be due to displacement of Ge atoms resulting from a two-step process in which the electron initially strikes a hydrogen atom which then collides with a lattice atom. The maximum energy transferred to the Ge atom in the two-step process is four time that for a direct electron-Ge collision; thus the threshold for producing a displacement by the two-step process should be about 100 kev. An order of magnitude calculation indicates that in the presence of 10^{18} hydrogen atoms/cm^3 there will be about 10^{-6} displaced Ge atoms/cm/incident electron at 300 kev. Comparison of irradiations of crystals grown in a hydrogen atmosphere with crystals grown in a vacuum shows that hydrogen-grown crystals have conductivity changes consistent with the above calculations, while vacuum-grown crystals are essentially unaffected by "below threshold" irradiation. The results suggest that the two-setp hypothesis is a likely explanation of the low-energy irradiation effects in Ge.

† Work supported by U. S. Atomic Energy Commission contract.

WA8. Low Temperature Annealing of Electron-Bombarded Ge.* E. E. KLONTZ AND J. W. MACKAY, *Purdue University.*—We previously[1] have reported the existence of two low temperature ranges for annealing of n-type germanium which has been irradiated, at liquid helium temperatures, with 1.1 Mev electrons. We associated the lower temperature range (about 35°K) with recombination of closest stable vacancy-interstitial pairs, and the higher temperature (about 64°K) with next-closest pairs. Further study reveals that the relative amount of annealing in each of these temperature ranges depends on the total flux which the sample receives. For fluxes less than 10^{16} electrons/cm^2, no appreciable annealing occurs in the 35°K stage. For more than 10^{17} electrons/cm^2, about half of the recovery is in each stage. These results indicate that the 35°K stage is probably not associated with primary defects. For sufficiently small irradiation, so that the 35°K stage is not observed, it is found that the percent recovery in the 64°K stage varies with the bombardment energy, from about 10% for 600 Kev electrons to about 50% for 1.0 Mev and above. This is consistent with results showing the existence of radiation annealing which is relatively more important at lower energies.

† Supported by the U. S. Atomic Energy Commission.
[1] J. W. Mackay and E. E. Klontz, J. Appl. Phys. **30**, 1269 (1959).

WA9. The Optical Absorption Edge of Very Impure Germanium. J. I. PANKOVE, *RCA Laboratories.*—Early theoretical treatments of the influence of donor impurities on the band structure of semiconductors have predicted a shift of the conduction band to a lower energy. This effect, which should occur in addition to the formation of a tail of density of states, has recently been calculated. The position of the conduction band edge can be measured directly by means of optical absorption. However, in a degenerate semiconductor, states near the band edge are occupied, thus forbidding the corresponding transitions and displacing the absorption threshold to a higher

energy. The absorption of arsenic-doped germanium (in the range 5×10^{18} to 6.2×10^{19} cm^{-3}) was measured at room temperature with an accuracy of about 1 cm^{-1} and a resolution of 0.0015 ev. The free carrier absorption, extrapolated to the range of across-the-gap transitions, was subtracted from the measured absorption coefficient. An approximate solution of the energy dependence of the absorption coefficient for the case of a degenerate parabolic band allows a Macfarlane-Roberts type of interpretation. The most striking effect is a shift of the whole conduction band by several hundredths of an ev closer to the edge of the valence band. The filling of the band by the Fermi sea is also evident.

WA10. Infrared Radiation-Induced Magnetoelectric Effect in Semiconductors. LOTHAR WANDINGER, *U. S. Army Signal Research and Development Laboratory.*—A magnetoelectric effect in germanium due to absorption of infrared radiation has been investigated in the temperature range of 300°K to 500°K. Samples of different conductivity type and different impurity content have been irradiated with infrared radiation above 2μ and a magnetoelectric effect of up to 30 μv at 1000 gauss has been measured. The incident radiation, the observed voltage between the ends of the semiconductor, and the direction of the magnetic field are perpendicular to each other. The experimental apparatus and problems for measuring the effect are discussed. Data on the variation of this effect with carrier type and density as a function of sample temperature are reported. Special arrangements (surface condition of sample, radiation source, etc.) assure that photoconductive, photoelectromagnetic, and Dember effects are negligible in comparison to the new magnetoelectric effect which apparently is caused by lattice absorption of the photons. The relation between this effect and the Nernst effect[1] outside the phonon-drag region and other magnetoelectric effects is indicated.

[1] H. Mette, W. W. Gaertner, and C. Loscoe, Phys. Rev. 115, 537 (1959).

WA11. Effective Mass Shifts in Cyclotron Resonances in Uniaxially Stressed Silicon. J. C. HENSEL, *Bell Telephone Laboratories.*—Subsequent to observations[1] of cyclotron resonances in the valance bands of silicon split by uniaxial stress, further investigation shows shifts in effective mass with changes in stress. The experiments were done at ~9000 Mc/sec and at 1.26°K on 5000 ohm-cm p-type samples subjected to uniaxial stresses up to 2200 kg/cm^2. Using white tungsten light to generate carriers, the stress-induced shifts were measured to be $\Delta m_\perp/\Delta T=+0.94\times10^{-6}$ cm^2/kg and $\Delta m_{\parallel}/\Delta T=-3.4\times10^{-6}$ cm^2/kg for stress T along the [001] axis, and $\Delta m_\perp/\Delta T=+22.9\times10^{-6}$ cm^2/kg and $\Delta m_{\parallel}/\Delta T=-8.25\times10^{-6}$ cm^2/kg for stress along the [111] axis. Extrapolation to zero stress gives the effective masses $m_\perp=0.2612\pm0.0002$, $m_{\parallel}=0.2010\pm0.0005$, and $m_\perp=0.3780\pm0.0005$, $m_{\parallel}=0.1412\pm0.0005$ for the [001] and [111] cases, respectively. The revised values for the valance-band inverse mass parameters are, accordingly, (in units of $\hbar^2/2m$) $A=-4.21\pm0.01$ and $|B|=0.86\pm0.02$ from the [001] case, and $A=-4.13\pm0.01$ and $|N|=8.87\pm0.04$ from the [111] case. Additional small line shifts are found to arise from the spectral distribution of the illumination. Measurements with monochromatic light show a decrease in the cyclotron mass for radiation near the band gap. This effect may be responsible for the remaining difference between the above quoted values for A.

[1] J. C. Hensel and G. Feher, Phys. Rev. Letters 5, 534 (1960).

WA12. Electron Spin Relaxation in Phosphorus-Doped Silicon. T. CASTNER, *General Electric Research Laboratory.*—Spin-lattice relaxation of phosphorus donor electrons in a silicon sample containing 9×10^{16}/cm^3 phosphorous impurities has been investigated between 4.2°K and 20.4°K at 9.3 kMc. The steady-state saturation method was used between 20.4°K and 10°K, and fast passage techniques were used between 10°K and 4.2°K to measure T_s ($\Delta M_s=\pm$, $\Delta M_I=0$ process). The T^{-7} temperature dependence of T_s found by Feher[1] is shown to continue up to 6.5°K. Between 6.5°K and 8.3°K the temperature dependence can best be fit by $T_sT^n=$constant, with $12<n<14$. Analysis of the saturation curves taken between 10°K and 20.4°K on the basis of the Portis theory[2] for inhomogeneously broadened lines assuming $T_1=T_2$ yields an exponential dependence of T_s on temperature. The dependence of T_s on the direction of the static magnetic field with respect to the crystallographic axes will also be considered. The results will be interpreted in terms of various Raman-type relaxation processes based on relaxation taking place via the intervalley states of the phosphorus donor electrons.

[1] G. Feher and E. A. Gere, Phys. Rev. 114, 1245 (1959).
[2] A. Portis, Phys. Rev. 91, 1071 (1953).

WA13. Pressure Energy, Source of Motive Power in the Pressure Theory of Thermo- and Photoelectricity. MILTON GREEN, *Burroughs Laboratories.*—The mathematical formulation of the pressure theory[1] of the thermoelectric and photoelectric effects is based on the hypothesis that the motive forces responsible for these effects are due to pressure gradients of holes, electrons, and phonons. For a nondegenerate semiconductor the pressures—P_p of holes, P_n of electrons—behave like ideal vapors, namely, $P_p=pkT$ etc. The energy density due to the pressure is proportional to it ($\frac{3}{2}P$ for an ideal monotonic gas) so that the flow of charge carriers down the pressure gradient, in accordance with the hypothesis $I_p=-\mu_p$ grad P_p etc., consititues a flow of energy from a region of higher energy density to a region of lower energy density (in agreement with the laws of thermodynamics). Charges flowing down the pressure gradient *against* an electrostatic field convert *pressure energy* into *electrostatic* energy, and conversely. Reversible equilibrium, $I_p=I_n=0$, is governed by a conservation type equation, namely, the sum of the electrostatic energy and the *pressure electromotive force energy* of a charge carrier is constant, i.e., $eV+kT\ln p=$const for holes, similarly for electrons.

[1] Milton Green, Bull. Am. Phys. Soc. 6, 28 (1961).

THURSDAY MORNING AT 9:30

Adams-Hamilton Room

(J. A. WHEELER presiding)

Theory, VII: General Theory, Mostly Relativity

WB1. Homogeneous Transformations. JANE ROBERG, *U. S. Naval Ordnance Laboratory* (introduced by J. H. Rosenbloom).—The Hamilton-Jacobi formalism in classical mechanics is based on the ordinary contact transformations. If one considers instead the homogeneous contact transformations to be basic, one obtains a theory which is distinct from that of Hamilton and Jacobi but which nevertheless bears a strong resemblance to it. The theory of doubly homogeneous

transformations has been developed, including tensor analysis. The most striking thing to come out of the equations is spinor analysis. Antisymmetric tensors play an essential role quite apart from that of the symmetric tensor. In fact, the theory has been developed so far without introducting a symmetric tensor so that it is completely nonmetrical in character. In order to have application to physics, symmetric tensors must be introduced.

WB2. Fundamental Postulates of the Special Theory of Relativity. M. Z. v. KRZYWOBLOCKI, *Michigan State University.*—The author proves that the two fundamental postulates of the special theory of relativity, i.e., the constancy of the speed of light and the invariance of the metric in the four-dimensional space, are not necessary for the validity of the main result of the special theory of relativitity, the equivalence of mass and energy.

WB3. Covariant Dynamics of Spinning Particles. G. SZAMOSI, *National Research Council, Ottawa.**—A system of equations describing the motion of a classical spinning particle is solved. The covariant solution is a helix-like curve in space-time. The axis of the helix lies along a time-like direction, while the circular sections of the helix are in spacelike planes. In the special system in which the three-momentum of the particle vanishes, the motion reduces to the Hönl-Papapetrou-Weysenhoff classical Zitterbewegung. The invariant phase occuring in the space-like circular motions may be expressed by means of the four coordinates of the time-like motion (translation). The wave number in the phase turns out to be proportional to the momentum of the translation.

*On leave from the Department of Physics, Israel Atomic Energy Commission, Rehovoth, Israel.

WB4. Electromagnetic Radiation by Electrically Charged Bodies in Gravitational Fields. WILLIAM H. CHERRY, *RCA Laboratories.*—Fundamental objections may arise when considering charged bodies under gravity within the framework of general relativity. Local equivalence implies that in a uniform gravitational field a freely falling body will not radiate. In a central field, as shown,[1] space-time curvature causes nonradiation electromagnetic field reaction to deflect the body from a geodesic. It therefore radiates. This argument includes orbital motion, but in spite of unsatisfactory features—dependence of radiation on mass, and radiative ineffectiveness of the oscillating charge—no obvious paradox is obtained because kinetic energy is always available to supply radiant energy. If, instead, the body is held stationary, equivalence implies a direct radiation process, as in eternal uniform acceleration, but no conceivable source of energy. However, there are difficulties of analysis and in formulating the essential operational procedure for extracting energy. More tractable is the case of oscillatory free fall through a diameter of the earth, with arrested motion for fixed periods at either extremity. This seemingly provides an unending source of extractable energy, which might be taken as reason for invalidating the space-time metric description of gravity.

[1] B. S. DeWitt and R. W. Brehme, Ann. Phys. 9, 220 (1960).

WB5. New Solution to the Einstein Field Equations.* JOHN STACHEL, *Lehigh University.*—Ehlers and Jordan,[1] generalizing the work of Beck[2] and Einstein and Rosen,[3] have shown the form that the empty-space field equations take when wave fronts with cylindrical symmetry occur. A solution of these equations is presented. In contrast to solutions of linear wave equations with cylindrical wave fronts, and to the Einstein-Rosen solutions, pulse solutions of this type do not develop "tails" in their wake, and are never purely wavelike, but contain a static part. The use of several proposed energy-momentum complexes to evaluate the energy flux carried by these waves is shown to lead to contradictory results. The Riemann tensor and polarization properties of this solution are discussed.

* Supported in part by the National Science Foundation.
[1] P. Jordan, *Research on the Theory of Relativity* (Aeronautical Research Lab. WCLJ TN 88-1.)
[2] G. Beck, Z. Physik **33**, 713 (1925).
[3] A. Einstein and N. Rosen, J. Franklin Inst. **223**, 43 (1937).

WB6. On Spherically Symmetric Solutions to the Field Equations of the Generalized Theory of Gravitation. R. D. WOODS, *University of Miami.*—The field equations for one of the spherically symmetric field types of Kursunoglu's version of Einstein's generalized theory of gravitation[1] have been investigated. These four equations reduce to three which are linearly dependent, hence two second-order equations remain to be solved, leaving, as expected, one of the field quantities to be chosen arbitrarily. This system of equations, which are nonlinear and contain the independent variable r, have two types of singular points, one for $r=\infty$, and the other for $r=0$. Series expansions, in powers of $1/r$, of the solutions shows that for r large, g_{23} goes as ϵ/r^2, while the symmetric part of g approaches Schwarzschild's solution. The preliminary results of an attempt to find numerically, with the aid of an electronic computer, solutions that have no singularity at $r=0$ will be presented.

[1] B. Kursunoglu, Nuovo cimento **15**, 729 (1960).

WB7. Group-Theoretical Considerations Concerning the Construction of Lorentz-Covariant "Observables" in General Relativity.* PETER G. BERGMANN, *Syracuse University.*—It has been suggested that the dynamical variables of general relativity should preferably be invariant with respect to gauge-type coordinate transformations, but noninvariant with respect to Lorentz-type transformations, both homogeneous and inhomogeneous. Such a program is feasible only if the totality of all transformations to be considered is a nonsimple group, that is, one which contains the gauge-type transformations as a normal subgroup. Such nonsimple groups can in fact be found, though there is some question as to whether they have the structure desired. The construction of dynamical variables with the transformation properties indicated will also be discussed.

* Work supported by the National Science Foundation and by AFOSR and WADD of the U. S. Air Force.

WB8. Spacelike Hypersurfaces in Quantized General Relativity.* JAMES L. ANDERSON, *Stevens Institute of Technology.*—In the general theory of relativity the metric tensor $g_{\mu\nu}$ describes not only the gravitational field but the geometry of the space-time manifold as well. As a consequence, the setting up of the initial value problem on the initial hypersurface is especially difficult, since the metric must be so chosen that the initial hypersurface is indeed spacelike and will remain so for at least a finite time into the future. In the quantum version of the theory we must likewise require that the initial hypersurface of each member of the ensemble corresponding to a given state functional be everywhere spacelike. Since the range of values of the $g_{rs}(r, s=1, 2, 3)$ is unrestricted, it would seem at first sight that very few state functionals would satisfy our requirement. We can overcome this difficulty by imposing the coordinate conditions $g_{12}=g_{23}=g_{31}=0$ and using as new field variables the quantities $g_1=\ln g_{11}$, etc. Then, even with unrestricted fluctuations of the g_i, two neighboring points for which $dx^0=0$ will always be spacelike.

* Supported in part by Wright Air Development Division, U. S. Air Force.

WB9. Spin-Statistics Theorem.* R. ARNOWITT, *Syracuse University,* AND S. DESER, *Brandeis University.*—A derivation of the connection between spin and statistics is obtained on

the basis of the specific set of postulates of the Schwinger action principle. These include that (1) the Hilbert space metric is positive-definite, (2) local commutativity and (3) proper Lorentz invariance hold, (4) the fields have local interactions, and (5) variations of field amplitudes either commute or anticommute with the fields themselves. Neither positive-definiteness of the Hamiltonian nor TCP invariance need then be involved to obtain the connection for charged and neutral spin 0 to 1 and for neutral spin $\frac{1}{2}$. Either of the last named assumptions may be used to guarantee the proper connection for the charged spin $\frac{1}{2}$ field, where the purely algebraic consistency proof used in the other cases is not sufficient.

* Supported in part by the National Science Foundation and Air Force Office of Scientific Research.

WB10. Generalized Free Fields and Local Field Theory Models. O. W. GREENBERG.* *M.I.T.*—A generalized free field $\phi(x)$ is a field which has a c-number commutator, and which has a positive frequency part which annihilates the vacuum. Each ϕ is specified by the Lehmann weight of its commutator. Such a ϕ satisfies the axioms of local field theory, transforms as a Heisenberg field under a representation U, which we exhibit, of the inhomogeneous Lorentz group, but has asymptotic fields which are not a complete set of fields. Given a ϕ, we construct a set of models which satisfy the axioms of local field theory, are not unitarily equivalent to any ϕ, transform as a Heisenberg field under the representation U which belongs to that ϕ, have S-matrix equal to 1, but are not in the Borchers class[1] of any ϕ. These models are specified by the Lehmann weight of their ϕ together with an arbitrary function of two variables. If the ϕ is chosen to be a mass m free field $\phi_0(x)$, the model reduces to a Wightman polynomial in ϕ_0.

* National Science Foundation Postdoctoral Fellow.
[1] H.-J. Borchers, Nuovo cimento 15, 784 (1960).

WB11. Triondynamics' Explanation of Geometrodynamics. JOSEPH G. BARREDO, *C.S.I.C.*—The chronosuperconductivity effect[1] explains geometrodynamics by demonstrating that the motion equation of mass-energy is $dx/dt = dn/dt = N^2 t^{-4}$, where t = time and N = number of charges. Furthermore, it defines the observable x as the fusion of two charges within a trion made up of three charges in a row, the middle one being of different sign than the other two. Triondynamics demonstrates: (1) the suggestion of Einstein, Podolsky, and Rosen that "wave function does not provide a complete description of physical reality,"[1] (2) Einstein's prediction that the basic equation of physics must be nonlinear and that mathematical physics will have to be redone, (3) that modern mathematical logic's preoccupation with classes and sets, i.e., with purely static entities, debars it from competence to explain reality, (4) that Euclid's negative definition of "line" is not improved by Peano's parametric equations based on Cantor's notion of equality of number between two sets of physical objects. This is why we use the word "row" in defining the trion, rather than "line". "Line" must be defined in terms of "observable," not vice-versa.

[1] J. A. Wheeler, Revs. Modern Phys. 33, 63 (1961); D. R. Inglis, *ibid.* 33, 1 (1961); J. G. Barredo, Naturwissenchaften 5, 546 (1956), Bull. Am. Phys. Soc. 5, 427 (1960).

THURSDAY AFTERNOON AT 1:30

Sheraton Hall

(W. V. HOUSTON presiding)

Invited Papers

X1. Lithium, Beryllium, and Boron in the Primary Cosmic Radiation. M. M. SHAPIRO, *U. S. Naval Research Laboratory.* (30 min.)

X2. Sources of X-Ray Emission in the Sun's Atmosphere. HERBERT FRIEDMAN, *U. S. Naval Research Laboratory.* (30 min.)

X3. Proton Energy-Spectra of the Inner Van Allen Belt. J. E. NAUGLE, *NASA Goddard Space Flight Center.* (30 min.)

THURSDAY AFTERNOON AT 1:30

Continental Room

(J. L. FOWLER presiding)

Nuclear Reactions, VII (Including Fission)

XA1. Gamma Yield From the Proton Bombardment of Tritium.* CALVIN C. GARDNER AND JOHN D. ANDERSON, *Lawrence Radiation Laboratory, Livermore.*—The Livermore 90-in. variable-energy cyclotron has been used to measure the 90° excitation function for the $T(p,\gamma)He^4$ reaction, for proton energies between 5.8 and 9.2 Mev. In addition, γ-ray angular distributions were measured at $E_p = 5.8$, 6.4, 7.7, 8.4, and 9.2 Mev. The γ radiation was produced in a 0.12-Mev-thick tritium gas target and detected in a 5-in.-diam by 6-in.-long NaI(Tl) crystal. No evidence was found for the excited states of He^4 recently reported by Milone.[1]

* Work done under the auspices of the U. S. Atomic Energy Commission.
[1] C. Milone, Phys. Rev. 120, 1302 (1960).

XA2. Angular Distributions of Neutrons From the $T(p,n)He^3$ Reaction. W. E. WILSON, R. L. WALTER, AND D. B. FOSSAN, *University of Wisconsin.**—Angular distributions of the neutrons from the $T(p,n)He^3$ reaction have been obtained at about $\frac{1}{2}$ Mev intervals from 5–13 Mev bombarding energy. Measurements were made at intervals of 10 deg up to 140 deg in the lab. Absolute cross sections were obtained by normalizing at 0° to telescope measurements of the forward yield.[1] A stilbene scintillator with pulse shape discrimination was used as a detector. Differential cross sections in the center-of-mass system have been fitted with a series of Legendre polynomials. Polynomials up to order 4 are sufficient to fit

the data in the energy region covered. When the angular distributions are integrated over solid angle, it is found that the total cross section varies approximately as E^{-1} in the region investigated. The agreement with other measurements of the angular distributions is satisfactory.[2]

* Work supported by the U. S. Atomic Energy Commission and the Wisconsin Alumni Research Foundation.
[1] W. E. Wilson, D. B. Fossan, and R. L. Walter, Bull. Am. Phys. Soc. 5, 410 (1960).
[2] M. D. Goldberg, J. D. Anderson, J. P. Stoering, and C. Wong, Bull. Am. Phys. Soc. 6, 60 (1961); and private communication.

XA3. Polarization of Protons From the $He^3(d,p)He^4$ Reaction.* R. I. Brown and W. Haeberli, *University of Wisconsin.*—The polarization of protons in the $He^3(d,p)He^4$ reaction has been measured from 20° to 100° for 6 and 8 Mev deuterons. The target was a 0.5-cm diameter cylinder with walls[1] 2.6 μ thick, containing He^3 at 16 atm. Left-right asymmetries of protons elastically scattered from carbon at a laboratory angle of 44° were measured with NaI crystals. Polyethylene foils were used to slow down the protons to an energy region where the analyzing power of carbon[2] is known. The $He^3(d,p)He^4$ polarization is positive (with respect to $\mathbf{k}_{in}\times\mathbf{k}_{out}$) for forward angles with maximum values at 30° ($+0.53\pm0.03$ at 6 Mev and $+0.82\pm0.05$ at 8 Mev), and negative for $\theta_{lab}>60°$ with maximum values at 100° (-0.66 ± 0.06 at 6 Mev and -0.06 ± 0.10 at 8 Mev). The uncertainties quoted are statistical errors in the present measurements only. Instrumental asymmetries lead to false polarizations no greater than ±0.04.

* Work supported by the U. S. Atomic Energy Commission and the Wisconsin Alumni Research Foundation.
[1] "Havar" foil, a high tensile strength alloy supplied by Hamilton Watch Company, Lancaster, Pennsylvania.
[2] S. Yamabe *et al.*, J. Phys. Soc. Japan 15, 2154 (1960).

XA4. Source of Polarized Deuterons. J. E. Sherwood, S. J. Ovenshine, and R. F. King, *Oak Ridge National Laboratory.*—The ORNL polarized ion source[1] consists of a Woods tube dissociator followed by a Stern-Gerlach polarizer and electron-bombardment ionizer. For the case of deuterium, the magnetic deflection permits selectron of either the $m_j=\frac{1}{2}$ or $m_j=-\frac{1}{2}$, ($m_i=0$, ±1) strong-field stomic states. When these states are ionized, the resultant deuteron spin populations are such as to yield a polarization of $\frac{1}{3}$. A convenient test for deuteron polarization, as pointed out by Galonsky, Willard, and Welton,[2] is to look for anisotropy in the neutron yield of the $T(d,n)He^4$ reaction. We have observed this anisotropy at a deuteron energy of 115 kev. At present, the polarized ion current is about 10^{-9} amp. The apparatus and its limitations will be discussed.

[1] Bull. Am. Phys. Soc. Ser. 5, 441 (1960).
[2] A. Galonsky, H. B. Willard, and T. A. Welton, Phys. Rev. Letters 2, 349 (1959).

XA5. Angular Correlation Chamber.* R. Weinberg, H. M. Dowds, and L. J. Lidofsky, *Columbia University.*—A 48-in.-diam angular correlation chamber has been built with independent angular motions provided for two counters. Counter "A" can be set remotely to any polar angle in the horizontal plane, while counter "B" can be positioned to any polar angle and to azimuthal angles of 120° to −120° as measured from the vertical plane. The motions are controlled and indicated by "Slo-Syn"[1] motors which permit the setting of angles in the horizontal plane with an error $<0.03°$, and in the vertical plane with an error $<0.1°$. Other features of the chamber and its mechanisms will be discussed.

* This work partially supported by the U. S. Atomic Energy Commission.
[1] Superior Electric Company, No. SS50-P1.

XA6. Reaction Cross Sections for Alpha Particles.* J. R. Huizenga, R. Vandenbosch, and H. Warhanek, *Argonne National Laboratory.*—The total fission cross sections have been measured for U^{238} and U^{232} targets bombarded with 18–43 Mev helium ions. Uniform targets were prepared by volatilization and electrodeposition and their thicknesses determined by α-particle counting and pulse height analysis. The fission fragments are detected with solid state counters in a small evacuated scattering chamber. The solid angles of the detectors are established with collimators and the cross section calculations utilize previous fission-fragment anisotropy measurements.[1] These targets were chosen because their fission cross sections represent most of the reaction cross section and, in addition, the spallation cross sections are known. The experimental reaction cross sections will be compared with those determined from optical model calculations[2] which utilize a complex nuclear potential derived from α-particle elastic scattering.

* Based on work performed under the auspices of the U. S. Atomic Energy Commission.
[1] R. Vandenbosch, H. Warhanek, and J. P. Huizenga, Bull. of Am. Phys. Soc. 5, 410 (1960).
[2] J. R. Huizenga and G. Igo (unpublished).

XA7. Delayed Gamma Rays from the Photodisintegration of U^{238}.* R. B. Walton, E. Haddad, J. C. Young, and C. W. Cook, *General Atomic.*—Delayed gamma-ray intensities have been measured from 30 μsec to 8 sec after the photodisintegration of U^{238}. A sample of U^{238} was placed in a well-collimated beam of x rays which were produced by bombarding a thin tungsten target with 5-μsec-wide pulses of 20-Mev electrons. A plastic scintillation detector was used to detect all delayed gamma rays having energies greater than 250 kev. The observed gamma-ray intensity falls with an apparent half-life of about 80 μsec in the interval from 30 μsec to 800 μsec, then remains almost constant for times up to 0.1 sec. After 0.1 sec, the intensity decreases at a rate consistent with previous measurements of delayed gamma rays from the thermal neutron fission of U^{235}. Gamma rays observed in this experiment probably resulted from the decay of fission products formed by U^{238} photofission; however, the possibility that the decay of U^{238} (γ,n) and $(\gamma,2n)$ reaction products contributed to the observed signal cannot be excluded. Measurements repeated with a 510-kev bias showed the same initial decay characteristic. In an attempt to evaluate neutron backgrounds using a mercury sample, gamma rays with energies less than about 510 kev and an apparent half-life of 102 μsec were observed.

* Work conducted under a U. S. Air Force contract.

XA8. Additional Long-Range Particles from the Spontaneous Fission of Cf^{252}.* H. E. Wegner, *Los Alamos Scientific Laboratory.*—A dE/dx and E mass identification detector system was used to observe long-range particles from the fission of Cf^{252}. The mass and energy scales of the detector system were calibrated with various reaction particles from light nuclei bombarded with 28-Mev α particles. More than 100 events corresponding to tritons were observed. The energy spectra of the deuterons and He^3 particles were not measured, and their association with the fission process rather than background effects has not been definitely established. The onset of the proton and triton energy spectra occurs at 5.5 ± 1.0 Mev; the spectra then rise rapidly to a maximum at 8.5 ± 1.0 Mev and gradually decrease to zero at 16 ± 1 Mev. With a long-range α-particle relative yield of 100, the proton yield is 2.2 ± 0.5; deuterons, <0.5; tritons, 6.0 ± 0.5; and He^3 particles, <0.5. The triton yield is in qualitative agreement with that of Watson.[1] Possible origins of these particles and further diagnostic experiments will be discussed.

* Work supported by the U. S. Atomic Energy Commission.
[1] J. C. Watson, Phys. Rev. 121, 230 (1961).

XA9. Delayed Gammas from Fission, I.* Philip C. Fisher, *Lockheed Missiles and Space Division and Los Alamos Scientific Laboratory,* and Leon B. Engle, *Los Alamos Scientific Laboratory.*—Measurements[1] have been made of the variation in

time and energy of the delayed gammas emitted between 0.15 Mev and 6.5 Mev after almost instantaneous neutron-induced fission. Seventeen bin distributions of the absolute number of photons/Mev/sec/fission have been derived from the overlapping sets of 100-channel pulse height analyzer data. Photons below 6.5 Mev were detected in five short time intervals between 0.2 sec and 45 sec after fast neutron fission of Th^{232}, U^{233}, U^{235}, U^{238}, and Pu^{239}. Furthermore, the time decay of gammas above several fixed pulse height biases was followed from 0.3 sec to 300 sec after fission. Some data from fast neutron fission of U^{234}, U^{236}, Np^{237}, and Pu^{240}, and thermal fission of U^{233}, U^{235}, and Pu^{239} also were obtained. Typical time decay and pulse height distribution data will be presented. The variation with time and the time integrated values of the number of photons/fission will be given for the first five isotopes listed above.

* Work performed under the auspices of the U. S. Atomic Energy Commission.
[1] P. C. Fisher, M. P. Kellogg, P. G. Koontz, and L. B. Engle, Bull. Am. Phys. Soc. **4**, 31 (1959).

XA10. Delayed Gammas from Fission, II.* LEON B. ENGLE, *Los Alamos Scientific Laboratory*, AND PHILIP C. FISHER, *Lockheed Missiles and Space Division and Los Alamos Scientific Laboratory* (introduced by Philip C. Fisher).—A response matrix has been constructed for the 4 in.×4 in. NaI total-absorption crystal spectrometer used for the measurements of Part I. The matrix was derived from line shapes obtained by measuring the gammas emitted by nine different radioactive sources and three different $(p,\alpha\gamma)$ reactions. Photon spectra were then derived by applying this matrix to the experimental data. So far no smoothing techniques have been employed. The following photon distributions will be intercompared: (a) one isotope for the five time intervals after fission, and (b) the five standard isotopes for one time interval after fission. Least-squares fits to the time-decay data have been used to determine apparent relative abundances, a_i, and periods, τ_i. Sets of a_i, τ_i for each of the five standard isotopes for eight different pulse height intervals were found. A comparison will be given of the relative rates of decay of the standard isotopes.

* Work performed under the auspices of the U. S. Atomic Energy Commission.

XA11. Fission Fragment Kinetic Energy Distributions for the Less Fissionable Elements.* R. VANDENBOSCH AND J. R. HUIZENGA, *Argonne National Laboratory*.—Kinetic energy distributions for deuteron and helium ion-induced fission of Bi, Pb, Tl and Au have been measured using surface barrier solid state detectors.[1] The kinetic energy distributions are symmetric and quite narrow. Comparison with mass distributions[2,3] for these elements shows that the width of the kinetic distributions arises in large part from the mass distribution. Total kinetic energies have been obtained by calibrating the detectors with Cf^{252} spontaneous fissions.

* Work performed under the auspices of the U. S. Atomic Energy Commission.
[1] We are indebted to D. M. Sparlin for supplying the solid state detectors.
[2] A. W. Fairhill, Phys. Rev. **102**, 1335 (1956).
[3] E. F. Neuzil, Ph.D. thesis, University of Washington, 1959 (unpublished). See R. C. Jensen and A. W. Fairhall, Phys. Rev. **118**, 771 (1960).

XA12. Fission Energetics of Th^{232}.* A. B. SMITH, A. M. FRIEDMAN, P. R. FIELDS, AND R. G. NOBLES, *Argonne National Laboratory*.—The distribution of the kinetic energy of fragments emitted as a result of the neutron-induced fission of Th^{232} has been determined. Incident neutron energies of 1475±35 kev and 1600±35 kev were used to observe fission below and at the peak of the large neutron resonance. The distributions at the two incident neutron energies are the same within the experimental errors. The measured total average fragment kinetic energy was 155±4.5 Mev. The most probable fragment mass ratio is 1.47±0.05, and the average kinetic energies of the light and heavy fragments are 95±2 and 60±3 Mev, respectively. The experimental results are related to the known systematics of neutron induced and spontaneous fission. The effect of collective nuclear rotations at the saddle point is discussed with particular emphasis on fission from specific rotational bands.

* Based on work performed under the auspices of the U. S. Atomic Energy Commission.

XA13. Dependence of Neutron Production in Fission on Rate of Change of Nuclear Potential. ROBERT W. FULLER, *Princeton University*.—Most prompt neutrons from fission are thought to come from separated fission fragments excited during scission. Can some come out in a prior process: excitation of individual nucleons in the dividing nucleus by nonadiabatic changes in the nuclear potential? J. A. Wheeler has raised the question: Can enough energy be transferred to some neutrons by the nonadiabatic distortion of the potential as the nucleus fissions to free them? To study this possibility we consider a square well containing a Fermi sea of nucleons in the middle of which is "erupting" an inverted square well "volcano." It rises and divides the original square well into the two fission fragments. The energy transferred to the nucleons can be calculated analytically for the two limiting cases, adiabatic and sudden changes of potential. The transition between these limiting situations has been studied on a computer. One finds that both the number of particles ejected and the mean energy transfer possess maxima for intermediate rise time T. This is reminiscent of the behavior of the mean energy transfer of a harmonic oscillator whose equilibrium position is jerked. For a particular model the fraction of nucleons that escapes for $T=10^{-22}$ sec is 0.13.

THURSDAY AFTERNOON AT 1:30

Franklin Room

(E. V. HAYWARD presiding)

Y. Post-Deadline Papers, if Any

THURSDAY AFTERNOON AT 1:30

National Bureau of Standards, East Building

(R. F. POST presiding)

Plasma, III

YA1. Frequency Dependence of Plasma Acceleration by rf Field Gradient.* G. A. SWARTZ, *RCA Laboratories*, AND T. T. REBOUL AND G. D. GORDON, *RCA Astro Electronics Division*.—Previous work[1] has shown that a plasma can be accelerated by an rf field gradient. Experimental confirmation was obtained by measuring the transit time of plasma elec-

trons between two probes. In the present work the transit time of the plasma ions was measured. The ion velocity showed a hyperbolic dependence on the maximum rf field amplitude which is consistent with the previous theory. To determine the frequency dependence, measurements were made at 140 and 330 Mc; the kinetic energy imparted by the rf field was found to be inversely proportional to the applied frequency. A comparison of the experimental data with the theory indicates that the ratio of the plasma frequency to the applied frequency was approximately unity. 500-kc oscillations in the ion current to the detection probes were observed when large rf fields were applied. The amplitude of oscillation decreased strongly when a magnetic field of ten gauss was applied in the rf field-plasma interaction region.

* Supported by ARPA through the U. S. Air Force Office of Scientific Research under contract.
[1] G. A. Swartz, T. T. Reboul, G. D. Gordon, and H. W. Lorber, Phys. Fluids 3, 973 (1960).

YA2. Electromagnetic Diffusion into a Cylindrical Plasma Column during the Early Stages of Pinch Formation.* JOSEPH L. NEURINGER, LESTER KRAUS, AND HERBERT MALAMUD, *Republic Aviation Corporation.*—The diffusion of electromagnetic energy into a cylindrical plasma column due to the discharge of the energy stored in a capacitor is formulated taking into account the effects of the capacitance and inductance of the discharge circuit. The discharge circuit reflects the linear pinch geometry in that the energy source is a charged condenser and the return lead is a perfectly conducting cylindrical shell concentric with the surrounding the plasma column. The plasma properties enter the formulation through an extended Ohm's law which includes the time rate of change of current density. Under the assumption that changes in the ionization density and collision frequency may be neglected, Maxwell's equations lead to a third-order linear partial differential equation for the diffusion current. An exact solution is obtained by Laplace transform techniques using appropriate initial and boundary conditions which take into account the finite external circuitry. The spatial and temporal behavior of the current density distribution as functions of the parameters which characterize both the circuit and the plasma are discussed and compared with that of an ordinary conductor obeying the simple Ohm's law.

* This work was supported in part by the U. S. Air Force Office of Scientific Research.

YA3. Instability of a Resistive Sheet Pinch.* JOHN KILLEEN AND HAROLD P. FURTH, *Lawrence Radiation Laboratory, Livermore.*—A resistive sheet pinch is subject to flutelike hydromagnetic instabilities, aligned in the direction of current flow. The basic concept has previously been presented qualitatively in an astrophysical context,[1] and in the context of the sheet pinch.[2] A complete analysis has now been made of a model using an incompressible fluid of infinite extent, with a sheetlike region of finite (isotropic) conductivity representing the pinch. The procedure is to assume perturbations in the magnetic field and plasma velocity, which in the infinite conductivity approximation would lead to stable hydromagnetic oscillations, and calculate their resistive relaxation. We obtain a pair of partial differential equations for the first-order perturbations in the magnetic field and plasma velocity. These equations are solved numerically, using an IBM 709 code. Unstable relaxations are found for wavelengths large compared to the thickness of the sheet pinch.

[1] J. W. Dungey, *Cosmic Electrodynamics* (Cambridge University Press, New York, 1958), pp. 98–102.
[2] H. P. Furth, Bull. Am. Phys. Soc. 6, 193 (1961).

YA4. Synoptic Analysis of a Dynamic Pinch. M. C. CHAPMAN, *Northrop Corporation, Norair Division,* AND RICHARD L. MOORE, *Richard L. Moore Consultants.*—The dynamic pinch experiments of Burkhardt and Lovberg[1] are shown to agree with a Gaussian density distribution with a vacuum plasma interface which moves radially under the action of the applied forces. Laws of continuity of motion and material are applied to obtain a self-consistent analysis of the motion. The interface is located by a variety of techniques based on the discontinuities of both hydrodynamics and Maxwell's equations. Use is made of the fields of $\partial\mathbf{B}/\partial t$, the discontinuity at the interface between the smooth internal function and the smooth external function of (a) $\mathbf{k}\cdot\nabla\times\mathbf{H}$ and (b) $1_0\cdot\nabla^2\mathbf{H}$. In addition, important information may be deduced from the variation of $1_0\cdot\nabla\times\mathbf{H}$ and $\mathbf{k}\cdot\nabla^2\mathbf{H}$. The existence of a snowplow density distribution at the interface is not substantiated by the experimental analysis.

[1] L. C. Burkhardt and R. Lovberg, in *Proceedings of the Second United Nations International Conference on the Peaceful Uses of Atomic Energy* (United Nations, New York, 1958), Vol. 32.

YA5. Acceleration of a Stabilized Pinch in a Rail Gun.* M. O. STERN, C. L. OXLEY, N. A. KRALL, R. L. MORSE, AND R. R. WILSON,† *General Atomic.*—Stabilization against Rayleigh-Taylor accelerative instabilities in a rail gun can theoretically be achieved[1] by incorporating a B_z field perpendicular to the rail faces in the plasma. In our gun, this has been accomplished in a stabilized pinch geometry, which also allows assembly and full ionization of the gas before acceleration. At one end of longitudinally slotted rails a B_z field is applied, and a hollow elliptical cylinder of gas is injected. Electrodes in the gas inlet provide preionization. Pinch current, fed to the gas symmetrically, rises in 5 μsec. A fast condenser system (1 μsec rise) applied to the rail ends accelerates the plasma. During acceleration, the width of the pinch is held constant by the locking of the B_z in the rail system. The back face of the pinch is accelerated by transverse fields, stabilized by B_z; the front face is accelerated by B_θ, stabilized by transverse fields. Pickup coils show reproducible trapping of the B_z field and its transport 50 cm to the end of the rails. Further diagnostic information will be given.

* This work supported by General Atomic and Texas Atomic Energy Research Foundation.
† Cornell University.
[1] Albares, Krall, and Oxley (submitted to Phys. Fluids).

YA6. Experiments With a Rail-Type Plasma Accelerator Using Ferrite Cores.* THOMAS L. THOURSON AND JOHN R. BASKETT, *Borg-Warner Corporation.*—A simple rail-type plasma accelerator[1] in which the plasma electrically connects the two parallel rails during acceleration has a basic weakness in that the accelerating magnetic field diverges to the side. The plasma, being diamagnetic, tends to migrate to the weaker part of the field, that is, to the side. Thus, a portion of the plasma soon passes out of the influence of the magnetic field and the plasma will eventually lose its identity. The diverging magnetic field lines can be straightened if the accelerator is surrounded with ferrite-core material reducing the tendency for the plasma to leak to the side. Experiments were performed using rail accelerators with and without a ferrite core. The plasma was metal derived. Results showed an increase in plasma mass although the plasma kinetic energy was unchanged. From these results one can conclude that the collimation of the plasma mass was improved.

* Supported in part by the Air Research and Development Command, Wright Air Development Division, U. S. Air Force.
[1] Korneff, Nadig, and Bohn, *Conference on Extremely High Temperatures* (John Wiley & Sons, New York, 1958).

YA7. Apparent Observation of Ionic Sound Waves in a Plasma. IGOR ALEXEFF AND RODGER NEIDIGH, *Oak Ridge National Laboratory.**—Oscillations have been observed in a magnetically supported cylindrical rod of plasma. An oscillation can be quite pure in frequency. Harmonics can also be excited alone. Radio frequency amplitudes of more than 20 v have been seen on a probe. The oscillation appears to be produced by a longitudinal standing ionic sound wave. The fre-

quency is given by the formula

$$f=\frac{1}{2l}\left(\frac{3kT_e}{m_i}\right)^{\frac{1}{2}}.$$

The electron temperature T_e is found to be roughly equal in energy to the first excitation potential in the un-ionized gas. The frequency dependence on ion mass m_i and on plasma column length l for ions of mass 1 to 201, and for columns of length 2.2 to 23.0 cm, will be discussed.

*Operated by Union Carbide Nuclear Company for the U. S. Atomic Energy Commission.

YA8. X-Ray Observations of Line Spectra from Highly Stripped Ions in a Magnetically Compressed Plasma.* F. L. RIBE, A. J. BEARDEN,† G. A. SAWYER, AND T. F. STRATTON, *Los Alamos Scientific Laboratory.*—A single-crystal x-ray diffraction spectrometer has been constructed and used to study the soft x rays emitted by the magnetically compressed Scylla plasma.[1] The diffracting element is a beryl crystal plate cut and ground parallel to the $10\bar{1}0$ planes ($2d=15.92$ KXU), polished and etched to give a uniform diffraction width of 40 sec of arc over its surface for Cu K_α radiation. When small amounts of oxygen are added to the deuterium gas of the discharge, spectral lines of the Lyman series of O VIII (series limit: 14.2 A) are observed. With neon added, lines of the singlet series, as well as intercombination transitions in the helium-like spectrum of Ne IX (series limit: 10.4 A) and Lyman lines of Ne X (series limit: 9.12 A) are observed. The Ne IX lines are observed to occur earlier during the magnetic compression than those of Ne X.

*Work performed under the auspices of the U. S. Atomic Energy Commission.
†Consultant, permanent address: Department of Physics, Cornell University, Ithaca, New York.
[1] K. Boyer, W. C. Elmore, E. M. Little, W. E. Quinn, and J. L. Tuck, Phys. Rev. 119, 831 (1960).

YA9. X-Ray Observations of the Emission Continuum from Scylla.* G. A. SAWYER, A. J. BEARDEN,† F. L. RIBE, AND T. F. STRATTON, *Los Alamos Scientific Laboratory.*—The beryl crystal diffraction spectrometer described in the previous paper has been used to measure the shape and intensity of the x-ray continuum spectrum from the magnetically compressed deuterium plasma of Scylla with no impurities added to the discharge gas. The shape of the continuum spectrum is found to be given by the function $\exp(-h\nu/kT_e)$, where the electron temperature thus determined is 345±40 ev. This temperature is larger than that deduced from previous x-ray absorption measurements.[1] The difference is accounted for by the presence of line radiation from wall impurities in the continuum wavelength region, whose effects are eliminated in the present measurements. In order to determine the absolute intensity of emission the reflection coefficient of the beryl crystal was determined over the range of wavelengths for which observations were made of the plasma x rays. This measurement was performed with characteristic line and continuum radiation from various targets in a demountable x-ray tube.

*Work performed under the auspices of the U. S. Atomic Energy Commission.
†Consultant, permanent address: Department of Physics, Cornell University, Ithaca, New York.
[1] F. C. Jahoda, E. M. Little, W. E. Quinn, G. A. Sawyer, and T. F. Stratton, Phys. Rev. 119, 843 (1960).

YA10. Experimental Evidence of Plasma Oscillations in Metals. P. R. WESSEL, *U. S. Naval Ordnance Laboratory.*—The radiation emitted from thin silver films, bombarded with 20 kev electrons, has been studied. This radiation exhibits the characteristics predicted by Ferrell[1] on the basis of plasma theory. Experimental results verify the existence of a strong peak in the radiation spectrum, occurring at the plasma frequency, which has the correct angular distribution and polarization for plasma radiation.

[1] R. A. Ferrell, Phys. Rev. 111, 1214 (1958).

YA11. Electron-Hole Plasma Pinching in *p*-type InSb. BETSY ANCKER-JOHNSON AND ROGER W. COHEN, *RCA Laboratories.*—Plasma pinching has been observed at 77°K in a single crystal of *p*-type InSb of hole density equal to 2.6×10^{15} cm^{-3}. A microsecond constant-current pulse was used to obtain the necessary electric fileds. Contacts to the sample were made in such a way that injection currents were essentially eliminated, or, on the other hand, were enhanced. The density of injected holes and electrons did not appreciably affect the current at which pinching began, which was about 2.5 amp (about 1250 amp/cm^2). The field strength at the onset of pinching, however, varied considerably with the quantity of injected holes and electrons, and has a maximum value of about 200 v/cm in the case of minimal injection. Pinch times of tenths of microseconds were measured, in agreement with theory.[1]

[1] M. Glicksman and R. A. Powlus, Phys. Rev. (to be published).

THURSDAY AFTERNOON AT 1:30

Cotillion Room, South

(V. W. HUGHES presiding)

Pions

Z1. Pion Photoproduction Recoil Nucleon Polarization Measurements Using Visual Detectors.* V. Z. PETERSON, *California Institute of Technology.*—Special problems exist in making measurements of the polarization of the recoil nucleon in pion photoproduction processes, such as $\gamma+p->p+\pi^0$, owing to the continuous energy spectrum of the incident bremsstrahlung. Knowledge of the scattering angle and energy loss of each scatter avoids systematic asymmetries and contamination of the sample by inelastic events The low flux of recoil protons (typically 10^7 less than cyclotron beams) involved in electron synchrotron pion photoproduction makes use of thin scatterers and good angular definition very difficult Use of bremsstrahlung cutoff to define inelasticity may introduce further asymmetries, and does not exclude all inelastic scatters. Visual scatterer-detectors (nuclear emulsion, nonhydrogen bubble chambers, and perhaps spark counters) have the advantages that individual scatters may be seen, obviously inelastic events can be readily eliminated, and the energy loss in the scattering process can be measured. Magnetic preselection does not introduce uncertainties in the scattering angle. Polarization in neutral pion photoproduction in the vicinity of the second resonance has been measured by nuclear emulsions and by propane bubble-chamber. Data will be presented for gamma-ray energies of 450 to 900 Mev and 90° c.m. production angle.

*This work was supported in part by the U. S. Atomic Energy Commission.

Z2. $\pi^-+p\rightarrow\pi^0+n$ Charge Exchange Cross Sections at 20.7 and 31.0 Mev.* K. MIYAKE, K. F. KINSEY, AND D. E. KNAPP, *The University of Rochester.*—A measurement has been made of the differential and total cross sections at 31.0 Mev and the total cross section at 20.7 Mev for the reaction $\pi^-+p\rightarrow\pi^0+n$. A thin-walled liquid hydrogen target was used. The gamma telescopes used a Čerenkov counter to identify the conversion electrons and a thin-lead converter to avoid complications from cascade processes. The angular distribution in mb/sr at 31.0 Mev is: $d\sigma/d\Omega=(1.00\pm0.02)[(0.51\pm0.04)-(0.61\pm0.11)P_1(\cos\theta)+(0.12\pm0.36)P_2(\cos\theta)]$. The total cross sections at 31.0 and 20.7 Mev are 6.5 ± 0.5 and 5.4 ± 0.4 mb, respectively. The data are also analyzed in terms of phase shifts. Assuming a linear momentum dependence of α_1 and α_3, the quantity $(a_1-a_3)=0.27\pm0.02$. This agrees with the prediction $(a_1-a_3)=0.245\pm0.01$[1] from photoproduction and the Panofsky ratio. There are theoretical and experimental grounds for a nonlinear behavior of α_3 and α_1, which would improve the agreement.

* This work partially supported by the U. S. Atomic Energy Commission.
[1] J. Hamilton and W. S. Woolcock, Phys. Rev. **118**, 291 (1960).

Z3. Interactions of 10 Bev/c π^- Mesons.* R. J. PREM, E. RAPOPORT, Y. PRAKASH, G. A. SNOW, AND P. H. STEINBERG, *University of Maryland.*—A stack of 42 emulsion pellicles ($40\times15\times0.06$ cm) was exposed to a negative secondary beam of 10 Bev/c at the CERN 25 Bev proton accelerator. The flux of beam particles was 2.5×10^4/cm^2. Scanning along beam tracks to locate interactions is in progress. Events in which only minimum tracks emerge from the point of interactions are given special attention. To date, 35 meters of beam track has been followed and 60 multiprong interactions have been found. This corresponds to a m.f.p. of 58 cm without correction for μ^- and e^- contamination in the beam. Further progress will be reported.

* This work is supported by the U. S. Atomic Energy Commission.

Z4. Meson-Nucleon Interactions in 10- to 1000-Bev Energy Range. P. L. JAIN, *University of Buffalo.*—A stack of nuclear emulsion consisting of 200 pellicles 60×30 cm, 600 μ thick, was exposed for 13 hr at 116 000 ft from Brownwood, Texas. By scanning the forward cone of half-opening angle of 1×10^{-2} rad around the shower axis of the singly charged and neutral high-energy jets with a dip angle $<17°$, we have recorded the charged and neutral secondary interactions which had five or more shower particles collimated in the forward direction of the original interactions. The angular distribution of shower particles by twenty nine charged and ten neutral secondary interactions was measured. These distributions will be discussed with respect to certain known models.

Z5. 1.97±0.06 Bev/c π^- Mesons in a Hydrogen Bubble Chamber. A. R. ERWIN, R. H. MARCH, AND W. D. WALKER, *Brookhaven National Laboratory and University of Wisconsin,* AND J. BALLAM, *Brookhaven National Laboratory and Michigan State University.*—Approximately 600 strange particle productions have been observed in a 1.97 bev/c π^- beam produced at the Brookhaven cosmotron. On the basis of these events it is estimated that about 2% (~0.6 mb) of all the interactions result in the production of strange particles. Associated production with at least one extra pion is very common at this energy. Analysis is especially simple for about 25% of the events because all three final state products are visible. The total absence of the $\pi^-+p\rightarrow\Sigma^++K^0+\pi^-$ reaction suggests that the $K-\pi$ system cannot appear in a pure $T=\frac{3}{2}$ state. The ratio $(\Sigma^-K^0\pi^+)/(\Sigma^-K^+\pi^0)\approx2$ further supports the idea that the $K-\pi$ system is predominantly $T=\frac{1}{2}$. Branching ratios for production and final state, two-body Q values will be presented. Decay asymmetry for the Λ^0's will be discussed.

Z6. π^--p Interactions at 1.97 Bev/c. W. D. WALKER, H. R. FECHTER, R. H. MARCH, D. LYON, P. SATTERBLOM, AND A. R. ERWIN, *Brookhaven National Laboratory and University of Wisconsin,* AND J. BALLAM, *Brookhaven National Laboratory and Michigan State University.*—The 14-in. hydrogen bubble chamber built by Adair and Leipuner was exposed to a π^- beam of 1.97 Bev/c momenta. An analysis has been made of some of the interactions which give rise to final states in which there are two and three π mesons. Of the two-pion production cases about 40% seem consistent with a simple π-π collision. The mass spectrum of the dipion system seems to be peaked at about 700 Mev for those cases which are consistent with a π-π collision. The remainder of the two-pion production involve large momentum transfers and are not understandable in any very simple way. The three-pion production processes seem to have almost isotropic angular distributions of all products. Examples have also been observed of four- and five-pion production processes.

THURSDAY AFTERNOON AT 1:30

Cotillion Room North

(K. LEHOVEC Presiding)

Semiconductors, II

ZA1. Lattice Absorption Bands and Clustering in Semiconductor Alloys. E. E. LOEBNER AND E. W. POOR, JR., *RCA Laboratories.*—Within the quaternary system Ga-P-Si-Zn, there exist substitutional semiconductor alloys, whose composition is $(16\ GaP)_{(1-x)}$ $(ZnGa_6Si_{17}P_{34})_x$ with $0<x<0.66$.[1] This system, characterized by a Si:Zn ratio of 17, has a linear variation with x of the sphalerite lattice parameter and of the optical energy gap.[1] An investigation of the infrared absorption spectrum up to 25 μ of samples having x of about 0.3 and 0.6 indicates the presence of bands having extrema at the same positions as those reported in pure GaP.[2] At frequencies intermediate to those for GaP and Si new bands appear. This frequency stability of lattice bands with changing alloy composition resembles the behavior of Si-Ge[3] and InP-InAs[4] alloy systems. The findings are interpreted to be due to atomic clusters whose composition is close to the termini of these systems. The clusters are estimated to contain 100–1000 atoms. The determinations of lattice parameters and energy gaps are based on effects averaged over many clusters. In contrast, combination bands are due to short wavelength phonons which are more localized. They probe selectively regions interior and exterior to the clusters.

[1] E. E. Loebner, I. J. Hegyi, and E. W. Poor, Jr., *Metallurgy of Elemental and Compound Semiconductors* (Interscience Publishers, Inc., New York, 1961).
[2] D. A. Kleinman and W. G. Spitzer, Phys. Rev. **118**, 110 (1960).
[3] R. Braunstein, Bull. Am. Phys. Soc. **5**, 198 (1960).
[4] F. Oswald, Z. Naturforsch. **14a**, 374 (1959).

ZA2. Oxide Formation on CdTe and ZnTe.* H. D. COGHILL, R. K. DICERBO, R. E. HALSTED, AND M. R. LORENZ, *General Electric Research Laboratory.*—Irreversible changes in the electrical and optical properties of surfaces of single crystals of CdTe and ZnTe occur on exposure to air. The reaction rate increases with increasing temperature. Electron diffraction measurements have established that these changes are due in part to the formation of TeO_2 surface films. This behavior is consistent with the oxygen-sulfide (e.g., ZnS) reaction in which SO_2 is an initial reaction product.[1] Beneath the transparent surface oxide film the oxygen interaction produces a "diffused impurity" layer which also has optical and electrical properties different from the initial sample. One might anticipate *n*-type conductivity in a layer containing Te vacancies or oxygen substituted for Te. However, *p*-type conductivity is observed. TeO_2 formation does not simply fit into previously proposed mechanisms for the interaction of oxygen with CdTe.[2] Alternative mechanisms remain to be established.

* Partially supported by the U. S. Air Force Air Research and Development Command.
[1] F. A. Kröger and J. A. M. Dikhoff, Electrochem. Soc. **99**, 144 (1952).
[2] Yu. A. Bodakov, G. A. Lomakina, G. P. Naumov, and Yu. P. Maslakovets, Soviet Phys.—Solid State **2**, 49 (1960).

ZA3. Correlation of ZnTe and other II-VI Compound Band Edge Emission Spectra. R. E. HALSTED AND M. AVEN, *General Electric Research Laboratory.*—At 20°K single crystal ZnTe exhibited five sets of emission "lines" with 0.0259 ±0.0005 ev phonon structure. The highest energy lines of four sets occur at 2.375, 2.329, 2.323, and 2.237 ev. An emission band was observed at 1.87 ev with phonon structure superimposed. Corresponding spectra for CdS, ZnSe, and CdTe are substantially consistent with prior work[1–3] and permit informative comparisons. Reststrahlen and dielectric constant data in these compounds correlate with longitudinal optical phonons. Such structure must generally characterize phonon emission processes within 0.3 ev (at 20°K) of band gap energy in II–VI compounds. The width, relative intensity, and number of satellite lines in a set increase for the more tightly bound recombination centers which are more strongly coupled to the lattice. However, variations observed in this trend help to characterize the recombination process involved. In ZnSe reversible changes in the edge emission spectra were produced by variation in stoichiometry. Several types of recombination mechanisms are necessary to account for the diversity of spectra and their dependence on bulk chemical properties.

[1] D. J. Thomas and J. J. Hopfield, Phys. Rev. **116**, 573 (1959).
[2] L. S. Pedrotti and D. C. Reynolds, Phys. Rev. **120**, 1664 (1960).
[3] Larson, Pedrotti, and Reynolds (to be published).

ZA4. Measurements of Piezoresistivity in Bi_2Te_3. T. J. DIESEL AND LEWIS E. HOLLANDER, JR., *Lockheed Missiles and Space Division.*—The piezoresistive effect has been measured in single crystals of *p*-type bismuth telluride, Bi_2Te_3, which were cleaved from an ingot along the (0001) cleavage plane. The room temperature value of the longitudinal piezoresistive coefficient π_L, measured along this cleavage plane, was found to be $+87\times10^{-12}$ cm²/d, and its temperature dependence was determined from −40° to +60°C. The hydrostatic coefficient π_H is about -40×10^{-12} cm²/d, indicating a negative transverse coefficient, which was qualitatively observed. Measurement of the Hall coefficient gave a carrier concentration of 5×10^{19} carriers/cm³, with a resistivity of 10^{-3} ohm cm. The piezoresistive coefficients were measured by compressing a specimen longitudinally to a stress of about 3×10^7 d/cm² and hydrostatically to 4×10^8 d/cm². Because of the high acceptor concentration of the samples studied, the many-valley energy surface theory is no longer valid, and the observed piezoresistive effect can be attributed to scattering.

ZA5. Reflectivity of *p*-Type Lead Telluride in the Infrared Region. JACK R. DIXON, *United States Naval Ordnance Laboratory.*—The reflectivity at near-normal incidence of *p*-type PbTe having hole concentrations varying from 3.0×10^{18} to 4.6×10^{19} cm⁻³ has been measured in the range from 3 to 32 μ. For the purest material, the reflectivity decreases regularly as the wavelength increases. In contrast, for heavily doped materials the wavelength dependence of the reflectivity is characterized by a distinct minimum followed at longer wavelengths by a region of high reflectivity. For example, the reflectivity of material having a hole concentration of 4.6×10^{19} cm⁻³ is 0.47 at 3 μ, decreases to a minimum of 0.17 at 11.6 μ, and then increases to 0.82 at 32 μ. Similar results applying to other semiconductors have been reported previously by Spitzer and Fan.[1] Such variations are attributed to the contribution of free carriers to the electric susceptibility. An analysis of the reflectivity data gives values of the susceptibility as a function of wavelength. This, in turn, yields a value of the susceptibility effective mass m_s of the holes. The effective masses determined in this way increase as the hole concentration increases. At hole concentrations of 3.0×10^{18} and 4.6×10^{19} cm⁻³, m_s was found to be 0.11 ± 0.02 and 0.20 ± 0.02 m_0, respectively, where m_0 is the rest mass of a free electron.

[1] W. G. Spitzer and H. Y. Fan, Phys. Rev. **106**, 882 (1957).

ZA6. Infrared Absorption Beyond the Fundamental Absorption Edge in PbS and PbTe. H. R. RIEDL, *United States Naval Ordnance Laboratory* (introduced by W. W. Scanlon).—Infrared absorption measurements have been made on PbS and PbTe in the 3 to 30 μ wavelength region at temperatures ranging from 18° to 300°K. It is found that the absorption coefficient due to free carriers is proportional to λ^n, where λ is the wavelength and n varies from 2.0 to 2.7. For example, in *p*-type PbS with a room temperature carrier concentration of 2.6×10^{18} holes/cm³, the absorption coefficient at 300°K, for λ between 4 and 9 μ, is $(1.29\pm0.13)\lambda^{2.45\pm0.05}$ cm⁻¹. In *p*-type PbTe, additional absorption varying more slowly with wavelength is also observed. This additional contribution is clearly seen from the fundamental absorption edge to about 15 μ at 300°K, and from the edge to about 11 μ at 195°K, and is stronger at 300°K.

ZA7. Absorption Edge in Degenerate *p*-Type GaAs.* I. KUDMAN AND T. SEIDEL, *RCA, Sommerville.*—Infrared absorption is studied at room temperature for *p*-type degenerate GaAs for various hole concentrations. A Burnstein-like[1] shift is observed for samples doped above 10^{19}/cm³, which is associated with a decrease in the valence band electron population. The data are also consistent with a large valence band effective mass and direct transitions where the matrix element does not depend strongly upon energy. Inflections are also detected in the absorption data. Resistivity vs carrier concentration (Hall effect) on similar material is presented. The mobility dependence on hole concentration is less strong than that observed for Ge for comparable doping.

* The work described was performed under the sponsorship of the Electronic Technology Laboratory, Wright Air Development Division, Air Research and Development Command, U. S. Air Force.
[1] E. Burstein, Phys. Rev. Letters **93**, 632 (1954).

ZA8. Irreversible Changes in the Space Region in Degenerate GaAs *p-n* Junctions.* ROBERT D. GOLD, BERNARD GOLDSTEIN, LEONARD R. WEISBERG, AND ROBERT M. WILLIAMS, *RCA Laboratories.*—The exponential dependence of the tunneling current through narrow *p-n* junctions on the width of the space charge region provides a very sensitive indication of changes in this width. The space charge region in GaAs tunnel diodes widens during operation at room temperature within hours. This is indicated by a decrease in junction capacitance, and is accompanied by an irreversible exponential decrease in peak tunneling current, together with a small decrease in valley current. These effects occur only when current flows in the forward injection region, and not when

tunnel current alone is present. Temperature by itself does not cause these effects since no decrease in peak current occurs when the diode is maintained at 200°C for several weeks with no current. Therefore, neither thermal diffusion nor field-enhanced diffusion can alone account for the redistribution of charge in the depletion layer. The measured junction temperature for currents sufficient to produce degradation (decrease in peak current) is considerably less than 200°C. However, the rate of degradation with such a current can be increased by more than two orders of magnitude for a temperature change from 25° to 150°C.

* Sponsored by the Electronics Research Directorate of the U. S. Air Force Research Division—Air Force Research and Development Command.

ZA9. Analysis of *p-n* Junctions and Junction Devices by a Flux Technique. J. P. McKELVEY, *Westinghouse Research Laboratories*.—A novel technique of analysis of excess carrier behavior in semiconductors,[1] based upon conservation of carrier fluxes, after allowing for generation and recombination, is applied to semiconductor *p-n* junctions and simple devices. It is assumed that the junction injects a flux of excess minority carriers into the bulk material on either side, and that the flux source strength is proportional to $\exp(eV/kT)$. In the case of the planar *p-n* junction in an infinite semiconductor, the usual exponential current-voltage dependence is obtained, but a more general expression for the saturation current than that obtained from conventional diffusion theory is exhibited. In particular it is shown that for sufficiently low carrier lifetime in the bulk material, the saturation current becomes independent of lifetime. The application of the method to a simple photovoltaic cell is also discussed. Here again the current-voltage dependence (which is related to the boundary condition at the junction rather than to diffusion and recombination phenomena in the bulk) is unaltered, but modified expressions for saturation and generation currents are obtained. Applicability of the method is currently limited to steady-state one-dimensional situations.

[1] J. P. McKelvey, R. L. Longini, and T. P. Brody, Bull. Am. Phys. Soc. 6, 28 (1961).

ZA10. Characteristics of *p-i-n* Junction Detectors. J. W. MAYER AND H. L. DUNLAP, *Hughes Aircraft Company*, AND H. E. WEGNER,* *Los Alamos Scientific Laboratory*.—Lithium-drifted *p-i-n* junction charged-particle detectors with active volumes between 1 and 4 mm thick have been constructed from *p*-type base material of 12 to 1400 ohm-cm resistivity following the technique of Pell.[1] The change in junction capacitance as a function of time indicates that lithium precipitation occurs, is present in all resistivities in the heavily doped front region, and results in increased depletion depths. Precipitation in the drifted region produces a decrease in the sensitive volume and was observed in all material with resistivities less than 1000 ohm cm. The precipitation time constant increases with increasing resistivity. A combination dE/dx and E gas ion chamber and *p-i-n* junction detector system was used to observe protons, deuterons, and tritons from C^{12} and Be^{9} bombarded with 17-Mev He^{3} ions. Electron response from 50 to 2000 kev was studied with a beta-ray spectrometer. Typical energy resolutions were 1% and 4% for 17-Mev deuterons and 1800-kev electrons, respectively.

* Work supported by the U. S. Atomic Energy Commission.
[1] E. M. Pell, J. Appl. Phys. 31, 291 (1960).

THURSDAY AFTERNOON AT 1:30

Adams-Hamilton Room

(R. A. SORENSEN presiding)

Theory, VIII: Nuclear Structure, II

ZB1. Effect of Finite Size of Protons on the Coulomb Energy of He^{3}. TAKASHI OHMURA AND HARUKO OHMURA, *Washington University*.—The experimental value of the difference between binding energies of H^{3} and He^{3} is 0.764 Mev, while the calculated Coulomb energy (abbreviated as CE, assuming the point protons) is about or more than 1.0 Mev, if the nuclear force has no repulsive core. It will be shown that, if the finite size of protons is taken into consideration, the CE of He^{3} is reduced by about 15∼20%. The effect of finite charge distribution is determined mainly by the mean square radius only, which is taken to be 0.8×10^{-13} cm. If there is a hard core (with radius D), the calculated CE (assuming point protons) is already smaller with the values 0.8∼0.9 Mev for $D=0.2\times10^{-13}$ cm, ∼0.7 Mev for $D=0.6\times10^{-13}$ cm The reduction of CE due to the finite size is about 8% and 3%, respectively.

ZB2. Positive Parity States of Be^{9} and C^{13}.* F. C. BARKER,† *M.I.T.*(introduced by Herman Feshbach).—The states produced by weakly coupling a 2*s*- or 1*d*-neutron to a core consisting of the ground or first excited state of C^{12} are mixed by means of a two-body central interaction and a one-body spin-orbit interaction of the type normally used in intermediate coupling calculations, to provide the low-lying positive parity eigenstates of C^{13} The positions and neutron widths of the states agree satisfactorily with experimental data, as do the calculated cross sections for photoneutron disintegration of C^{13}, however, in order to obtain agreement with other data involving $E1$ radiation widths the single particle shell model wave functions must be modified so as to have the correct asymptotic forms. Similar calculations are performed for the Be^{9} positive parity states, about which little is known experimentally.

* This work is supported in part by funds provided by the U. S. Atomic Energy Commission, the Office of Naval Research, and the Air Force Office of Scientific Research.
† On leave from the Australian National University.

ZB3. Pairing Plus Long-Range Force for Spherical Nuclei.* L. S. KISSLINGER, *Western Reserve University*, AND R. A. SORENSEN, *Columbia University*.—The independent particle model with a two-body residual interaction, consisting of a pairing force and a long-range part, is considered for spherical nuclei, $A \geq 48$ [1] The pairing force, assumed to be effective only for pairs of the same kind (neutrons or protons), is treated in the quasi-particle approximation. The long-range force, taken to be a quadrupole-quadrupole interaction is treated by the Sawada approximation. In the adiabatic limit, these approximations are equivalent to a collective model of nuclear vibrations about a spherical equilibrium shape. The deformed region corresponds to a zero (or imaginary) vibrational frequency. The parameters, which are assumed to be smoothly varying functions of A, include the strength of the pairing force, the strengths of the *n-n*, *p-p*, and *n-p* quadrupole forces, and the separation of the independent particle levels The low energy

properties of odd-A and even-even nuclei, including the energy leyels, transition rates, and static moments are calculated and compared to experiment.

* Supported in part by the National Science Foundation, the U. S. Army Office of Ordnance Research, and the U. S. Atomic Energy Commission.
[1] L. S. Kisslinger and R. A. Sorenson, Kgl. Danske Videnskab. Selskab, Mat.—fys. Medd. **32**, [9] (1960).

ZB4. Structure of the First Excited States of Even-Even Nuclei and $2_-(\beta)2_+(\gamma)0_+$ Transitions.* M. MORITA AND I-TUNG WANG, *Columbia University*, Z. MATUMOTO, *Japan Atomic Energy Research Institute*, AND M. YAMADA, *Waseda University of Japan*.—Successive beta and gamma decays of the odd-odd nuclei with spin 2_- have been investigated theoretically in connection with the structure of the first excited states of even-even nuclei.[1] The study is repeated, since accurate experimental data are available now. The beta decay to the first excited state ($2_- \rightarrow 2_+$) involves six nuclear matrix elements. All of them other than B_{ij} are zero, if the j-j coupling shell model or rotational excitation are strictly valid. However, this is not the case, as follows from the measured beta-ray spectra. Approximate validity of the selection rules due to the above nuclear models together with the large Z approximation makes the formula for β-γ directional correlation very simple. It depends upon only two parameters, which are the ratios between nuclear matrix elements. Furthermore, a relation between these two parameters is given by combining the measured ft values of the beta decays with the calculated ratio of the B_{ij}'s for ($2_- \rightarrow 2_+$) and for the ground state transition ($2_- \rightarrow 0_+$). The numerical analysis of experimental data on the β-γ directional correlation shows that the two selection rules are distinguishable in some cases.

* This work partially supported by the U. S. Atomic Energy Commission.
[1] Z. Matumoto, M. Morita, and M. Yamada, Bull. Kobayashi Inst. Phys. Research **5**, 210 (1955).

ZB5. Collective States of Spherical Nuclei. Giant Dipole State. J. SAWICKI AND TOSHIO SODA, *University of California, Berkeley*.—A new method of treating certain collective states of finite nuclei based on the linearized equations for the density matrix is developed. The Hartree-Fock exchange terms are included. Certain self-energy terms are discussed. Equations are obtained for calculating collective states of definite angular momentum, parity, spin, and isotopic spin. Particular application is made to the case of the giant dipole state of O^{16} with the use of finite range forces with different parameters of exchange interactions and radial shapes. Satisfactory agreement with experiment is obtained. Extension of this theory is being made to include corrections of terms nonlinear in the density operators.

ZB6. Damping of the Giant-Dipole Resonance.* RICHARD A. FERRELL, *University of Maryland*.—The excited configurations in the shell model which account for the collective behavior of the giant dipole resonance,[1] and whose coherent superposition produces an interaction energy shift away from the single-particle energies,[2] are not the same configurations which are responsible for the damping of the giant-dipole. To describe the damping it is necessary to admix single-nucleon wave functions from the continuum which correspond to a single-nucleon energy equal to the total energy of the resonance. These wave functions are quantitatively different from the bound single-nucleon wave functions which are responsible for the dynamics of the resonance. Branching ratios based on the latter lead to erroneous conclusions. Furthermore, the energy shift separates the giant dipole from the single-particle resonances and tends to inhibit the damping.

* Research supported in part by the Atomic Energy Commission and by the Office of Naval Research.
[1] D. M. Brink, Nuclear Phys. **4**, 215 (1957).
[2] R. A. Ferrell, Bull. Am. Phys. Soc. **3**, 49 (1958).

ZB7. Extended Shell Model Calculations and the Giant $E1$ Resonance in Deformed Nuclei.* S. G. NILSSON, J. SAWICKI, AND N. K. GLENDENNING, *Lawrence Radiation Laboratory and University of California, Berkeley*.—Certain collective states of finite nuclei may be reasonably well described by a modified random-phase approximation based on a linearized system of equations for the components of the single-particle density matrix. The exchange terms corresponding to the antisymmetrized wave function are included and certain self-energy terms are discussed. This so-called extended shell model formulation is applied to deformed nuclei. For even-even nuclei the giant $E1$ resonance generally separates into two groups corresponding to $K=0,1$. We have first studied the simplified case of the spin-orbit splitting being neglected. The $E1$ states then separate additionally into ($T=1,S=0$), ($T=1,S=1$), ($T=0,S=0$), ($T=0,S=1$) groups. The giant $E1$ resonance occurs within the first group. Various different forms of the two-body interaction are investigated. The numerical results obtained for the C^{12} nucleus reproduce quantitatively recent experimental data. The work with a more realistic single-particle potential is in progress with particular application also to Mg^{24}.

* Work performed under the auspices of the U. S. Atomic Energy Commission.

ZB8. Some Isotopic-Spin Effects in Heavier Nuclei.* J. B. FRENCH AND M. H. MACFARLANE, *University of Rochester*.—The isotopic-spin quantum number is redundant for the ground states of heavier nuclei, being simply half the neutron excess; this, however, is not the case for states in which a proton is excited to an orbit not filled for neutrons or a neutron promoted from an orbit not empty for protons. Some consequences of this will be discussed. One in particular is an isotopic-spin splitting of giant resonances in particle (and hole) reactions, which is expected even in certain cases where there may be sizable isotopic-spin admixtures in the individual excited states. Another consequence is that simple relationships exist between the spectra of nuclei which are isotopically spin related when described by means of the shell model.

* Supported in part by the U. S. Atomic Energy Commission and the National Science Foundation.

ZB9. Center of Mass Effects in the Shell Model.* CHONG WAN LEE AND ELIZABETH BARANGER, *University of Pittsburgh*.—The usual shell model harmonic oscillator wavefunctions used for describing states of nuclei are known to be partly spurious, unless they belong to the lowest configuration allowed by the Pauli principle.[1] One can construct nonspurious states by subtracting the spurious part and renormalizing. By dividing out the center of mass motion one obtains a wavefunction depending only on internal coordinates, and this can usually be given a simple cluster interpretation. The electromagnetic transition matrix elements are computed by calculating matrix elements of the corrected operators[2] between such states. In calculating transitions to the ground state, one will thus obtain a factor $(1-\alpha^2)^{-1}$, where α is the amount of spurious state admixed into the excited shell model state, which multiplies the matrix element of the corrected operator between the shell model states. This factor has been ignored in the past. Further applications of the use of these states will be discussed.

* Work done in the Radiation Laboratory and assisted by the joint program of the Office of Naval Research and the U. S. Atomic Energy Commission.
[1] J. P. Elliott and T. H. R. Skyrme, Proc. Roy. Soc. (London) **A232**, 561 (1955).
[2] S. Gartenhaus and C. Schwartz, Phys. Rev. **108**, 482 (1957).

SUPPLEMENTARY PROGRAMME

SP1. Miniature Coils for High Magnetic Field Research.* R. W. DE BLOIS, *General Electric Research Laboratory.*—Pulsed magnetic fields greater than 100 koe and of μ-sec duration are reported here to be readily producible in 1-mm diam coils supplied by energy storage units of only several joules capacity. Demonstrative experiments are described which show the magnetic-state transitions of a 20 μg specimen of MnAs near 90 koe, the shift in transition temperature when the specimen and coil are subjected to hydrostatic pressures up to 850 atm, and the reversal of magnetization of a 0.5 μg iron cube from which all reverse nuclei were presumably driven.

* To be given at the end of Session BA if the chairman rules that time permits.

SP2. Magnetic Moment in the Radional Field. ANATOL J. SHNEIDEROV, *Polycultural Institution of America.**—A macrocosmic or a microcosmic body spinning in the radional field (see Abstract No. CBX 11) produces a quasi-vortical anisotropy in the field around the body, representing its magnetic field. A formula for magnetic moment is derived: $\mu_g = (bJ_t)^{\frac{1}{2}}\beta Q\cdot(2/5)r^2\cdot(v/c)/2\pi r$ ergs per gauss for homogeneous, spherical *macro*bodies; and its variant: $\mu_s = 4\pi a^2 J_t^{\frac{1}{2}}\cdot kr^2\cdot(v/c)2\pi r$ ergs per gauss for *micro*bodies, where a is radius of the microbody, r is radius of its rotation; M is mass; $J_t = 1.12\cdot10^{31}$ d/cm^2 is pressure of the radional field; $b = 2.98\cdot10^{-16}$ is a ratio of the sum of volumes of elementary particles (protons, neutrons, electrons, etc.) each assigned a mean mass $\bar{m}$, and a number n of which constitute a body of unit density, to the volume of such a body; $\beta = 4.46\cdot10^{-12}$ cm^2/g is radional absorption coefficient; v is equatorial rotation velocity; c is speed of light; k is moment of inertia coefficient; δ is $Q/(4/3)\pi r^3$; $x = r\delta\beta$, and

$$Q = \sum_1^n \bar{m} = (4/3)Mx/[1-(1/2x^2)+(e^{-2x}/2x^2)+(e^{-2x}/x)].$$

Magnetic moments calculated for Bohr magneton, the moon, the earth, the sun, and several stars agree satisfactorily with the experimental or observed values.

* To be called for at the end of Session CB if the Chairman rules that time permits.

SP3. Theory of Space Charge in High-Pressure Inert Gas Diodes.* R. FORMAN, *Union Carbide Corporation.*—A theory for space charge conditions in high-pressure diodes has been developed which shows that the current obeys a V^1 power relation rather than the usual assumed V^2 relation. This interesting result has been verified experimentally and data in argon and helium filled diodes will be presented to illustrate the validity of the theory.

* To be called for at the end of Session M if the Chairman rules that time permits.

SP4. On the Transients of Wave Propagation in Liquids and Liquid Mixtures.* E. TERNER, *Armour Research Foundation.*—Shock tubes have been used extensively for the study of various phenomena in gases; here the use of a shock tube is described which contains a liquid under pressure in the driver chamber. On sudden decompression a pulse is propagated along the tube and is subsequently multiply reflected. This wave motion has been observed by taking suitable pressure recordings along the tube and it is possible to study various properties of the fluids concerned by this experimental means. Among the liquids used were water and carbon tetrachloride; the wave propagation was also studied in aerated water as well as isopropanol water mixtures. Interesting effects are observed if the liquid is preheated and is allowed to boil under pressure, thus containing some nuclei at decompression.

* To be called for at the end of Session Q if the Chairman rules that time permits.

Pertaining to the Oliver E. Buckley Solid-State Physics Prize

(Item added to proof and not proofread.)

By order of the Council, members of the Society are invited to propose candidates for the 1962 Oliver E. Buckley Solid-State Physics Prize, and this they may do by writing to Dr. Benjamin Lax, Lincoln Laboratory, M.I.T., Cambridge 39, Massachusetts, who is Chairman of the Committee appointed to nominate candidates.

This prize is to be awarded for the making of "a most important contribution to the advancement of knowledge in solid-state physics" during the five years immediately preceding the award and "in the United States of America and its possessions or in the neighboring countries included in the continent of North America and its insular environs." No stipulation is made as to the nationality of the prize-winner. The prize may not be divided between two or more recipients.

Author Index to Papers Presented at the 1961 Washington Meeting

Abeledo, D.—T4
Adams, B.—GA2
Adams, E. D.—MA9
Adams, H. S.—GA14
Alburger, David E.—AA8
Alder, Bernie—TA10
Alexeff, Igor—YA7
Allison, S. K.—F2
Almqvist, E.—RA10
Alston, Margaret—T7
Altman, Albert—AA2
Alvarez, L. W.—T7
Amar, Henri—QA2
Ames, I.—M5
Ammar, R. G.—T4
Ancker-Johnson, Betsy—YA11
Anderson, C. E.—RA11
Anderson, Charles H.—N2, QB2
Anderson, Hugh R.—LA1
Anderson, James L.—WB8
Anderson, John D.—XA1
Anderson, K. A.—LA6
Anderson, Roy S.—G3, G6, G7
Arai, Tadashi—QB4
Arakawa, E. T.—M7
Armstrong, J. A.—D8
Arnowitt, R.—WB9
Arns, R. G.—E8
Atkinson, John H., Jr.—F10
Aubrey, B. B.—G10
Austern, N.—GA8
Aven, M.—ZA3

Bahcall, J. N.—MB3
Baker, D. A.—VA6, VA7
Baker, D. J.—R6
Baker, George A., Jr.—FB4
Baker, Milton R.—N3
Ball, J. B.—NA2
Ballam, J.—Z5, Z6
Banister, John R.—Q4, VA9
Baranger, Elizabeth—ZB9
Barash, Lee F.—D12
Bardwick, John—KA6
Barker, F. C.—ZB2
Barker, William A.—U7
Barnard, A. C. L.—KA7, KA8
Baroody, E. M.—TA8
Barr, Ronald—L14
Barredo, Joseph G.—WB11
Barschall, H. H.—UA1
Bartholomew, G. A.—DA13
Bartlett, A. A.—F5, KA11
Bartolini, W.—S5
Barton, G.—JB6
Bashkin, S.—AA4
Baskett, John R.—YA6
Bassani, Franco—TA3
Bauer, Ernest—N7
Bauer, R. W.—A4
Bazley, N. W.—QB9
Bearden, A. J.—YA8, YA9
Bearden, J. A.—U4
Becker, Richard L.—L13
Beckner, E. H.—AA10
Bedo, D. E.—R6
Benedek, G. B.—D3, D8
Benenson, W.—H11
Bennett, Lawrence H.—D2
Bent, R. D.—GA6, GA15
Bergmann, Peter G.—WB7
Berk, H. L.—DA3
Berkowitz, E.—AA4
Bernheim, R. A.—D4
Bernstein, A. M.—A1
Bertanza, L.—T2
Bertozzi, W.—DA7, H2, H3
Bevington, P. R.—H9
Bhattacharya, Dwijendra—MA2
Biedenharn, L. C.—NA12
Biggerstaff, J. A.—AA6
Bilhorn, D. E.—TB6
Billings, James J.—Q9
Bina, Melvin J.—AA11
Birkhoff, R. D.—M7
Bishara, B. A.—E1
Biswas, S.—LA3
Bjørnholm, S.—E9
Blair, J. M.—AA1
Bleuler, E.—J5
Bloch, B.—W2
Block, R. C.—P4
Blosser, H. G.—J8
Boedeker, Richard—L14
Bollinger, L. M.—P2, P3, P10
Bolotin, H.—P1
Bonner, T. W.—DA5
Borchers, R. R.—H10, H11
Bowers, Raymond—L4
Boyarski, A.—F14, W3
Bozorth, R. M.—BA5
Bradner, H.—T5
Bradt, H. V.—LA4
Braid, T. H.—NA3, NA4, NA5
Brajovic, V. M.—L7
Bray, P. J.—A8, D7, G1
Bray, T. M.—D1
Breitenberger, Ernst—U2
Brice, D. K.—BA10
Britt, H. C.—RA6, RA7
Brockhouse, B. N.—L4
Brodwin, M. E.—WA2
Broek, H. W.—NA3, NA4, NA5
Bromley, D. A.—RA11
Brout, R.—FB5
Brown, G. C.—D1
Brown, R. I.—AA9, XA3
Browne, C. P.—AA7
Broyles, A. A.—FB7
Brungs, R. A.—TA9
Bryant, P. J.—QA3
Buchsbaum, S. J.—SA8
Buechner, W. W.—J3, KA9
Bulewicz, E. M.—K8, K9
Bunker, M. E.—B9
Burke, E. R.—FA4
Burt, P. B.—VA11
Butcher, B. M.—FA10
Butler, J. P.—GA11

Cameron, A. G. W.—R10
Campbell, E. C.—H6
Capps, Richard H.—JB3
Carlson, T. A.—B1, B2
Carmichael, H.—LA7
Carovillano, R. L.—NA9
Carter, E. B.—AA13, DA2, J2
Castner, T.—WA12
Chan, Sunney I.—N3
Chang, Chieh C.—Q1
Chapman, M. C.—YA4
Chase, L. F., Jr.—DA8
Chen, Francis F.—SA5
Cherry, William H.—WB4
Cheston, W.—FB2
Chi, B. E.—CB9
Chilton, Frank—JB9
Chinowsky, W.—T5, T10
Chisholm, L. D.—F3
Chopra, K. P.—Q3
Chow, L. Y.—G10
Choy, L.—T4
Chrien, R. E.—P1
Christensen, R. L.—M5
Christian, R. S.—J7
Christofilos, N.—SA6
Cipollini, Ernesto—K7
Clark, G. W.—LA4
Clark, M. A.—GA3
Clarke, George A.—G9
Cline, J. E.—B8, E10
Cline, Thomas L.—LA9
Coensgen, F.—EA2
Coghill, H. D.—ZA2
Cohen, Roger W.—YA11
Colgate, Stirling A.—R11, VA3
Connolly, P. L.—T2
Contogouris, A. P.—JB7
Cook, C. W.—XA7
Coopersmith, M.—FB5
Cormack, A. M.—S4
Costello, D. G.—GA13
Coté, R. E.—P3, P10
Cotter, M. J.—L8
Cotts, R. M.—A3
Crane, L. T.—FA12
Crayton, N.—T4
Crowe, Kenneth M.—W4
Cuevas, J.—F2
Cullen, J. R.—FB3
Culvahouse, J. W.—G4
Culwick, B. B.—T2
Cummings, F. W.—N7
Curtis, Cyril D.—J9
Curtis, R. B.—MB3
Cutkosky, R. E.—JB2

Dalitz, R. H.—MB2
Dance, W. E.—F3
Daum, C.—KA1
Davidson, J. P.—CB7, CB8, CB9
Davies, J.—AA4
Davis, D. D.—BA5
Davis, H. L.—Q4
Davis, R., Jr.—PA8
Davis, R. H.—AA5, AA13, DA2, GA1, J2
Day, Paul—E11
De Benedetti, S.—HA3
De Blois, R. W.—BA9, SP1
DeFelice, J.—PA6, PA7

Delaney, Robert—L14
Demos, P. T.—DA7, H2, H3
dePackh, D. C.—M10, M11
De Pangher, J.—H13
deParry, T.—J4
Deser, S.—WB9
DeSorbo, Warren—MA1
De Swart, J. J.—MB6, MB7
Deutsch, M.—A4
De Vries, C.—S2
DiCerbo, R. K.—ZA2
Dickinson, W. C.—L1, S5
Diesel, T. J.—ZA4
Din, Ghias Ud—DA5
Dixon, Jack R.—ZA5
Dodson, R. W.—PA10
Doggett, Wesley O.—FB14
Doherty, Patrick—L14
Dorenbusch, W. E.—AA7
Douglass, D. H., Jr.—MA6
Dowds, H. M.—XA5
Drell, S. D.—JB8
Drevinsky, P. J.—PA9
Drew, Russell—K6
Dropesky, B. J.—B9
Drummond, J. A.—EA4
Dullemond, C.—MB6, MB7
Dunlap, H. L.—ZA10
Dupree, Thomas H.—SA1

Eberhard, P.—T7
Eccleshall, D.—GA2
Edelstein, R.—W2
Ederer, D. L.—R6
Edge, R. D.—U3
Edwards, H. H.—MA5
Efremov, Nicholas—MB12
Eichler, E.—B5
Eidson, W. W.—GA6, GA15
Eisler, F. R.—T2
Ek, F.—Q5
Elmgren, J. A.—WA4
El-Wahab, M. A.—F8, J1
Ely, John T. A.—PA4
Ely, R. P.—T3
Emery, Guy T.—B11
Enge, H. A.—J3
Engle, Leon B.—XA9, XA10
Erskine, J. R.—AA7
Erwin, A. R.—Z5, Z6
Ewan, G. T.—E4

Fairbank, W. M.—MA8, MA9
Fechter, H. R.—Z6
Feher, G.—W1
Ferguson, A. J.—DA1
Ferrell, Richard A.—FA4, FB3, L12, ZB6
Fickinger, W.—W8
Fields, P. R.—XA12
Fields, T. H.—F9
Filz, R.—PA2
Finkel, J.—QB1
Finkelstein, David—SA9
Fireman, E. L.—PA6, PA7
Firk, F. W. K.—H7, P9
Fischbeck, Helmut J.—E3
Fisher, David E.—LA11
Fisher, Philip C.—XA9, XA10
Fishman, F.—Q8
Fisk, H. E.—T11
Ford, Kenneth W.—MB1
Forman, R.—M1, SP3
Forsyth, P. D.—AA12, KA8
Fossan, D. B.—XA2
Fowler, H. A.—M3, M4
Fowler, J. L.—H6
Fox, D. W.—QB9
Fox, J. D.—GA14
Fox, John N.—FB8
Francis, N. C.—TB13
Frank, A. L.—M7
Freeman, A. J.—D9
Freier, Phyllis—LA3
French, J. B.—ZB8
Friedlander, G.—PA10
Friedman, A. M.—XA12
Friedman, Herbert—X2
Friedman, L.—WA3
Fujimoto, Minoru—G7
Fukui, K.—PA3
Fuller, Robert W.—XA13
Fulmer, C. B.—NA2
Fumi, Fausto—TA4, TA5
Fung, S. Y.—T3
Furdyna, J. K.—WA2
Furth, Harold P.—YA3

Garcia-Munoz, M.—F2
Gardner, Calvin C.—XA1
Garvey, G.—RA8
Geiger, J. S.—E4
Geller, S.—BA4
Gerritsen, H. J.—D11
Gibbons, J. H.—H7
Gibbs, W. R.—DA6, TB5
Gidal, G.—T3
Giddings, L. E., Jr.—N8
Gilliam, O. R.—G2, G8
Gilmer, George H.—TA11
Ginther, R. J.—P9
Gittleman, J. I.—MA7
Glahe, H. C.—T9
Glendenning, N. K.—ZB7
Gluckstern, R. L.—J6
Goebel, Charles J.—JB5
Gold, Robert D.—ZA8
Goldberger, M. L.—V1
Goldhaber, G.—T5
Goldhaber, S.—T5
Goldman, D. T.—TB2, TB3, TB13
Goldstein, Bernard—ZA8
Good, M. L.—T7
Good, W. M.—H5
Goodkind, J. M.—MA8
Goodman, C. D.—NA2
Gordon, G. D.—YA1
Gordon, M. M.—J8
Gordy, Walter—K1, K2, K3, K4, K5, K6, K7
Gove, H. E.—GA3
Graham, R. L.—E4
Grasberger, William H.—R11
Graziano, W.—T7
Green, K.—J10
Green, M. S.—R12
Green, Milton—WA13
Greenberg, J. S.—M5
Greenberg, O. W.—WB10
Grench, H. A.—DA10
Greyber, Howard—R9
Griffioen, Roger D.—RA13
Griffy, T. A.—NA12
Grover, Richard—TA10

Haddad, E.—XA7
Haeberli, W.—AA9, XA3
Haertle, Richard A.—CB2
Haigh, P. J.—D6
Halbert, M. L.—RA3
Hall, J. L.—G5
Hall, W. S.—NA13
Halpern, O.—L1, S5
Halsted, R. E.—ZA2, ZA3
Hamilton, D. R.—A1
Hammel, J. E.—VA6, VA7
Harlan, R. A.—GA9
Harris, D. L.—A2
Harris, E. G.—VA11
Harris, R. W.—AA10
Harte, William E.—FA3
Hartman, Charles W.—VA3
Havens, W. W.—L6
Hayward, R. W.—HA1
Heath, R. L.—B8
Hecht, K. T.—KA3
Heckman, Harry H.—RA12
Heller, P.—D3
Hellwarth, R. W.—M9
Henderson, Dale J.—E11
Henderson, Jerry D.—DA9
Henkel, John H.—TA7
Hensel, J. C.—WA11
Herb, R. G.—GA13
Herling, G. H.—TB12
Herman, Robert—S2, S3
Heydenburg, N. P.—GA14
Hines, R. L.—FA5
Hinrichs, C. K.—T1
Hintz, Norton M.—KA12, KA13
Hobbie, R. K.—AA1
Hoffman, R. A.—S6, S7
Hofmann, Fritz W.—R2
Hofstadter, Robert—S1, S2, S3
Hollander, Lewis E., Jr.—ZA4
Holliday, J. E.—R8
Holstein, T.—WA3
Holtebekk, T.—KA4
Hood, R. F.—AA6
Hoogenboom, A. M.—KA9
Hooper, H. O.—D7
Huang, Justin C.—MB10
Hudis, J.—PA10
Hudson, C. I., Jr.—H4
Hudson, D. E.—WA4
Huff, Robert W.—MB2
Hughes, Vernon W.—G10, M5, MB1, W6
Huizenga, J. R.—KA10, XA6, XA11
Humphrey, William E.—T8
Hunt, W. E.—AA5, GA1

Imhof, W. L.—DA10
Ingraham, R. L.—FB6
Innes, Frederick R.—QB7
Innes, K. K.—N8

Jackson, H. E.—P2
Jacobsmeyer, V. P.—TA9
Jaffey, A. H.—F6
Jain, A. P.—P1

Jain, P. L.—T9, Z4
James, H. M.—WA7
Jänecke, Joachim—B4, KA5
Jarmie, Nelson—DA12
Jaseja, Thadho S.—G3
Jastram, P. S.—E1
Jeffries, C. D.—A7
Jenkins, Alvin W., Jr.—BA6
Jog, S. D.—QB5
Johnson, C. H.—B1, B2, UA4
Johnson, Noah R.—B5
Johnson, O. E.—B6
Johnson, R. C.—N1
Johnson, R. G.—DA8, D10
Johnson, W. B.—R1
Johnson, W. P.—DA4
Jones, C. M.—AA10
Jones, G. A.—NA7, NA8
Jones, Richard D.—VA9
Jung, Horst—B4

Kacser, C.—JB6
Kagan, M. R.—U9
Kahn, A.—JA4
Kaiser, H. F.—M6
Kalkstein, M. I.—B10, PA9
Kanazawa, Akira—JB1
Kanda, Y.—N5
Kane, J. V.—F8, J1
Kantele, Juhani—H12
Kaplan, Harvey—QA4
Kashy, E.—KA9
Katayama, Mikio—K5
Kaufman, A. N.—FB10
Kavaloski, C. D.—KA13
Keck, J. C.—Q8
Keffer, F.—QA8
Kelley, J. G.—RA9
Kellogg, Paul J.—LA10, VA3
Kerst, D. W.—SA10, VA8
Kessler, K. G.—HA2
Keyes, Robert W.—FA14
Kiel, A.—D1
Killeen, John—YA3
Kim, C. C.—KA7
King, R. F.—XA4
Kinsey, K. F.—Z2
Kip, A. F.—C2
Kirz, Janos—T8
Kisslinger, L. S.—ZB3
Klontz, E. E.—WA8
Knapp, D. E.—Z2
Knight, J. D.—B9
Knox, Robert S.—TA3
Knutsen, A. B.—E9
Kobe, D.—FB2
Koga, Toyoki—VA2
Kohin, Roger P.—G6, G7
Kohn, Hedwig—R2
Kovacs, J. S.—MB8, MB10
Kowalski, S.—DA7
Krall, N. A.—YA5
Kranzer, Herbert C.—SA7
Kraus, Lester—YA2
Kraushaar, J. J.—KA11
Kritz, Arnold H.—SA2
Kroger, H.—R5
Krone, R. W.—GA12
Kruger, Hans—W4
Kuan, Hsin-Min—DA5
Kudman, I.—ZA7
Kuehner, J. A.—RA10
Kunzler, J. E.—V3
Kurss, Herbert—TA1
Kuyatt, C. E.—M2

Lafferty, D. L.—M12, M13, M14
Lambe, J.—U5, U6
Lamborn, B. N. A.—M12, M13, M14
Lapointe, Serge M.—LA5
La Salle, R. A.—GA6
Laurance, Neal—U5, U6
Laurie, Victor W.—N4
Lawrence, Thomas R.—N2
Lebowitz, Joel L.—SA3
Lee, Chong Wan—ZB9
Lee, Kiuck—CB1, CB2
Lee, L. L., Jr.—KA12
Lee, Sook—G1
Lee, W.—T5
Lefevre, H. W.—H10, H11
Lefrançois, J.—S6, S7
Legg, J. C.—GA4
Lehovec, Kurt—WA1
Leifson, O. S.—A7
Leitner, Jack—T8
Levi-Setti, R.—T4
Levine, M. A.—VA5
Levy, P. W.—G2, G8
Levy, S. L.—QA3
Lewis, H. R., Jr.—E5
Lewis, H. W.—H9
Li, Angela C.—B12
Libby, W. F.—V2
Lichtenberg, D. B.—MB4
Lidofsky, L. J.—XA5
Lieb, E.—BA8
Liefeld, Robert J.—R7
Lindsay, William F.—F13
Lipas, P. O.—CB8
Litherland, A. E.—GA2, GA3
Liu, S. H.—BA1
Loebner, E. E.—ZA1
Loh, E.—W3
Long, R. L.—M5
Lorenz, M. R.—ZA2
Low, C. A., Jr.—GA7
Lowe, J.—J1
Lubitz, C. R.—TB3, TB13
Lupton, William H.—L12
Lyon, D.—Z6

MacDonald, William M.—AA2
MacFarlane, M. H.—ZB8
MacFarlane, Ronald D.—RA13
MacKay, J. W.—WA8
Maier, E. J.—W2
Malamud, Herbert—YA2
Malik, F. B.—QB3
Mallmann, C. A.—F6
Mani, G. S.—AA12, KA8
Manson, Donald—L14
Maradudin, A. A.—JA2
March, R. H.—L4, Z5, Z6
Marcinkowski, Chester J.—QB12
Marcus, Paul M.—MA3
Marion, J. P.—P3
Marion, Jerry B.—AA2
Marshak, H.—P5, P6
Martin, J. H.—J4
Marton, L.—M4
Mason, E. A.—FB12
Mathur, R. N.—J5
Matthias, B. T.—V4
Mattis, D.—BA8
Matumoto, Z.—ZB4
Maxson, D. R.—DA11
May, T. H.—H11
Mayer, J. W.—ZA10
Mazur, Paul—U1
McAvoy, N.—U9
McCallum, G. J.—DA1
McConnell, D. B.—H2, H3
McCracken, K. G.—LA8
McCullen, J. D.—A2, KA11
McDonald, D. G.—AA9
McEllistrem, M. T.—AA6
McGowan, F. K.—NA6
McGrath, J. W.—A6
McIntosh, J. S.—TB11
McIntyre, J. A.—RA14
McIrvine, E. C.—U5, U6
McKelvey, J. P.—ZA9
McMillan, Juan A.—D10
McReynolds, A. W.—L10, L11
McWhorter, A. L.—WA6
Mead, James B.—NA11
Mehta, M. K.—AA5, GA1
Meijer, Paul H. E.—FA13, FB8
Meister, R. P.—VA5
Mendelson, S.—QA12
Meservey, R.—MA10
Mette, Herbert—TA12
Metzger, F. R.—B3, GA10
Micheletti, Sergio—NA11
Mielczarek, Eugenie V.—FA13
Miles, D. O.—TA13
Miller, D. W.—DA4, NA13
Miller, Max G.—QA5
Minshall, F. Stanley—Q9
Mintzer, David—SA2
Misho, R. H.—R3
Mitchell, G. E.—AA13, DA2
Mitchell, J. W.—QA1
Miyake, K.—Z2
Mobley, R. C.—F3
Mohling, Franz—CB5
Monchick, L.—FB12
Montgomery, D. J.—R3
Moon, R. M.—L2
Moore, M. S.—P8
Moore, Richard L.—VA4, YA4
Moore, W. E.—DA15
Morita, M.—ZB4
Morris, E.—SA3
Morris, T. W.—T2
Morse, R. L.—YA5
Moss, S. J.—AA9
Moszkowski, S. A.—CB3
Moyer, B. J.—T1
Muenzer, H.—H5
Muether, H. R.—L9
Mullins, W. W.—TA2
Munir, B.—W7
Murri, E. L.—E10
Muss, D. R.—FA7, FA8
Myers, V. W.—L7, L8

Naber, J. A.—WA7
Narasimha Rao, D. V. G. L.—K3

Narchal, Mohan Lal—U7
Naugle, J. E.—X3
Naumann, R. A.—E5
Neal, Laurance—U6
Neher, D. H.—GA12
Neidigh, Rodger—YA7
Neiler, J. H.—F4
Nelson, J. W.—DA2, GA1
Neuringer, Joseph L.—YA2
Neuringer, L.—A9
Newhouse, V. L.—MA5
Newman, E.—RA5
Newson, H. W.—H8
Nichols, Glenn E.—MA1
Nielsen, O. B.—E9
Niemela, L. Q.—F14, W3
Nilsson, S. G.—CA2, ZB7
Nishida, Y.—TB12
Nishimura, K.—H5
Nobles, R. G.—XA12
Norbeck, E.—AA4
Northcliffe, L. C.—F7

Ogden, P. M.—T1
O'Halloran, T.—T5
Ohkawa, T.—SA10, VA8
Ohlmann, R. C.—BA7
Ohmura, Haruko—ZB1
Ohmura, Takashi—ZB1
Okaya, Akira—D12
O'Keefe, J. G.—A8
O'Kelley, G. D.—B5
Olness, D.—N6
Otnes, K.—L3
Ovenshine, S. J.—XA4
Oxley, C. L.—YA5
Ozaki, S.—W3

Padley, P. J.—K8, K9
Palevsky, H.—L3, L7, L8, P1
Palmer, R. B.—T2
Palmieri, J. N.—S4
Pan, Y. L.—T3
Pankove, J. I.—WA9
Park, S. C.—TB11
Parkinson, W. C.—KA2, KA6
Passell, L.—L1, S5
Pati, J. C.—MB11
Patten, Raymond—K4
Pearson, J. J.—QA9
Percus, Jerome K.—FB1, QB11
Perkins, W. A.—VA10
Petersen, F. R.—A5
Peterson, T. J., Jr.—R4
Peterson, V. Z.—Z1
Petry, R. F.—E2
Petschek, H. E.—Q8
Pfann, W. G.—WA5
Phillips, G. C.—AA10, TB7
Pickup, E.—W7, W8, W9
Pinkerton, James N.—QB2
Platzman, Philip M.—SA8
Pleasonton, Frances—B1, B2
Plendl, H. S.—AA5
Poirier, J. A.—T1
Pool, M. L.—E6
Poor, E. W., Jr.—ZA1
Poppe, C. H.—H10
Posner, M.—A1
Post, R. F.—EA3, VA10
Postma, H.—P5, P6
Powell, W. M.—T3
Power, J. L.—E5
Prager, Stephen—FB11
Prakash, Y.—Z3
Pratt, R. H.—JB8
Prem, R. J.—Z3
Prepost, R.—W1
Prodell, A. G.—T2
Prosser, F. W., Jr.—GA12
Prowse, D. J.—T11

Quinn, John J.—FA2
Quinton, A. R.—RA6, RA7
Quisenberry, K. S.—GA7

Ralph, D. C.—F3
Ramanaiah, P.—Q1
Ramaswamy, M. K.—E1
Ramsey, Norman F.—N2, U10
Rapoport, E.—Z3
Rasmussen, John O.—CB6
Rasmussen, V. K.—GA10
Rawitscher, G. H.—TB11, W5
Rayburn, L. A.—H14
Raymund, M.—T4
Reames, Donald V.—RA12
Reboul, T. T.—YA1
Reeves, Hubert—TB10
Reich, C. W.—B8
Reinhardt, G. C.—H1
Rexroad, Harvey N.—K2
Reynolds, C. A.—P5, P6
Rhode, J. I.—B6
Ribe, F. L.—YA8, YA9
Riedl, H. R.—ZA6
Rimai, L.—A9
Ristinen, Robert A.—F5, KA11
Ritchie, R. H.—M7
Ritson, D.—W3
Roberg, Jane—WB1
Roberts, L. D.—BA3
Robinson, D. K.—W7, W8, W9
Robinson, R. L.—B5, NA6
Rockwood, Curtis C.—F11
Rose, D. C.—LA5
Rose, M. H.—FB13
Rosenberg, Leonard—QB6
Rosenfeld, Arthur H.—T8
Rosenthal, Jenny E.—U8
Rost, E.—GA8
Rubin, A. G.—VA5
Rubin, R. J.—JA1
Rudinger, George—Q7
Ruff, A. W., Jr.—FA9
Ruoff, A. L.—FA10
Rush, J. J.—L6
Rustgi, M. L.—TB9

Sabisky, E.—D11
Sachs, A. M.—W1
Sachs, M.—RA11
Sack, R. A.—TA6
Saffren, Melvin M.—QB8
Sailor, V. L.—P5, P6
Salant, E. O.—W7, W8, W9
Samios, N. P.—T2
Santry, D. C.—GA11
Sapp, R. C.—BA10
Sargent, C. P.—DA7, H2, H3
Sasakawa, T.—CB10
Sastry, K. S. R.—E2
Satchler, G. R.—GA8, UA3
Sato, Hiroshi—FA11
Satterblom, P.—Z6
Sauder, William C.—U4
Sawicki, J.—ZB5, ZB7
Sawyer, G. A.—YA8, YA9
Sayres, A.—DA14
Schaeffer, O. A.—PA10
Scharff-Goldhaber, Gertrude—B11
Schermer, R. I.—L5, QA7
Schiffer, J. P.—NA7, NA8
Schiller, Ralph—JB12, QB10
Schmidt, George—SA9
Schmitt, H. W.—F4
Schmorak, Marcel—B11, B12
Schreiber, D. S.—A3
Schultz, T.—BA8
Schumacher, R. T.—G5
Schwarz, Helmut—FA6
Schwartz, M.—JB12
Schwarzschild, A.—B12
Scott, T. A.—D6
Seemann, K. W.—DA15
Segel, Ralph E.—AA11
Segrè, E.—T10
Seidel, T.—ZA7
Sekerka, R. F.—TA2
Seth, K. K.—H8, H9
Shafroth, S. M.—B7
Shapiro, M. M.—X1
Sheline, R. K.—E7, GA9
Shelley, D.—FA13
Sherwood, J. E.—XA4
Sherwood, R. C.—BA4
Shields, Howard—K1
Shirer, D.—J4
Shneiderov, Anatol J.—CB11, SP2
Shore, F. J.—P5, P6
Shugart, H. A.—A5
Shull, C. G.—L2
Shuskus, A. J.—G2, G8
Siegel, R. T.—W2
Signell, Peter—MB5
Silbert, M. G.—DA12
Silva, R. J.—F4
Silver, A. H.—D5
Silverstein, Seth D.—FA1
Silvidi, A. A.—A6
Simon, William G.—RA12
Simpson, J. Arol—M2, M4
Simpson, O. D.—P8
Singh, Virendra—JB4
Skeel, W. L.—E1
Skjeggestad, O.—T4
Slater, W.—T5
Slaughter, G. G.—P9
Slepian, Joseph—SA11
Slifkin, Lawrence—QA5
Smaller, Bernard—D10
Smith, A. B.—XA12
Smith, A. M.—RA8, RA9
Smith, Darryl B.—DA12
Smith, Kenneth—MB2
Smith, W. G.—B6
Smith, W. R.—Q6
Snider, J. L.—A1
Snow, G. A.—Z3
Snowdon, S. C.—J7

Snyder, H. A.—Q2
Sobolak, E.—JB10
Soda, Toshio—MA11, ZB5
Sorensen, R. A.—ZB3
Sperber, Daniel—CB4
Sponer, H.—N5, N6
Spruch, Larry—QB6
Stachel, John—WB5
Staehle, G. G.—E6
Starner, J. W.—B9
Stearns, R. L.—L9
Stehle, P.—JB10
Steigert, F. E.—RA8, RA9
Stein, W.—LA3
Steinberg, D. J.—S4
Steinberg, P. H.—Z3
Steljes, J. F.—LA7
Stelson, P. H.—NA6
Stern, Edward A.—FA3, MA2
Stern, M. O.—YA5
Sternglass, E. J.—JB13
Sternheim, Morton M.—JB11
Stetson, R. F.—M12
Stewart, Ellen S.—QA11
Stewart, James L.—QA11
Stoenner, R. W.—PA8
Stolovy, A.—P7
Stork, D.—T5
Stovall, Tannie—KA12, KA13
Stratton, T. F.—YA8, YA9
Strauss, Michael G.—F11
Strohm, W. W., Jr.—BA10
Stroke, Henry H.—D13
Stubbs, T.—T5
Stump, Robert—F1
Suarez-Etchepare, J.—F6
Sugawara, Masao—JB1
Sullivan, John J.—QA4
Summerfield, George C.—MB9
Sund, R. E.—E8
Suter, T.—F6
Swann, C. P.—GA10
Swanson, N.—M4
Swartz, G. A.—YA1
Swift, R.—G10
Swihart, James C.—MA4
Szamosi, G.—WB3

Tabony, R. H.—H8
Tanaka, Tomoyasu—FB8
Taylor, T. I.—L6
Temmer, G. M.—GA14
Terhune, R. W.—U5
Terner, E.—Q10, SP4
Thomas, T. Darrah—TB4
Thompson, R. W.—F9
Thomsen, John S.—U4
Thomson, J. O.—BA3
Thorndike, E. H.—S6, S7
Thornton, W. A.—M8
Thourson, Thomas L.—YA6
Thurston, R. N.—WA5
Ticho, H. K.—T5, T7
Tickle, R. S.—KA3, KA6
Tidman, Derek A.—VA1
Tilles, D.—PA6, PA7
Tobocman, W.—DA6, TB5, TB6
Tomboulian, D. H.—R4, R5
Tombrello, T. A.—TB7
Tosi, Mario—TA4, TA5
Toth, Kenneth S.—RA4
Toth, Robert S.—FA11
Townsend, J. R.—FA7, FA8
Townsend, VW. T.—U9
Trammell, G. T.—TB8
Trefftz, E.—QB3
Trehan, P. N.—NA1
Trombka, J. I.—F12
Tterlikkis, Lambros—BA6
Turchinetz, W.—DA7, H2, H3
Turk, E. H.—B8
Turnbull, David—TA11
Turner, C. H. M.—J4

Udgaonkar, B. M.—JB4
Ulrich, P. B.—M10
Unruh, W. P.—G4

Van Allen, J. A.—PA5
Vandenbosch, R.—XA6, XA11
Vandenbosch, Susanne E.—E11
Van Patter, D. M.—NA1
Vasudevan, R.—MA11
Vaughn, F. J.—DA8
Vervier, J. F.—DA13
Vogt, Rochus—LA2
Volkoff, G. M.—QB5
Von der Lage, F. C.—P4
v. Krzywoblocki, M. Z.—WB2

Wakuta, Y.—L9
Walker, L. R.—HA4
Walker, W. D.—Z5, Z6
Walker, W. Scott—H4
Wall, N. S.—NA10
Wallis, R. F.—JA3
Walter, F. J.—F4
Walter, R. L.—XA2
Walters, W. L.—GA13
Walton, R. B.—XA7
Wandinger, Lothar—WA10
Wang, I-Tung—ZB4
Warburton, E. K.—DA3
Warhanek, H.—XA6
Warner, L. B.—E7
Wasson, J. T.—PA9
Watson, K. M.—FB10
Watson, R. E.—D9
Watson, W. W.—RA9
Watts, T. L.—RA14
Weatherly, T. L.—N1
Webb, W. W.—QA6
Weber, A. H.—L14
Weber, M. J.—A9
Wegner, H. E.—NA13, XA8, ZA10
Weinberg, R.—XA5
Weinberg, Steven—CA1
Weinstein, R.—W3
Weisberg, Leonard R.—ZA8
Weiss, George H.—VA1
Wenger, Wayne R.—TA12
Wernick, J. H.—BA2, BA5
Werntz, Carl—TB1
Wertheim, G. K.—BA2
Wessel, P. R.—YA10
Weston, L. W.—H8, P4
White, H.—T3
White, Richard H.—R11
Whitehead, W. D.—H1
Whittemore, W. L.—L10, L11
Wiedenbeck, Marcellus L.—E3, E8, F12
Wild, R. L.—QA10
Wildermuth, Karl—NA9, UA2
Wilenzick, R. M.—H9
Wilkinson, R. G.—E2
Williams, D. J.—RA8
Williams, H. J.—BA4
Williams, Quitman—N1
Williams, Robert M.—ZA8
Williams, S. A.—CB7
Willis, Charles R.—FB9
Wills, John G.—MB1
Wilson, Richard—S6, S7
Wilson, R. G.—E6
Wilson, R. R.—KA11, YA5
Wilson, W. E.—XA2
Wing, J.—KA10
Wojcicki, S. G.—T7
Woods, A. D. B.—L4
Woods, R. D.—WB6
Wright, I. F.—RA1

Yagoda, Herman—PA1, PA2, PA3
Yamada, M.—ZB4
Yates, M.—GA2
Yevick, George J.—FB1, QB11
Yin, L. I.—E8
Yntema, J. L.—AA3, NA3, NA4, NA5
Yoder, Richard—MB5
Yoshikawa, S.—SA4
Young, C. G.—G8
Young, J. C.—XA7

Zatzick, M. R.—DA11
Zeidman, B.—AA3, NA3, NA4, NA5
Ziering, S.—Q5
Zimmerman, J. E.—FA12
Zorn, B. Sechi—W10
Zucker, A.—RA2

SHERATON-PARK HOTEL, WASHINGTON, D. C. 1961

AMERICAN PHYSICAL SOCIETY

Please Reserve:	☐ Economy	☐ Standard	☐ Luxury
☐ Single with Bath	9.85	12.50–14.50	20.00
☐ Twins with Bath	13.85	16.50–18.50	20.00
☐ Parlor and One Bedroom Suites (Bath)	20.00	25.00–30.00	35.00
☐ Parlor and Two Bedroom Suites (Bath)		55.00	65.00

ALL ROOMS WITH BATH, AIR CONDITIONED, RADIO & TV

If rate category requested is unavailable, room in next highest category will be assigned.

TO ENABLE US TO CONFIRM YOUR REQUEST, RESERVATIONS MUST BE RECEIVED NOT LATER THAN APRIL 18

An advance deposit or written Guarantee of Payment is necessary to hold your room if arrival is scheduled after 8:00 p.m.

NAME .....

ADDRESS .....

CITY ..... STATE .....

Name(s) of other occupants .....

DATE ARRIVING ..... ARRIVAL HOUR .....

DATE DEPARTING .....

Preliminary Announcement of the 1961 Mexico Meeting*

(Three copies of each abstract, please!)

Those who attended either of our two previous meetings in Mexico will be delighted, and all others should be allured, by the news that arrangements for the meeting of June 22–24, 1961, are well under way. This, like the Congress of 1955, will be a joint meeting of the Sociedad Mexicana de Fisica and our Society, and its scene will be the Ciudad Universitaria on the southern boundary of Mexico City. Committees each composed of a member of each Society are now planning groups of invited papers in cosmic-ray physics, low-energy nuclear physics, theoretical physics, and solid-state physics. Our Divisions of Electron Physics, Fluid Dynamics and Plasma Physics will all three take part.

Deadline will be Friday, April 7. Abstracts are to be sent to the office of the Society at Columbia University, New York 27, New York. *Three copies of each abstract are requested:* one copy will be sent forthwith to Mexico City for translation into Spanish and publication in the announcement of the Sociedad Mexicana de Fisica.

Rooms have been booked for our members in hotels of three categories. The *de luxe* category includes the Hotel del Prado, Alffer, Bamer, Continental Hilton: its price range is $16 to $13.60 double, $14 to $12 single. Of the "superior first-class" category are the Cristobal Colon, San Francisco, Diplomatico ($10 to $8 double, $7.20 to $8 single). Of the "first-class" category are the Prince, Regis, Metropol ($8.80 to $6.80 double, $7.60 to $4.80 single). These prices are quoted in U.S.A. currency; they do not include any meals.

All hotel reservations are to be made by writing to Pancho Lona Tours, Balderas 32 (primer piso), Mexico 1, D.F., Mexico. Use 7-cent airmail stamp. Make deposit for one night when you make your reservation; it will be refunded if you give 72 hours notice of cancellation. All reservations are to be made before June 10.

* Item added in proof and not proofread.

Announcement of the 1961 Thanksgiving Meeting at Chicago

The 1961 Thanksgiving Meeting will be held at Chicago, in the buildings of the University of Chicago, on Friday and Saturday, November 24 and 25. The official hotel will be the Windermere, at 1642 East 56th Street, Chicago 37, Illinois. Deadline for receipt of abstracts will be September 22.

1961 International Conference on Photoconductivity

The "1961 International Conference on Photoconductivity" will be held at Cornell University, Ithaca, New York, on August 21–24. This is accepted as a "topical conference" by The American Physical Society, and other sponsors are the International Union of Pure and Applied Physics and the Office of Naval Research. The emphasis of this conference will be on the fundamental aspects of photoconductivity and phenomena directly related thereto. The conference will conform to the pattern of the 1954 conference on photoconductivity held at Atlantic City. Parallel sessions will not be allowed, and so the programme must include not more than about twenty half-hour papers and forty 15-minute papers, probably only a small percentage of those that may be contributed. Papers on specific devices and applications will be excluded. All members of the Society are allowed to attend this Conference, but those who wish to go must signify their wish **not later than July 1** to the Conference Secretary, Dr. A. R. Hutson, Bell Telephone Laboratories, Murray Hill, New Jersey. To him must go also the abstracts of contributed papers, and these must conform to the same rules as are imposed on those submitted to general meetings of the Society. **Deadline for abstracts is March 31, 1961.**

1961 Gaseous Electronics Conference

The 1961 Gaseous Electronics Conference, fourteenth of the series, will be held at the General Electric Research Laboratories ("the Knolls") at Schenectady, New York, on October 11–13. Former conferences were sponsored by our Division of Electron Physics, which still contributes a member to the Organizing Committee. This Conference has been accepted as a Topical Conference of The American Physical Society. Like its predecessors it is to deal with the basic collision processes occurring in ionized gases, with the mechanisms of electrical breakdown and those of operation of electrical discharges, and with plasma physics in general, but papers on specific devices are excluded. All members of the Society have the right to attend this Conference and to submit contributed papers, but the Organizing Committee may accept or reject these as it chooses.

Abstracts of contributed papers are to be sent to C. J. Gallagher, General Electric Research Laboratories, Schenectady, New York, and must reach him not later than August 25, 1961. Abstracts must conform to the same regulations as are imposed on those submitted for general meetings of the Society. The Organizing Committee will not accept a greater number of contributed papers than is compatible with its intent to keep the meeting within three days, to avoid simultaneous sessions, and to provide adequate time for presentation and discussion of the papers that are accepted.

1961 Spring Meeting of the New York State Section

The 1961 Spring Meeting of the New York State Section will be held on Friday and Saturday, April 14 and 15, at Lemoyne College, Syracuse, New York. It will consist principally of a symposium on atomic and molecular amplifiers, comprising masers of various kinds. Advance registration by mail will be required, since the space available is limited. This should be made by writing to Oran E. Miller, B-65, 1669 Lake Avenue, Kodak Park, Rochester 4, New York. Additional information about the meeting may be obtained from him.

Topical Conference on Planetary Science

A topical conference on planetary science has been arranged for April 19–21 by H. E. Newall and R. Jastrow of the American Geophysical Union. The sponsorship of that Union, of the American Astronomical Society, and of our Society has been accorded to it. The conference will be held in the Auditorium of the Department of the Interior, on C Street between 18th and 19th Streets N.W., Washington, D. C. The titles of the sessions and the names of their chairmen are: Moon and Planets, P. H. Abelson (April 19 at 9:00 a.m.); Meteorites, E. Anders (April 19 at 2:00 p.m.); Trapped Particles, J. A. Van Allen (April 20 at 8:30 a.m.); Interplanetary Plasma, J. A. Simpson (April 20 at 1:30 p.m.); Solar Cosmic Rays: Solar Physics, John Winckler (April 20 at 3:30 p.m.); Atmospheres of the Planets, J. W. Chamberlain (April 21 at 9:00 a.m.); Hydromagnetic Effects, A. J. Dessler (April 21 at 11:00 a.m.). Of great interest, especially to those members of the sponsoring societies who cannot be at the earlier sessions, is the final session to be held on Friday, April 21, at 2:00 p.m. At this session all of the Chairmen named in the foregoing lines will review the outstanding features of their respective sessions and survey developments of significance which have occurred in their respective fields in the past year. H. C. Urey will be Chairman of this closing session.

Important Notice to Members and Fellows of The American Physical Society

A new Membership List of The American Physical Society will be issued in 1961, and it is highly desirable that this be as nearly complete as possible. By the time you read this you should have received by first-class mail, in a window envelope, a return-addressed postal card bearing your name and address of present record, together with instructions for its immediate return emended as necessary. If you have not received this postal card, notify the undersigned of your name and address as you wish them to appear in the Membership List. If your professional affiliation does not appear in your address, this additional information is requested.

SHIRLEY L. QUIMBY
Pupin Physics Laboratories
Columbia University
New York 27, New York

MEETINGS AND DEADLINES THROUGH JANUARY 1962

Place	*Meeting dates*	*Deadline date*
Washington	April 24–27	February 10
Mexico City	June 22–24	April 7
Chicago	November 24–25	September 22
Los Angeles*	December 27–29	October 20
New York	January 24–27, 1962	November 10

Abstracts for the meeting marked with an asterisk are to be sent to Professor H. A. Shugart, University of California, Berkeley 4, California, and must reach his office not later than the corresponding deadline date. Abstracts for the other meetings listed above are to be sent to Karl K. Darrow, American Physical Society, Columbia University, New York 27, New York, and must reach his office not later than the corresponding deadline date. Take note that abstracts mailed the day before deadline day often fail to arrive in time: the last postal delivery of the day usually comes to our office before 2 p.m. For meetings handled at this office, *allow at least two days for abstracts sent by airmail from points east of the Mississippi, and longer for those sent from farther west.* Abstracts postmarked (at the point of dispatch) on deadline day are instantly rejected. No abstract postmarked (at the point of dispatch) on deadline day ever reaches the office on time, nor does any abstract postmarked at any point west of the Rockies on the day before deadline day. Some abstracts arrive with covering letters dated three or more days before the postmark; it may be a good idea for you to put your abstract into a United States mail box with your own hands. Finally, if time is scant, fold your abstract and mail it in an envelope of size $9\frac{1}{2}$ by $4\frac{1}{4}$ inches or thereabouts; for if you mail it in a "manila" envelope large enough to accommodate it without folding, it may very well arrive after the deadline. *The privilege of contributing papers to meetings of The American Physical Society is restricted to the members of the Society and to nonmembers whose papers are sponsored by members.*

SECTIONAL MEETINGS AND TOPICAL CONFERENCES (see pages 183 and 184)

Syracuse	New York Section	April 14–15	—
Ithaca	Photoconductivity	August 21–24	March 31
Schenectady	Gaseous Electronics	October 11–13	August 25

RULES AND INSTRUCTIONS FOR THE PREPARATION OF ABSTRACTS

The Council has ordered that abstracts shall be not longer than two hundred (200) words or the equivalent thereof. In reckoning equivalence, a footnote is equated to ten words or to its actual length in words, whichever is the greater; each line in a table to ten words; a "display" formula—one that requires a line to itself—is an expensive luxury equated to forty words. By-lines are not counted as part of the 200 words, and therefore addresses are condensed to the minimum in them. If you want to spend a lot of your precious 200 words in describing your exact location and the exact compartment of your organization in which you work, you have that privilege.

Two copies of each abstract must be sent to the appropriate office. They must be typewritten; *one must be an original*, the other may be an original or a carbon copy. *Carbon copies will not be accepted in lieu of originals:* they smear. *Abstracts* (including titles, by-lines, and footnotes) *must be double-spaced:* single-spaced manuscripts are too crowded to permit the editorial markings to be made with ease and clearness. *Each abstract must be confined to a single page:* if it is too long for a single page it is too long to be printed. If we receive an abstract typed on two pages, we print only its first page. *Write each abstract as a single paragraph:* the suppression of paragraphs costs time and labor to the editors. *Do not use very thin paper:* a sheet of very thin paper may cause extraordinary trouble when mixed with sheets of reasonable thickness. *Tables too broad to fit into one column of the Bulletin will be left out.* The American Institute of Physics will bless you if you type first the title of your abstract in lower-case with capitalized initials, then your name in capitals, then the name of your institution in lower-case underlined with capitalized initials. It is a pleasure to report that those who qualify for this blessing are increasing in number but are still quite a bit short of 100% of the total. Issues of the *Bulletin* are always appreciably delayed because the editors have to do what the authors should have done.

Remember the rule of the Council that, if an author submits more than one abstract, all but one must go into the Supplementary Programme. In enforcing this rule, an abstract is credited to the author whose name appears first in the by-line.

It has now become an expensive business to make any change in an abstract, even the smallest, after it has been received. By order of our Council "A change in an abstract will be permitted only at the discretion of the Secretary or his deputy, and only if TEN DOLLARS is enclosed with the letter in which the change is requested." As heretofore, an abstract will not be withdrawn from proof unless the asker sends ten dollars with his request.

New Instructions

(a) If it is wished that two abstracts be scheduled consecutively, write on the first "To be scheduled before abstract ..... by ....." and on the second "To be scheduled after abstract ..... by ....."

(b) In general, all instructions about an abstract should be typed at the bottom of the page that has the abstract on it, never in a covering letter. Covering letters get separated from abstracts!

(c) If a member insists that his paper be scheduled for a particular day or not on a particular day, he will get his wish, but usually at the price of having his contribution included in a session to which it is irrelevant.

The American Physical Society

OFFICERS OF THE SOCIETY FOR 1961

President	FREDERICK SEITZ	University of Illinois
Vice-President	W. V. HOUSTON	William Marsh Rice University
Secretary	K. K. DARROW	Bell Telephone Laboratories (*retired*) (Office at Columbia University)
Treasurer	S. L. QUIMBY	Columbia University
Managing Editor	S. A. GOUDSMIT	Brookhaven National Laboratory

Past Presidents now on Council: W. F. G. Swann, J. W. Beams, G. E. Uhlenbeck, and V. F. Weisskopf.

Other members of the Council: W. A. Fowler, Charles Kittel, Harvey Brooks, Charles Hard Townes, N. E. Bradbury, D. W. Kerst, L. G. Elliott, and P. Kusch.

Deputy Secretary	W. W. HAVENS, JR.	Columbia University
Deputy Secretary for the Pacific Coast	E. L. HAHN	University of California, Berkeley

Memoranda

Memoranda

Memoranda